Xenobiotic-metabolizing enzymes elevated in multiple mouse models of slow aging

by

Michael John Steinbaugh

A dissertation submitted in partial fulfillment
of the requirements for the degree of
Doctor of Philosophy
(Cellular and Molecular Biology)
in The University of Michigan
2012

Doctoral Committee:

Professor Richard A. Miller, Chair
Professor Gary D. Hammer
Associate Professor David O. Ferguson
Associate Professor Mats Ljungman
Assistant Professor Ao-Lin Hsu

ACKNOWLEDGEMENTS

First and foremost, I would like to thank my mentor, Rich Miller, for helping me develop as a scientist. During my tenure in his laboratory, I greatly improved my experimental technique, writing ability, and presentation style. I would also like to thank my thesis committee members: David Ferguson, Gary Hammer, Ao-Lin Hsu, and Mats Ljungman. Their feedback during meetings over the years was invaluable and helped me focus my thesis research.

The other members of the Miller lab have provided much support over the years. Thank you to Lisa Burmeister and Sabrina Friedline, as well as Maggie Vergara and Jessica Sewald, for managing the mice used during my thesis research and additional technical assistance. Thank you to Liou Sun, misguided Spurs fan, who was like a second mentor in the lab. Additional thanks to Jim Harper, Gonzalo Garcia, Bill Swindell, Amir Sadighi-Akha, Min Wang, Najoua Elbourakadi, Weiquan Li, Ayesha Rahman, Scott Leiser, Adam Salmon, Varol Ulas Ozkurede, Maria Alvarellos, Bill Kohler, and Melissa Han for their assistance.

I would like to acknowledge my previous research mentors, Ken Bradley, Lisa Ellerby, and Michelle Lafevre-Bernt. I began my science career in Ken's lab at UCLA alongside Francisco Maldonado-Arocho (Jedi Master), David Banks, Ana Sanchez, Sabrina Ward, Marissa Caldwell-Oakland, and Eugene Gillespie. I

was also fortunate to intern at the Buck Institute in the Ellerby Lab under Michelle's tutelage.

Additional thanks to the teachers that made an impact on my math, science, and writing ability: Augusto Andres, Jerry Childers, Fernando Cruz, Peter Foster, Dave Lapp, Patricia Holland, Jeffrey Miller, Sherie Morrison, Lee Pando, Larry Simpson, Mike Tate, and Jerome Zack.

Thanks to my friends in Ann Arbor who kept me grounded during the stressful times of graduate school: Dave Thal, Matt Molusky, Bev Piggott, Paul Moore, Heather Krueger Moore, Ryan Evans, Kevin Vannella, Levi Blazer, Alina Sobiesiak, Paul Marinec, Nicolle Marinec, Dan Foster, Sean Ferris, Ashley Carpenter, Justin Colacino, Kelly Bakulski, Ashley DeHudy, Jen Massie, Matt Smith, Gabe Richards, Jason Norman, and Zach Dalebroux.

Lastly, I would not have made it through graduate school without the support of my family. Thank you to my parents, Bob and Kathy, for being such great role models. Thanks and congratulations to my sister Christine, who will be completing her graduate studies this May. Finally, I would like to acknowledge my cousin, Grady Chaltain, who has been battling cancer this past year with unparalleled bravery and character.

PREFACE

The experimental research conducted during my tenure at the University of Michigan can be summarized as a work in two acts: (A) a collaborative research study with postdoctoral researcher Dr. Liou Y. Sun on the biochemical changes that occur in response to stress in long-lived dwarf mice, which identified the mitogen-activated protein kinase (MAPK) signal cascade as being differentially regulated in dwarf mice, and (B) an independent study of the changes that occur in xenobiotic metabolism in response to genetic, dietary, and pharmacological interventions associated with delayed aging in mice.

The majority of the work presented in this thesis was conducted independently, but it most be noted that select experiments were performed in collaboration with other members of the Miller laboratory. In particular, Figure 2-5, Figure 2-6, and Figure 2-7, Figure 2-11, Figure 2-12, Table 3-9, and Table 3-16 were the result of work conducted by both myself and Dr. Sun. The data presented in Figure 4-3 and Figure 4-4 were a collaborative effort with research assistant Varol Ulas Ozkurede.

TABLE OF CONTENTS

LIST OF FIGURES

LIST OF TABLES

LIST OF ABBREVIATIONS

ABC	ATP-binding cassette
AhR	Aryl hydrocarbon receptor
AL	Ad libitum
ALT	Alanine transaminase
AMP	Adenosine monophosphate
AMPK	Adenosine monophosphate-activated protein kinase
ANOVA	Analysis of variance
ARE	Antioxidant response element
BCA	Bicinchoninic acid
BP	Binding protein
BSA	Bovine serum albumin
CA	Cholic acid
CAR	Constitutive androstane receptor
cDNA	Complementary DNA
CL	Crowded litter
CR	Caloric restriction
CYP	Cytochrome P450
DAF	Dauer formation
DMEM	Dulbecco's modified Eagle’s medium
DNA	Deoxyribonucleic acid
DR	Dietary restriction
DRE	Dioxin-responsive element
ECF	Enhanced chemifluorescence
ECL	Enhanced chemiluminescence
ERK	Extracellular signal-regulated kinase
EROD	Ethoxyresorufin
FAD	Flavin adenine dinucleotide
FCS	Fetal calf serum
FIRKO	Fat-specific insulin receptor knockout
FMO	Flavin monooxygenase
FOXO	Forkhead box O
FXR	Farnesoid X receptor
GAP	GTPase activating protein
GEF	Guanine nucleotide exchange factor
GH	Growth hormone
GHR	Growth hormone receptor
GHRBP	Growth hormone receptor binding protein
GHRH	Growth hormone releasing hormone

GHRHR	Growth hormone releasing hormone receptor
GHRKO	Growth hormone receptor knockout
GPCR	G-protein coupled receptor
GPX	Glutathione peroxidase
GSH	Glutathione
GST	Glutathione S-transferase
GTP	Guanosine triphosphate
HAO	Hydroxyacid oxidase
HMOX	Heme oxygenase
HSP	Heat-shock protein
IEG	Immediate early gene
IGF	Insulin-like growth factor
IGFBP	Insulin-like growth factor binding protein
IGF-1R	Insulin-like growth factor 1 receptor
IIS	Insulin/IGF-1 signaling
IP	Intraperitoneal
IRS	Insulin receptor substrate
ITP	Interventions Testing Program
JAK	Janus kinase
JNK	c-Jun N-terminal kinase
KEAP	Kelch-like ECH-associated protein
LDH	Lactate dehydrogenase
LD_{50}	Lethal dose 50%, median lethal dose
MAPEG	Membrane-associated proteins in eicosanoid and glutathione
MAPK	Mitogen activated protein kinase
MDR	Multidrug resistance protein
MEK	MAPK/ERK kinase
MGST	Microsomal glutathione S-transferase
MIFKO	Macrophage inhibitory factor knockout
MMS	Methyl methanesulfonate
MR	Methionine restriction
mRNA	Messenger RNA
MROD	Methoxyresorufin
MT	Metallothionein
NADPH	Nicotinamide adenine dinucleotide phosphate
NIA	National Institute on Aging
NLS	Nuclear localization sequence
NQO	NAD(P)H dehydrogenase, quinone
NR	Nuclear receptor
NRF	Nuclear erythroid 2 p45-related factor
PAPPA	Pregnancy-associated plasma protein A
PAPPA-KO	Pregnancy-associated plasma protein A knockout
PAPS	3'-phosphoadenosine 5'-phosphosulfate
PAPSS	3'-phosphoadenosine 5'-phosphosulfate synthase

PBREM	Phenobarbital responsive enhancer module
PBS	Phosphate buffered saline
PCR	Polymerase chain reaction
PDK	Phosphoinositide-dependent kinase
PIT1	Pituitary-specific positive transcription factor 1
PI3K	Phosphoinositide 3-kinase
PKC	Protein kinase C
POR	Cytochrome P450 reductase
PPAR	Peroxisome proliferator-activated receptor
PPRE	PPAR response element
PROD	Pentoxyresorufin
PROP1	Prophet of Pit1
PTEN	Phosphatase and tensin homolog
PXR	Pregnane X receptor
RNA	Ribonucleic acid
RNAi	RNA interference
ROS	Reactive oxygen species
RT-PCR	Real-time polymerase chain reaction
RXR	Retinoid X receptor
SDR	Short-chain dehydrogenase/reductase
SDS-PAGE	Sodium dodecyl sulfate polyacrylamide gel electrophoresis
SFN	Sulforaphane
SOD	Superoxide dismutase
SPF	Specific pathogen-free
STAT	Signal transducer and activator of transcription
SULT	Sulfotransferase
S6K	Ribosomal S6 kinase
tBHQ	Tert-butylhydroquinone
TBS	Tris buffered saline
TBST	Tris buffered saline/Tween-20
TEMT	Indolethylamine N-methyltransferase
TH	Thyroid hormone
TNF	Tumor necrosis factor
TOR	Target of rapamycin
TORC	Target of rapamycin complex
TSH	Thyroid stimulating hormone
UCUCA	University Committee on the Use and Care of Animals
UDCA	Ursodeoxycholic acid
UDPGA	UDP-glucuronic acid
UGT	UDP-glucuronosyltransferase
UPS	Ubiquitin/proteasome system
UV	Ultraviolet
WST-1	Water-soluble tetrazolium
XAP	X-associated protein

XME	Xenobiotic-metabolizing enzyme
XREM	Xenobiotic responsive enhancer module
3-NPA	3-nitropropionic acid
4E-BP	Eukaryotic translation initiation factor 4E-binding protein

CHAPTER 1

Introduction

Aging is a process in which young adult organisms becoming increasingly susceptible to injury, illness, and death (1). Following this definition, age-associated changes begin at maturity, even though age-related pathologies do not emerge until late in life. Changes associated with aging occur in most, if not all, cell types and tissues in humans (2). Many theories have been proposed for the biochemical processes that promote aging, such as free radical damage or genomic instability, but a unified theory that explains how organisms can live anywhere from days to decades and still experience similar age-related declines in vitality has not been achieved (3).

1-1. Theories of aging

Multiple theories have been proposed for the biochemical basis of aging, over 300 by one estimate (4). Many have been formed without a strong foundation of empirical evidence. The most relevant theories of aging in relation to the work presented in this thesis are the free radical theory, somatic mutation theory, and the waste accumulation theory.

Free radical theory of aging

The free radical theory of aging proposes that long-term damage caused by reactive oxygen species (ROS) generated during cellular metabolism is the central force behind aging (5). According to this theory, aging is regulated as a balance of free radical-mediated damage, cellular defenses that modify toxic intermediates, and repair systems that fix damaged macromolecules. An important modification to this theory was the discovery that the most commonly produced free radical, superoxide, is generated by oxidative phosphorylation reactions in mitochondria (6). Mitochondrial ROS has been proposed to damage mitochondrial DNA, leading to dysfunctional mitochondria that generate higher levels of ROS, which eventually damage the genome and other organelles (7). This model has garnered support since its inception, backed by indirect evidence obtained from studies of caloric restriction and long-lived genetic mutants that demonstrate reductions in lipid peroxidation and DNA damage. However, there is little direct evidence to support the basis of ROS as the main driver of aging, since short-lived free radicals are difficult to measure. According to this model, two predictions should hold true: (A) increasing anti-oxidant defenses should reduce long-term oxidative damage and increase lifespan; and (B) decreasing anti-oxidant defenses should increase long-term oxidative damage and shorten lifespan. Studies of model organisms treated with antioxidants and genetic mutants with increased or decreased expression of antioxidant enzyme do not report consistent changes in lifespan (8-11). Oxidative stress appears to play a

role in regulation of healthspan but contributes to the rate of aging in a much more limited role than initially proposed.

Somatic mutation theory of aging

Maintenance of the genome has been proposed to be a critical regulator of aging (12). The genome can be modified by chemical damage, such as ROS and UV light, or by polymerase-mediated copy errors during replication. DNA damage can lead to permanent mutations that affect gene regulation or protein function and activate cellular responses associated with cell death or senescence (13), both of which have been proposed to contribute to age-related pathologies. Double-stranded breaks accumulate during aging in multiple tissues in mice (14). An increase in genomic translocations has been observed in the lymphatic system in old mice compared to young mice (15) and mutation frequencies increase in T cells with age (16). Clearer support for the role of DNA damage in aging could come from interventions that modify protection or repair systems and show a reduction in damage levels as well as an extension of lifespan. However, to date there are no published studies demonstrating lifespan extension in transgenic mouse models that overexpress DNA repair genes, suggesting that DNA repair is unlikely to be the rate-limiting step in aging.

Age-related changes of cellular components likely differ for cell types with differing proliferative capacities. Post-mitotic cells experience “chronological aging,” characterized by a gradual loss in structure and function over time. Highly proliferative cells, such as those that constitute epithelia and the lymphatic

system, are under additional pressure of “replicative aging,” which includes genomic instability and telomere shortening, and may be more susceptible to ROS-mediated damage and replicative senescence (17). Adult stem cells maintain organismal regenerative capacity and are subject to both chronological and replicative aging effects (18). There is no evidence that the longevity of an organism is limited by stem cell regenerative capacity; adult stem cells either maintain an excessive replicative capacity or have a way to replenish using another source (19). Stem cell functional potential decreases with age but is strongly influenced by extracellular factors in the surrounding niche. Supplementation of the microenvironment from young adult organisms can restore regenerative capacity and function of aged stem cells (20, 21). Stem cell populations may both respond and contribute to aging. However, it remains to be seen whether enhancement of stem cell function in select tissues or multiple tissue types has an effect on lifespan.

Waste accumulation theory of aging

The waste accumulation theory of aging proposes that damage caused by free radicals and other reactive chemicals is neutralized in young animals by detoxification enzymes, molecular chaperones, the ubiquitin/proteasome system (UPS) and autophagy, but that the ability of these systems to effectively deal with intracellular toxic species declines with age. As a result, damaged molecules build up inside the cell and are responsible for accelerating the aging process (22). Like the somatic mutation theory of aging, the damage that occurs over time

is driven by reactive free radicals but it is the breakdown in cellular repair machinery that is responsible for age-related pathologies.

The xenobiotic-metabolizing enzymes (XME) are a diverse group of detoxification enzymes responsible for neutralizing carcinogens, drugs, and other toxins. They are also responsible for disposal of endobiotics, some of which, but not all, are generated by free radicals. Their activity is primarily localized to the smooth ER, which acts as an intracellular filter for toxins, utilizing phase I and II metabolism enzymes for conjugation and export from the cell in association with phase III transporters. Multiple XME genes have been identified to be upregulated in slow-aging worms (23) and mice (24). Xenobiotic metabolism is the primary topic of my thesis research and is covered in more extensive detail in Section 1-7.

In addition to detoxification enzymes, cells possess multiple systems to regulate intracellular protein and organelle quality, including molecular chaperones, the UPS, and autophagy (25). Proteins are synthesized and degraded in a continuous renewal process that serves to maintain functionality (26). Decline of protein homeostasis is observed in multiple tissues in aged organisms, which may be attributed to progressive decline of these quality control systems along with increased generation of cytotoxic byproducts during cellular metabolism (27).

Heat-shock proteins (Hsp) are molecular chaperones that serve as active or passive facilitators of protein folding, as well as sensors of protein quality (28,

29). Increasing chaperone expression has been shown to enhance longevity and stress resistance in invertebrates (30-34). However, lifelong elevation of chaperone expression may be detrimental in the context of mammalian aging, since it has been shown that long-term upregulation of chaperones can promote malignancy, based on stimulation of cell proliferation and survival pathways (35). Additionally, higher constitutive expression of chaperones found in tissues from old organisms can be reversed by caloric restriction (CR) (36, 37). Maintenance of the chaperone adaptive response to stress, rather than constitutive elevation, may better protect against age-associated decline of protein homeostasis.

The UPS is responsible for cytosolic degradation of damaged or misfolded proteins. Misfolded proteins in organelles can also be retrotranslocated into the cytosol, in order to maintain organelle integrity (38). Downregulation of proteasome subunits and functional decline of the proteasome system has been observed in multiple tissues in aged rodents (39-43). Interestingly, CR has been shown to be effective at preventing age-associated functional decline in proteasome activity in rodents (40, 44-47).

In addition to molecular chaperones and the UPS, the lysosome plays a major role in maintenance of the proteome and organelle integrity. Lysosome-mediated degradation of intracellular components is known as autophagy, which can be grouped into 3 distinct types: macroautophagy, microautophagy, and chaperone-mediated autophagy (48, 49). Macroautophagy is the best studied type of autophagy in the context of aging. Upregulation of macroautophagy has

been identified in multiple invertebrate models with extended lifespan, particularly in mutants with altered IIS (50, 51) or TOR signaling (52). Additionally, mutants with feeding defects that mimic CR have elevations of macroautophagy (50-54). Morphological changes of the lysosome consistent with dysregulation have also been observed in aged organisms, including expansion of the lysosomal compartment and accumulation of lipofuscin, which interferes with lysosome function by decreasing acidification (55).

1-2. Caloric intake is a regulator of aging

Sustained research on caloric restriction (CR) in the context of aging has been conducted since the 1930s. The first published study compared ad libitum fed rats to reduced energy intake groups restricted for 700 or 900 days. Both restricted groups lived longer than controls and the authors concluded that growth retardation was responsible for the changes observed in lifespan (56). Four years later, the same research group showed that the reduction in caloric intake rather than slowed growth rate was responsible for the previously reported increase in lifespan (57). Similar lifespan extension is observed when CR is started at both 6 weeks and 6 months of age, and aging is delayed by CR started at 12 months of age (58, 59). CR has been shown to effectively increase longevity in multiple rodent stocks (60), as well as in genetically heterogeneous mice (61).

CR extends lifespan and decreases the risk of cancer and other age-associated pathologies in rodents, including signs of oxidative damage (60, 62-

64). Long-term CR in rodents increases insulin sensitivity (glucose uptake and utilization) and reduces circulating insulin levels ~2-fold in comparison to control animals (65, 66). Improved insulin responsiveness may be a factor that contributes to delayed aging (67). Cells cultured with serum obtained from CR animals have been reported to be resistant to H_2O_2 and heat shock (68), but primary dermal fibroblasts cultured from mice on long-term CR were not found to be resistant to H_2O_2, $CdCl_2$, or UV-C light at 4 and 18 months of age (69). However, mice on CR have elevated antioxidant defenses (70, 71) and are resistant to multiple hepatotoxins (69, 70). Reduction in vitamins (72), lipids (73), minerals (73), or protein (74) are not responsible for CR-mediated lifespan extension. CR-induced effects on gene function have been described for over 25 years (75) and numerous microarray studies have been published characterizing detailed mRNA expression changes associated with CR, with some of the largest changes seen in xenobiotic metabolism genes (76, 77).

Specific restriction of the amino acid methionine (MR) has been shown to extend lifespan in both rats and mice (78-80), and like CR, reduces serum levels of IGF-1, insulin, glucose, and thyroid hormone T4. MR mice are also resistant to acetaminophen-induced hepatotoxicity (81). However, unlike CR mice, MR mice were not found to have increased phosphorylation of ERK1/2 and p38 or reduced TOR and 4E-BP1 phosphorylation (80). Therefore, while CR and MR mice have much in common, the beneficial effects of dietary restriction cannot be attributed solely to a reduction in specific amino acids.

Short-term CR specifically during early development has been shown to enhance longevity in mice (80). Transient nutrient restriction can be imposed prior to weaning by manipulating the number of pups per mother. Crowded litter (CL) mice have been produced by expanding the normal liter size of 8 pups/mother to 12 pups/mother during the 3 weeks before weaning. The CL intervention is only applied during the first 3 weeks of life and yet these mice have an 18% increase in median lifespan (80). Additionally, these mice were reported to have lower serum IGF-1 levels during development and also maintain a small, but significant reduction in body weight throughout adulthood (80). The biochemical processes altered by CR during development have not been identified but have been proposed to result in epigenetic reprogramming of pro-aging pathways.

1-3. Invertebrate models implicate insulin signaling as a regulator of aging

The discovery that single gene mutations can significantly alter the rate of aging has enabled gerontologists to study differences in the aging process by comparing young adult long-lived mutants to littermate controls, rather than young versus old cohorts of the same genotype. This approach is advantageous in two ways: (A) it reduces the influence of age-associated pathologies, deconfounding aging from the effects of disease, and (B) it allows for identification of causal pathways that are altered early in life that directly regulated the aging process. Multiple conserved genetic mechanisms of aging have been identified with invertebrate models, thanks in part to their rapid

developmental life cycles and short lifespans. Genetic manipulation of the nematode worm (*Caenorhabditis elegans*), budding yeast (*Saccharomyces cerevisiae*), and fruit fly (*Drosophila melanogaster*) has implicated several specific genes and protein signaling networks in aging (82-85) (Figure 1-1).

Genetic studies in *C. elegans* have yielded multiple significant discoveries that have shed light on the biology of aging (86, 87). Genetic knockout and RNA interference (RNAi) lifespan screens have identified over 300 genes that extend lifespan in worms (88). *C. elegans* is a powerful tool for studying aging due to its relative ease of maintenance, simple body plan (959 somatic cells), rapid development (3 days), and short lifespan (2-3 weeks). Endocrine signaling, genomic maintenance, metabolism, reproduction, and stress resistance have all been implicated in controlling the rate of worm aging. Random mutagenesis studies first isolated long-lived mutants with defects in development, food intake, movement, and reproduction (89). The specific genes mutated in these long-lived *C. elegans* strains were initially unknown but found to be heritable and segregate as single gene mutations. The first single gene longevity-associated mutation identified was *age-1*, which encodes the ortholog of phosphoinositide 3-kinase (PI3K) p110 catalytic subunit (90, 91). Ablation of *daf-2*, which encodes the ortholog of the insulin/IGF-1 receptor, was later found to double the lifespan of *C. elegans* (92). *Daf-2* and *age-1* were then identified as components of an insulin signaling cascade in worms that is conserved in mammals (93). Signaling initiated through DAF-2 activates a transcriptional response regulated by DAF-16,

the ortholog of mammalian FOXO transcription factors (94, 95). DAF-16 regulates expression of stress-response genes, detoxification genes, and genes that control metabolism (96-100). Lifespan extension in *daf-2* worms is dependent on *daf-16* (92, 93), which supports the hypothesis that enhanced resistance to cytotoxic stress delays aging.

Insulin or IGF-1R activation results in downstream signaling through the IRS-PI3K-Akt-FOXO pathway (Figure 1-1). In *C. elegans*, mutation of *daf-2* (IGF-1R ortholog) increases lifespan and elevates the level of active DAF-16 (FOXO ortholog) (93, 95, 101). In the absence of insulin or growth factors, FOXO is localized to the nucleus and can transcriptionally activate stress resistance, cell cycle arrest, or cell death-associated programs. Conversely, upon activation of the insulin signaling cascade, phosphorylated AKT translocates to the nucleus and suppresses FOXO by phosphorylation. Nuclear p-FOXO interacts with 14-3-3 and subsequently RanGTP, which facilitate export to the cytosol, where FOXO maintains an inactive state (102, 103). In nematodes, DAF-16 serves as a regulator of entry into the stress-resistant dauer larvae. Mammalian FOXO transcription factors have not been conclusively linked with aging but have been shown to be associated with enhanced stress resistance (104).

Long-lived single gene mutants have also been identified in *D. melanogaster* (105). The first long-lived fly mutant *methuselah* (*mth*) was generated with *P*-element transposon insertional mutagenesis (106). Molecular cloning of *methuselah* cDNA revealed that the gene encodes a protein with G-

protein coupled receptor (GPCR)-like function. Mutation of *Indy*, an ortholog of sodium dicarboxylate cotransporters, was found to extend lifespan, and may play a role in regulating metabolism (107). *Chico*, the ortholog of insulin receptor substrate, was the first component of the insulin signaling cascade to be associated with longevity (108). Heteroallelic recombination of *InR* alleles was shown to produce viable, dwarf flies that are long-lived, but this effect was sex-specific to females (109). Overexpression of antioxidant genes (catalase, Cu/ZnSOD) and *hsp70* also have been reported to extend lifespan and be associated with enhanced stress resistance in *D. melanogaster* (31, 110, 111). Similar lifespan extension was observed in yeast with deletion of *SOD1* or *SOD2* (112, 113).

These studies demonstrate that diminished insulin signaling extends lifespan and delays aging in worms and flies (114, 115). A common hallmark of many of these long-lived single gene mutants is enhanced resistance to multiple forms of cytotoxic stress (e.g. oxidation, heavy metals, UV light, heat) (30, 116-118). Conversely, organisms selected for their enhanced resistance to stress also tend to be long-lived (119).

1-4. The somatotropic axis regulates mouse aging

Single gene mutations associated with reduced growth hormone (GH) and/or IGF-1 action (Figure 1-2; Figure 1-3) have some of the largest reported effects on mouse lifespan (120) (Table 1-1). Long-lived GH/IGF-1-deficient mice also tend to have increased resistance to multiple types of cytotoxic stress (121-

126). These observations have raised the possibility that reduction in steady-state levels of the somatotropic hormone axis alter downstream protein signaling cascades in a manner that leads to elevated stress resistance and delayed aging (127, 128).

Snell dwarf mice (129) are homozygous for the *dw* mutant allele at the pituitary-specific positive transcription factor 1 (*Pit1*) locus, rendering them defective in the pathway responsible for development of pituitary lactotrophs, somatotrophs, and thyrotrophs (130). These mice are unable to produce GH, thyroid-stimulating hormone (TSH), and prolactin; as a result they have low circulating levels of IGF-1 and thyroid hormones. The *dw/dw* genotype extends lifespan ~40% depending on gender and genetic background when compared to non-dwarf heterozygous littermate controls (131, 132). Ames dwarf mice, first characterized in 1961 (133), are homozygous for the *df* mutant allele at the prophet of Pit1 (*Prop1*) locus and are also long-lived (134-136). Ames mice on CR live longer than ad libitum-fed controls, suggesting that CR and mutations affecting pituitary function extend lifespan at least partially through different mechanisms (137).

Elevated systemic resistance to oxidative toxins, such as acetaminophen, 3-nitropropionic acid (3-NPA), and paraquat, is a hallmark of long-lived dwarf mice (126, 138-140) (Table 1-1). Primary dermal fibroblasts cultured for 3 weeks maintain a stable enhanced stress resistance response to multiple cytotoxic agents, including cadmium chloride, hydrogen peroxide, methyl

methanesulfonate (MMS), paraquat, and UV-C light (122, 123, 141). Additionally, Snell dwarf fibroblasts are resistant to metabolic stresses such as glucose deprivation and rotenone exposure (142). These fibroblasts are resistant to oxygen-induced growth arrest at both low oxygen (3%) and high oxygen (20%) culture conditions (143). DNA repair of UV-induced lesions (e.g. cyclobutane pyrimidine dimers, 6-4 photoproducts) is enhanced in Snell dwarf fibroblasts (144). The enhanced multiplex stress resistance phenotype of dwarf mice is dependent on reduced circulating GH. Ames dwarf mice injected with GH once daily for 6 weeks starting at 2 weeks of age have similar median lifespan as littermate control mice and no difference in cellular stress resistance to cadmium, glucose deprivation, MMS, paraquat, or rotenone exposure (145). Additionally, catalase and SOD activity are reduced in hepatocytes treated with GH or IGF-1 and in transgenic mice overexpressing GH (146, 147). These experiments demonstrate that reduced circulating GH/IGF-1 enhances resistance to cytotoxic stress in a primary fibroblast culture model and in vivo.

Improper pituitary development in Snell and Ames dwarf mice results in impaired secretion of GH and subsequent IGF-1 production by the liver. Targeted knockout of the growth hormone receptor (*Ghr/bp*$^{-/-}$ or "GHRKO") increases lifespan in mice (148, 149) (Table 1-1). Cultured GHRKO fibroblasts are resistant to multiple cytotoxic stresses (e.g. hydrogen peroxide, paraquat, UV), similar to cells from long-lived Snell dwarf mice (123). Genetic knockout of growth hormone releasing hormone (GHRH) receptor (*Ghrhr*$^{lit/lit}$ or "Little") impairs GHRH-

mediated secretion of GH by somatotrophs (150). These Ghrhr-null mice are long-lived (131) and resistant to hepatotoxins (acetaminophen, bromobenzene, and carbon tetrachloride) as well as paralyzing agents (zoxazolamine) (140). Targeted disruption of GH production extends lifespan and increases stress resistance, similar to that observed in Snell and Ames dwarf mice.

IGF-1 receptor knockout mice (*IGF-1R*$^{-/+}$) were initially reported to be long-lived (33% increase in females; 16% but statistically insignificant increase in males) and resistant to paraquat-induced oxidative stress in vivo (121). Recently, this mutation was tested in a new lifespan study by an independent laboratory, which found that the differences in lifespan were much smaller than initially reported (less than 5% and insignificant for females; no difference for males) (151). Although *IGF-1R*$^{-/+}$ mice are not invariably long-lived, mice lacking the insulin receptor in specifically in adipose tissue (fat-specific insulin receptor knockout or "FIRKO") live longer (18%) than wild-type mice in both sexes (152). Heterozygous deletion of insulin receptor substrate 1 (*IRS1*$^{-/+}$) has been reported to extend lifespan in female mice (32%) but not in males (153). Whole body or brain-specific deletion of IRS2 (*IRS2*$^{-/-}$) has been shown to increase lifespan (18%) in both sexes (154). Therefore, although heterozygosity of IGF-1R may not be sufficient to extend lifespan in mice, there is additional strong evidence from studies of mice with mutations in the insulin receptor and insulin/IGF-1R signal cascade (e.g. IRS proteins) that support the role of IGF-1 signals in aging. These

studies are in agreement with published reports of long-lived *C. elegans* and *D. melanogaster* mutants with reduced insulin signaling.

Maintenance of local IGF-1 availability to the IGF-1 receptor may also play a role in aging. IGF binding proteins (IGFBP) can sequester IGF-1 and regulate local IGF-1 concentrations available to interact with the receptor. Pregnancy-associated plasma protein A (PAPPA) is a protease that cleaves IGFBPs (IGFBP-4, possibly IGFBP-2,5) (155). PAPPA knockout (*PAPPA*$^{-/-}$ or "PAPPA-KO") mice are long-lived (30-40% increase) but do not have decreased circulating GH and IGF-1 in the blood (156) (Table 1-1). These mice are an attractive new long-lived model because their enhanced lifespan is linked to IGF-1 signaling, like the Snell dwarf mouse, but they do not have systemic alterations in endocrine function. However, the tissues where local IGF-1 is reduced and that exhibit diminished IGF-1R signaling have not been identified.

1-5. TOR is a nutrient-sensing protein kinase that regulates aging

Target of rapamycin (TOR) acts as an evolutionarily conserved intracellular rheostat that integrates diverse inputs associated with nutrient levels, growth factors, and stress response (157, 158) (Figure 1-3). TOR signaling controls multiple biochemical processes including cell growth, rate of translation, autophagy, and stress response. Rapamycin, first extracted from *Streptomyces hygroscopicus* in soil from the island of Rapa Nui, is a compound with potent antifungal and immunosuppressive properties (159). Rapamycin treatment studies in *S. cerevisiae* identified FK506-binding protein of 12 kDa (FKBP12 or

FRP1 gene) as the intracellular drug-binding receptor (160, 161). Genetic screens of rapamycin-resistant mutants identified dominant gain-of-function point mutations in *TOR1* and *TOR2* that do not bind complexed FKBP12 and rapamycin (162, 163). Yeast with reduced TOR activity were reported to be long-lived in chronological lifespan experiments (164, 165). The TOR proteins are integrated into two complexes with distinct functions that are conserved in mammals: TORC1 (rapamycin sensitive) regulates cell growth and TORC2 (rapamycin insensitive) controls spatial aspects of growth, such as regulation of the actin cytoskeleton (166, 167).

In contrast to yeast, only a single TOR ortholog is encoded in worms (168), flies (169, 170), and mammals (171-175). Deletion of TOR in these models results in developmental arrest and lethality (168, 169, 176). Mutants that express a dominant negative form of TOR are long-lived in *D. melanogaster* (177), and downregulation of TOR by RNAi during adulthood extends lifespan in *C. elegans* (178). TOR is activated in multicellular organisms in response to the insulin/IGF-1 signaling (IIS) cascade, but also functions in parallel to growth factor signaling (179, 180). In mammals, TORC1 regulates protein synthesis primarily through activation of S6K1 and inhibition of 4E-BP1 (181). Since TOR inhibition is associated with enhanced longevity in invertebrate models, TOR has been proposed to also be a regulator of aging in mammals. In agreement with this hypothesis, Ames dwarf mice have reduced hepatic phosphorylation of S6K1 and increased expression of 4E-BP1 (182). Additionally, knockout of S6K1 in

mice extends lifespan in mice in a sex-specific manner, with a 20% increase in longevity reported in females (183). S6K1 knockout mice are also more insulin sensitive and resistant to high-fat diet-induced obesity (184).

Pharmacological repression of the TOR pathway by rapamycin has recently been shown to extend lifespan, protect against high-fat diet-induced obesity, and enhance hematopoietic stem cell function in mice (185-189). Rapamycin was first reported by the National Institute on Aging Interventions Testing Program (ITP) (190) to extend lifespan in a genetically heterogeneous mouse population (UM-HET3), when the drug was given in the diet starting at 20 months of age. The effect was seen in both males (9% increase in mean lifespan) and females (14%) (187). Similar lifespan extension was observed in HET3 cohorts administered rapamycin starting at 9 months of age (187, 188). Intermittent feeding of rapamycin (2 weeks per month) starting at 2 months of age was also recently reported to increase longevity in female 129/Sv mice (189).

TOR activity is controlled by upstream AMP-dependent kinase (AMPK) signaling (Figure 1-3). AMPK can inhibit TORC1 signaling through TSC2 and raptor (191, 192). AMPK is activated by a decrease in cellular energy and inhibited by sestrins, which are induced by genotoxic stress through p53-mediated transcription initiation (193). AMPK activity is increased by the pharmacological agonist metformin, a biguanide compound with anti-diabetic effects. Metformin has been reported to extend lifespan in female mice by ~10%

(males were not reported) in two studies (194, 195) but does not extend lifespan in rats (196).

1-6. MAPK signal cascades may influence the rate of aging

Ras GTPases play an important role in the regulation of cell growth, differentiation, and stress resistance. *RAS1* and *RAS2* orthologs have been shown to regulate longevity in *S. cerevisiae.* Deletion of *RAS1* extends replicative lifespan and deletion of *RAS2* extends chronological lifespan (113, 197). However, deletion of *RAS*2 has been shown to shorten replicative longevity (197). Attenuated Ras signaling is also associated with enhanced stress resistance in yeast (165, 198). Ras functions downstream of the insulin/IGF-1 receptor in mammals and its GTPase activity is regulated by Ras-guanine nucleotide exchange factors (GEF) and Ras-GTPase-activating proteins (GAP). Ras-GEFs have been proposed to play a conserved role in the regulation of aging (199). Recently, homozygous deletion of the Ras-GEF RasGrf1 was found to extend lifespan 19% in mice (200, 201). Decreased Ras-GEF activity is associated with a reduction in downstream Ras pathway activation.

A major downstream mediator of Ras function is the MEK/ERK MAPK cascade. MAPKs comprise a ubiquitous group of signaling proteins that play a prominent role in regulating cell proliferation, differentiation and adaptation. Members of each major MAPK subfamily, the extracellular signal regulated protein kinases (ERK), the c-Jun N-terminal kinases (JNK) and p38 MAPK, have been implicated in cell injury and disease (202, 203). The MAPK signaling

module is defined by a three-tiered kinase cascade, resulting in phosphorylation of a conserved Thr-X-Tyr activation motif by an upstream dual specificity MAPK kinase (202). In particular, ERK1 and ERK2, which are activated by the MAPK/ERK kinase-1/2 (MEK1/2), are important regulators of cellular responses to various stimuli (204).

ERK signaling is tightly regulated at multiple levels to achieve signaling specificity that controls diverse cellular functions. This is proposed to be controlled in the following ways: (A) distinct duration and strength of the signal, (B) presence of components with differing specificities in each level of the cascade, (C) interaction with scaffold proteins, (D) crosstalk with other signal cascades, and (E) distinct subcellular localizations that may compartmentalize MEK/ERK cascade components (205, 206). ERK signal duration is tightly linked to the localization of pathway activation, which is thought to be influenced by MEK/ERK scaffold proteins. MEK/ERK scaffolds have been shown to be localized to multiple places inside the cell, including the plasma membrane, early endosome, and Golgi (207). Scaffold proteins are capable of inducing faster kinetics of activation, different duration and intensity, and cross talk with other signaling components.

1-7. Intracellular detoxification may contribute to the rate of aging

The waste disposal theory of aging postulates that the ability of organisms to deal with intracellular toxic byproducts declines with age. XMEs, which are primarily active in the liver, play a major role in detoxification of a diverse range of

damaging agents (Figure 1-4). Xenobiotic metabolism is divided into three phases: (A) phase I, in which cytochrome P450s and flavin monooxygenases add reactive or polar groups onto compounds targeted for removal, and metallothioneins regulate metal ion homeostasis, (B) phase II, in which glutathione S-transferases (GST), sulfotransferases (SULT), UDP-glucuronosyltransferases (UGT) conjugate charged species (e.g. glutathione, sulfate, glucuronic acid) onto the activated metabolites produced by phase I biotransformation, and (C) phase III, in which multidrug resistance proteins (MDR) and ATP-binding cassette (ABC) transporter proteins facilitate export of the conjugates and metabolites produced by phase II reactions.

Phase I biotransformation

The largest and best studied group of phase I enzymes are the cytochrome P450 (CYP) monooxygenases. CYP enzymes catalyze the first step in metabolism of lipophilic xenobiotics by making them more water-soluble. The CYP enzymes play a major role in drug metabolism and bioinactivation, and induction or inhibition of these enzymes are responsible for most drug interactions in humans (208, 209). CYP enzymes were first studied in the context of drug, carcinogen, and steroid metabolism in the 1940s (210) and later isolated by purification in the 1970s (211, 212). 102 putatively functional and 88 pseudogenes have been identified in mice, whereas 57 putatively functional and 58 pseudogenes have been identified in humans (213). There are 9 named clusters or “clans” of related CYP enzymes in vertebrates: CYP2 clan

(CYP1,2,17,21 genes), CYP3 clan (CYP3,5 genes), CYP4 clan (CYP4 genes), CYP7 clan (CYP7,8,39 genes), CYP19 clan (CYP19 genes), CYP20 clan (CYP20 genes), CYP26 clan (CYP26 genes), CYP51 clan (CYP51 genes), and the mitochondrial clan (CYP11,24,27 genes) (213, 214). The CYP2, CYP3, CYP4, and mitochondrial clans are also functionally conserved in invertebrates (214, 215).

The CYP2 and CYP3 clans are primarily involved in drug and steroid metabolism. Phenobarbital is a potent inducer of CYP2 gene expression (216-218). CYP2 genes are positively regulated by Ca^{2+} release via calmodulin-dependent kinase as well as protein kinase C but are negatively regulated by GH, cytokines, and the cAMP/PKA pathway (219-221). In humans, Cyp3a4 has been reported to account for 30-80% of total CYP expression in the liver, as well as to catalyze the metabolism of over 50% of drugs in clinical use (222). CYP4 enzymes are hydroxylases that metabolize fatty acids and arachidonic acid (223). CYP4 genes are transcriptionally upregulated in response to aberrant hepatic lipid metabolism and increased levels of lipid peroxidation (224, 225). While there is significant overlap in the functions of CYP clans between humans mice, individual genes can behave very differently between these species (209).

Flavin-containing monooxygenases (FMO) are flavin adenine dinucleotide (FAD) or reduced nicotinamide adenine dinucleotide phosphate (NADPH)-dependent enzymes that activate sulfur or nitrogen-containing xenobiotics by oxidation or hydroxylation reactions (226). Mammals encode 5 FMO variants

(Fmo1-5) (227). Fmo3 is the best characterized of the 5 variants, since it highly polymorphic in humans and has been proposed to contribute to differential drug response (228). Fmo3 expression is upregulated during post-natal development, which may serve to protect the liver from early exposure to environmental toxicity (229). Additionally, Fmo3 has been shown to affect sulfoxidation of methionine (230, 231), which is of interest in the context of aging, since long-lived dwarf mice have elevated methionine metabolism (232).

Metallothioneins (MT) are stress-responsive regulators of metal ion homeostasis, cell survival, and pathways associated with inflammation or apoptosis (233-235). Ten MT isoforms are encoded in humans, grouped into four families (MT-1, MT-2, MT-3, MT-4). Only four MT genes are encoded in the mouse genome (*Mt1*, *Mt2*, *Mt3*, *Mt4*). *Mt1* and *Mt2* are best conserved across species and expressed across most tissues in the mouse (235). MT genes include response elements for multiple transcription factors, including the metal response element, antioxidant response element (ARE), glucocorticoid response element, and well as binding sites for transducers and activators of transcription (STAT). Mice that overexpress metallothionein, especially the human metallothionein-IIa gene (236), were reported to have increased resistance to doxorubicin (236) and a 14% increase in mean lifespan (237). In addition, cells that overexpress MT have been shown to be resistant to multiple forms of cytotoxic stress, including paraquat and tert-butyl hydroperoxide (238-240). Conversely, mice that do not express metallothionein 1 and 2 (*Mt1/2*$^{-/-}$) were

found to be more susceptible to high-fat-diet-induced obesity (241) and cells from MT-null mice have been shown to be susceptible to multiple oxidative stress agents (242, 243).

Phase II biotransformation

GSTs mediate detoxification of electrophilic xenobiotics activated by phase I biotransformation, as well as endogenous epoxides, hydroperoxides, and quinones formed as secondary metabolites during oxidative stress, through conjugation, reduction, and isomerization reactions (244). Three families of GSTs exist in mammals, defined primarily by their localization to the cytosol, microsomes, or mitochondria. Microsomal GSTs, also referred to as membrane-associated proteins in eicosanoid and glutathione (MAPEG) metabolism (245), do not structurally resemble cytosolic and mitochondrial GSTs. Cytosolic GSTs are the best characterized family in the context of xenobiotic metabolism. Based on amino acid sequence similarities, seven classes of cytosolic GSTs have been defined in mammals: Gsta (α, alpha), Gstz (ζ, zeta), Gstt (θ, theta), Gstm (μ, mu), Gstp (π, pi), Gsts (σ, sigma), and Gsto (ω, omega) (246-249). Cytosolic GST isoenzymes, on average, share > 40% identity within a class between rodents and humans. These enzymes catalyze nucleophilic attack along with reduced glutathione (GSH) on nonpolar compounds that contain an electrophilic carbon, nitrogen, or sulfur atom (244).

Sulfotransferases are another major class of phase II enzymes involved in detoxification, drug metabolism, and hormone regulation (250). Sulfotransferases

perform sulfurylation reactions through catalytic transfer of a sulfuryl group (SO_3) from a donor molecule, typically 3'-phosphoadenosine 5'-phosphosulfate (PAPS) to amine or hydroxyl substrates on the target molecule. The formation of these sulfate conjugates is an effective method to detoxify carcinogens or inactivate hormones (251). Sulfotransferases are classified into cytosolic or membrane-associated groups based on their localization in the cell. Cytosolic sulfotransferases are better characterized in the context of xenobiotic metabolism and their nomenclature is defined primarily by substrate specificity (250). Cytosolic sulfotransferases can metabolize a wide variety of substrates, including phenols and catecholamines (Sult1a1, Sult1a2, Sult1a3), thyroid hormones (Sult1b1), aryl hydroxylamines (Sult1c1, Sult1c2), estrogens (Sult1e1), and hydroxysteroids (Sult1a1, Sult2a1, Sult2a2).

UGT-catalyzed glucuronidation is considered to be the most common phase II reaction, accounting for up to 35% of phase II biotransformation (252-254). Similar to cytochrome p450s, UGT enzymes are localized on the ER. UGTs are responsible for metabolism of a wide variety of phenolic compounds, environmental toxins, and carcinogens (255, 256). UGTs most commonly utilize UDP-glucuronic acid (UDPGA) as a co-substrate. Natural phenolic compounds including flavonoids (e.g. epigallocatechin gallate) and stilbenes (e.g. resveratrol) are primarily metabolized by UGT enzymes. Additionally, synthetic phenolic compounds including nonsteroidal anti-inflammatory drugs (e.g. acetaminophen), immunosuppressants, and decongestants are targeted by UGTs (254). After

UGT-mediated transformation, phenolic glucuronides are much more hydrophilic and readily transported out of the cell by phase III biotransformation. Mammalian UGTs are classified into four families: UGT1, UGT2, UGT3, and UGT8, based on amino acid sequence identity (257). The most important drug-conjugating UGTs belong to UGT1 and UGT2 families. In mice, the UGT1 subfamily consists of 9 enzymes (Ugt1a1, Ugt1a2, Ugt1a5, Ugt1a6a, Ugt1a6b, Ugt1a7c, Ugt1a8, Ugt1a9, and Ugt1a10) and five pseudogenes (Ugt1a3, Ugt1a4, Ugt1a7a, Ugt1a7b, and Ugt1a11). The 7 UGT2 genes in mice include Ugt2b1, Ugt2b5, Ugt2b34, Ugt2b35, Ugt2b36, Ugt2b37, and Ugt2b38 (257, 258).

Regulation of xenobiotic metabolism by intracellular receptors

Nuclear receptors (NR) mediate the intracellular adaptive response to xenobiotics. Pregnane X receptor (PXR), constitutive androstane receptor (CAR), and peroxisome proliferator activated receptors (PPAR) are the major regulators of cytochrome P450 enzymes (259). NRs have a shared modular structure characterized by a ligand-binding/dimerization domain, a DNA-binding/weak dimerization domain, and a transactivation domain (260). In general, PXR and CAR regulate CYP2 and CYP3 genes, and PPARα regulates CYP4 genes (261). Additionally, the aryl hydrocarbon receptor (AhR), a basic helix-loop-helix/Per-ARNT-Sim (bHLH/PAS) transcription factor, is a key regulator of CYP1 gene expression (259). NRs are also capable of regulating phase II XMEs, including GST, ST, and UGT enzymes (262).

PXR is the most studied NR regulator of cytochrome P450s, since it has been identified to induce CYP3A genes, the most abundantly expressed cytochrome P450 family in humans (263). The ligand-binding specificity of PXR varies greatly between species. For example, phenobarbital and rifampicin activate PXR in humans but have little effect in rodents. Conversely, pregnenolone 16α-carbonitrile activates PXR in rodents but not in humans. Differential activation of NRs between mice and humans has been a major problem for successful drug development. Transgenic mice that express only the human NR variant have been reported to have a more “humanized” xenobiotic response that may be useful for pharmacological studies (264). In both rodents and humans, PXR transcriptional activity is dependent upon heterodimerization with the retinoid X receptor (RXR) and subsequent binding of the xenobiotic responsive enhancer module (XREM) (263, 265, 266). In addition to playing a major role in drug metabolism, PXR is a regulator of bile acid metabolism. In response to high intracellular bile acid concentrations, PXR induces CYP3A genes and represses CYP7A genes, which catalyze the conversion of cholesterol to bile acids (267).

CAR is a phenobartibal-responsive NR that regulates XME gene expression through the phenobarbital responsive enhancer module (PBREM) (268, 269). Similar to PXR, activated CAR translocates from the cytosol to the nucleus, where it heterodimerizes with RXR and acts as a transcription factor, primarily of CYP2B and CYP3A gene expression (270). CAR exhibits a high

degree of redundancy with PXR in regulation of XME gene expression, particularly with regard to CYP2B and CYP3A genes (271, 272). CAR also functions as a regulator of bile acid and thyroid hormone metabolism. Wild-type mice treated with CAR activator TCPOBOP have lower circulating levels of thyroxine (T4) relative to *CAR*$^{-/-}$ mice treated with TCPOBOP, attributed, at least in part, to induction of UGT1 and SULT enzymes (273, 274). Additionally, CAR plays a role in metabolism of phenolic compounds (e.g. acetaminophen). CAR-null mice have increased susceptibility to acetaminophen-induced hepatotoxicity, due primarily to deficiency in the induction of phase II GSTp enzymes (275). Along with PXR, CAR protects against bile acid-induced toxicity (e.g. lithocholic acid exposure) (276) and accumulation of bile acid precursors (267, 277, 278), but this appears to be secondary to the farnesoid X receptor (FXR), which is a regulator of CYP7 and CYP8 gene expression (279, 280). PXR and CAR function as broad regulators of XME gene expression, with both parallel and overlapping effects on phase I and phase II enzymes (260).

PPARs regulate XME gene expression, in addition to carbohydrate and lipid metabolism, insulin action, inflammation, and the immune response (281). Mammals encode three subtypes of PPAR proteins, expressed in different tissues and at different times during development: PPARα, PPARβ/δ, and PPARγ (282). PPARγ is a key regulator of adipogenesis (283, 284) and has been extensively studied in the context of diabetes treatment, since activation of PPARγ has been shown to increase insulin sensitivity (285). The function of

PPARβ/δ is still unclear, but it may contribute to regulation of lipid metabolism (286). PPARα is enriched in tissues that perform fatty acid oxidation, particularly in hepatocytes (260). Similar to PXR and CAR, PPARα forms a heterodimeric complex with RXR in the nucleus that interacts with PPAR response elements (PPRE) (287). Natural PPARα ligands include arachidonic acid, lineolic acid, oleic acid, and palmitic acid. PPARα can also be activated by hypolipidemic drugs (e.g. clofibrate, ciprofibrate), phthalates, and steroids (e.g. dehydroepiandrosterone) (260). PPARα is a regulator of XME genes including the CYP4A family, which are involved in hydroxylation of fatty acid derivatives and cholesterol metabolism, and the SULT2 family (288-290).

The AhR is a soluble, ligand-activated bHLH/Per-ARNT-Sim transcription factor that regulates xenobiotic metabolism through the dioxin-responsive element (DRE, also referred to as AHRE or XRE) (291, 292). AhR is normally sequestered in the cytosol in a complex with Hsp90 and X-associated protein 2 (XAP2). Upon ligand binding, the nuclear localization sequence (NLS) on AhR is exposed by release of XAP2 (293, 294). The AhR-Hsp90 complex then translocates to the nucleus, where Hsp90 is displaced by the AhR nuclear translocator (ARNT) (295, 296). The AhR-ARNT complex is then able to bind DNA at the DRE. Similar to the NRs PXR, CAR, and PPARα, AhR regulates the adaptive response of XME genes. Cyp1a1 was the first XME identified to be regulated by AhR, in response to 2,3,7,8-tetrachlorodibenzo-p-dioxin exposure

(297-299). AhR also regulates other CYP1 genes including Cyp1a2 and Cyp1b1, as well as phase II Gsta, NQO1, and UGT1 enzymes (300).

Regulation of xenobiotic metabolism by Nrf2

NF-E2-related factor 2 (Nrf2) is a Cap'n'Collar (CNC) transcription factor that regulates several enzymatic pathways, phase I and phase II biotransformation (301-304). Other members of the CNC family include Nrf1, Nrf3, and p45 NF-E2, as well as two distantly related proteins named Bach1, and Bach2 (302, 305-307, 307-311). These proteins contain a DNA-binding CNC domain and a conserved basic-region leucine zipper (bZip) domain that interacts with small Maf proteins (303, 312). Nrf2 was initially identified as the transcription factor whose binding motif interacts with the ARE (313). The ARE is a cis-acting promoter element that found in many phase II detoxification genes (314). Microarray studies have identified over 200 genes that are under transcriptional control of Nrf2/ARE, and are involved primarily in the maintenance of intracellular redox balance (302).

Nrf2 activity is regulated post-translationally through rapid turnover by the proteasome. Nrf2 has an estimated half-life time of 30 min (315) and is repressed under homeostatic conditions (312, 316). Nrf2 is regulated via its trans-activation domain, which is the binding site of Kelch-like ECH-associated protein 1 (Keap1) (317). Keap1 binds Nrf2 as a dimer and sequesters it in the cytosol by interaction with the actin cytoskeleton, where Keap1 then functions as an adaptor for Cul3-based E3 ligase to regulate proteasomal degradation of Nrf2 (318). In response

to oxidative stress, Nrf2/Keap1 binding is disrupted, and Nrf2 translocates to the nucleus where it acts as a transcription factor (302, 319) (Figure 1-5). This model is supported by studies of Nrf2 activator compounds, which have been reported to increase steady-state Nrf2 protein levels but not mRNA levels (320-322). Keap1 association with Nrf2 is mediated by conserved cysteine residues (C151, C273, and C288) that are affect the protein conformation and binding affinity of Keap1 (302). Keap1 monitors intracellular oxidative stress levels through these thiol groups, which form disulfide linkages under high oxidative stress conditions (302, 323-325). Nrf2 activators (e.g. tert-butylhydroquinone [tBHQ] and sulforaphane [SFN]) induce Nrf2 through modification of these cysteines on Keap1 (326-329). Therefore, Keap1 likely functions as a molecular switch, maintaining low Nrf2 protein expression when cellular redox status is in balance, and promoting Nrf2/ARE-regulated transcriptional upregulation of XME genes when oxidative stress is high (330).

In addition to Keap1, Nrf2 activation has been proposed to be regulated by phosphorylation, which may stabilize Nrf2 and prevent proteasomal degradation (302). Phosphorylation of Nrf2 has been linked to PI3K, MAPK, and PKC signal transduction pathways (331), but whether Nrf2 activity is regulated through a Keap1-independent mechanism remains controversial. The studies that implicate these signal cascades in the regulation of Nrf2 have been largely correlative and non-mechanistic, often using broad spectrum inhibitors. Inhibition of PI3K with wortmannin or LY 294002 has been reported to prevent induction of Nrf2-

regulated target genes (332, 333). Nrf2 is tethered to the membrane by Keap1-actin association under basal conditions, possibly allowing for PI3K or PKC to directly phosphorylate Nrf2 at the membrane (333). ERK has been also implicated as a potential regulator of Nrf2 activity, based on data showing that some Nrf2 activators increase phosphorylation of ERK1/2 (334, 335), and that PD98059-mediated inhibition of MEK/ERK decreased Nrf2/ARE-regulated gene expression (336). However, there are conflicting reports that Nrf2 activity is unaffected by MAPK inhibitors (337, 338). The best-defined signal transduction pathway responsible for Nrf2 activation is the protein kinase C (PKC) pathway. PKC has been reported to phosphorylate Nrf2 at Ser40 (339), and activation of PKC has also been reported to increase Nrf2/ARE activation (337). Conversely, PKC inhibition has been reported to suppress Nrf2/ARE activation (337). These studies provide preliminary evidence that Nrf2 activity may be regulated by multiple pathways, but Keap1 is best supported by experimental evidence as the primary regulator of Nrf2 activity.

Studies of transgenic mice with altered Nrf2 or Keap1 expression have provided direct evidence in support of the role of Nrf2 as a key regulator of xenobiotic metabolism in vivo. Nrf2-null mice are viable, suggesting that Nrf2 is not required during development (340). Nrf2-null mice have increased sensitivity to multiple xenobiotics (341), including acetaminophen (342), benzo(a)pyrene (343), butylated hydroxytoluene (344), diesel exhaust (345), dimethyl-benz(a)anthracene (346), cigarette smoke (347), and 3-nitropropionic acid (348).

Whole body knockout of Keap1 is lethal due to lesions from hyperkeratotic outgrowth of the esophagus and forestomach (349-351), but mice with hepatocyte-specific knockout of Keap1 (*Alb-Cre::Keap1*$^{flox/-}$) are phenotypically normal (351). *Alb-Cre::Keap1*$^{flox/-}$ mice were reported to have increased Nrf2 nuclear localization and enhanced resistance to acetaminophen toxicity (351). These data support the role of Nrf2 as a key mediator of cytotoxic stress resistance in vivo (342, 352). Additionally, mice with Nrf2 or Keap1 mutations have altered expression of multiple phase II enzymes, including NAD(P)H:quinone oxidoreductase (Nqo1) (351, 353-355), heme oxygenase 1 (Hmox1) (356), glutathione peroxidases (GPX) (351, 357), peroxiredoxins (358, 359), GSTs (321, 351, 351, 360-363), and SULTs (351). Interestingly, these studies have revealed that Nrf2 also regulates heat shock proteins Hsp40 (364) and Hsp70 (365), as well as multiple phase I XMEs (304), including CYP1 genes (366), CYP2 genes (351, 366, 367), FMOs (351, 368, 369), and carbonyl reductases (351, 370). The mechanism of Nrf2-regulated phase I gene expression is not well understood but may be associated with NR activation. In Nrf2-null mice, mRNA levels of PXR, CAR, and AhR were reported to be lower relative to littermate control mice (366).

Xenobiotic metabolism in the context of aging

Xenobiotic metabolism genes were first identified as being transcriptionally upregulated in long-lived organisms in a *C. elegans* microarray study of *daf-2* mutants (23). CYP, UGT, and short-chain dehydrogenase/reductase (SDR)

enzymes were found to be elevated in the insulin signaling-deficient *daf-2* mutants. Similar results were obtained in microarrays performed on long-lived mouse models, including Ames (371, 372), GHRKO (373), Little (371), Snell (372, 374, 375), and CR mice (376, 377). XMEs were found to have some of the largest changes in gene expression in long-lived mice relative to control mice. Meta-analysis of CR and long-lived dwarf mice microarrays revealed that phase I enzymes in particular were elevated in liver tissue (378). Additionally, Fmo1 and Fmo5 were reported to be transcriptionally upregulated in *Irs1*$^{-/-}$ mice, implicating the IGF-1R-IRS pathway in regulation of FMOs (379, 380). The phase I DMEs shown to be differentially expressed in long-lived dwarf mice have been reported in other models to be regulated by CAR and/or PXR (381-387). However, experiments utilizing *Ghrhr*$^{lit/lit}$ mice crossed with CAR/PXR or FXR knockouts showed that FXR and not CAR/PXR is the nuclear receptor that predominantly regulates phase I gene expression in *Ghrhr*$^{lit/lit}$ mice (140). Regulation of xenobiotic metabolism has not been tested using nuclear receptor knockout crosses in other dwarf models, but there is additional data that suggests phase I gene expression may be controlled by multiple factors. PPAR and RXR levels are elevated in Ames dwarf and GHRKO liver tissue (281), and multiple Nrf2-regulated genes are also elevated in Ames and Snell dwarf liver tissue (388, 389). However, there are hundreds of genes involved in xenobiotic metabolism, many of which exhibit redundancy, making single gene analysis of effects on

lifespan difficult. Presently, the influence of xenobiotic metabolism and aging is poorly characterized with regard to transgenic mouse models.

The role of Nrf2 in aging has been studied primarily in the context of the *C. elegans* ortholog SKN-1. In worms, SKN-1 functions in the intestines and ASI neurons, in support of a neuroendocrine regulatory circuit of life-span control. SKN-1 is negatively regulated by IIS in parallel to the DAF-16, which can also inhibit SKN-1 directly (390). Unlike mammalian Nrf2, SKN-1 functions as a homodimer in worms and is activated in response to stress by p38 and GSK-3 (391, 392). *Skn-1* is also necessary for DR-mediated lifespan extension, and overexpression of SKN-1 has been shown to increase longevity and oxidative stress resistance (390, 393, 394). SKN-1 regulates glutathione synthesis and quinone reduction, similar to Nrf2 in mammals, and downstream targets of SKN-1 have been shown to overlap with DR-responsive signal pathways (390). An ortholog of Nrf2 in *D. melanogaster* has only been recently identified and is not well characterized (395). However, heterozygous knockout of the Keap1 ortholog increases stress resistance and lifespan in male flies (395). These findings in invertebrate models demonstrate a direct role for SKN-1 in aging, as well as mediating lifespan extension through DR and reduced IIS signaling.

Nrf2 has not been shown to directly regulate aging in mammals but has been shown to be a potent regulator of the stress response and protect against cancer (330). Nrf2-null mice on CR still exhibit improved insulin sensitivity and lifespan extension but are more susceptible to cancer (396). Interestingly, Nrf2

steady-state levels have been shown to decrease with age in multiple human and rodent tissues (397-399). Nrf2 has also been shown to play a protective role in multiple age-related diseases, including Alzheimer's disease, Parkinson's disease, cardiovascular disease, emphysema, and macular degeneration (400). Nrf2 can be activated by a chemically diverse group of pharmacological agents (401), and clinical studies of Nrf2 activators have reported potent chemopreventive effects, suggesting that Nrf2-mediated regulation of XMEs may be a promising approach to prevent age-related disease, cancer, and possibly aging (402, 403).

1-8. Figures

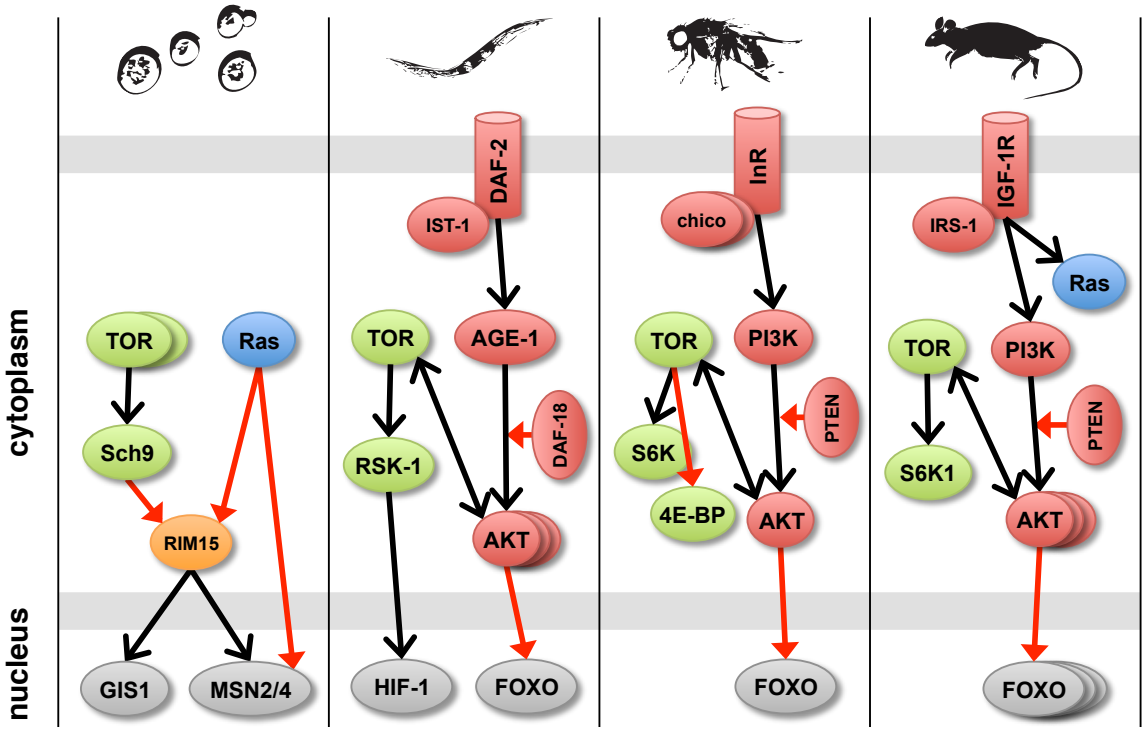

Figure 1-1. Nutrient signaling pathways associated with aging (404).

Insulin/IGF-1 and TOR signaling in four model organisms (from left): the yeast *S. cerevisiae*, the nematode worm *C. elegans*, the fruit fly *D. melanogaster*, and the mouse *M. musculus*. Ras is only indicated in yeast and mice, where manipulation of Ras signaling has been shown to extend lifespan. Black lines with arrowheads denote activating interactions and red lines with arrowheads denote inhibitory interactions.

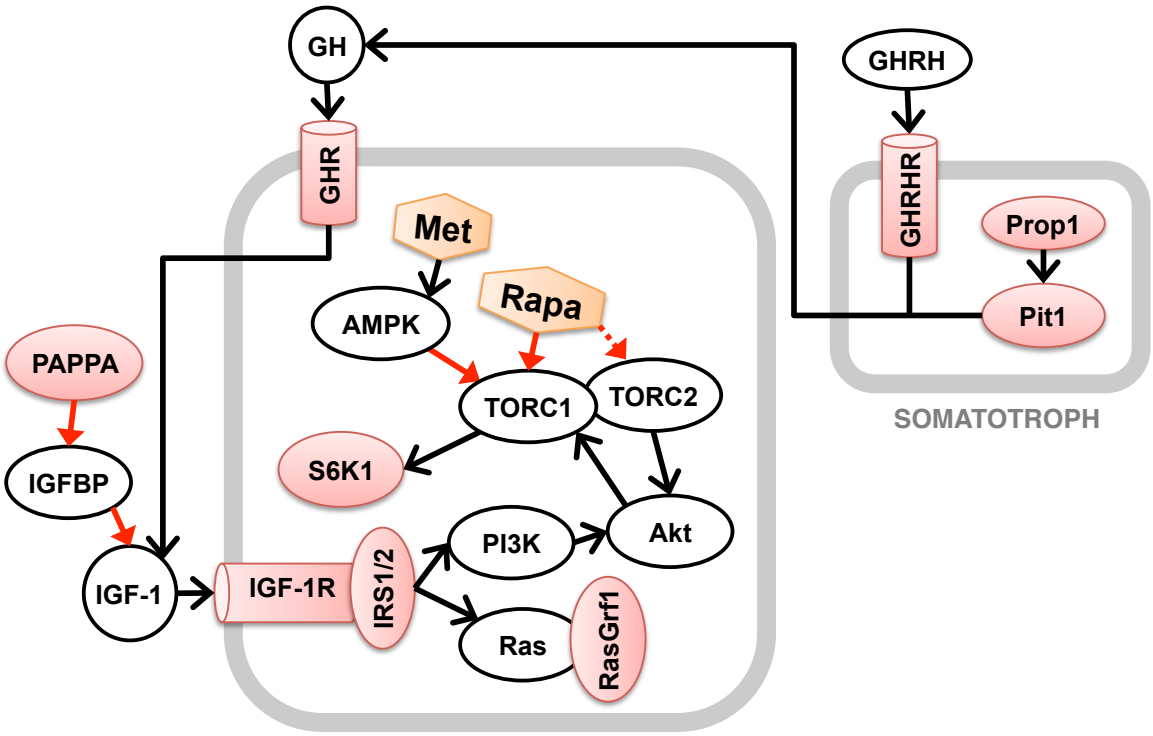

Figure 1-2. Components of GH, IGF-1, and TOR signal networks that affect longevity in mice.

Factors that have been shown to extend lifespan in transgenic mouse models are colored in red (GHR, GHRHR, IGF-1R, IRS1, IRS2, PAPPA, Pit1, Prop1, RasGrf1, S6K1). Pharmacological agents that have been shown to extend lifespan in mice are colored in orange (metformin, rapamycin). Black lines with arrowheads denote activating interactions and red lines with arrowheads denote inhibitory interactions.

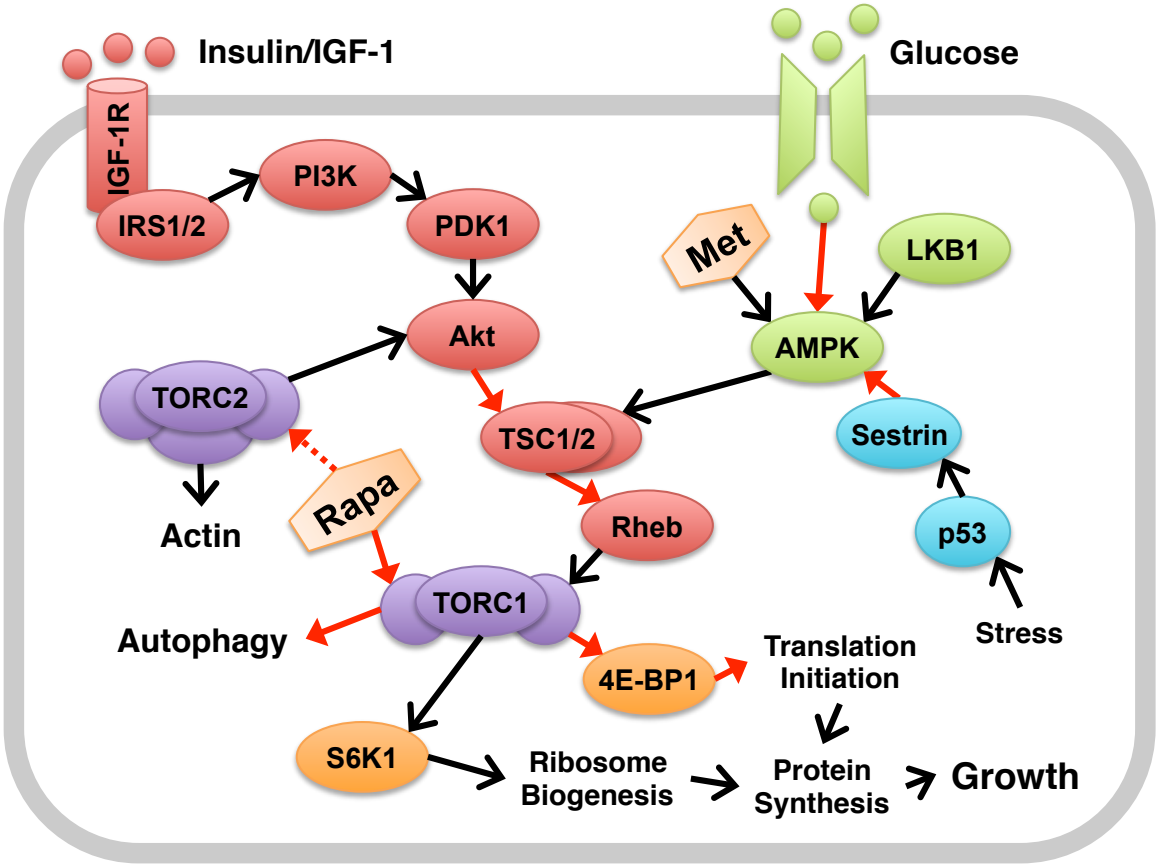

Figure 1-3. TOR signaling in mammals (185).

TOR acts as an intracellular rheostat of signals from growth factors (insulin, IGF-1), nutrients (glucose) and stress to regulate cell growth and autophagy through TORC1, and cellular morphology through TORC2. Black lines with arrowheads denote activating interactions and red lines with arrowheads denote inhibitory interactions.

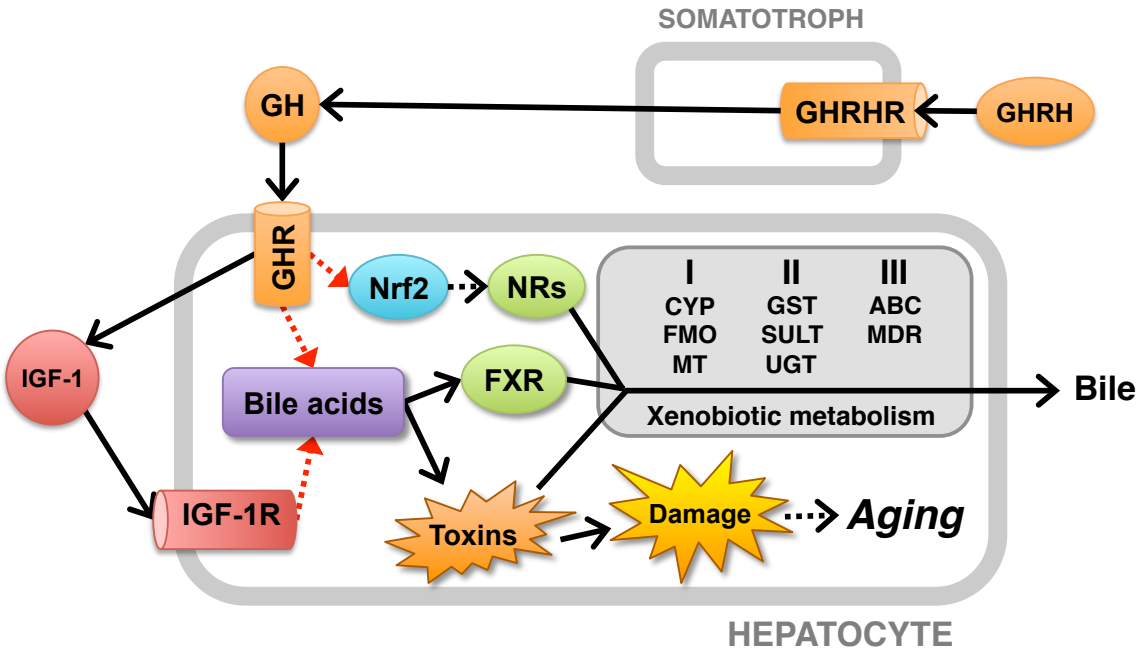

Figure 1-4. Model of hepatic xenobiotic metabolism regulation in GH/IGF-1-deficient dwarf mice (405).

GH and IGF-1 signaling are proposed to regulate bile acid levels and Nrf2 activation, which in turn influence nuclear receptor expression (PXR, CAR, AhR, FXR) and XME transcriptional activation (phase I-III). Solid black lines with arrowheads denote activating interactions and dashed red lines with arrowheads denote proposed but unconfirmed interactions.

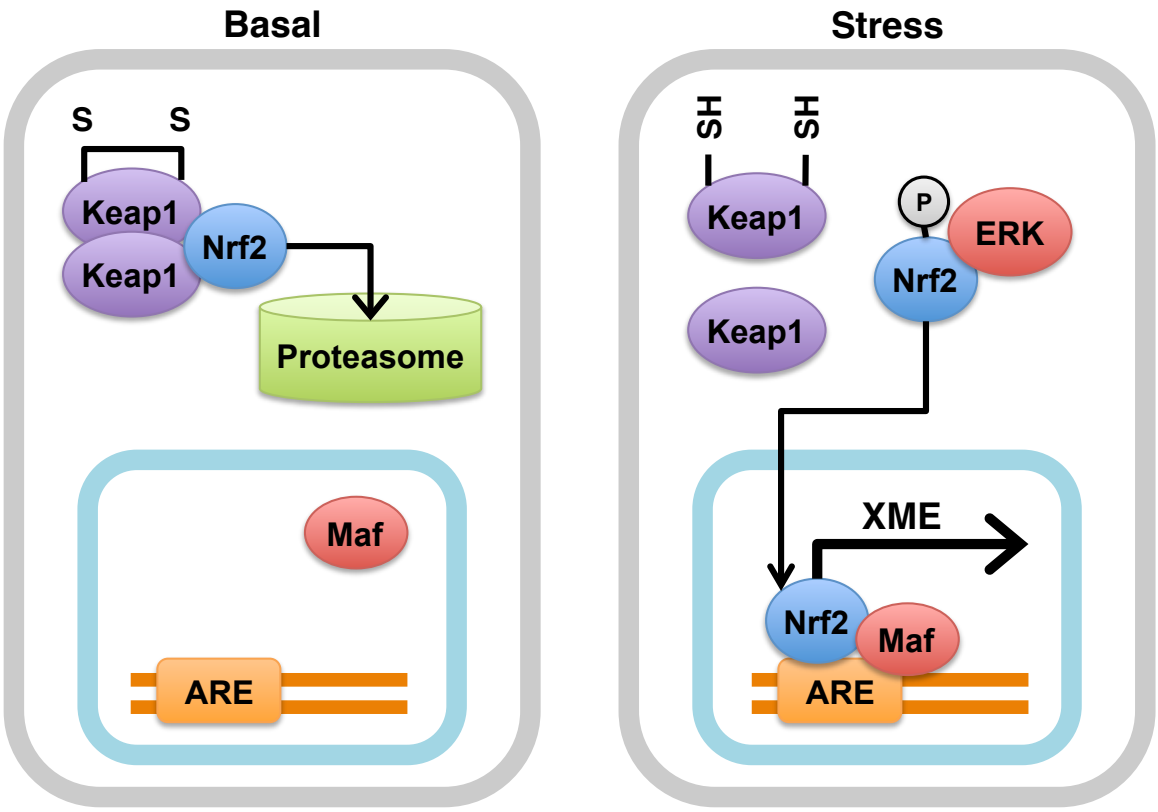

Figure 1-5. Nrf2 activation in response to stress in mammals.

Under basal conditions, Nrf2 is sequestered in the cytosol by interaction with dimeric Keap1. Keap1 serves as an adaptor for E3 ligase, which facilitates proteasomal degradation. In response to stress, cysteine residues on Keap1 are oxidized, resulting in a conformational change that releases Nrf2. Nrf2 has also been proposed to be activated via phosphorylation by ERK. Unbound Nrf2 translocates to the nucleus, where, in association with small Maf proteins, binds the ARE and induces transcription of XME gene expression.

1-9. Tables

	Ames	Snell	Little	GHRKO	PAPPA-KO
Gene	*Prop-1*	*Pit-1*	*Ghrhr*	*Ghr/bp*	*Pappa*
Lifespan (♂)	49%	> 40%	> 20%	> 35%	> 25%
Lifespan (♀)	68%	> 40%	> 25%	> 35%	> 25%
Strain	Heterogen.	*dw*/J x C3H/HeJ	C57BL/6J	129/Ola x BALB/c	C57BL/6J x 129SV/E
Body weight	⬇	⬇	⬇	⬇	⬇
Plasma GH	⬇	⬇	⬇	⬆	NC
Plasma IGF-1	⬇	⬇	⬇	⬇	NC
Insulin sensitivity	⬆	⬆	⬆	⬆	ND
Fibroblast stress resistance	⬆	⬆	ND	⬆	NC
In vivo stress resistance	⬆	⬆	ND	ND	ND

Table 1-1. Phenotypes of long-lived mice with altered GH/IGF-1 signaling.

1-10. References

1. Miller RA (1999) Kleemeier award lecture: are there genes for aging? *J Gerontol A Biol Sci Med Sci* 54:B297–307.

2. Finch CE (2007) *The Biology of Human Longevity* (Academic Press).

3. Finch CE (1994) *Longevity, Senescence, and the Genome* (University Of Chicago Press).

4. Medvedev ZA (1990) An attempt at a rational classification of theories of ageing. *Biol Rev Camb Philos Soc* 65:375–398.

5. Harman D (1956) Aging: a theory based on free radical and radiation chemistry. *J Gerontol* 11:298–300.

6. Harman D (2006) Free radical theory of aging: an update: increasing the functional life span. *Ann N Y Acad Sci* 1067:10–21.

7. Gruber J, Schaffer S, Halliwell B (2008) The mitochondrial free radical theory of ageing--where do we stand? *Front Biosci* 13:6554–6579.

8. Pérez VI et al. (2009) Is the oxidative stress theory of aging dead? *Biochim Biophys Acta* 1790:1005–1014.

9. Lapointe J, Hekimi S (2010) When a theory of aging ages badly. *Cell Mol Life Sci* 67:1–8.

10. Salmon AB, Richardson A, Pérez VI (2010) Update on the oxidative stress theory of aging: does oxidative stress play a role in aging or healthy aging? *Free Radic Biol Med* 48:642–655.

11. Van Raamsdonk JM, Hekimi S (2010) Reactive Oxygen Species and Aging in Caenorhabditis elegans: Causal or Casual Relationship? *Antioxid Redox Signal* 13:1911–1953.

12. Promislow DE (1994) DNA repair and the evolution of longevity: a critical analysis. *J Theor Biol* 170:291–300.

13. Lou Z, Chen J (2006) Cellular senescence and DNA repair. *Exp Cell Res* 312:2641–2646.

14. Sedelnikova OA et al. (2004) Senescing human cells and ageing mice accumulate DNA lesions with unrepairable double-strand breaks. *Nat Cell Biol* 6:168–170.

15. Tucker JD, Spruill MD, Ramsey MJ, Director AD, Nath J (1999) Frequency of spontaneous chromosome aberrations in mice: effects of age. *Mutat Res* 425:135–141.

16. Dempsey JL, Odagiri Y, Morley AA (1993) In vivo mutations at the H-2 locus in mouse lymphocytes. *Mutat Res* 285:45–51.

17. Collado M, Blasco MA, Serrano M (2007) Cellular senescence in cancer and aging. *Cell* 130:223–233.

18. Rando TA, Chang HY (2012) Aging, rejuvenation, and epigenetic reprogramming: resetting the aging clock. *Cell* 148:46–57.

19. Liu L, Rando TA (2011) in *Handbook of the Biology of Aging*, eds Masoro EJ, Austad SN (Academic Press), pp 141–161. 7th Ed. Available at: http://dx.doi.org/10.1016/B978-0-12-378638-8.00006-3.

20. Conboy IM, Conboy MJ, Smythe GM, Rando TA (2003) Notch-mediated restoration of regenerative potential to aged muscle. *Science* 302:1575–1577.

21. Dorshkind K, Montecino-Rodriguez E, Signer RAJ (2009) The ageing immune system: is it ever too old to become young again? *Nat Rev Immunol* 9:57–62.

22. Terman A, Brunk UT (2004) Aging as a catabolic malfunction. *Int J Biochem Cell Biol* 36:2365–2375.

23. Gems D, McElwee JJ (2005) Broad spectrum detoxification: the major longevity assurance process regulated by insulin/IGF-1 signaling? *Mech Ageing Dev* 126:381–387.

24. Swindell WR (2007) Genotype-by-age interaction and identification of longevity-associated genes from microarray data. *AGE* 29:97–102.

25. Kaushik S, Cuervo AM (2011) in *Handbook of the Biology of Aging*, eds Masoro EJ, Austad SN (Academic Press), pp 297–317. 7th Ed. Available at: http://dx.doi.org/10.1016/B978-0-12-378638-8.00013-0.

26. Ciechanover A (2005) Proteolysis: from the lysosome to ubiquitin and the proteasome. *Nat Rev Mol Cell Biol* 6:79–87.

27. Morimoto RI, Cuervo AM (2009) Protein homeostasis and aging: taking care of proteins from the cradle to the grave. *J Gerontol A Biol Sci Med Sci* 64:167–170.

28. Bukau B, Weissman J, Horwich A (2006) Molecular chaperones and protein quality control. *Cell* 125:443–451.

29. Liberek K, Lewandowska A, Zietkiewicz S (2008) Chaperones in control of protein disaggregation. *EMBO J* 27:328–335.

30. Lithgow GJ, White TM, Melov S, Johnson TE (1995) Thermotolerance and extended life-span conferred by single-gene mutations and induced by thermal stress. *Proc Natl Acad Sci USA* 92:7540–7544.

31. Tatar M, Khazaeli AA, Curtsinger JW (1997) Chaperoning extended life. *Nature* 390:30.

32. Shama S, Lai CY, Antoniazzi JM, Jiang JC, Jazwinski SM (1998) Heat stress-induced life span extension in yeast. *Exp Cell Res* 245:379–388.

33. Kurapati R, Passananti HB, Rose MR, Tower J (2000) Increased hsp22 RNA levels in Drosophila lines genetically selected for increased longevity. *J Gerontol A Biol Sci Med Sci* 55:B552–9.

34. Hsu A-L, Murphy CT, Kenyon C (2003) Regulation of aging and age-related disease by DAF-16 and heat-shock factor. *Science* 300:1142–1145.

35. Söti C, Csermely P (2007) Protein stress and stress proteins: implications in aging and disease. *J Biosci* 32:511–515.

36. Cao SX, Dhahbi JM, Mote PL, Spindler SR (2001) Genomic profiling of short- and long-term caloric restriction effects in the liver of aging mice. *Proc Natl Acad Sci USA* 98:10630–10635.

37. Weindruch R, Kayo T, Lee CK, Prolla TA (2001) Microarray profiling of gene expression in aging and its alteration by caloric restriction in mice. *J Nutr* 131:918S–923S.

38. Yorimitsu T, Nair U, Yang Z, Klionsky DJ (2006) Endoplasmic reticulum stress triggers autophagy. *J Biol Chem* 281:30299–30304.

39. Conconi M, Szweda LI, Levine RL, Stadtman ER, Friguet B (1996) Age-related decline of rat liver multicatalytic proteinase activity and protection from oxidative inactivation by heat-shock protein 90. *Arch Biochem Biophys* 331:232–240.

40. Shibatani T, Nazir M, Ward WF (1996) Alteration of rat liver 20S proteasome activities by age and food restriction. *J Gerontol A Biol Sci Med Sci* 51:B316–22.

41. Bulteau AL, Petropoulos I, Friguet B (2000) Age-related alterations of proteasome structure and function in aging epidermis. *Exp Gerontol* 35:767–777.

42. Keller JN, Huang FF, Markesbery WR (2000) Decreased levels of proteasome activity and proteasome expression in aging spinal cord. *Neuroscience* 98:149–156.

43. Petropoulos I et al. (2000) Increase of oxidatively modified protein is associated with a decrease of proteasome activity and content in aging epidermal cells. *J Gerontol A Biol Sci Med Sci* 55:B220–7.

44. Lee CK, Klopp RG, Weindruch R, Prolla TA (1999) Gene expression profile of aging and its retardation by caloric restriction. *Science* 285:1390–1393.

45. Zhang L, Li F, Dimayuga E, Craddock J, Keller JN (2007) Effects of aging and dietary restriction on ubiquitination, sumoylation, and the proteasome in the spleen. *FEBS Lett* 581:5543–5547.

46. Hepple RT, Qin M, Nakamoto H, Goto S (2008) Caloric restriction optimizes the proteasome pathway with aging in rat plantaris muscle: implications for sarcopenia. *Am J Physiol Regul Integr Comp Physiol* 295:R1231–7.

47. Dasuri K et al. (2009) Aging and dietary restriction alter proteasome biogenesis and composition in the brain and liver. *Mech Ageing Dev* 130:777–783.

48. Mizushima N, Levine B, Cuervo AM, Klionsky DJ (2008) Autophagy fights disease through cellular self-digestion. *Nature* 451:1069–1075.

49. He C, Klionsky DJ (2009) Regulation mechanisms and signaling pathways of autophagy. *Annu Rev Genet* 43:67–93.

50. Meléndez A et al. (2003) Autophagy genes are essential for dauer development and life-span extension in C. elegans. *Science* 301:1387–1391.

51. Hars ES et al. (2007) Autophagy regulates ageing in C. elegans. *Autophagy* 3:93–95.

52. Hansen M et al. (2008) A role for autophagy in the extension of lifespan by dietary restriction in C. elegans. *PLoS Genet* 4:e24.

53. Jia K, Levine B (2007) Autophagy is required for dietary restriction-mediated life span extension in C. elegans. *Autophagy* 3:597–599.

54. Tóth ML et al. (2008) Longevity pathways converge on autophagy genes to regulate life span in Caenorhabditis elegans. *Autophagy* 4:330–338.

55. Cuervo AM et al. (2005) Autophagy and aging: the importance of maintaining “clean” cells. *Autophagy* 1:131–140.

56. McCay CM, Crowell MF, Maynard LA (1935) The effect of retarded growth upon the length of life span and upon the ultimate body size. *Nutrition* 10:63–70.

57. McCay CM, Maynard LA, Sperling G, Barnes LL (1939) Retarded growth, life span, ultimate body size, and age changes in the albino rat after feeding diets restricted in calories. *J Nutr* 18:1–13.

58. Weindruch R, Walford RL (1982) Dietary restriction in mice beginning at 1 year of age: effect on life-span and spontaneous cancer incidence. *Science* 215:1415–1418.

59. Yu BP, Masoro EJ, McMahan CA (1985) Nutritional influences on aging of Fischer 344 rats: I. Physical, metabolic, and longevity characteristics. *J Gerontol* 40:657–670.

60. Masoro EJ (2010) in *Calorie Restriction, Aging and Longevity*, eds Everitt AV, Rattan SIS, Couteur D, de Cabo R (Springer), pp 3–14.

61. Flurkey K, Astle CM, Harrison DE (2010) Life extension by diet restriction and N-acetyl-L-cysteine in genetically heterogeneous mice. *J Gerontol A Biol Sci Med Sci* 65:1275–1284.

62. Weindruch R, Walford RL (1988) *The Retardation of Aging and Disease by Dietary Restriction* (Charles C Thomas, Springfield, IL).

63. Sohal RS, Weindruch R (1996) Oxidative Stress, Caloric Restriction, and Aging. *Science* 273:59–63.

64. Yu BP (1996) Aging and oxidative stress: modulation by dietary restriction. *Free Radic Biol Med* 21:651–668.

65. Masoro EJ, McCarter RJ, Katz MS, McMahan CA (1992) Dietary restriction alters characteristics of glucose fuel use. *J Gerontol* 47:B202–8.

66. Dhahbi JM et al. (2001) Caloric restriction alters the feeding response of key metabolic enzyme genes. *Mech Ageing Dev* 122:1033–1048.

67. Bonkowski MS, Rocha JS, Masternak MM, Al-Regaiey KA, Bartke A (2006) Targeted disruption of growth hormone receptor interferes with the beneficial actions of calorie restriction. *Proc Natl Acad Sci USA* 103:7901–7905.

68. de Cabo R et al. (2003) An in vitro model of caloric restriction. *Exp Gerontol* 38:631–639.

69. Harper JM et al. (2006) Stress resistance and aging: influence of genes and nutrition. *Mech Ageing Dev* 127:687–694.

70. Yu BP, Chung HY (2001) Stress resistance by caloric restriction for longevity. *Ann N Y Acad Sci* 928:39–47.

71. Liang H et al. (2003) Genetic mouse models of extended lifespan. *Exp Gerontol* 38:1353–1364.

72. Yu BP, Masoro EJ, Murata I, Bertrand HA, Lynd FT (1982) Life span study of SPF Fischer 344 male rats fed ad libitum or restricted diets: longevity, growth, lean body mass and disease. *J Gerontol* 37:130–141.

73. Iwasaki K et al. (1988) Influence of the restriction of individual dietary components on longevity and age-related disease of Fischer rats: the fat component and the mineral component. *J Gerontol* 43:B13–21.

74. Masoro EJ et al. (1989) Dietary modulation of the progression of nephropathy in aging rats: an evaluation of the importance of protein. *Am J Clin Nutr* 49:1217–1227.

75. Birchenall-Sparks MC, Roberts MS, Rutherford MS, Richardson A (1985) The effect of aging on the structure and function of liver messenger RNA. *Mech Ageing Dev* 32:99–111.

76. Swindell WR (2008) Genes regulated by caloric restriction have unique roles within transcriptional networks. *Mech Ageing Dev* 129:580–592.

77. Swindell WR (2008) Comparative analysis of microarray data identifies common responses to caloric restriction among mouse tissues. *Mech Ageing Dev* 129:138–153.

78. Orentreich N, Matias JR, DeFelice A, Zimmerman JA (1993) Low methionine ingestion by rats extends life span. *J Nutr* 123:269–274.

79. Richie JP et al. (1994) Methionine restriction increases blood glutathione and longevity in F344 rats. *FASEB J* 8:1302–1307.

80. Sun L, Sadighi Akha AA, Miller RA, Harper JM (2009) Life-span extension in mice by preweaning food restriction and by methionine restriction in middle age. *J Gerontol A Biol Sci Med Sci* 64:711–722.

81. Miller RA et al. (2005) Methionine-deficient diet extends mouse lifespan, slows immune and lens aging, alters glucose, T4, IGF-I and insulin levels, and increases hepatocyte MIF levels and stress resistance. *Aging Cell* 4:119–125.

82. Tissenbaum HA, Guarente LP (2002) Model organisms as a guide to mammalian aging. *Dev Cell* 2:9–19.

83. Antebi A (2007) Genetics of aging in Caenorhabditis elegans. *PLoS Genet* 3:1565–1571.

84. Bishop NA, Guarente LP (2007) Genetic links between diet and lifespan: shared mechanisms from yeast to humans. *Nat Rev Genet* 8:835–844.

85. Vermeulen CJ, Loeschcke V (2007) Longevity and the stress response in Drosophila. *Exp Gerontol* 42:153–159.

86. Kenyon C (2005) The plasticity of aging: insights from long-lived mutants. *Cell* 120:449–460.

87. Wolff S, Dillin A (2006) The trifecta of aging in Caenorhabditis elegans. *Exp Gerontol* 41:894–903.

88. Braeckman BP, Vanfleteren JR (2007) Genetic control of longevity in C. elegans. *Exp Gerontol* 42:90–98.

89. Klass MR (1983) A method for the isolation of longevity mutants in the nematode Caenorhabditis elegans and initial results. *Mech Ageing Dev* 22:279–286.

90. Friedman DB, Johnson TE (1988) A mutation in the age-1 gene in Caenorhabditis elegans lengthens life and reduces hermaphrodite fertility. *Genetics* 118:75–86.

91. Morris JZ, Tissenbaum HA, Ruvkun G (1996) A phosphatidylinositol-3-OH kinase family member regulating longevity and diapause in Caenorhabditis elegans. *Nature* 382:536–539.

92. Kenyon C, Chang J, Gensch E, Rudner A, Tabtiang R (1993) A C. elegans mutant that lives twice as long as wild type. *Nature* 366:461–464.

93. Kimura KD, Tissenbaum HA, Liu Y, Ruvkun G (1997) daf-2, an insulin receptor-like gene that regulates longevity and diapause in Caenorhabditis elegans. *Science* 277:942–946.

94. Lin K, Dorman JB, Rodan A, Kenyon C (1997) daf-16: An HNF-3/forkhead family member that can function to double the life-span of Caenorhabditis elegans. *Science* 278:1319–1322.

95. Ogg S et al. (1997) The Fork head transcription factor DAF-16 transduces insulin-like metabolic and longevity signals in C. elegans. *Nature* 389:994–999.

96. Yu H, Larsen PL (2001) DAF-16-dependent and independent expression targets of DAF-2 insulin receptor-like pathway in Caenorhabditis elegans include FKBPs. *J Mol Biol* 314:1017–1028.

97. Lee SS, Kennedy S, Tolonen AC, Ruvkun G (2003) DAF-16 target genes that control C. elegans life-span and metabolism. *Science* 300:644–647.

98. Murphy CT et al. (2003) Genes that act downstream of DAF-16 to influence the lifespan of Caenorhabditis elegans. *Nature* 424:277–283.

99. McElwee J, Bubb K, Thomas JH (2003) Transcriptional outputs of the Caenorhabditis elegans forkhead protein DAF-16. *Aging Cell* 2:111–121.

100. McCarroll SA et al. (2004) Comparing genomic expression patterns across species identifies shared transcriptional profile in aging. *Nat Genet* 36:197–204.

101. Berdichevsky A, Viswanathan M, Horvitz HR, Guarente L (2006) C. elegans SIR-2.1 interacts with 14-3-3 proteins to activate DAF-16 and extend life span. *Cell* 125:1165–1177.

102. Tran H, Brunet A, Griffith EC, Greenberg ME (2003) The many forks in FOXO's road. *Sci STKE* 2003:RE5.

103. Greer EL, Brunet A (2005) FOXO transcription factors at the interface between longevity and tumor suppression. *Oncogene* 24:7410–7425.

104. Kops GJPL et al. (2002) Forkhead transcription factor FOXO3a protects quiescent cells from oxidative stress. *Nature* 419:316–321.

105. Aigaki T, Seong K-H, Matsuo T (2002) Longevity determination genes in Drosophila melanogaster. *Mech Ageing Dev* 123:1531–1541.

106. Lin YJ, Seroude L, Benzer S (1998) Extended life-span and stress resistance in the Drosophila mutant methuselah. *Science* 282:943–946.

107. Rogina B, Reenan RA, Nilsen SP, Helfand SL (2000) Extended life-span conferred by cotransporter gene mutations in Drosophila. *Science* 290:2137–2140.

108. Clancy DJ et al. (2001) Extension of life-span by loss of CHICO, a Drosophila insulin receptor substrate protein. *Science* 292:104–106.

109. Tatar M et al. (2001) A mutant Drosophila insulin receptor homolog that extends life-span and impairs neuroendocrine function. *Science* 292:107–110.

110. Orr WC, Sohal RS (1994) Extension of life-span by overexpression of superoxide dismutase and catalase in Drosophila melanogaster. *Science* 263:1128–1130.

111. Sun J, Tower J (1999) FLP recombinase-mediated induction of Cu/Zn-superoxide dismutase transgene expression can extend the life span of adult Drosophila melanogaster flies. *Mol Cell Biol* 19:216–228.

112. Parkes TL et al. (1998) Extension of Drosophila lifespan by overexpression of human SOD1 in motorneurons. *Nat Genet* 19:171–174.

113. Fabrizio P et al. (2003) SOD2 functions downstream of Sch9 to extend longevity in yeast. *Genetics* 163:35–46.

114. Barbieri M, Bonafè M, Franceschi C, Paolisso G (2003) Insulin/IGF-I-signaling pathway: an evolutionarily conserved mechanism of longevity from yeast to humans. *Am J Physiol Endocrinol Metab* 285:E1064–71.

115. Tatar M, Bartke A, Antebi A (2003) The endocrine regulation of aging by insulin-like signals. *Science* 299:1346–1351.

116. Larsen PL (1993) Aging and resistance to oxidative damage in Caenorhabditis elegans. *Proc Natl Acad Sci USA* 90:8905–8909.

117. Murakami S, Johnson TE (1996) A genetic pathway conferring life extension and resistance to UV stress in Caenorhabditis elegans. *Genetics* 143:1207–1218.

118. Barsyte D, Lovejoy DA, Lithgow GJ (2001) Longevity and heavy metal resistance in daf-2 and age-1 long-lived mutants of Caenorhabditis elegans. *FASEB J* 15:627–634.

119. Rose MR, Vu LN, Park SU, Graves JL (1992) Selection on stress resistance increases longevity in Drosophila melanogaster. *Exp Gerontol* 27:241–250.

120. Bartke A (2011) Pleiotropic effects of growth hormone signaling in aging. *Trends Endocrinol Metab* 22:437–442.

121. Holzenberger M et al. (2003) IGF-1 receptor regulates lifespan and resistance to oxidative stress in mice. *Nature* 421:182–187.

122. Murakami S, Salmon A, Miller RA (2003) Multiplex stress resistance in cells from long-lived dwarf mice. *FASEB J* 17:1565–1566.

123. Salmon AB et al. (2005) Fibroblast cell lines from young adult mice of long-lived mutant strains are resistant to multiple forms of stress. *Am J Physiol Endocrinol Metab* 289:E23–9.

124. Bartke A (2008) Impact of reduced insulin-like growth factor-1/insulin signaling on aging in mammals: novel findings. *Aging Cell* 7:285–290.

125. Salmon AB, Sadighi Akha AA, Buffenstein R, Miller RA (2008) Fibroblasts from naked mole-rats are resistant to multiple forms of cell injury, but sensitive to peroxide, ultraviolet light, and endoplasmic reticulum stress. *J Gerontol A Biol Sci Med Sci* 63:232–241.

126. Bokov AF, Lindsey ML, Khodr C, Sabia MR, Richardson A (2009) Long-lived ames dwarf mice are resistant to chemical stressors. *J Gerontol A Biol Sci Med Sci* 64:819–827.

127. Johnson TE, Lithgow GJ, Murakami S (1996) Hypothesis: interventions that increase the response to stress offer the potential for effective life prolongation and increased health. *J Gerontol A Biol Sci Med Sci* 51:B392–5.

128. Brown-Borg HM (2006) Longevity in mice: is stress resistance a common factor? *AGE* 28:145–162.

129. Snell GD (1929) Dwarf, a new recessive character of the house mouse. *Proc Natl Acad Sci USA* 15:733–734.

130. Smith PE, MacDowell EC (1931) The differential effect of hereditary mouse dwarfism on the anterior pituitary hormones. *Anat Rec* 50:85–93.

131. Flurkey K, Papaconstantinou J, Miller RA, Harrison DE (2001) Lifespan extension and delayed immune and collagen aging in mutant mice with defects in growth hormone production. *Proc Natl Acad Sci USA* 98:6736–6741.

132. Flurkey K, Papaconstantinou J, Harrison DE (2002) The Snell dwarf mutation Pit1(dw) can increase life span in mice. *Mech Ageing Dev* 123:121–130.

133. Schaible R, Gowen JW (1961) A new dwarf mouse. *Genetics* 46:896.

134. Chandrashekar V, Bartke A (1993) Induction of endogenous insulin-like growth factor-I secretion alters the hypothalamic-pituitary-testicular function in growth hormone-deficient adult dwarf mice. *Biol Reprod* 48:544–551.

135. Brown-Borg HM, Borg KE, Meliska CJ, Bartke A (1996) Dwarf mice and the ageing process. *Nature* 384:33.

136. Sornson MW et al. (1996) Pituitary lineage determination by the Prophet of Pit-1 homeodomain factor defective in Ames dwarfism. *Nature* 384:327–333.

137. Bartke A et al. (2001) Extending the lifespan of long-lived mice. *Nature* 414:412.

138. Bartke A et al. (2001) Prolonged longevity of hypopituitary dwarf mice. *Exp Gerontol* 36:21–28.

139. Madsen MA et al. (2004) Altered oxidative stress response of the long-lived Snell dwarf mouse. *Biochem Biophys Res Commun* 318:998–1005.

140. Amador-Noguez D et al. (2007) Alterations in xenobiotic metabolism in the long-lived Little mice. *Aging Cell* 6:453–470.

141. Murakami S (2006) Stress resistance in long-lived mouse models. *Exp Gerontol* 41:1014–1019.

142. Leiser SF, Salmon AB, Miller RA (2006) Correlated resistance to glucose deprivation and cytotoxic agents in fibroblast cell lines from long-lived pituitary dwarf mice. *Mech Ageing Dev* 127:821–829.

143. Maynard SP, Miller RA (2006) Fibroblasts from long-lived Snell dwarf mice are resistant to oxygen-induced in vitro growth arrest. *Aging Cell* 5:89–96.

144. Salmon AB, Ljungman M, Miller RA (2008) Cells from long-lived mutant mice exhibit enhanced repair of ultraviolet lesions. *J Gerontol A Biol Sci Med Sci* 63:219–231.

145. Panici JA et al. (2010) Early life growth hormone treatment shortens longevity and decreases cellular stress resistance in long-lived mutant mice. *FASEB J* 24:5073–5079.

146. Brown-Borg HM, Rakoczy SG (2000) Catalase expression in delayed and premature aging mouse models. *Exp Gerontol* 35:199–212.

147. Brown-Borg HM, Rakoczy SG, Romanick MA, Kennedy MA (2002) Effects of growth hormone and insulin-like growth factor-1 on hepatocyte antioxidative enzymes. *Exp Biol Med (Maywood)* 227:94–104.

148. Coschigano KT, Clemmons D, Bellush LL, Kopchick JJ (2000) Assessment of growth parameters and life span of GHR/BP gene-disrupted mice. *Endocrinology* 141:2608–2613.

149. Coschigano KT et al. (2003) Deletion, but not antagonism, of the mouse growth hormone receptor results in severely decreased body weights, insulin, and insulin-like growth factor I levels and increased life span. *Endocrinology* 144:3799–3810.

150. Godfrey P et al. (1993) GHRH receptor of little mice contains a missense mutation in the extracellular domain that disrupts receptor function. *Nat Genet* 4:227–232.

151. Bokov AF et al. (2011) Does Reduced IGF-1R Signaling in Igf1r Mice Alter Aging? *PLoS ONE* 6:e26891.

152. Blüher M, Kahn BB, Kahn CR (2003) Extended longevity in mice lacking the insulin receptor in adipose tissue. *Science* 299:572–574.

153. Selman C et al. (2008) Evidence for lifespan extension and delayed age-related biomarkers in insulin receptor substrate 1 null mice. *FASEB J* 22:807–818.

154. Taguchi A, Wartschow LM, White MF (2007) Brain IRS2 signaling coordinates life span and nutrient homeostasis. *Science* 317:369–372.

155. Boldt HB, Conover CA (2007) Pregnancy-associated plasma protein-A (PAPP-A): a local regulator of IGF bioavailability through cleavage of IGFBPs. *Growth Horm IGF Res* 17:10–18.

156. Conover CA, Bale LK (2007) Loss of pregnancy-associated plasma protein A extends lifespan in mice. *Aging Cell* 6:727–729.

157. Fingar DC, Blenis J (2004) Target of rapamycin (TOR): an integrator of nutrient and growth factor signals and coordinator of cell growth and cell cycle progression. *Oncogene* 23:3151–3171.

158. Kapahi P, Kockel L (2011) in *Handbook of the Biology of Aging*, eds Masoro EJ, Austad SN (Academic Press), pp 203–214. 7th Ed. Available at: http://dx.doi.org/10.1016/B978-0-12-378638-8.00009-9.

159. Sehgal SN (2003) Sirolimus: its discovery, biological properties, and mechanism of action. *Transplant Proc* 35:7S–14S.

160. Harding MW, Galat A, Uehling DE, Schreiber SL (1989) A receptor for the immunosuppressant FK506 is a cis-trans peptidyl-prolyl isomerase. *Nature* 341:758–760.

161. Siekierka JJ, Hung SH, Poe M, Lin CS, Sigal NH (1989) A cytosolic binding protein for the immunosuppressant FK506 has peptidyl-prolyl isomerase activity but is distinct from cyclophilin. *Nature* 341:755–757.

162. Heitman J, Movva NR, Hall MN (1991) Targets for cell cycle arrest by the immunosuppressant rapamycin in yeast. *Science* 253:905–909.

163. Cafferkey R et al. (1993) Dominant missense mutations in a novel yeast protein related to mammalian phosphatidylinositol 3-kinase and VPS34 abrogate rapamycin cytotoxicity. *Mol Cell Biol* 13:6012–6023.

164. Powers RW, Kaeberlein M, Caldwell SD, Kennedy BK, Fields S (2006) Extension of chronological life span in yeast by decreased TOR pathway signaling. *Genes Dev* 20:174–184.

165. Wei M et al. (2008) Life span extension by calorie restriction depends on Rim15 and transcription factors downstream of Ras/PKA, Tor, and Sch9. *PLoS Genet* 4:e13.

166. Loewith R et al. (2002) Two TOR complexes, only one of which is rapamycin sensitive, have distinct roles in cell growth control. *Mol Cell* 10:457–468.

167. Jacinto E et al. (2004) Mammalian TOR complex 2 controls the actin cytoskeleton and is rapamycin insensitive. *Nat Cell Biol* 6:1122–1128.

168. Long X et al. (2002) TOR deficiency in C. elegans causes developmental arrest and intestinal atrophy by inhibition of mRNA translation. *Curr Biol* 12:1448–1461.

169. Oldham S, Montagne J, Radimerski T, Thomas G, Hafen E (2000) Genetic and biochemical characterization of dTOR, the Drosophila homolog of the target of rapamycin. *Genes Dev* 14:2689–2694.

170. Zhang H, Stallock JP, Ng JC, Reinhard C, Neufeld TP (2000) Regulation of cellular growth by the Drosophila target of rapamycin dTOR. *Genes Dev* 14:2712–2724.

171. Brown EJ et al. (1994) A mammalian protein targeted by G1-arresting rapamycin-receptor complex. *Nature* 369:756–758.

172. Chen Y et al. (1994) A putative sirolimus (rapamycin) effector protein. *Biochem Biophys Res Commun* 203:1–7.

173. Chiu MI, Katz H, Berlin V (1994) RAPT1, a mammalian homolog of yeast Tor, interacts with the FKBP12/rapamycin complex. *Proc Natl Acad Sci USA* 91:12574–12578.

174. Sabers CJ et al. (1995) Isolation of a protein target of the FKBP12-rapamycin complex in mammalian cells. *J Biol Chem* 270:815–822.

175. Sabatini DM, Pierchala BA, Barrow RK, Schell MJ, Snyder SH (1995) The rapamycin and FKBP12 target (RAFT) displays phosphatidylinositol 4-kinase activity. *J Biol Chem* 270:20875–20878.

176. Hentges KE et al. (2001) FRAP/mTOR is required for proliferation and patterning during embryonic development in the mouse. *Proc Natl Acad Sci USA* 98:13796–13801.

177. Kapahi P et al. (2004) Regulation of lifespan in Drosophila by modulation of genes in the TOR signaling pathway. *Curr Biol* 14:885–890.

178. Vellai T et al. (2003) Genetics: influence of TOR kinase on lifespan in C. elegans. *Nature* 426:620.

179. Marygold SJ, Leevers SJ (2002) Growth signaling: TSC takes its place. *Curr Biol* 12:R785–7.

180. Shamji AF, Nghiem P, Schreiber SL (2003) Integration of growth factor and nutrient signaling: implications for cancer biology. *Mol Cell* 12:271–280.

181. Ma XM, Blenis J (2009) Molecular mechanisms of mTOR-mediated translational control. *Nat Rev Mol Cell Biol* 10:307–318.

182. Sharp ZD, Bartke A (2005) Evidence for down-regulation of phosphoinositide 3-kinase/Akt/mammalian target of rapamycin

(PI3K/Akt/mTOR)-dependent translation regulatory signaling pathways in Ames dwarf mice. *J Gerontol A Biol Sci Med Sci* 60:293–300.

183. Selman C et al. (2009) Ribosomal protein S6 kinase 1 signaling regulates mammalian life span. *Science* 326:140–144.

184. Um SH et al. (2004) Absence of S6K1 protects against age- and diet-induced obesity while enhancing insulin sensitivity. *Nature* 431:200–205.

185. Tsang CK, Qi H, Liu LF, Zheng XFS (2007) Targeting mammalian target of rapamycin (mTOR) for health and diseases. *Drug Discov Today* 12:112–124.

186. Chen C, Liu Y, Liu Y, Zheng P (2009) mTOR regulation and therapeutic rejuvenation of aging hematopoietic stem cells. *Sci Signal* 2:ra75.

187. Harrison DE et al. (2009) Rapamycin fed late in life extends lifespan in genetically heterogeneous mice. *Nature* 460:392–395.

188. Miller RA et al. (2011) Rapamycin, but not resveratrol or simvastatin, extends life span of genetically heterogeneous mice. *J Gerontol A Biol Sci Med Sci* 66:191–201.

189. Anisimov VN et al. (2011) Rapamycin increases lifespan and inhibits spontaneous tumorigenesis in inbred female mice. *Cell Cycle* 10:4230–4236.

190. Miller RA et al. (2007) An Aging Interventions Testing Program: study design and interim report. *Aging Cell* 6:565–575.

191. Inoki K, Zhu T, Guan K-L (2003) TSC2 mediates cellular energy response to control cell growth and survival. *Cell* 115:577–590.

192. Gwinn DM et al. (2008) AMPK phosphorylation of raptor mediates a metabolic checkpoint. *Mol Cell* 30:214–226.

193. Budanov AV, Karin M (2008) p53 target genes sestrin1 and sestrin2 connect genotoxic stress and mTOR signaling. *Cell* 134:451–460.

194. Anisimov VN et al. (2005) Effect of metformin on life span and on the development of spontaneous mammary tumors in HER-2/neu transgenic mice. *Exp Gerontol* 40:685–693.

195. Anisimov VN et al. (2008) Metformin slows down aging and extends life span of female SHR mice. *Cell Cycle* 7:2769–2773.

196. Smith DL et al. (2010) Metformin supplementation and life span in Fischer-344 rats. *J Gerontol A Biol Sci Med Sci* 65:468–474.

197. Sun J, Kale SP, Childress AM, Pinswasdi C, Jazwinski SM (1994) Divergent roles of RAS1 and RAS2 in yeast longevity. *J Biol Chem* 269:18638–18645.

198. Fabrizio P, Pozza F, Pletcher SD, Gendron CM, Longo VD (2001) Regulation of longevity and stress resistance by Sch9 in yeast. *Science* 292:288–290.

199. Mirisola MG, Longo VD (2011) Conserved role of Ras-GEFs in promoting aging: from yeast to mice. *AGING* 3:340–343.

200. Borrás C et al. (2011) RasGrf1 deficiency delays aging in mice. *AGING* 3:262–276.

201. Ratajczak MZ et al. (2011) RasGrf1: genomic imprinting, VSELs, and aging. *AGING* 3:692–697.

202. Chang L, Karin M (2001) Mammalian MAP kinase signalling cascades. *Nature* 410:37–40.

203. Junttila MR, Li S-P, Westermarck J (2008) Phosphatase-mediated crosstalk between MAPK signaling pathways in the regulation of cell survival. *FASEB J* 22:954–965.

204. Roux PP, Blenis J (2004) ERK and p38 MAPK-activated protein kinases: a family of protein kinases with diverse biological functions. *Microbiol Mol Biol Rev* 68:320–344.

205. Murphy LO, Blenis J (2006) MAPK signal specificity: the right place at the right time. *Trends Biochem Sci* 31:268–275.

206. Shaul YD, Seger R (2007) The MEK/ERK cascade: from signaling specificity to diverse functions. *Biochim Biophys Acta* 1773:1213–1226.

207. Kolch W (2005) Coordinating ERK/MAPK signalling through scaffolds and inhibitors. *Nat Rev Mol Cell Biol* 6:827–837.

208. Lin JH, Lu AY (1998) Inhibition and induction of cytochrome P450 and the clinical implications. *Clin Pharmacokinet* 35:361–390.

209. Guengerich FP (2008) Cytochrome p450 and chemical toxicology. *Chem Res Toxicol* 21:70–83.

210. Mueller GC, Miller JA (1948) The metabolism of 4-dimethylaminoazobenzene by rat liver homogenates. *J Biol Chem* 176:535–544.

211. Imai Y, Sato R (1974) A gel-electrophoretically homogeneous preparation of cytochrome P-450 from liver microsomes of phenobarbital-pretreated rabbits. *Biochem Biophys Res Commun* 60:8–14.

212. Haugen DA, van der Hoeven TA, Coon MJ (1975) Purified liver microsomal cytochrome P-450. Separation and characterization of multiple forms. *J Biol Chem* 250:3567–3570.

213. Nelson DR et al. (2004) Comparison of cytochrome P450 (CYP) genes from the mouse and human genomes, including nomenclature recommendations for genes, pseudogenes and alternative-splice variants. *Pharmacogenetics* 14:1–18.

214. Nelson DR (1999) Cytochrome P450 and the individuality of species. *Arch Biochem Biophys* 369:1–10.

215. Gilbert LI ed. (2011) *Insect Molecular Biology and Biochemistry* (Academic Press).

216. Stupans I, Ikeda T, Kessler DJ, Nebert DW (1984) Characterization of a cDNA clone for mouse phenobarbital-inducible cytochrome P-450b. *DNA* 3:129–137.

217. Nemoto N, Sakurai J (1995) Glucocorticoid and sex hormones as activating or modulating factors for expression of Cyp2b-9 and Cyp2b-10 in the mouse liver and hepatocytes. *Arch Biochem Biophys* 319:286–292.

218. Damon M, Fautrel A, Guillouzo A, Corcos L (1996) Genetic analysis of the phenobarbital regulation of the cytochrome P-450 2b-9 and aldehyde dehydrogenase type 2 mRNAs in mouse liver. *Biochem J* 317 (Pt 2):481–486.

219. Shapiro BH, Pampori NA, Lapenson DP, Waxman DJ (1994) Growth hormone-dependent and -independent sexually dimorphic regulation of phenobarbital-induced hepatic cytochromes P450 2B1 and 2B2. *Arch Biochem Biophys* 312:234–239.

220. Abdel-Razzak Z, Corcos L, Fautrel A, Guillouzo A (1995) Interleukin-1 beta antagonizes phenobarbital induction of several major cytochromes P450 in adult rat hepatocytes in primary culture. *FEBS Lett* 366:159–164.

221. Marc N et al. (2000) Regulation of phenobarbital induction of the cytochrome P450 2b9/10 genes in primary mouse hepatocyte culture. Involvement of calcium- and cAMP-dependent pathways. *Eur J Biochem* 267:963–970.

222. Guengerich FP (1999) Cytochrome P-450 3A4: regulation and role in drug metabolism. *Annu Rev Pharmacol Toxicol* 39:1–17.

223. Leclercq IA et al. (2000) CYP2E1 and CYP4A as microsomal catalysts of lipid peroxides in murine nonalcoholic steatohepatitis. *J Clin Invest* 105:1067–1075.

224. Kroetz DL, Yook P, Costet P, Bianchi P, Pineau T (1998) Peroxisome proliferator-activated receptor alpha controls the hepatic CYP4A induction adaptive response to starvation and diabetes. *J Biol Chem* 273:31581–31589.

225. Leone TC, Weinheimer CJ, Kelly DP (1999) A critical role for the peroxisome proliferator-activated receptor alpha (PPARalpha) in the cellular fasting response: the PPARalpha-null mouse as a model of fatty acid oxidation disorders. *Proc Natl Acad Sci USA* 96:7473–7478.

226. Fraaije MW, Mattevi A (2000) Flavoenzymes: diverse catalysts with recurrent features. *Trends Biochem Sci* 25:126–132.

227. Lawton MP et al. (1994) A nomenclature for the mammalian flavin-containing monooxygenase gene family based on amino acid sequence identities. *Arch Biochem Biophys* 308:254–257.

228. Zhou J, Shephard EA (2006) Mutation, polymorphism and perspectives for the future of human flavin-containing monooxygenase 3. *Mutat Res* 612:165–171.

229. Cherrington NJ, Cao Y, Cherrington JW, Rose RL, Hodgson E (1998) Physiological factors affecting protein expression of flavin-containing monooxygenases 1, 3 and 5. *Xenobiotica* 28:673–682.

230. Duescher RJ, Lawton MP, Philpot RM, Elfarra AA (1994) Flavin-containing monooxygenase (FMO)-dependent metabolism of methionine and evidence for FMO3 being the major FMO involved in methionine sulfoxidation in rabbit liver and kidney microsomes. *J Biol Chem* 269:17525–17530.

231. Krause RJ et al. (1996) Characterization of the methionine S-oxidase activity of rat liver and kidney microsomes: immunochemical and kinetic

evidence for FMO3 being the major catalyst. *Arch Biochem Biophys* 333:109–116.

232. Uthus EO, Brown-Borg HM (2006) Methionine flux to transsulfuration is enhanced in the long living Ames dwarf mouse. *Mech Ageing Dev* 127:444–450.

233. Dutsch-Wicherek M, Sikora J, Tomaszewska R (2008) The possible biological role of metallothionein in apoptosis. *Front Biosci* 13:4029–4038.

234. Inoue K-I, Takano H, Shimada A, Satoh M (2009) Metallothionein as an anti-inflammatory mediator. *Mediators of Inflammation* 2009:101659.

235. Swindell WR (2011) Metallothionein and the biology of aging. *Ageing Res Rev* 10:132–145.

236. Kang YJ, Chen Y, Yu A, Voss-McCowan M, Epstein PN (1997) Overexpression of metallothionein in the heart of transgenic mice suppresses doxorubicin cardiotoxicity. *J Clin Invest* 100:1501–1506.

237. Yang X et al. (2006) Metallothionein prolongs survival and antagonizes senescence-associated cardiomyocyte diastolic dysfunction: role of oxidative stress. *The FASEB Journal* 20:1024–1026.

238. Bakka A, Johnsen AS, Endresen L, Rugstad HE (1982) Radioresistance in cells with high content of metallothionein. *Experientia* 38:381–383.

239. Schwarz MA et al. (1994) Cytoplasmic metallothionein overexpression protects NIH 3T3 cells from tert-butyl hydroperoxide toxicity. *J Biol Chem* 269:15238–15243.

240. Suzuki Y, Apostolova MD, Cherian MG (2000) Astrocyte cultures from transgenic mice to study the role of metallothionein in cytotoxicity of tert-butyl hydroperoxide. *Toxicology* 145:51–62.

241. Sato M et al. (2010) Development of high-fat-diet-induced obesity in female metallothionein-null mice. *The FASEB Journal* 24:2375–2384.

242. Lazo JS et al. (1995) Enhanced sensitivity to oxidative stress in cultured embryonic cells from transgenic mice deficient in metallothionein I and II genes. *J Biol Chem* 270:5506–5510.

243. Yang H-Y, Wang Y-M, Peng S-Q (2009) Basal expression of metallothionein suppresses butenolide-induced oxidative stress in liver homogenates in vitro. 53:246–253.

244. Hayes JD, Flanagan JU, Jowsey IR (2005) Glutathione transferases. *Annu Rev Pharmacol Toxicol* 45:51–88.

245. Jakobsson PJ, Morgenstern R, Mancini J, Ford-Hutchinson A, Persson B (1999) Common structural features of MAPEG -- a widespread superfamily of membrane associated proteins with highly divergent functions in eicosanoid and glutathione metabolism. *Protein Sci* 8:689–692.

246. Hayes JD, Pulford DJ (1995) The glutathione S-transferase supergene family: regulation of GST and the contribution of the isoenzymes to cancer chemoprotection and drug resistance. 30:445–600.

247. Armstrong RN (1997) Structure, catalytic mechanism, and evolution of the glutathione transferases. *Chem Res Toxicol* 10:2–18.

248. Hayes JD, McLellan LI (1999) Glutathione and glutathione-dependent enzymes represent a co-ordinately regulated defence against oxidative stress. *Free Radic Res* 31:273–300.

249. Sheehan D, Meade G, Foley VM, Dowd CA (2001) Structure, function and evolution of glutathione transferases: implications for classification of non-mammalian members of an ancient enzyme superfamily. *Biochem J* 360:1–16.

250. Chapman E, Best MD, Hanson SR, Wong C-H (2004) Sulfotransferases: structure, mechanism, biological activity, inhibition, and synthetic utility. *Angew Chem Int Ed Engl* 43:3526–3548.

251. Clarke C, Thorburn P, McDonald D, Adams JB (1982) Enzymic synthesis of steroid sulphates. XV. Structural domains of oestrogen sulphotransferase. *Biochim Biophys Acta* 707:28–37.

252. Evans WE, Relling MV (1999) Pharmacogenomics: translating functional genomics into rational therapeutics. *Science* 286:487–491.

253. Ishii Y, Nurrochmad A, Yamada H (2010) Modulation of UDP-glucuronosyltransferase activity by endogenous compounds. *Drug Metab Pharmacokinet* 25:134–148.

254. Wu B, Kulkarni K, Basu S, Zhang S, Hu M (2011) First-pass metabolism via UDP-glucuronosyltransferase: a barrier to oral bioavailability of phenolics. *J Pharm Sci* 100:3655–3681.

255. Tukey RH, Strassburg CP (2000) Human UDP-glucuronosyltransferases: metabolism, expression, and disease. *Annu Rev Pharmacol Toxicol* 40:581–616.

256. Iyanagi T (2007) Molecular mechanism of phase I and phase II drug-metabolizing enzymes: implications for detoxification. *Int Rev Cytol* 260:35–112.

257. Mackenzie PI et al. (2005) Nomenclature update for the mammalian UDP glycosyltransferase (UGT) gene superfamily. *Pharmacogenet Genomics* 15:677–685.

258. Owens IS, Basu NK, Banerjee R (2005) UDP-glucuronosyltransferases: gene structures of UGT1 and UGT2 families. *Meth Enzymol* 400:1–22.

259. Williams SN, Dunham E, Bradfield CA (2005) in *Cytochrome P450*, ed Ortiz de Montellano PR (Kluwer Academic/Plenum Publishers), pp 323–346.

260. Omiecinski CJ, Vanden Heuvel JP, Perdew GH, Peters JM (2011) Xenobiotic metabolism, disposition, and regulation by receptors: from biochemical phenomenon to predictors of major toxicities. *Toxicol Sci* 120 Suppl 1:S49–75.

261. Waxman DJ (1999) P450 gene induction by structurally diverse xenochemicals: central role of nuclear receptors CAR, PXR, and PPAR. *Arch Biochem Biophys* 369:11–23.

262. Ueda A et al. (2002) Diverse roles of the nuclear orphan receptor CAR in regulating hepatic genes in response to phenobarbital. *Mol Pharmacol* 61:1–6.

263. Goodwin B, Redinbo MR, Kliewer SA (2002) Regulation of cyp3a gene transcription by the pregnane x receptor. *Annu Rev Pharmacol Toxicol* 42:1–23.

264. Xie W et al. (2000) Humanized xenobiotic response in mice expressing nuclear receptor SXR. *Nature* 406:435–439.

265. Mangelsdorf DJ, Evans RM (1995) The RXR heterodimers and orphan receptors. *Cell* 83:841–850.

266. Goodwin B, Hodgson E, Liddle C (1999) The orphan human pregnane X receptor mediates the transcriptional activation of CYP3A4 by rifampicin through a distal enhancer module. *Mol Pharmacol* 56:1329–1339.

267. Staudinger JL et al. (2001) The nuclear receptor PXR is a lithocholic acid sensor that protects against liver toxicity. *Proc Natl Acad Sci USA* 98:3369–3374.

268. Trottier E, Belzil A, Stoltz C, Anderson A (1995) Localization of a phenobarbital-responsive element (PBRE) in the 5'-flanking region of the rat CYP2B2 gene. *Gene* 158:263–268.

269. Honkakoski P, Negishi M (1997) Characterization of a phenobarbital-responsive enhancer module in mouse P450 Cyp2b10 gene. *J Biol Chem* 272:14943–14949.

270. Moreau A, Vilarem M-J, Maurel P, Pascussi J-M (2008) Xenoreceptors CAR and PXR activation and consequences on lipid metabolism, glucose homeostasis, and inflammatory response. *Mol Pharm* 5:35–41.

271. Moore LB et al. (2000) Orphan nuclear receptors constitutive androstane receptor and pregnane X receptor share xenobiotic and steroid ligands. *J Biol Chem* 275:15122–15127.

272. Pascussi JM, Gerbal-Chaloin S, Drocourt L, Maurel P, Vilarem MJ (2003) The expression of CYP2B6, CYP2C9 and CYP3A4 genes: a tangle of networks of nuclear and steroid receptors. *Biochim Biophys Acta* 1619:243–253.

273. Maglich JM et al. (2004) The nuclear receptor CAR is a regulator of thyroid hormone metabolism during caloric restriction. *J Biol Chem* 279:19832–19838.

274. Qatanani M, Zhang J, Moore DD (2005) Role of the constitutive androstane receptor in xenobiotic-induced thyroid hormone metabolism. *Endocrinology* 146:995–1002.

275. Zhang J, Huang W, Chua SS, Wei P, Moore DD (2002) Modulation of acetaminophen-induced hepatotoxicity by the xenobiotic receptor CAR. *Science* 298:422–424.

276. Zhang J, Huang W, Qatanani M, Evans RM, Moore DD (2004) The constitutive androstane receptor and pregnane X receptor function coordinately to prevent bile acid-induced hepatotoxicity. *J Biol Chem* 279:49517–49522.

277. Xie W et al. (2001) An essential role for nuclear receptors SXR/PXR in detoxification of cholestatic bile acids. *Proc Natl Acad Sci USA* 98:3375–3380.

278. Goodwin B et al. (2003) Identification of bile acid precursors as endogenous ligands for the nuclear xenobiotic pregnane X receptor. *Proc Natl Acad Sci USA* 100:223–228.

279. Modica S, Bellafante E, Moschetta A (2009) Master regulation of bile acid and xenobiotic metabolism via the FXR, PXR and CAR trio. *Front Biosci* 14:4719–4745.

280. Wollam J, Antebi A (2011) Sterol regulation of metabolism, homeostasis, and development. *Annu Rev Biochem* 80:885–916.

281. Masternak MM, Bartke A (2007) PPARs in Calorie Restricted and Genetically Long-Lived Mice. *PPAR Res* 2007:28436.

282. Vanden Heuvel JP (2004) Diet, fatty acids, and regulation of genes important for heart disease. *Curr Atheroscler Rep* 6:432–440.

283. Tontonoz P, Hu E, Graves RA, Budavari AI, Spiegelman BM (1994) mPPAR gamma 2: tissue-specific regulator of an adipocyte enhancer. *Genes Dev* 8:1224–1234.

284. Tontonoz P, Hu E, Spiegelman BM (1994) Stimulation of adipogenesis in fibroblasts by PPAR gamma 2, a lipid-activated transcription factor. *Cell* 79:1147–1156.

285. Semple RK, Chatterjee VKK, O'Rahilly S (2006) PPAR gamma and human metabolic disease. *J Clin Invest* 116:581–589.

286. Wang Y-X et al. (2003) Peroxisome-proliferator-activated receptor delta activates fat metabolism to prevent obesity. *Cell* 113:159–170.

287. Tugwood JD et al. (1992) The mouse peroxisome proliferator activated receptor recognizes a response element in the 5' flanking sequence of the rat acyl CoA oxidase gene. *EMBO J* 11:433–439.

288. Reddy JK, Hashimoto T (2001) Peroxisomal beta-oxidation and peroxisome proliferator-activated receptor alpha: an adaptive metabolic system. *Annu Rev Nutr* 21:193–230.

289. Johnson EF, Hsu M-H, Savas U, Griffin KJ (2002) Regulation of P450 4A expression by peroxisome proliferator activated receptors. *Toxicology* 181-182:203–206.

290. Fang H-L et al. (2005) Regulation of human hepatic hydroxysteroid sulfotransferase gene expression by the peroxisome proliferator-activated receptor alpha transcription factor. *Mol Pharmacol* 67:1257–1267.

291. Hankinson O (1995) The aryl hydrocarbon receptor complex. *Annu Rev Pharmacol Toxicol* 35:307–340.

292. Bock KW, Köhle C (2009) The mammalian aryl hydrocarbon (Ah) receptor: from mediator of dioxin toxicity toward physiological functions in skin and liver. *Biol Chem* 390:1225–1235.

293. Ikuta T, Eguchi H, Tachibana T, Yoneda Y, Kawajiri K (1998) Nuclear localization and export signals of the human aryl hydrocarbon receptor. *J Biol Chem* 273:2895–2904.

294. Pollenz RS, Barbour ER (2000) Analysis of the complex relationship between nuclear export and aryl hydrocarbon receptor-mediated gene regulation. *Mol Cell Biol* 20:6095–6104.

295. Reyes H, Reisz-Porszasz S, Hankinson O (1992) Identification of the Ah receptor nuclear translocator protein (Arnt) as a component of the DNA binding form of the Ah receptor. *Science* 256:1193–1195.

296. Probst MR, Reisz-Porszasz S, Agbunag RV, Ong MS, Hankinson O (1993) Role of the aryl hydrocarbon receptor nuclear translocator protein in aryl hydrocarbon (dioxin) receptor action. *Mol Pharmacol* 44:511–518.

297. Israel DI, Whitlock JP (1983) Induction of mRNA specific for cytochrome P1-450 in wild type and variant mouse hepatoma cells. *J Biol Chem* 258:10390–10394.

298. Israel DI, Whitlock JP (1984) Regulation of cytochrome P1-450 gene transcription by 2,3,7, 8-tetrachlorodibenzo-p-dioxin in wild type and variant mouse hepatoma cells. *J Biol Chem* 259:5400–5402.

299. Ko HP, Okino ST, Ma Q, Whitlock JP (1996) Dioxin-induced CYP1A1 transcription in vivo: the aromatic hydrocarbon receptor mediates transactivation, enhancer-promoter communication, and changes in chromatin structure. *Mol Cell Biol* 16:430–436.

300. Nebert DW et al. (2000) Role of the aromatic hydrocarbon receptor and [Ah] gene battery in the oxidative stress response, cell cycle control, and apoptosis. *Biochem Pharmacol* 59:65–85.

301. Motohashi H, O'Connor T, Katsuoka F, Engel JD, Yamamoto M (2002) Integration and diversity of the regulatory network composed of Maf and CNC families of transcription factors. *Gene* 294:1–12.

302. Kensler TW, Wakabayashi N, Biswal S (2007) Cell survival responses to environmental stresses via the Keap1-Nrf2-ARE pathway. *Annu Rev Pharmacol Toxicol* 47:89–116.

303. Blank V (2008) Small Maf proteins in mammalian gene control: mere dimerization partners or dynamic transcriptional regulators? *J Mol Biol* 376:913–925.

304. Martín-Montalvo A, Villalba JM, Navas P, de Cabo R (2011) NRF2, cancer and calorie restriction. *Oncogene* 30:505–520.

305. Chan JY, Han XL, Kan YW (1993) Cloning of Nrf1, an NF-E2-related transcription factor, by genetic selection in yeast. *Proc Natl Acad Sci USA* 90:11371–11375.

306. Chan JY, Han XL, Kan YW (1993) Isolation of cDNA encoding the human NF-E2 protein. *Proc Natl Acad Sci USA* 90:11366–11370.

307. Kobayashi A et al. (1999) Molecular cloning and functional characterization of a new Cap“n” collar family transcription factor Nrf3. *J Biol Chem* 274:6443–6452.

308. Moi P, Chan K, Asunis I, Cao A, Kan YW (1994) Isolation of NF-E2-related factor 2 (Nrf2), a NF-E2-like basic leucine zipper transcriptional activator that binds to the tandem NF-E2/AP1 repeat of the beta-globin locus control region. *Proc Natl Acad Sci USA* 91:9926–9930.

309. Itoh K, Igarashi K, Hayashi N, Nishizawa M, Yamamoto M (1995) Cloning and characterization of a novel erythroid cell-derived CNC family transcription factor heterodimerizing with the small Maf family proteins. *Mol Cell Biol* 15:4184–4193.

310. Oyake T et al. (1996) Bach proteins belong to a novel family of BTB-basic leucine zipper transcription factors that interact with MafK and regulate transcription through the NF-E2 site. *Mol Cell Biol* 16:6083–6095.

311. Muto A et al. (1998) Identification of Bach2 as a B-cell-specific partner for small maf proteins that negatively regulate the immunoglobulin heavy chain gene 3' enhancer. *EMBO J* 17:5734–5743.

312. Motohashi H, Katsuoka F, Engel JD, Yamamoto M (2004) Small Maf proteins serve as transcriptional cofactors for keratinocyte differentiation in the Keap1-Nrf2 regulatory pathway. *Proc Natl Acad Sci USA* 101:6379–6384.

313. Venugopal R, Jaiswal AK (1998) Nrf2 and Nrf1 in association with Jun proteins regulate antioxidant response element-mediated expression and coordinated induction of genes encoding detoxifying enzymes. *Oncogene* 17:3145–3156.

314. Jaiswal AK (2004) Nrf2 signaling in coordinated activation of antioxidant gene expression. *Free Radic Biol Med* 36:1199–1207.

315. McMahon M, Itoh K, Yamamoto M, Hayes JD (2003) Keap1-dependent proteasomal degradation of transcription factor Nrf2 contributes to the negative regulation of antioxidant response element-driven gene expression. *J Biol Chem* 278:21592–21600.

316. Motohashi H, Yamamoto M (2004) Nrf2-Keap1 defines a physiologically important stress response mechanism. *Trends Mol Med* 10:549–557.

317. Itoh K et al. (1999) Keap1 represses nuclear activation of antioxidant responsive elements by Nrf2 through binding to the amino-terminal Neh2 domain. *Genes Dev* 13:76–86.

318. Zhang DD, Lo S-C, Cross JV, Templeton DJ, Hannink M (2004) Keap1 is a redox-regulated substrate adaptor protein for a Cul3-dependent ubiquitin ligase complex. *Mol Cell Biol* 24:10941–10953.

319. Osburn WO, Kensler TW (2008) Nrf2 signaling: an adaptive response pathway for protection against environmental toxic insults. *Mutat Res* 659:31–39.

320. Itoh K et al. (2003) Keap1 regulates both cytoplasmic-nuclear shuttling and degradation of Nrf2 in response to electrophiles. *Genes Cells* 8:379–391.

321. Nguyen T, Sherratt PJ, Huang H-C, Yang CS, Pickett CB (2003) Increased protein stability as a mechanism that enhances Nrf2-mediated transcriptional activation of the antioxidant response element. Degradation of Nrf2 by the 26 S proteasome. *J Biol Chem* 278:4536–4541.

322. Stewart D, Killeen E, Naquin R, Alam S, Alam J (2003) Degradation of transcription factor Nrf2 via the ubiquitin-proteasome pathway and stabilization by cadmium. *J Biol Chem* 278:2396–2402.

323. Dinkova-Kostova AT et al. (2002) Direct evidence that sulfhydryl groups of Keap1 are the sensors regulating induction of phase 2 enzymes that protect against carcinogens and oxidants. *Proc Natl Acad Sci USA* 99:11908–11913.

324. Levonen A-L et al. (2004) Cellular mechanisms of redox cell signalling: role of cysteine modification in controlling antioxidant defences in response to electrophilic lipid oxidation products. *Biochem J* 378:373–382.

325. Hong F, Sekhar KR, Freeman ML, Liebler DC (2005) Specific patterns of electrophile adduction trigger Keap1 ubiquitination and Nrf2 activation. *J Biol Chem* 280:31768–31775.

326. Zhang DD, Hannink M (2003) Distinct cysteine residues in Keap1 are required for Keap1-dependent ubiquitination of Nrf2 and for stabilization of Nrf2 by chemopreventive agents and oxidative stress. *Mol Cell Biol* 23:8137–8151.

327. Eggler AL, Liu G, Pezzuto JM, van Breemen RB, Mesecar AD (2005) Modifying specific cysteines of the electrophile-sensing human Keap1 protein is insufficient to disrupt binding to the Nrf2 domain Neh2. *Proc Natl Acad Sci USA* 102:10070–10075.

328. Eggler AL, Luo Y, van Breemen RB, Mesecar AD (2007) Identification of the highly reactive cysteine 151 in the chemopreventive agent-sensor Keap1 protein is method-dependent. *Chem Res Toxicol* 20:1878–1884.

329. Luo Y et al. (2007) Sites of alkylation of human Keap1 by natural chemoprevention agents. *J Am Soc Mass Spectrom* 18:2226–2232.

330. Lau A, Villeneuve NF, Sun Z, Wong PK, Zhang DD (2008) Dual roles of Nrf2 in cancer. *Pharmacol Res* 58:262–270.

331. Nguyen T, Yang CS, Pickett CB (2004) The pathways and molecular mechanisms regulating Nrf2 activation in response to chemical stress. *Free Radic Biol Med* 37:433–441.

332. Kang KW, Ryu JH, Kim SG (2000) The essential role of phosphatidylinositol 3-kinase and of p38 mitogen-activated protein kinase activation in the antioxidant response element-mediated rGSTA2 induction by decreased glutathione in H4IIE hepatoma cells. *Mol Pharmacol* 58:1017–1025.

333. Kang KW, Cho MK, Lee CH, Kim SG (2001) Activation of phosphatidylinositol 3-kinase and Akt by tert-butylhydroquinone is responsible for antioxidant response element-mediated rGSTA2 induction in H4IIE cells. *Mol Pharmacol* 59:1147–1156.

334. Yu R et al. (1999) Role of a mitogen-activated protein kinase pathway in the induction of phase II detoxifying enzymes by chemicals. *J Biol Chem* 274:27545–27552.

335. Yu R et al. (2000) p38 mitogen-activated protein kinase negatively regulates the induction of phase II drug-metabolizing enzymes that detoxify carcinogens. *J Biol Chem* 275:2322–2327.

336. Zipper LM, Mulcahy RT (2000) Inhibition of ERK and p38 MAP kinases inhibits binding of Nrf2 and induction of GCS genes. *Biochem Biophys Res Commun* 278:484–492.

337. Huang HC, Nguyen T, Pickett CB (2000) Regulation of the antioxidant response element by protein kinase C-mediated phosphorylation of NF-E2-related factor 2. *Proc Natl Acad Sci USA* 97:12475–12480.

338. Kang KW, Park EY, Kim SG (2003) Activation of CCAAT/enhancer-binding protein beta by 2“-amino-3-”methoxyflavone (PD98059) leads to the induction of glutathione S-transferase A2. *Carcinogenesis* 24:475–482.

339. Huang H-C, Nguyen T, Pickett CB (2002) Phosphorylation of Nrf2 at Ser-40 by protein kinase C regulates antioxidant response element-mediated transcription. *J Biol Chem* 277:42769–42774.

340. Itoh K et al. (1997) An Nrf2/small Maf heterodimer mediates the induction of phase II detoxifying enzyme genes through antioxidant response elements. *Biochem Biophys Res Commun* 236:313–322.

341. Baird L, Dinkova Kostova AT (2011) The cytoprotective role of the Keap1-Nrf2 pathway. *Arch Toxicol* 85:241–272.

342. Enomoto A et al. (2001) High sensitivity of Nrf2 knockout mice to acetaminophen hepatotoxicity associated with decreased expression of ARE-regulated drug metabolizing enzymes and antioxidant genes. *Toxicol Sci* 59:169–177.

343. Ramos-Gomez M et al. (2001) Sensitivity to carcinogenesis is increased and chemoprotective efficacy of enzyme inducers is lost in nrf2 transcription factor-deficient mice. *Proc Natl Acad Sci USA* 98:3410–3415.

344. Chan K, Kan YW (1999) Nrf2 is essential for protection against acute pulmonary injury in mice. *Proc Natl Acad Sci USA* 96:12731–12736.

345. Aoki Y et al. (2001) Accelerated DNA adduct formation in the lung of the Nrf2 knockout mouse exposed to diesel exhaust. *Toxicol Appl Pharmacol* 173:154–160.

346. Xu C et al. (2006) Inhibition of 7,12-dimethylbenz(a)anthracene-induced skin tumorigenesis in C57BL/6 mice by sulforaphane is mediated by nuclear factor E2-related factor 2. *Cancer Res* 66:8293–8296.

347. Rangasamy T et al. (2004) Genetic ablation of Nrf2 enhances susceptibility to cigarette smoke-induced emphysema in mice. *J Clin Invest* 114:1248–1259.

348. Calkins MJ et al. (2005) Protection from mitochondrial complex II inhibition in vitro and in vivo by Nrf2-mediated transcription. *Proc Natl Acad Sci USA* 102:244–249.

349. Wakabayashi N et al. (2003) Keap1-null mutation leads to postnatal lethality due to constitutive Nrf2 activation. *Nat Genet* 35:238–245.

350. Wakabayashi N et al. (2004) Protection against electrophile and oxidant stress by induction of the phase 2 response: fate of cysteines of the Keap1 sensor modified by inducers. *Proc Natl Acad Sci USA* 101:2040–2045.

351. Okawa H et al. (2006) Hepatocyte-specific deletion of the keap1 gene activates Nrf2 and confers potent resistance against acute drug toxicity. *Biochem Biophys Res Commun* 339:79–88.

352. Umemura T et al. (2006) A crucial role of Nrf2 in in vivo defense against oxidative damage by an environmental pollutant, pentachlorophenol. *Toxicol Sci* 90:111–119.

353. Favreau LV, Pickett CB (1991) Transcriptional regulation of the rat NAD(P)H:quinone reductase gene. Identification of regulatory elements controlling basal level expression and inducible expression by planar aromatic compounds and phenolic antioxidants. *J Biol Chem* 266:4556–4561.

354. Li Y, Jaiswal AK (1992) Regulation of human NAD(P)H:quinone oxidoreductase gene. Role of AP1 binding site contained within human antioxidant response element. *J Biol Chem* 267:15097–15104.

355. Nolan KA et al. (2010) Pharmacological inhibitors of NAD(P)H quinone oxidoreductase, NQO1: structure/activity relationships and functional activity in tumour cells. *Biochem Pharmacol* 80:977–981.

356. Prestera T et al. (1995) Parallel induction of heme oxygenase-1 and chemoprotective phase 2 enzymes by electrophiles and antioxidants: regulation by upstream antioxidant-responsive elements (ARE). *Mol Med* 1:827–837.

357. Banning A et al. (2008) Glutathione Peroxidase 2 Inhibits Cyclooxygenase-2-Mediated Migration and Invasion of HT-29 Adenocarcinoma Cells but Supports Their Growth as Tumors in Nude Mice. *Cancer Res* 68:9746–9753.

358. Chang X-Z et al. (2007) Identification of the functional role of peroxiredoxin 6 in the progression of breast cancer. *Breast Cancer Res* 9:R76.

359. Cao J et al. (2009) Prdx1 inhibits tumorigenesis via regulating PTEN/AKT activity. *EMBO J* 28:1505–1517.

360. Friling RS, Bensimon A, Tichauer Y, Daniel V (1990) Xenobiotic-inducible expression of murine glutathione S-transferase Ya subunit gene is controlled by an electrophile-responsive element. *Proc Natl Acad Sci USA* 87:6258–6262.

361. Rushmore TH, Pickett CB (1990) Transcriptional regulation of the rat glutathione S-transferase Ya subunit gene. Characterization of a xenobiotic-responsive element controlling inducible expression by phenolic antioxidants. *J Biol Chem* 265:14648–14653.

362. Reinhart J, Pearson WR (1993) The structure of two murine class-mu glutathione transferase genes coordinately induced by butylated hydroxyanisole. *Arch Biochem Biophys* 303:383–393.

363. Efferth T, Volm M (2005) Glutathione-related enzymes contribute to resistance of tumor cells and low toxicity in normal organs to artesunate. *In Vivo* 19:225–232.

364. Mitra A, Shevde LA, Samant RS (2009) Multi-faceted role of HSP40 in cancer. *Clin Exp Metastasis* 26:559–567.

365. Wang H et al. (2010) Expression of Hsp27 and Hsp70 in lymphocytes and plasma in healthy workers and coal miners with lung cancer. *J Huazhong Univ Sci Technol Med Sci* 30:415–420.

366. Anwar-Mohamed A et al. (2011) The effect of Nrf2 knockout on the constitutive expression of drug metabolizing enzymes and transporters in C57Bl/6 mice livers. *Toxicol In Vitro* 25:785–795.

367. Muguruma M et al. (2006) Molecular pathological analysis for determining the possible mechanism of piperonyl butoxide-induced hepatocarcinogenesis in mice. *Toxicology* 228:178–187.

368. Bae S-Y et al. (2006) Effects of genetic polymorphisms of MDR1, FMO3 and CYP1A2 on susceptibility to colorectal cancer in Koreans. *Cancer Science* 97:774–779.

369. Fialka F et al. (2008) CPA6, FMO2, LGI1, SIAT1 and TNC are differentially expressed in early- and late-stage oral squamous cell carcinoma--a pilot study. *Oral Oncol* 44:941–948.

370. Lal S et al. (2008) CBR1 and CBR3 pharmacogenetics and their influence on doxorubicin disposition in Asian breast cancer patients. *Cancer Science* 99:2045–2054.

371. Amador-Noguez D, Yagi K, Venable S, Darlington G (2004) Gene expression profile of long-lived Ames dwarf mice and Little mice. *Aging Cell* 3:423–441.

372. Boylston WH, Deford JH, Papaconstantinou J (2006) Identification of longevity-associated genes in long-lived Snell and Ames dwarf mice. *AGE* 28:125–144.

373. Rowland JE et al. (2005) In vivo analysis of growth hormone receptor signaling domains and their associated transcripts. *Mol Cell Biol* 25:66–77.

374. Dozmorov I, Bartke A, Miller RA (2001) Array-based expression analysis of mouse liver genes: effect of age and of the longevity mutant Prop1df. *J Gerontol A Biol Sci Med Sci* 56:B72–80.

375. Dozmorov I et al. (2002) Gene expression profile of long-lived snell dwarf mice. *J Gerontol A Biol Sci Med Sci* 57:B99–108.

376. Tsuchiya T et al. (2004) Additive regulation of hepatic gene expression by dwarfism and caloric restriction. *Physiol Genomics* 17:307–315.

377. Dhahbi JM, Mote PL, Fahy GM, Spindler SR (2005) Identification of potential caloric restriction mimetics by microarray profiling. *Physiol Genomics* 23:343–350.

378. Swindell WR (2007) Gene expression profiling of long-lived dwarf mice: longevity-associated genes and relationships with diet, gender and aging. *BMC Genomics* 8:353.

379. Lattard V, Lachuer J, Buronfosse T, Garnier F, Benoit E (2002) Physiological factors affecting the expression of FMO1 and FMO3 in the rat liver and kidney. *Biochem Pharmacol* 63:1453–1464.

380. Janmohamed A, Hernandez D, Phillips IR, Shephard EA (2004) Cell-, tissue-, sex- and developmental stage-specific expression of mouse flavin-containing monooxygenases (Fmos). *Biochem Pharmacol* 68:73–83.

381. Bertilsson G et al. (1998) Identification of a human nuclear receptor defines a new signaling pathway for CYP3A induction. *Proc Natl Acad Sci USA* 95:12208–12213.

382. Blumberg B et al. (1998) SXR, a novel steroid and xenobiotic-sensing nuclear receptor. *Genes Dev* 12:3195–3205.

383. Kliewer SA et al. (1998) An orphan nuclear receptor activated by pregnanes defines a novel steroid signaling pathway. *Cell* 92:73–82.

384. Wei P, Zhang J, Egan-Hafley M, Liang S, Moore DD (2000) The nuclear receptor CAR mediates specific xenobiotic induction of drug metabolism. *Nature* 407:920–923.

385. Xie W et al. (2000) Reciprocal activation of xenobiotic response genes by nuclear receptors SXR/PXR and CAR. *Genes Dev* 14:3014–3023.

386. Sonoda J, Pei L, Evans RM (2008) Nuclear receptors: decoding metabolic disease. *FEBS Lett* 582:2–9.

387. Tolson AH, Wang H (2010) Regulation of drug-metabolizing enzymes by xenobiotic receptors: PXR and CAR. *Adv Drug Deliv Rev* 62:1238–1249.

388. Leiser SF, Miller RA (2010) Nrf2 signaling, a mechanism for cellular stress resistance in long-lived mice. *Mol Cell Biol* 30:871–884.

389. Sun LY, Bokov AF, Richardson A, Miller RA (2011) Hepatic response to oxidative injury in long-lived Ames dwarf mice. *FASEB J* 25:398–408.

390. Tullet JMA et al. (2008) Direct inhibition of the longevity-promoting factor SKN-1 by insulin-like signaling in C. elegans. *Cell* 132:1025–1038.

391. Inoue H et al. (2005) The C. elegans p38 MAPK pathway regulates nuclear localization of the transcription factor SKN-1 in oxidative stress response. *Genes Dev* 19:2278–2283.

392. An JH et al. (2005) Regulation of the Caenorhabditis elegans oxidative stress defense protein SKN-1 by glycogen synthase kinase-3. *Proc Natl Acad Sci USA* 102:16275–16280.

393. Bishop NA, Guarente L (2007) Two neurons mediate diet-restriction-induced longevity in C. elegans. *Nature* 447:545–549.

394. Onken B, Driscoll M (2010) Metformin induces a dietary restriction-like state and the oxidative stress response to extend C. elegans Healthspan via AMPK, LKB1, and SKN-1. *PLoS ONE* 5:e8758.

395. Sykiotis GP, Bohmann D (2008) Keap1/Nrf2 signaling regulates oxidative stress tolerance and lifespan in Drosophila. *Dev Cell* 14:76–85.

396. Pearson KJ et al. (2008) Nrf2 mediates cancer protection but not prolongevity induced by caloric restriction. *Proceedings of the National Academy of Sciences* 105:2325–2330.

397. Suh JH et al. (2004) Decline in transcriptional activity of Nrf2 causes age-related loss of glutathione synthesis, which is reversible with lipoic acid. *Proc Natl Acad Sci USA* 101:3381–3386.

398. Collins AR et al. (2009) Age-accelerated atherosclerosis correlates with failure to upregulate antioxidant genes. *Circ Res* 104:e42–54.

399. Shih P-H, Yen G-C (2007) Differential expressions of antioxidant status in aging rats: the role of transcriptional factor Nrf2 and MAPK signaling pathway. *Biogerontology* 8:71–80.

400. Zhang DD (2006) Mechanistic studies of the Nrf2-Keap1 signaling pathway. *Drug Metab Rev* 38:769–789.

401. Hur W, Gray NS (2011) Small molecule modulators of antioxidant response pathway. *Curr Opin Chem Biol* 15:162–173.

402. Kensler TW, Wakabayashi N (2010) Nrf2: friend or foe for chemoprevention? *Carcinogenesis* 31:90–99.

403. Boutten A, Goven D, Artaud-Macari E, Boczkowski J, Bonay M (2011) NRF2 targeting: a promising therapeutic strategy in chronic obstructive pulmonary disease. *Trends Mol Med* 17:363–371.

404. Alic N, Partridge L (2011) Death and dessert: nutrient signalling pathways and ageing. *Curr Opin Cell Biol* 23:738–743.

405. Gems D (2007) Long-lived dwarf mice: are bile acids a longevity signal? *Aging Cell* 6:421–423.

CHAPTER 2

Differential activation of the MAPK pathway in long-lived dwarf mice

2-1. Abstract

Primary dermal fibroblasts from long-lived dwarf mice, including Snell and growth hormone receptor knockout (GHRKO) mice, are resistant to multiple forms of cytotoxic stress, but the molecular mechanisms for their enhanced resistance are unknown. This study demonstrates that ERK1/2, but not JNK or p38 phosphorylation, induced by hydrogen peroxide (H_2O_2), cadmium chloride ($CdCl_2$), or paraquat is attenuated in fibroblasts from Snell dwarf and GHRKO mice. UV-C light, hyperosmolarity (excess NaCl), and tumor necrosis factor alpha (TNF-α) induce ERK phosphorylation in Snell and GHRKO cells to a similar extent as littermate control cells. Attenuation of ERK phosphorylation is also observed in liver tissue from Snell dwarf mice exposed to diquat. *Portions of this data set* (Figure 2-5; Figure 2-6; Figure 2-7) *were previously published in Free Radical Biology and Medicine* (1).

2-2. Introduction

Loss-of-function mutations that diminish GH/IGF-1 signaling action have been shown to delay aging and increase mouse lifespan (2, 3). The Snell ($Pit1^{dw/dw}$) and Ames ($Prop1^{dw/dw}$) dwarf mouse models are the best-studied slow-

aging mutants with altered circulating GH/IGF-1 levels (4, 5). Multiple age-associated phenotypes are delayed in these mice, including cataracts, collagen cross-linking, immunosenescence, kidney disease, and neoplasia, as well as impaired learning ability, locomotion, or memory (5-8). Snell and Ames dwarf mice undergo improper embryonic development of the anterior pituitary, resulting in impaired secretion of GH, prolactin, and TSH. This results in additional reduction of circulating IGF-1 and thyroid hormones (TH) levels. The Snell and Ames mutations increase lifespan ~40% in both sexes and in multiple genetic backgrounds (4, 5, 8). GHRKO mice were developed by targeted disruption of the *Ghr/Ghrbp* gene and do not express the GH receptor (9). These mice have elevated levels of circulating GH levels but are GH resistant due to a lack of functional GH receptor. Similar to Snell and Ames mice, GHRKO mice have diminished circulating levels of IGF-1 and insulin, increased lifespan, and multiple indices associated with delayed aging (8-10).

Dysregulation of IGFBPs has also recently been shown to extend lifespan in mice. Targeted disruption of PAPPA, an IGFBP protease that regulates function of IGFBPs (IGFBP-4, possibly -2,5) through cleavage, increases longevity in mice (11) (Table 1-1). Interestingly, these mice are long-lived but have no observed decrease in circulating GH or IGF-1 levels. PAPPA-KO mice have been proposed to be long-lived due to a reduction in local, rather than circulating IGF-1 concentration, due to increased expression of IGFBPs (12, 13).

Whether cells from PAPPA-KO mice are resistant to cytotoxic stress, similar to Snell, Ames, and GHRKO mice, has not been determined.

Longevity extension has previously been shown to be associated with increased resistance to multiple forms of stress in yeast, worms, and flies (14-16). Enhanced multiplex stress resistance may also play a role in mammalian aging (17). Primary dermal fibroblasts of adult Snell, Ames, and GHRKO mice are resistant to death induced by oxidative (H_2O_2, paraquat), nonoxidative (MMS, UV-C light), and mixed ($CdCl_2$, heat) stresses (18, 19). Cells from Snell mice are also resistant to metabolic stress induced by glucose deprivation or rotenone exposure (20), are better protected against oxygen stress-induced senescence (21), and are faster to resume transcription after UV irradiation (22). Resistance to stress has been shown to be positively associated with lifespan across specials of mammals (23, 24) and birds (25). However, the molecular basis of enhanced cellular stress resistance is not defined.

Since mutations that affect insulin signaling and increase longevity in worms and flies have been shown to be associated with enhanced stress resistance (26), we hypothesized that altered insulin/IGF-1R signaling is responsible for the multiplex enhanced cellular stress resistance phenotype of long-lived dwarf fibroblasts. The insulin/IGF-1R signaling cascade forks into two main branches: (A) the PI3K-AKT pathway controls nutrient metabolism including glucose uptake and suppression of gluconeogenesis, and (B) the Ras-MAPK

pathway mediates gene expression. These two pathways have also been shown to interact to regulate cell growth and differentiation (27).

Activation of Akt by the insulin/IGF-1 receptor is mediated by the IRS-PI3K-Akt kinase cascade (28). Akt can act as a negative regulator of stress resistance primarily through inhibitory phosphorylation of the Forkhead Box-O (FOXO) transcription factor (29). In worms and flies, lifespan extension observed in insulin receptor mutants has been shown to be dependent on FOXO activity (30-32). In contrast, there is little direct evidence in support of the IRS-PI3K-Akt-FOXO pathway regulating mammalian aging (2). Some insight has been obtained from dietary restriction studies. Akt phosphorylation has been shown to be reduced in liver samples from CR and MR mice (33). The observations that $IRS1^{-/+}$ (34) and $IRS2^{-/+}$ (35) mutant mice are long-lived suggests that this pathway may play a role in regulation of mammalian aging.

MAPKs comprise a ubiquitous group of signaling proteins that play a prominent role in regulating cell proliferation, differentiation, and adaptation (36). The MAPK signaling module is defined by a three-tiered kinase cascade, resulting in phosphorylation of a conserved Thr-X-Tyr activation motif by an upstream dual-specificity MAPK kinase (37). ERK, JNK, and p38 are the major subfamilies of the MAPK signal network. ERK1/2 is canonically activated by the Ras/Raf/MEK pathway, and Ras has been implicated as a regulator of longevity in yeast (38). Ras activity is controlled in mammals by insulin/IGF-1 receptor

signaling mediated through IRS1/2 and Grb2-Sos, parallel to the PI3K-Akt pathway (27).

The multiplex stress resistance phenotype of dwarf mice appears to be valid in vivo as well. IGF-1R$^{+/-}$ mice are resistant to intraperitoneal (IP) administration of the oxidative toxin paraquat compared to littermate control mice (39). Ames mice also survive exposure to diquat and paraquat longer than littermate control mice (40). Resistance in both the IGF-1R$^{-/-}$ and Ames studies were measured as survival time in response to a single, lethal stress dose. The enhanced resistance of IGF-1R$^{-/-}$ mice to paraquat was only observed in females (39), but both sexes of Ames mice were resistant to stress (40). Diquat and paraquat are frequently used to generate oxidative stress in cells and whole animals (41, 42). Diquat is a redox cycler that can be converted to a free radical intermediate, which upon combination with molecular oxygen generates superoxide anions. Paraquat catalyzes oxidation of intracellular NADPH as well as superoxide formation (43). In addition, both diquat and paraquat can peroxidize lipid membranes (42).

The goal of this component of my research project was to test the hypothesis that the enhanced stress resistance phenotype of dwarf mice is associated with altered Akt pathway or MAPK cascade activation. Akt phosphorylation was measured in Snell skin-derived fibroblasts in response to IGF-1 or insulin stimulation, and MAPK phosphorylation was evaluated in Snell and GHRKO skin fibroblasts in response to cytotoxic stress exposure ($CdCl_2$,

H_2O_2, paraquat, UV-C light). Additionally, differential activation of the MAPK pathway was examined in multiple tissues of Snell dwarf mice challenged with a single IP injection of diquat.

2-3. Materials and Methods

Animals

Snell dwarf (*dw/dw*) and heterozygote (*dw/+*) control mice were bred as the progeny of (DW/J x C3H/HeJ)F1 *dw/+* females and (DW/J x C3H/HeJ)F1 *dw/+* males; the sires had been treated with growth hormone and thyroxine to increase their fertility (44).

GHRKO mice and littermate controls were maintained in the laboratory of Dr. Andrzej Bartke at Southern Illinois University from stock produced by Dr. John Kopchick's group at Ohio University, as previously described (9). The genetic background of these animals is derived from 129/Ola embryonic stem cells and includes contributions from BALB/c, C57BL/6, and C3H inbred strains.

PAPPA-KO mice used in this study were generated from breeding colonies at the University of Michigan, initiated from a breeding pair generously provided by Dr. Cheryl A. Conover at the Mayo Clinic. These mice were originally generated using targeted disruption of the PAPPA gene at exon 4 (11). PAPPA-KO were maintained on a mixed C57BL/6-129SV/E genetic background.

Tail skin biopsies for fibroblast culture were taken from male Snell and PAPPA-KO mice 3-4 months of age. Tail skin biopsies GHRKO mice were obtained from male mice 3-6 months of age shipped overnight on ice to the

University of Michigan in Dulbecco's modified Eagle's medium (DMEM) supplemented with 20% heat-inactivated fetal calf serum (FCS), penicillin, streptomycin, Fungizone, and 10 mM Hepes.

Diquat dibromide monohydrate (Chem Service, West Chester, PA, USA) was dissolved in 0.9% saline and delivered via intraperitoneal injection in a volume adjusted to deliver 50 mg per kg body weight, as previously described (40). After 6 h of treatment, diquat and saline-treated control mice were euthanized by CO_2 asphyxiation. Tissues were immediately dissected, snap frozen in liquid nitrogen, and stored at -80°C.

Animal use in these experiments was approved by the University Committee on the Use and Care of Animals (UCUCA) at the University of Michigan.

Cell culture

Fibroblasts from Snell, GHRKO, and PAPPA-KO, and respective littermate control tail skin biopsies were isolated following our standardized, previously published protocol (18). Tail snips of ~5 mm in length were minced with a scalpel and placed into a 35-mm dish with 1.5 mL of "complete" medium (high glucose DMEM variant without sodium pyruvate [Gibco/Life Technologies, Carlsbad, CA, USA], 1X Antibiotic-Antimycotic solution of penicillin/streptomycin/Fungizone [Gibco], 10% heat-inactivated FCS [Hyclone/Thermo Scientific, Logan, UT, USA]) containing collagenase (1000 U/ml; Gibco) in a humidified CO_2 incubator at 37°C with 20% O_2. After overnight collagenase digestion, the cell suspension was

pipetted repeatedly to dislodge fibroblasts, passed through a sterile nylon cell strainer (BD Biosciences, San Jose, CA, USA) into 50 mL tubes to remove debris, and centrifuged for 5 min at 200 g in 15 mL tubes. The resulting cell pellet was resuspended in 3 mL of complete medium, transferred to a 25-cm^2 flask (passage 0). Every 3 days, 2/3 of cell culture medium was replaced with fresh complete medium. When cells approached confluence ~1 week later, the monolayer was trypsinized, resuspended in complete medium, and counted with a hemacytometer. 0.75 x 10^6 cells were then passaged into 75-cm^2 flasks (passage 1). The following week, when cells approached confluence, the cultures were passaged into T175 flasks at a density of 1.75 x 10^6 cells per flask (passage 2). The same duration and flask volume was used for passage 3 cells. All fibroblast experiments described used cell cultures at passage 3 from Snell, GHRKO, PAPPA-KO, and respective littermate control mice propagated and tested independently in parallel. Serum deprivation was conducted in DMEM containing 2% bovine serum albumin (BSA; Gemini Bio-Science, Logan, UT, USA) without FCS for 18-24 h.

Multiplex cellular stress resistance assay

Snell and PAPPA-KO fibroblast survival was measured with a test based on metabolic conversion of WST-1 reagent, as previously described (18). Cells were seeded in triplicate in clear, flat bottom 96-well plates at a density of 30,000 cells/well. After 24 h incubation in complete medium, cells were washed 2x with PBS and incubated in serum-free medium for 18 h. Chemical stressors ($CdCl_2$,

H_2O_2 , NaCl, paraquat [all from Sigma-Aldrich, St. Louis, MO, USA]) were prepared in serial dilutions the day of the experiment in DMEM without BSA or FCS and applied to cells for 6 hours. For UV stress, cells were incubated in PBS and briefly exposed to UV-C light using a Stratagene Stratalinker. Cells were then allowed to recover in serum-free medium for 18 hours. Colorimetric change due to reduction of the tetrazolium dye WST-1 (Roche Applied Science, Indianapolis, IN, USA) after 4 hours was measured by spectrophotometry (Molecular Dynamics) following the recommended protocol specified by the manufacturer.

Antibodies

Antibodies for immunoblotting were obtained as follows: p38 MAPK, phospho-p38 MAPK (Thr180/Tyr182), ERK, phospho-ERK (Thr202/Tyr204), JNK, phospho-JNK (Thr183/Tyr185), phospho-Akt (Ser473), phospho-Akt (Thr308), and Akt (pan) were from Cell Signaling Technology (Beverly, MA, USA); β-actin was from Sigma-Aldrich (St. Louis, MO, USA); and goat anti-rabbit and goat anti-mouse antibodies were from Santa Cruz Biotechnology (Santa Cruz, CA, USA).

Western blot analysis

After stress or mock treatment, cells were washed in cold PBS and harvested by scraping in 1 mL of RIPA lysis buffer (Pierce/Thermo Scientific, Rockford, IL, USA) containing 1X HALT protease inhibitor cocktail (Pierce) and PhosSTOP phosphatase inhibitor cocktail (Roche). Lysates were centrifuged at 12,000 rpm for 40 min at 4°C and stored at -80°C. Protein concentrations were

determined using the bicinchoninic acid (BCA) assay (Pierce) according to the manufacturer's recommended microplate protocol. Samples were then prepared for immunoblot by adding Laemmli buffer and boiling for 5 min. Sodium dodecyl sulfate polyacrylamide gel electrophoresis (SDS-PAGE) was performed using 40 μg protein per lane and Criterion XT gels (Bio-Rad, Hercules, CA, USA) at 100 V. Wet-transfer was then performed for 1 h at 100 V using 0.45 μM PVDF membrane (Millipore). Membranes were briefly incubated in pH 7.6 Tris-buffered saline (TBS) and blocked with 3% BSA in TBS plus 0.05% Tween 20 (TBST) for 1 h at room temperature. Blots were briefly washed with TBST and incubated with primary Ab diluted at the manufacturer's recommended concentration in 1% BSA/TBST solution overnight at 4°C. After primary Ab incubation, blots were washed for 15 min 3X with TBST and then incubated with secondary Ab in 1% BSA/TBST overnight at 4°C. Enhanced chemiluminescence (ECL) substrate (Pierce) and X-OMAT film was used for visualization of phospho-Akt and total proteins. Phospho-MAPK proteins were visualized with enhanced chemifluorescence (ECF) substrate (GE Healthcare) and digital image processing using a STORM 860 molecular imager (Molecular Dynamics, Sunnyvale, CA, USA). Quantification of immunoblot band intensities was performed using ImageQuant 5.2 software (Molecular Dynamics).

Statistical analyses

All graphs show mean values ± SEM. Differences between normal and dwarf fibroblasts in the levels of protein phosphorylation were evaluated using a

paired t-test, with each time point considered separately, at a criterion of $p < 0.05$ for statistical significance. For analysis of diquat-treated tissue samples, differences between dwarf and control mice were performed using an unpaired t-test. Interaction of genotype and diquat exposure was calculated using 2-way analysis of variance (ANOVA) in Prism 5 software (GraphPad Software, La Jolla, CA, USA).

2-4. Results

Phosphorylation of Akt in response to IGF-1 and insulin treatment does not differ between Snell dwarf and control fibroblasts

The insulin/IGF-1 receptor has been implicated in stress response control and delayed aging in multiple models of aging. Snell mice have reduced circulating IGF-1 and insulin resulting from improper pituitary development and subsequent reduction of GH secretion. The enhanced stress resistance phenotype of Snell dwarf fibroblasts is epigenetically stable, and thus maintained through multiple passages in culture containing high levels of growth factors, including insulin. We hypothesized that part of this epigenetically stable phenomenon that contributes to enhanced stress resistance in fibroblasts is altered insulin/IGF-1R sensitivity. To test this hypothesis, we treated cultured fibroblasts with IGF-1 or insulin and evaluated downstream PI3K-Akt signaling activity via Akt phosphorylation. PDK1, regulated by PI3K, phosphorylates Akt at the Thr308 residue. Additionally, the TORC2 complex regulates Akt activity by phosphorylation at the Ser473 residue. We measured phosphorylation at both of

these sites to determine if differential activation of downstream Akt signaling occurs through PI3K or TOR-dependent mechanisms.

Cells were deprived of serum for 24 h and then exposed to graded doses of IGF-1 (1, 10, 100 ng/ml) or insulin (1, 10, 100 μg/ml) for 15 or 60 min. Equivalent, dose-dependent increases in Akt phosphorylation were observed in response to IGF-1 at both Thr308 (Figure 2-1A) and Ser473 (Figure 2-1B). Follow-up analysis with additional time points (2, 4, 8, 30, 60, 240 min) confirmed that the kinetics of IGF-1-mediated Akt phosphorylation are the same between Snell and control fibroblasts (Figure 2-2). IGF-1 induced robust Akt phosphorylation after only 2 minutes of treatment, with a diminution in Akt phosphorylation observed starting at 30 minutes. Insulin stimulation induced similar changes in Akt Thr308 phosphorylation between Snell and control cells (Figure 2-3), consistent with the IGF-1 treatment experiments (Figure 2-1). These results suggest that cultured dwarf and normal fibroblasts maintain the same responsiveness to IGF-1 and insulin.

Primary dermal fibroblasts from PAPPA-KO mice are not resistant to multiple forms of stress

Since Snell dwarf fibroblasts do not maintain stable, increased sensitivity to IGF-1 or insulin as initially hypothesized, we sought to determine whether diminished GH/IGF-1 action is in fact associated with enhanced stress resistance in long-lived mice. PAPPA-KO mice are long-lived but do not have reduced circulating levels of IGF-1. PAPPA is a protease that cleaves IGFBP-4, and possibly IGFBPs-2,5. In the absence of PAPPA, IGFBP activity is increased

resulting in tissue-specific reductions of local IGF-1 concentration (12, 13). PAPPA-KO mice have normal circulating levels of GH and IGF-1 (Table 1-1). We hypothesized that tissue-specific reduction of IGF-1 would still enhance cellular stress resistance in multiple tissues of PAPPA-KO mice. We measured cytotoxic stress resistant in primary dermal fibroblasts cultured from PAPPA-KO and littermate control mice. We observed no difference in resistance to $CdCl_2$, (Figure 2-4A), H_2O_2 (Figure 2-4B), paraquat (Figure 2-4C), and UV-C light (Figure 2-4D) with the WST-1 assay. No significant difference in resistance was observed between PAPPA-KO and littermate control cells to any of the stressors tested. These data contradicted our initial hypothesis, but are consistent with the observations that enhanced cellular stress resistance is specific to long-lived dwarf mice with reduced circulating GH or IGF-1 action.

ERK phosphorylation is attenuated in Snell dwarf and GHRKO fibroblasts in response to multiple cytotoxic stresses

Since IGF-1 and insulin increased Akt phosphorylation similarly in Snell and control cells (Figure 2-1; Figure 2-2; Figure 2-3), we shifted focus to whether differential activation of MAPK family members may contribute to the resistance to stress in dwarf fibroblasts. We examined the levels of the phosphorylation of ERK1/2, JNK1/2, and p38 in response to 100 μM H_2O_2 (Figure 2-5A,B), 10 μM $CdCl_2$ (Figure 2-5C,D), 10 mM paraquat (Figure 2-6A,B), and 40 mJ/cm^2 UV-C light (Figure 2-6C,D). The stressor concentrations evaluated were approximately equal to the LD_{50} values obtained in the previously published multiplex stress resistance experiments (18, 19). We found that H_2O_2 exposure increased

phosphorylation of ERK1/2 in a dose-dependent manner in both Snell dwarf cells and control cells. Interestingly, the phosphorylation of ERK1/2 by H_2O_2 was dramatically attenuated in dwarf fibroblasts compared with normal fibroblasts (Figure 2-5A,B). By 60 min, phosphorylation levels had increased in control cells 3-fold, compared to a 50% increase in dwarf cells. Cadmium and paraquat induced similar levels of ERK1/2 phosphorylation, which were also significantly attenuated in dwarf cells compared to controls (Figure 2-5C,D and Figure 2-6A,B). This effect appears to be ERK-specific, since phosphorylation of JNK1/2 or p38 was not increased by H_2O_2 exposure, and there was no observed difference in basal phosphorylation levels (Figure 2-5A,B). Cadmium, paraquat, and UV-C light also did not induce JNK phosphorylation in Snell or control cells (Figure 2-5; Figure 2-6).

Skin-derived primary fibroblasts from GHRKO mice also show diminished ERK phosphorylation in response to H_2O_2 and paraquat

GHRKO mice are not responsive to GH signals and have suppressed circulating levels of IGF-1 and insulin (Table 1-1). Similar to Snell and Ames mice, fibroblasts from GHRKO mice were found to be resistant to 100 μM H_2O_2, 10 mM paraquat, and 40 mJ/cm^2 UV-C light compared to fibroblasts from littermate control mice, but for unknown reasons do not show differential sensitivity to $CdCl_2$ (19). We sought to determine whether attenuated ERK phosphorylation is a conserved phenotype in multiple long-lived mouse mutants (Table 1-1) with enhanced cellular stress resistance. We observed that H_2O_2 and paraquat selectively induced phosphorylation of ERK1/2, but not of JNK or p38,

in GHRKO and control cells (Figure 2-7). Similar to the results from cells from Snell dwarf mice, stress-induced ERK1/2 activation was significantly attenuated in GHRKO cells compared with controls (Figure 2-7).

ERK phosphorylation is equivalent in Snell dwarf and control cells in response to UV-C light, NaCl, and TNF-α

The blunted ERK phosphorylation response was observed in dwarf fibroblasts exposed to H_2O_2 (Figure 2-5A,B; Figure 2-7A,B), paraquat (Figure 2-6A,B; Figure 2-7C,D), and cadmium (Figure 2-5C,D). However, UV-C light induced ERK phosphorylation to a similar extend in both Snell and control cells (Figure 2-6C,D). Cells were exposed to a single pulse of UV irradiation and harvested at various times after treatment instead of being under continuous stress exposure as in the tests of soluble agents. Similar results were obtained in Snell and control cells exposed to osmotic stress by exposure to 0.5 M NaCl (Figure 2-8) or stimulated with 10 ng/ml TNF-α (Figure 2-9). The time course of the increase in ERK phosphorylation after TNF-α was very different from that seen using the other stressors. The peak of TNF-α-induced ERK phosphorylation was observed at 5 min, instead of in the 30-90 min range. Snell and control fibroblasts were equally susceptible to death induced by osmotic shock (Figure 2-10), consistent with the ERK phosphorylation results (Figure 2-8). Additionally, Snell and control fibroblasts are equally susceptible to death induced by TNF-α (Yasumura and Miller, unpublished). These data suggest that the attenuated ERK phosphorylation response in dwarf cells is specific to oxidative stress.

Blunted ERK phosphorylation is observed in vivo in diquat-treated Snell dwarf liver tissue

Based on experiments with Snell and GHRKO fibroblasts that demonstrated phosphorylation of ERK1/2 was attenuated in dwarf cells compared to controls (Figure 2-5; Figure 2-6; Figure 2-7), we hypothesized that differential activation of the ERK pathway would also be observed in vivo in a tissue-specific manner, and serve to identify organs that may directly contribute to enhancing stress resistance. Initial analysis of MAPK phosphorylation in response to stress in vivo was evaluated in diquat-treated liver samples from Ames dwarf mice (45). There was no observable difference in basal hepatic ERK phosphorylation (i.e. prior to diquat exposure) between Ames and control mice. However, as seen in the fibroblast studies, ERK phosphorylation was robustly increased by diquat exposure in control mouse liver tissue, but no change was observed in dwarf mouse liver tissue (45).

To address the question of whether differential MAPK activation was observed in multiple tissues of long-lived dwarf mice, we injected Snell mice with diquat following the same protocol used for the Ames diquat exposure survival study (40). Snell mice were injected with a single IP dose of 50 mg/kg diquat and sacrificed 6 h after initial exposure. We first measured diquat-induced changes in ERK phosphorylation in Snell and control mouse liver tissue. There was no observable difference in basal ERK phosphorylation between Snell and control mice, but ERK phosphorylation was increased in diquat-treated control mouse liver tissue with no change in dwarf mouse liver tissue (Figure 2-11). These

results were consistent with the data obtained from diquat-treated Ames mouse liver tissue (45), as well as Snell (Figure 2-5; Figure 2-6) and GHRKO (Figure 2-7) fibroblast experiments, suggesting that differential MAPK activation might be a conserved phenotype in multiple long-lived dwarf stocks.

Differential ERK phosphorylation is not a conserved, multi-organ phenotype in Snell mice

Since differential activation of ERK was observed in Snell liver tissue, we next sought to address whether such a phenotype was also apparent in other tissue types. We measured ERK phosphorylation in hippocampus (Figure 2-12), heart (Figure 2-13), skeletal muscle (Figure 2-14), lung (Figure 2-15), and kidney tissue (Figure 2-16) from Snell dwarf and control mice exposed to diquat for 6 h. The pattern of ERK phosphorylation seen in dwarf liver and dermal fibroblasts was not observed in any of the other tissue types we evaluated. Diquat induced robust and equivalent ERK phosphorylation in both Snell and control mouse hippocampi (Figure 2-12). No change in ERK phosphorylation was seen in Snell and control cardiac tissue (Figure 2-13). The study of skeletal muscle tissue did not yield consistent or statistically significant results: one control mouse did show high levels of ERK phosphorylation in skeletal muscle, but there were no significant differences between dwarf and control mice when all of the data were combined (Figure 2-14). In lung tissue, dwarf baseline ERK phosphorylation was found to be elevated, unlike liver, but with no statistical difference from littermate control baseline levels. In control mice, ERK was found to be phosphorylated in response to diquat, just as observed in the liver. Diquat also stimulated ERK

phosphorylation in dwarf mice, but with much variation and no statistical difference from baseline levels (Figure 2-15). Therefore, although diquat increased ERK phosphorylation in the lung, the overall pattern of phosphorylation changes were very different from that observed the liver. In kidney, diquat produced a small and statistically insignificant increase in control mice, with no change in phosphorylation observed in dwarf kidney tissue (Figure 2-16). We were able to detect only a single ERK isoform in both hippocampus and kidney samples (Figure 2-12; Figure 2-16). These results do not support our initial hypothesis that blunted phosphorylation of ERK in response to stress is a conserved phenotype across Snell dwarf organs. Instead, we propose that differential activation of MAPK signal cascades may instead be associated with tissue-specific IGF-1 expression levels. Local IGF-1 expression in the liver is markedly reduced in Ames mice (46). However, no difference in IGF-1 mRNA expression is observed in the hippocampus between Ames and control mice (46). Similar patterns of IGF-1 expression have been observed in liver and hippocampus tissue of Snell dwarf mice, and reductions in IGF-1 mRNA expression have been observed in other somatic tissues in Snell mice (Sun LY; personal communication). These alterations in local IGF-1 expression may mediate the observed differences among tissues in the extent to which ERK signals are modified in Snell dwarf mice.

2-5. Discussion

The association of mutations that increase lifespan in worms and flies with enhanced resistance to multiple forms of lethal stress (47) suggests that the lifespan extension observed in these mutants is a consequence of their protection from stress. Gene expression studies of CR and GH or insulin/IGF-1-deficient signaling mutants have revealed that specific regulatory networks are altered in slow-aging organisms (48, 49). These factors may regulate coordinated resistance to multiple forms of cytotoxic stress, including oxidative damage and genotoxic insults. The underlying model here is that the rate of aging, whether influenced by diet (50, 51), single gene mutations (4, 5, 52), or evolutionary divergence might also reflect modulation of cellular stress resistance properties (17).

Fibroblasts from long-lived dwarf mice have been shown to be resistant in culture to multiple forms of cytotoxic stress and injury (18, 19). Multiplex stress resistance has also been shown to be correlated with maximal lifespan in studies that compare cells from different species (23, 25, 53, 54). These findings provide indirect evidence in support of the idea that stress resistance influences the rate of aging. However, the biological processes responsible for enhancing stress resistance and the extent to which increased stress resistance of fibroblasts in culture mimics whole organ responses are not well defined. The goal of the experiments described in this chapter was to identify biochemical pathways that might mediate the enhanced stress resistance phenotype of long-lived dwarf

mice and to determine whether such changes were conserved throughout multiple tissue types.

We directed our initial search for signaling networks that may be differentially regulated in dwarf mice to cascades implicated in stress response regulation downstream of the insulin/IGF-1 receptor. First, we sought to measure PI3K-Akt pathway activation, since downstream factors such as FOXO proteins have been shown to regulate insulin receptor-mediated lifespan extension and stress resistance in *C. elegans* and *D. melanogaster* (30-32). We treated Snell and littermate control fibroblasts with IGF-1 or insulin and found no detectable differences in Akt phosphorylation intensity or kinetics between Snell and control cells (Figure 2-1; Figure 2-2; Figure 2-3). These results demonstrate that Snell fibroblasts do not have differential sensitivity to IGF-1 or insulin and that the downstream PI3K-Akt pathway is not differentially activated in primary cultured fibroblasts of Snell mice in response to hormonal stimulation.

MAPK activation is associated with resistance to oxidative damage both in vitro and in vivo (55, 56). ERK is partially regulated through the insulin/IGF-1 receptor by the Grb2-Sos-Ras-Raf-MEK cascade (57)**.** ERK activation has differing effects on stress resistance and apoptosis depending on the duration, intensity, and intracellular localization of activation (58). For example, ERK has been shown to promote cell survival (59, 60) or increase sensitivity to oxidative stress (61). In Snell and GHRKO fibroblasts, ERK phosphorylation is attenuated in response to multiple forms of cytotoxic stress (H_2O_2, $CdCl_2$, paraquat) (Figure

2-5; Figure 2-6; Figure 2-7). Differential ERK phosphorylation is stress-specific and not observed in Snell fibroblasts treated with UV-C light (Figure 2-6C,D), hypertonic NaCl (Figure 2-8), or TNF-α (Figure 2-9). Similar changes in ERK phosphorylation were observed in liver homogenates from Snell (Figure 2-11) and Ames (45) dwarf mice injected with diquat.

These results have several implications concerning the mechanism of multiplex stress resistance in long-lived dwarf mice. It is not well characterized how chemical stress (e.g. H_2O_2, $CdCl_2$, paraquat) induces ERK phosphorylation, and it is likely that the activation process differs for each agent. Paraquat augments oxidative damage caused by mitochondrial free radicals (41, 42). Hydrogen peroxide induces cellular damage primarily by lipid peroxidation (62). Our experiments show that early activation of ERK phosphorylation is not observed in dwarf cells in response to oxidative stress (H_2O_2, $CdCl_2$, paraquat) but can be rapidly increased by other forms of stress (UV-C light, NaCl, TNF-α). Therefore, dwarf fibroblasts are likely less susceptible to early stage activation in one or more of these damage-detection pathways. For example, dwarf cells may be less susceptible or rapidly repair H_2O_2-mediated membrane peroxidation that normally triggers the ERK cascade in control cells. Experiments that evaluate early stage damage and upstream MAPK kinase activity will be needed to address these concerns.

Immediate early genes (IEG) are rapidly and transiently synthesized in response to stress or mitogenic stimuli (63, 64). PI3K-Akt and MAPK signaling

have been shown to regulate IEG induction (65). Expression of the IEGs Egr-1, Fos, and Jun was evaluated in Snell dwarf fibroblasts exposed to 100 μM H_2O_2 for 1 h and found to increase more in dwarf cells in response to stress. This response was dependent on MEK activity, since increased mRNA expression was not observed in fibroblasts pretreated with the MEK inhibitor PD98059 (1). Similar trends of IEG expression were reported in H_2O_2-treated GHRKO fibroblasts, with the exception that Jun induction did not differ from control cells (1). These observed results in fibroblasts are paradoxical, since ERK phosphorylation was found to be attenuated in Snell and GHRKO mice in response to stress, and suggest that a MEK/ERK-independent mechanism is responsible for the adaptive response of these IEGs. However, a different pattern of IEG expression in response to diquat-induced oxidative stress was observed in Ames dwarf liver tissue. Basal expression of Egr-1, Fos, and Jun mRNA was found to be elevated in Snell (Sun LY; personal communication) and Ames (45) liver tissue compared to control mice. Increased hepatic expression of Egr-1 and Fos but not Jun were observed in diquat-treated Snell mice (Sun LY; personal communication). Egr-1, Fos, and Jun expression was found to significantly increase more in diquat-treated control mice compared to Snell mice (Sun LY; personal communication). In Ames mice, No significant change in hepatic IEG expression was detected in diquat-treated animals, but control mice had increased expression of Egr-1 and Fos mRNA (45). These experiments demonstrate that in addition to altered ERK phosphorylation observed in

fibroblast cell culture and in liver tissue lysates, IEG expression differs between dwarf and control mice.

No detectable change in JNK or p38 phosphorylation was observed in Snell, GHRKO and littermate control-matched fibroblasts exposed to stress (Figure 2-5; Figure 2-6; Figure 2-7) or in tissue lysates from diquat-treated Snell and littermate control mice (not shown). However, a blunted p38 response, similar to that we observed with ERK, was detected in diquat-treated Ames liver tissue (45). Additionally, differential activation of p38 was reported in Ames dwarf fibroblasts in response to H_2O_2, 3-NPA, antimycin A and rotenone (66). JNK phosphorylation was observed to increase in liver samples from Ames mice exposed to diquat compared to controls, opposite to what was observed with ERK. Therefore, it remains plausible that differential activation of JNK and p38 MAPKs also contributes to enhanced stress resistance. Experiments that evaluate additional time points and test other forms of stress will be required to test the proposed hypotheses that differences in the activation pattern of ERK, JNK, and p38 contribute to enhanced stress resistance and delayed aging in dwarf mice.

Although long-lived dwarf mice are able to survive oxidative stress challenge (e.g. diquat, paraquat) longer than littermate controls (39, 40), increased apoptosis and toxicity has been observed in the liver of these mice in response to stress (40). Ames mice challenged with diquat had a ~3-fold increase in apoptosis as measured by double strand DNA breaks (40).

Additionally, Snell and GHRKO mice are more sensitivity to acetaminophen exposure than littermate control mice (53). This is in contrast to Little (67) and CR (53) mice, which have been reported to be resistant to acetaminophen challenge. The mechanistic basis for this difference in chemical stress resistance is not known, but may be due to differences in intracellular redox homeostasis, xenobiotic metabolism, or control of apoptosis. Multiple proapoptotic genes, such as Bad and Bax, have been reported to be constitutively elevated at the mRNA level in dwarf mice (45, 68). Snell fibroblasts are also more susceptible to chemical agents (thapsigargin, tunicamycin) that induce ER stress-mediated apoptosis (22). Higher expression of CHOP, enhanced caspase 3 and 12 activity, and diminished Xbp1 splicing, all associated with a shift in favor of apoptosis, are observed in Snell dwarf fibroblasts (69). CHOP (Gadd153), which is induced by oxidative stress and mediates ER stress-induced programmed cell death (70-72), is upregulated in Ames liver tissue in response to diquat (45). Higher apoptosis in proliferative tissue, such as liver, has been proposed to promote regeneration of new, undamaged cells in response to cytotoxic stress (73). Therefore, the observed increase in apoptosis in Ames liver may provide an advantage to the mice by eliminating damaged cells more rapidly.

The experiments described in this chapter demonstrate that differential MAPK activation is a conserved phenotype across multiple long-lived dwarf mice of different genetic backgrounds (Snell, Ames, GHRKO) both in fibroblast culture models in response to multiple cytotoxic stresses and in vivo in response to

diquat. We propose that this effect is due to reduced circulating GH/IGF-1 levels and subsequent alteration of insulin/IGF-1R signaling. In long-lived PAPPA-KO mice, which do not have lower circulating levels of IGF-1, there is no observed difference in cellular stress resistance (Figure 2-4). Similarly, Ames dwarf mice injected with GH for 6 weeks starting at 2 weeks of age have similar median lifespan as littermate control mice and no observed difference in cellular stress resistance (74), consistent with the model that reduced circulating GH/IGF-1 is required to establish an epigenetically stable enhanced stress resistance phenotype in skin-derived fibroblasts. In Snell mice treated with diquat, attenuation of ERK phosphorylation was only observed in liver tissue, which has a low level of local IGF-1 expression (Sun LY, personal communication). In contrast, robust ERK phosphorylation was observed in the hippocampus, which maintains a normal level of local IGF-1 (46, 75). Therefore, we propose that differential MAPK phosphorylation in dwarf mice in response to stress is influenced by local IGF-1 concentration. These in vivo stress experiments were performed at a single dose and time point, and serve as a preliminary first step toward developing a comprehensive picture of how stress resistance is differentially regulated in throughout the whole dwarf mouse. The differential activation of these signaling components likely reflects a single aspect of a more complex network of homeostatic circuits, with survival of both specific cell types, and survival of the mouse itself, influenced by cellular repair processes,

inflammation, redox balance, and the rate of stressor detoxification mediated by xenobiotic metabolism.

2-6. Acknowledgments

This work was supported by National Institute on Aging grants AG-023122 and AG-019899. We thank John Kopchick for the gift of breeding pairs for the GHRKO mouse stock. We thank Maggie Lauderdale, William Kohler, and Lisa Burmeister for technical assistance.

2-7. Figures

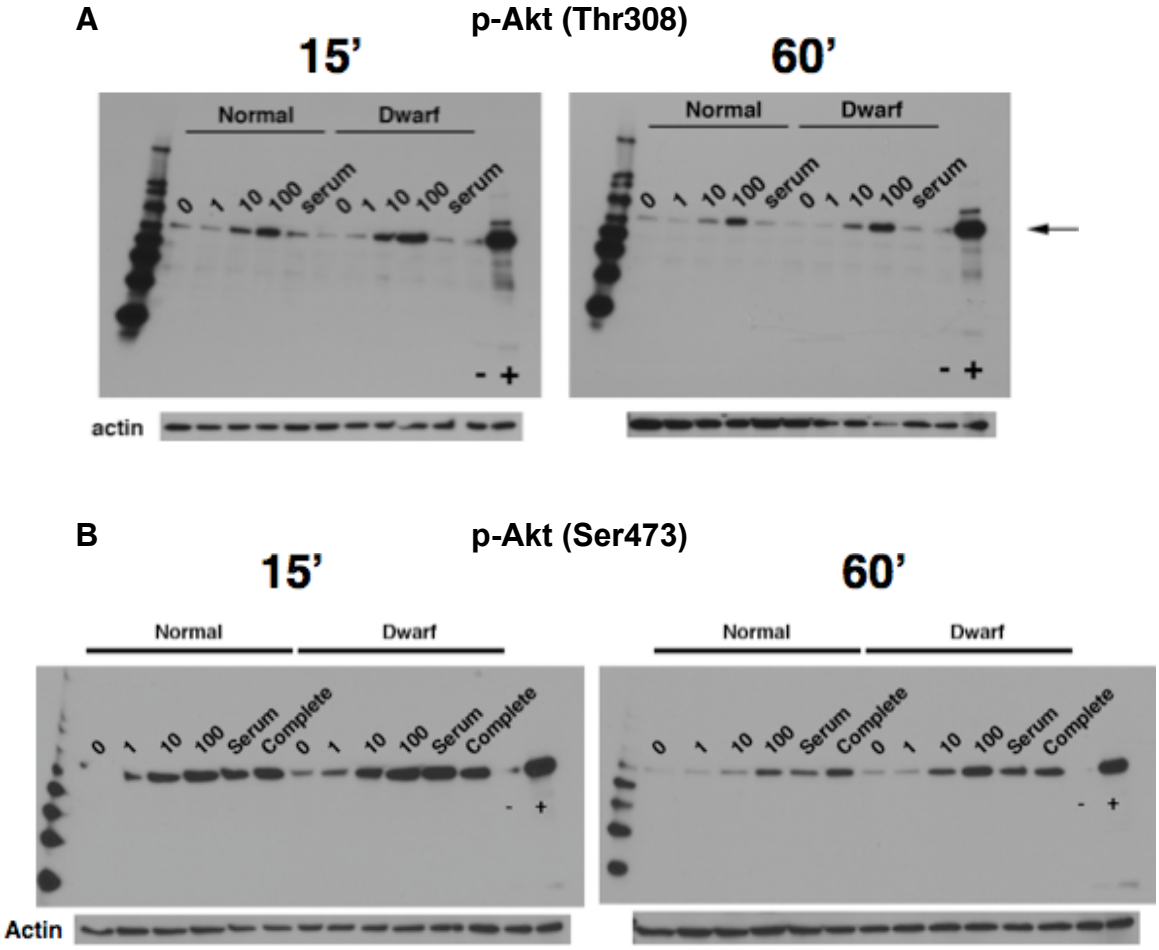

Figure 2-1. Similar phosphorylation of Akt at Thr308 and Ser473 observed in Snell and control fibroblasts in response to IGF-1.

After overnight serum removal, cells were treated with IGF-1 for 15' or 60' at 3 doses (1, 10, 100 ng/mL). Phospho-Akt controls: Jurkat cells treated with LY294002 (-) or calyculin A (+). Serum lane denotes cells that underwent serum removal and subsequent addition of serum-containing complete medium. Complete lane denotes cells that were kept in complete medium without serum removal. Representative immunoblots of p-Akt and actin at the 15' and 60' time points are shown. IGF-1 induced Akt phosphorylation at both residues and both time points in a dose-dependent manner, but no significant difference was observed between Snell dwarf and littermate control cells (n = 4).

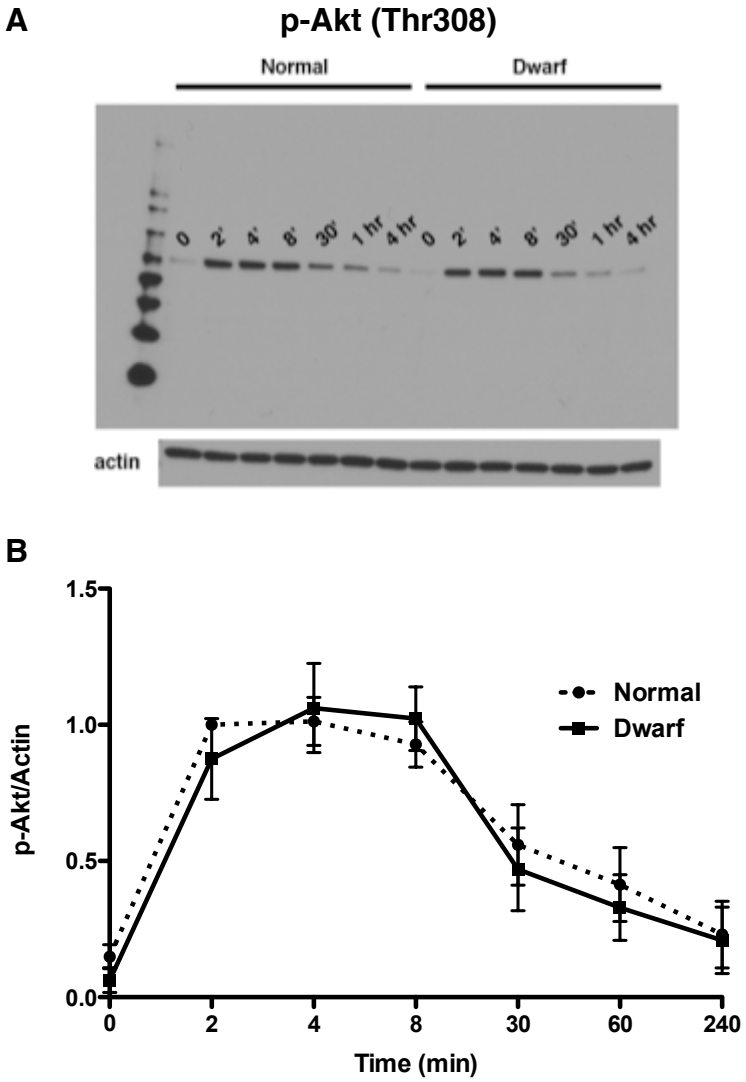

Figure 2-2. Snell dwarf and control fibroblasts have similar Akt phosphorylation kinetics at Thr308 in response to IGF-1.

After overnight serum removal, cells were treated with IGF-1 (10 ng/ml) and lysed at multiple time intervals (0, 2', 4', 8', 30', 60', 240'). (A) Representative immunoblots of p-Akt and actin are shown. Akt is rapidly phosphorylated in response to IGF-1 stimulus, with high levels of phosphorylation observed at 2-8 minutes. Phosphorylation levels are attenuated after 30 minutes of treatment. (B) No significant difference was observed between Snell dwarf and littermate control cells (n = 2).

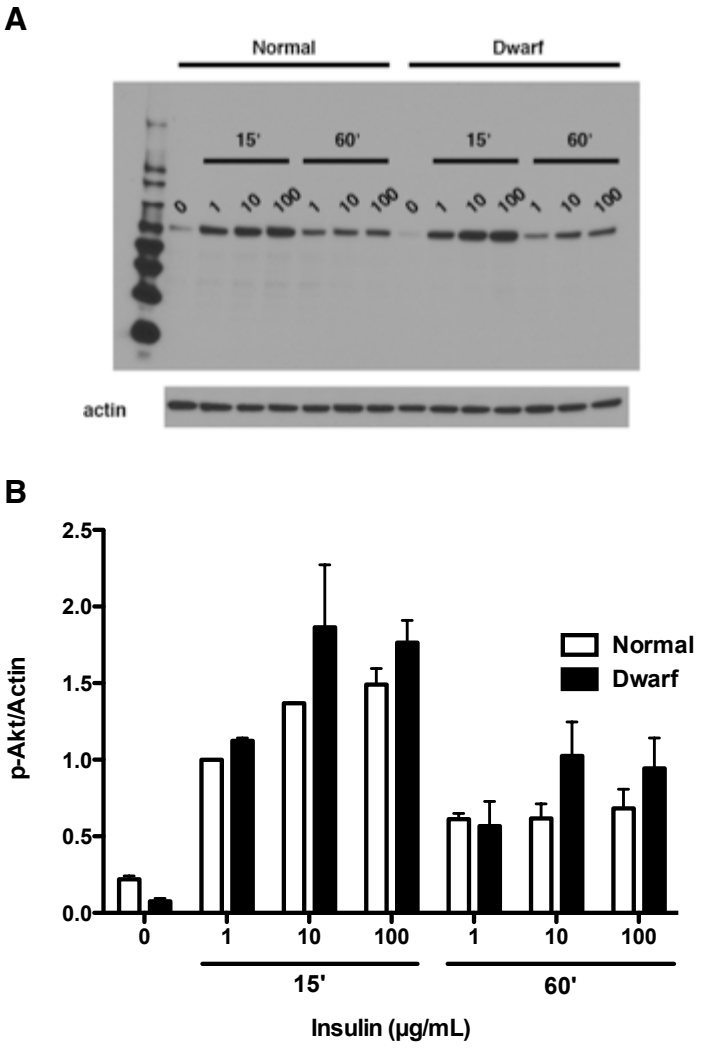

Figure 2-3. Similar phosphorylation of Akt at Thr308 in Snell and control fibroblasts is observed in response to insulin.

After overnight serum removal, cells were treated with insulin for 15' or 60' at 3 doses (1, 10, 100 μg/mL). (A) Representative immunoblots of p-Akt and actin are shown. Insulin induced Akt phosphorylation at both time points. (B) Means and SEMs for ratio of p-Akt to actin in normal and dwarf cells at the indicated doses and time points. No significant difference was observed between genotypes (n = 4).

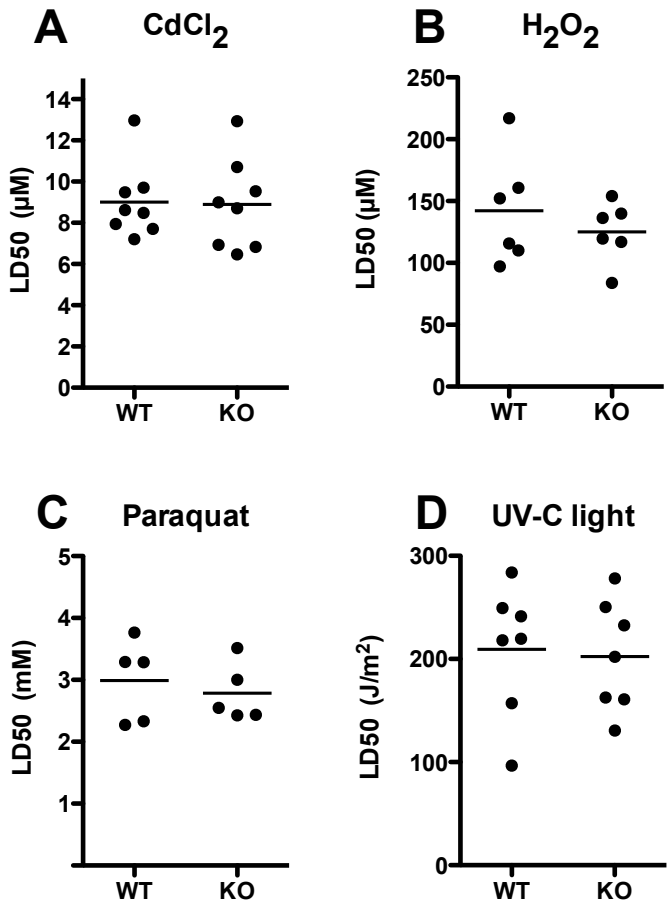

Figure 2-4. PAPPA-KO dermal fibroblasts are not resistance to multiple forms of cytotoxic stress.

PAPPA-KO and control cells were allowed to adhere for 24 h and deprived of serum overnight. The cells were exposed varying doses of (A) $CdCl_2$, (B) H_2O_2, or (C) paraquat for 6 h. (D) UV-treated cells were exposed to a single pulse and then incubated in serum-free media for 6 h during the stress period. LD_{50}, the dose of stress that led to death of 50% of the cells, was calculated from the dose-response curve. No significant difference in resistance was found between PAPPA-KO and controls. PAPPA-KO and littermate control cells have LD_{50} values that resemble those previously obtained from Snell dwarf littermate controls (18, 19).

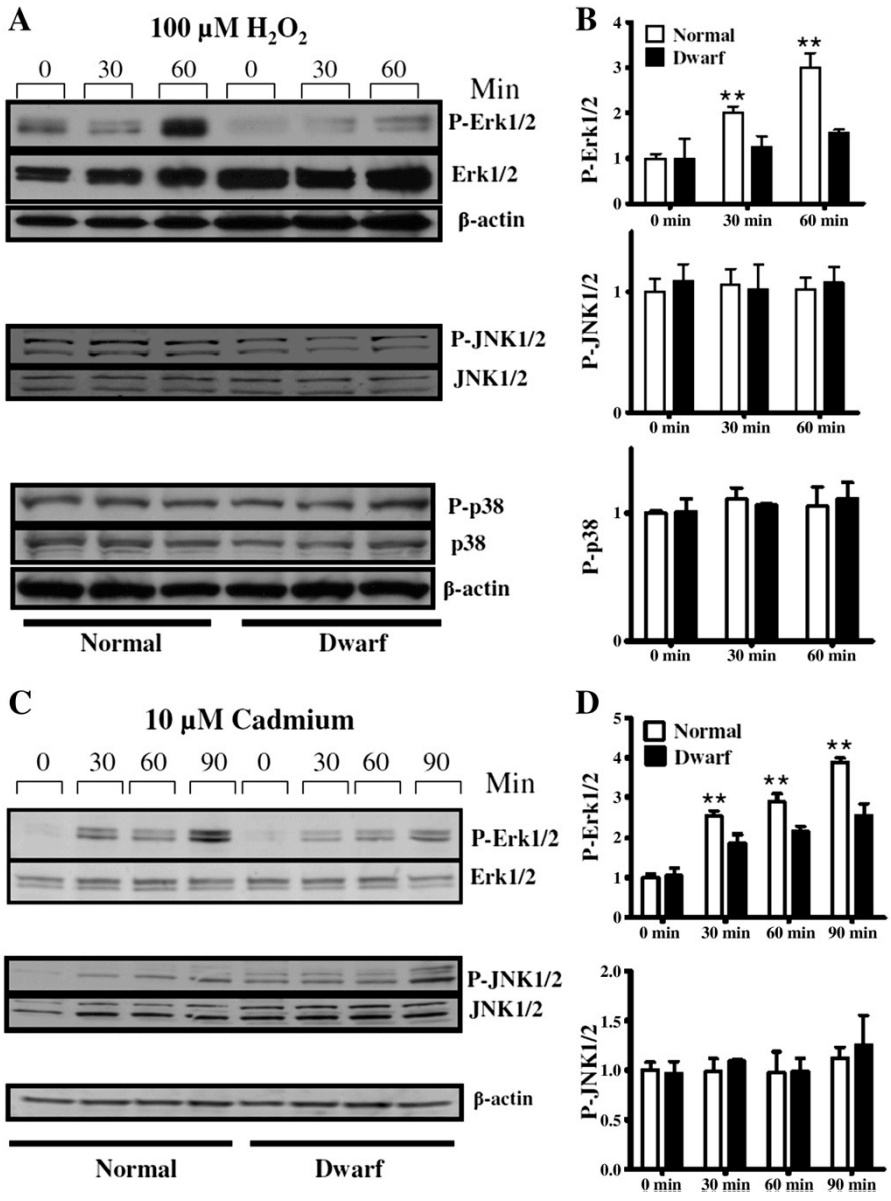

Figure 2-5. Phosphorylation of ERK1/2, JNK1/2, and p38 in skin-derived primary fibroblasts from Snell dwarf and normal mice in response to (A,B) H_2O_2 and (C,D) cadmium.

After overnight serum removal, cells were treated with H_2O_2 (100 μM, equivalent to 600 nmol of H_2O_2 per 10^6 cells) or cadmium (10 μM) for the indicated time intervals. (A,C) Representative immunoblots for phosphorylated and total forms of ERK1/2, JNK1/2 and p38 proteins are shown. (B,D) The means and SEM, presented as ratios to unstressed control cells at the start of treatment (n = 6; $p < 0.01$**).

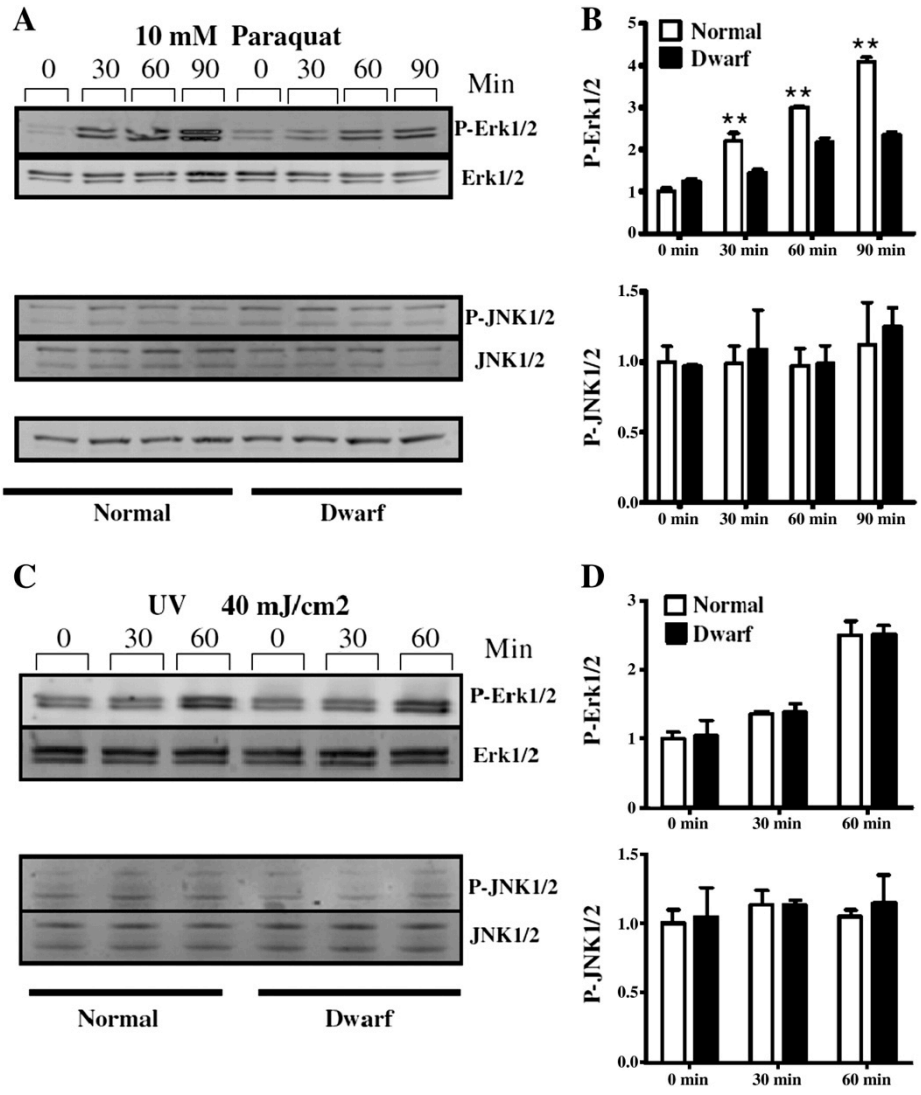

Figure 2-6. Phosphorylation of ERK1/2 and JNK1/2 in skin-derived primary fibroblasts from Snell dwarf and normal mice in response to (A,B) paraquat and (C,D) UV-C light.

After overnight serum removal, cells were treated with paraquat (10 mM) or exposed to UV-C light (40 mJ/cm^2) for the indicated time intervals.
(A,C) Representative immunoblots for phosphorylated and total forms of ERK1/2 and JNK1/2 proteins are shown. (B,D) The means and SEM, presented as ratios to unstressed controls at the start of treatment ($n = 6$; $p < 0.01$**).

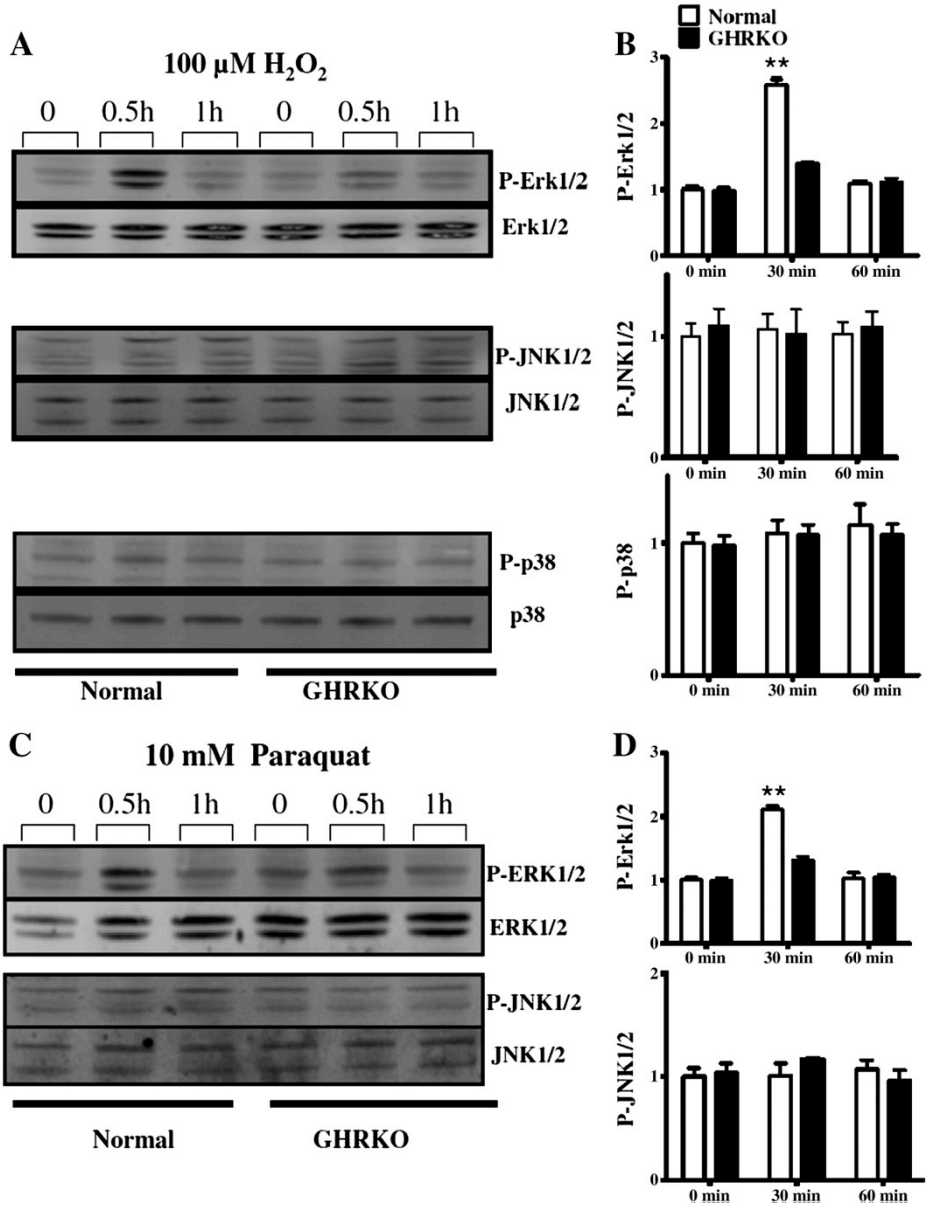

Figure 2-7. Phosphorylation of ERK1/2, JNK1/2, and p38 signaling in skin-derived primary fibroblasts from GHRKO and normal mice in response to (A,B) H_2O_2 and (C,D) paraquat.

After overnight serum removal, cells were treated with H_2O_2 (100 μM; equivalent to 600 nmol of H_2O_2 per 10^6 cells) or paraquat (10 mM) for the indicated time intervals. (A,C) Representative immunoblots for the phosphorylated and total forms of ERK1/2, JNK1/2, and p38 proteins are shown. (B,D) The means and SEM, presented as ratios to unstressed control cells at the start of treatment ($n = 5$; $p < 0.01$**).

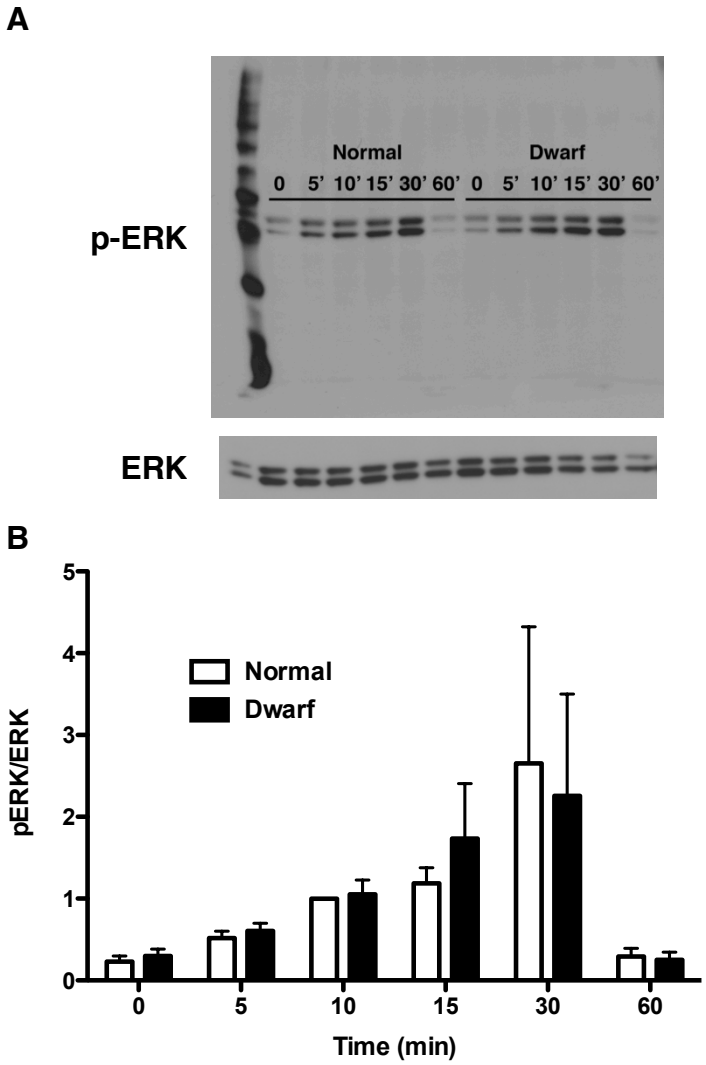

Figure 2-8. Delayed and transient ERK1/2 phosphorylation is observed in Snell and control fibroblasts in response to osmotic stress.

Snell and control fibroblasts were allowed to adhere for 48 h and deprived of serum overnight. The cells were exposed to 0.5 M NaCl added to base DMEM (320-355 mOsm/kg). (A) Representative immunoblots of p-ERK1/2 and total ERK1/2 proteins are shown. (B) Relative pERK/ERK intensity was expressed in comparison to levels seen in normal cells at the 10' time point. No significant genotypic difference between normal and dwarf cells was observed in signal intensity or kinetics (n = 4).

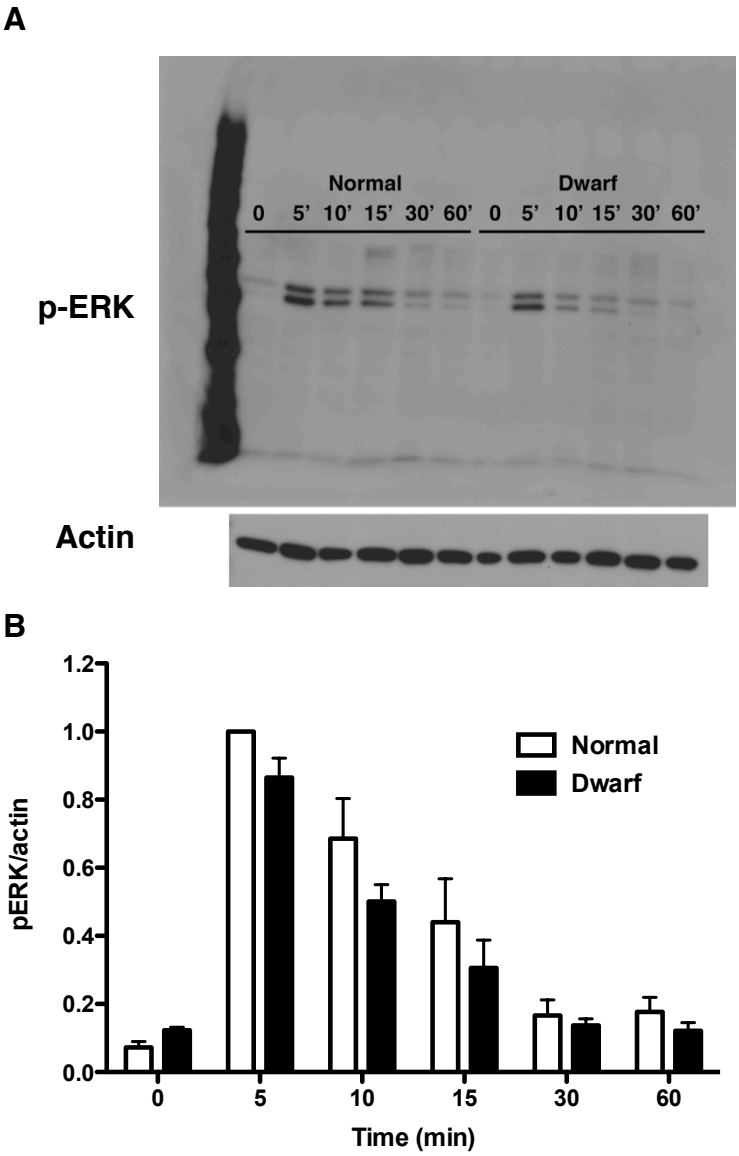

Figure 2-9. Rapid and transient ERK1/2 phosphorylation is observed in Snell and control fibroblasts in response to TNF-α.

Snell and control fibroblasts were allowed to adhere for 48 h, and then deprived of serum overnight. Cells were treated with TNF-α (10 ng/ml). (A) Representative immunoblots of p-ERK1/2 and total ERK1/2 proteins are shown. (B) Relative pERK/ERK intensity was normalized to the ratio seen in normal cells at the 5' time point. No significant genotypic difference between normal and dwarf cells was observed in peak levels or kinetics of ERK phosphorylation (n = 3).

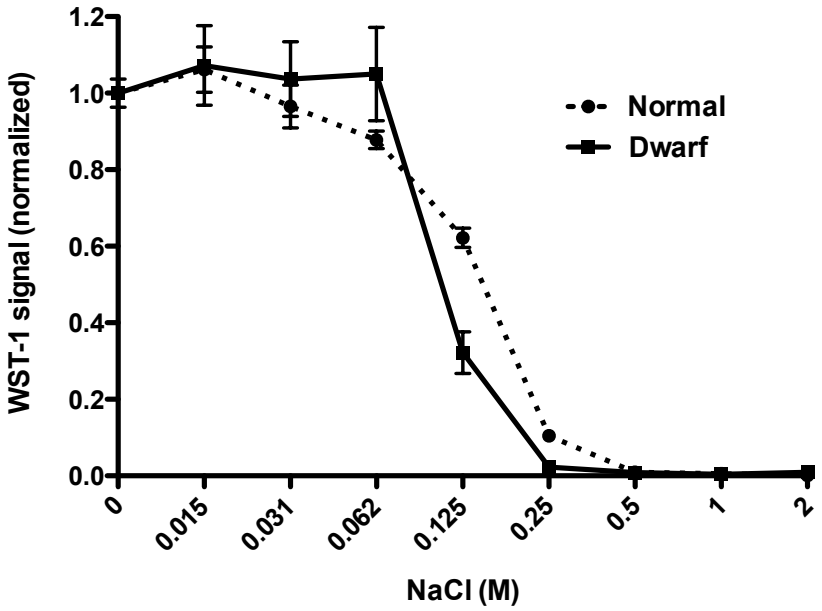

Figure 2-10. Snell dwarf dermal fibroblasts are not resistant to osmotic stress-induced death by sodium chloride.

Snell and control fibroblasts were allowed to adhere for 24 h and deprived of serum overnight. The cells were exposed to NaCl added to base DMEM (320-355 mOsm/kg) at various doses for 6 h. Cells were then washed with PBS and allowed to recover overnight in serum-free media. WST-1 was added for 3 h and analyzed by spectrophotometry. No significant difference in dose-sensitivity was observed between normal and dwarf cells (n = 2).

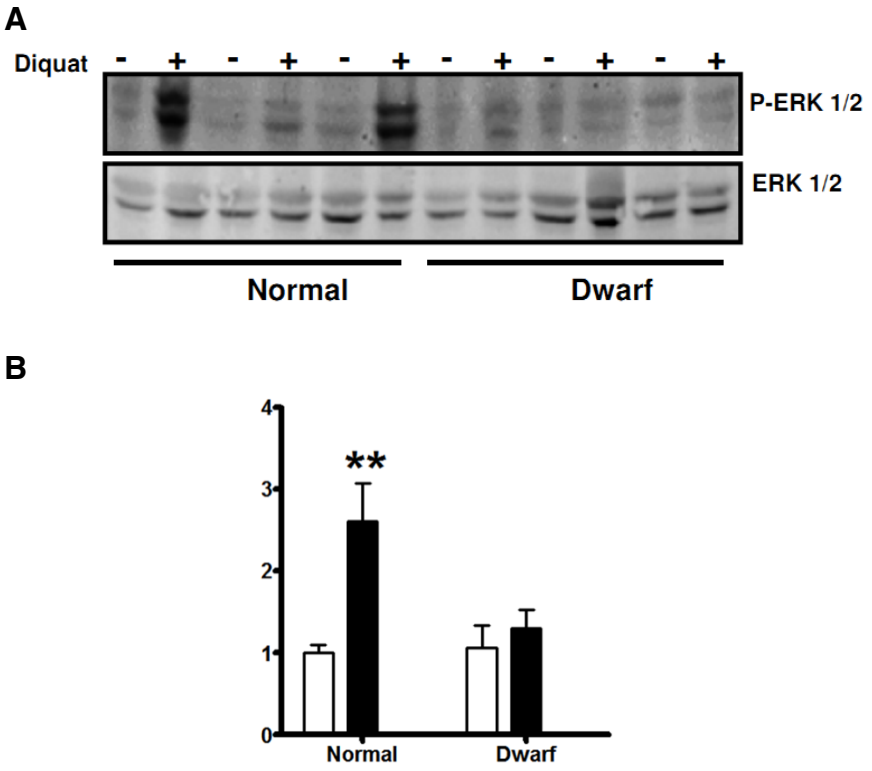

Figure 2-11. Phosphorylation of ERK1/2 in the liver of Snell and control mice in response to diquat exposure.

Snell and control mice were injected with diquat (50 mg/kg body weight) or saline and sacrificed after 6 h exposure. (A) Representative immunoblots of p-ERK1/2 and total ERK1/2 liver proteins are shown. (B) The means and SEM, presented as ratios to saline-injected control mice ($n = 6$; $p < 0.01$**).

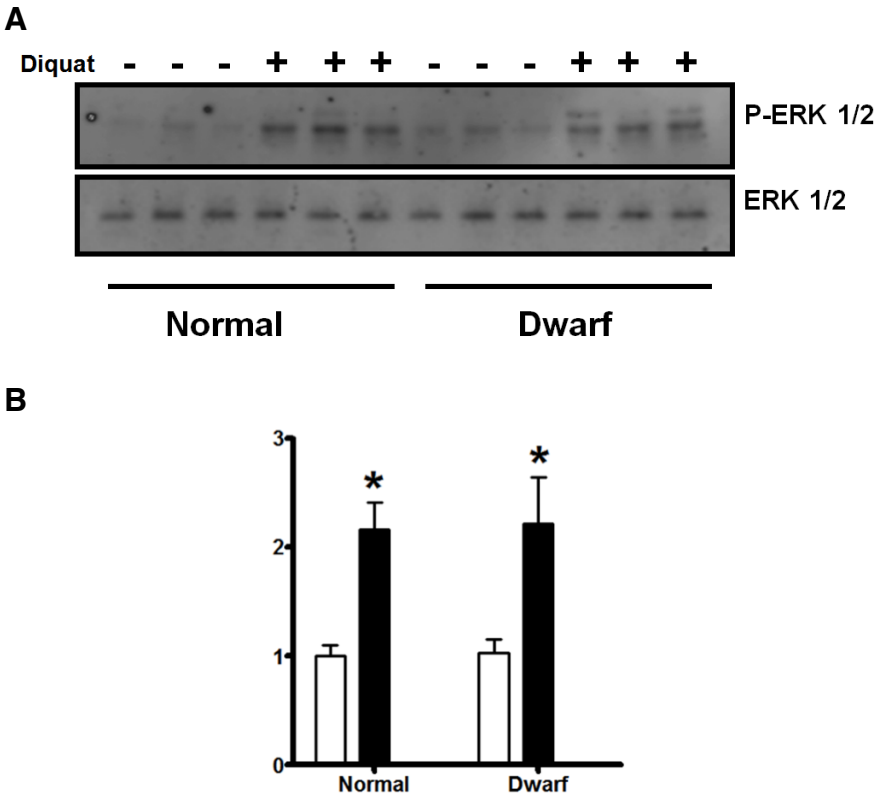

Figure 2-12. Phosphorylation of ERK1/2 in the hippocampus of Snell and control mice in response to diquat exposure.

Snell and control mice were injected with diquat (50 mg/kg body weight) or saline and sacrificed after 6 h exposure. (A) Representative immunoblots of p-ERK1/2 and total ERK1/2 hippocampal proteins are shown. (B) The means and SEM are presented as ratios to saline-injected control mice ($n = 6$; $p < 0.05$*).

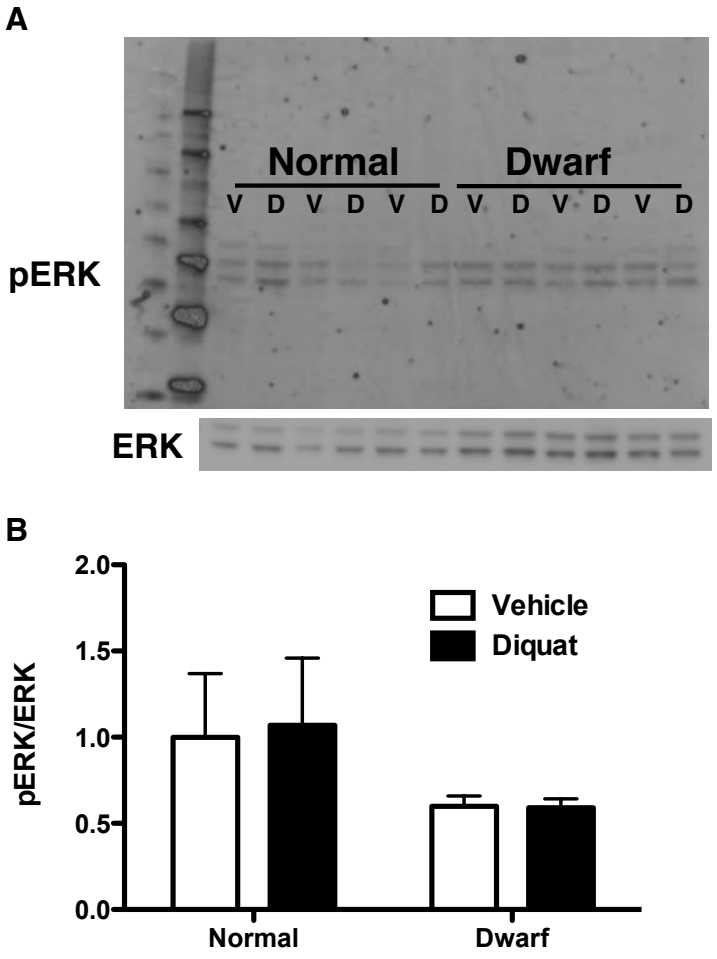

Figure 2-13. Phosphorylation of ERK1/2 in the heart of Snell and control mice in response to diquat exposure.

Snell and control mice were injected with diquat (50 mg/kg body weight) or saline and sacrificed after 6 h exposure. (A) Representative immunoblots of p-ERK1/2 and total ERK1/2 cardiac proteins are shown. (B) The means and SEM are presented as ratios to saline-injected control mice (n = 3).

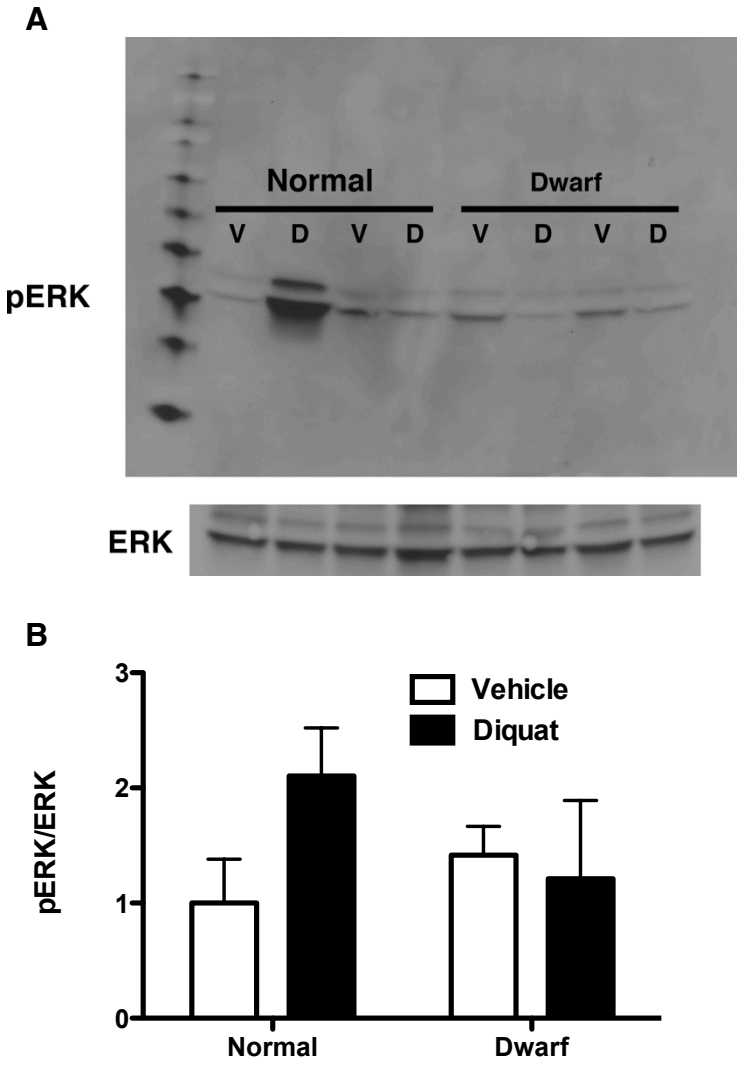

Figure 2-14. Phosphorylation of ERK1/2 in skeletal muscle of Snell and control mice in response to diquat exposure.

Snell and control mice were injected with diquat (50 mg/kg body weight) or saline and sacrificed after 6 h exposure. (A) Representative immunoblots of p-ERK1/2 and total ERK1/2 muscle proteins are shown. (B) The means and SEM are presented as ratios to saline-injected control mice (n = 3).

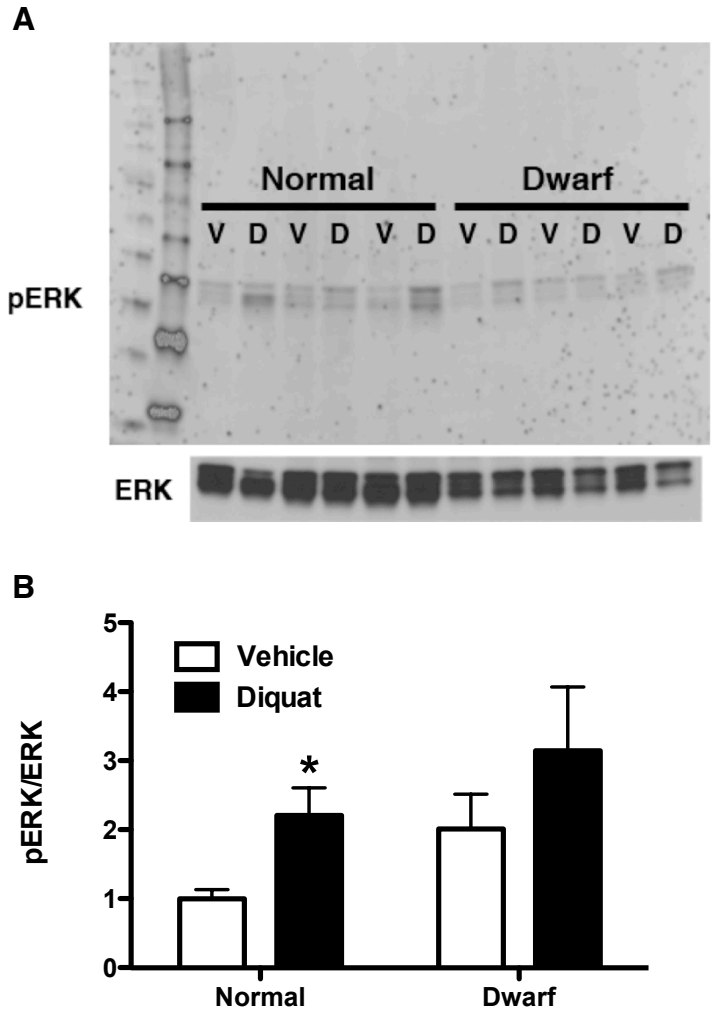

Figure 2-15. Phosphorylation of ERK1/2 in the lung of Snell and control mice in response to diquat exposure.

Snell and control mice were injected with diquat (50 mg/kg body weight) or saline and sacrificed after 6 h exposure. (A) Representative immunoblots of p-ERK1/2 and total ERK1/2 lung proteins are shown. (B) The means and SEM are presented as ratios to saline-injected control mice ($n = 5$; $p < 0.05$*).

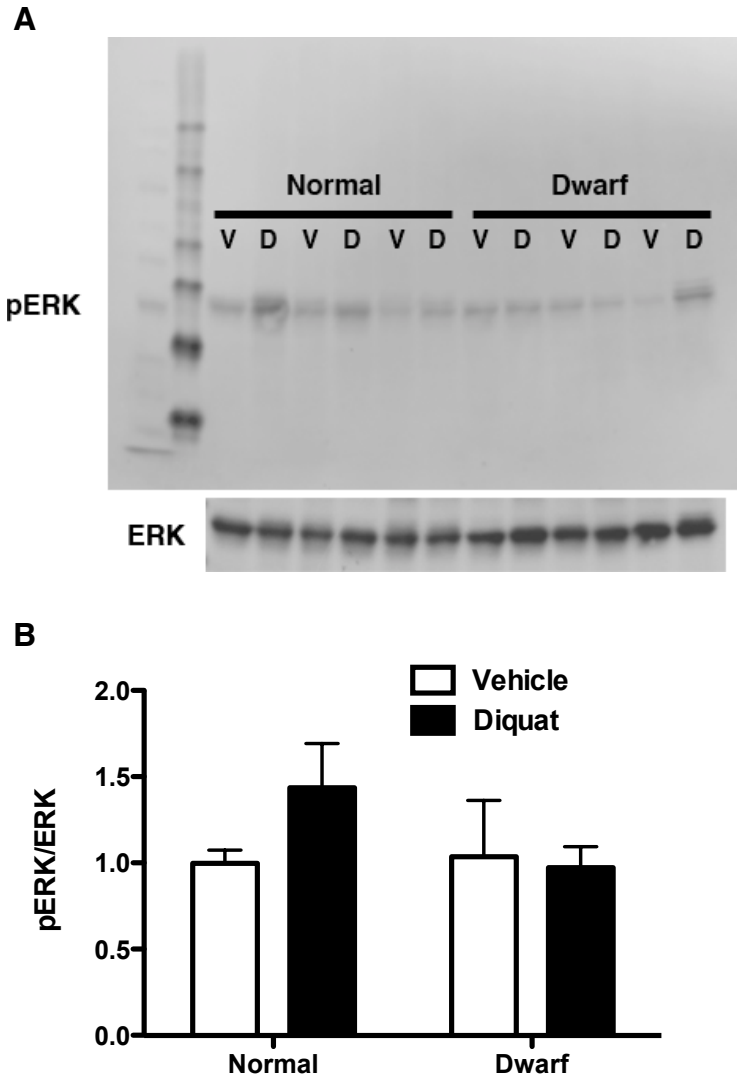

Figure 2-16. Phosphorylation of ERK1/2 in the kidney of Snell and control mice in response to diquat exposure.

Snell and control mice were injected with diquat (50 mg/kg body weight) or saline and sacrificed after 6 h exposure. (A) Representative immunoblots of p-ERK1/2 and total ERK1/2 kidney proteins are shown. (B) The means and SEM are presented as ratios to saline-injected control mice (n = 5).

2-8. References

1. Sun LY, Steinbaugh MJ, Masternak MM, Bartke A, Miller RA (2009) Fibroblasts from long-lived mutant mice show diminished ERK1/2 phosphorylation but exaggerated induction of immediate early genes. *Free Radic Biol Med* 47:1753–1761.

2. Spong A, Bartke A (2010) in *The Comparative Biology of Aging*, ed Wolf NS (Springer), pp 43–68.

3. Brown-Borg HM (2011) in *Handbook of the Biology of Aging*, eds Masoro EJ, Austad SN (Academic Press), pp 25–45. 7th Ed. Available at: http://dx.doi.org/10.1016/B978-0-12-378638-8.00002-6.

4. Brown-Borg HM, Borg KE, Meliska CJ, Bartke A (1996) Dwarf mice and the ageing process. *Nature* 384:33.

5. Flurkey K, Papaconstantinou J, Miller RA, Harrison DE (2001) Lifespan extension and delayed immune and collagen aging in mutant mice with defects in growth hormone production. *Proc Natl Acad Sci USA* 98:6736–6741.

6. Kinney BA, Meliska CJ, Steger RW, Bartke A (2001) Evidence that Ames dwarf mice age differently from their normal siblings in behavioral and learning and memory parameters. *Hormones and behavior* 39:277–284.

7. Ikeno Y, Bronson RT, Hubbard GB, Lee S, Bartke A (2003) Delayed occurrence of fatal neoplastic diseases in ames dwarf mice: correlation to extended longevity. *J Gerontol A Biol Sci Med Sci* 58:291–296.

8. Bartke A (2005) Minireview: role of the growth hormone/insulin-like growth factor system in mammalian aging. *Endocrinology* 146:3718–3723.

9. Zhou Y et al. (1997) A mammalian model for Laron syndrome produced by targeted disruption of the mouse growth hormone receptor/binding protein gene (the Laron mouse). *Proc Natl Acad Sci USA* 94:13215–13220.

10. Bonkowski MS, Rocha JS, Masternak MM, Al-Regaiey KA, Bartke A (2006) Targeted disruption of growth hormone receptor interferes with the beneficial actions of calorie restriction. *Proc Natl Acad Sci USA* 103:7901–7905.

11. Conover CA, Bale LK (2007) Loss of pregnancy-associated plasma protein A extends lifespan in mice. *Aging Cell* 6:727–729.

12. Boldt HB, Conover CA (2007) Pregnancy-associated plasma protein-A (PAPP-A): a local regulator of IGF bioavailability through cleavage of IGFBPs. *Growth Horm IGF Res* 17:10–18.

13. Conover CA (2010) PAPP-A: a new anti-aging target? *Aging Cell* 9:942–946.

14. Larsen PL (1993) Aging and resistance to oxidative damage in Caenorhabditis elegans. *Proc Natl Acad Sci USA* 90:8905–8909.

15. Martin GM, Austad SN, Johnson TE (1996) Genetic analysis of ageing: role of oxidative damage and environmental stresses. *Nat Genet* 13:25–34.

16. Lin YJ, Seroude L, Benzer S (1998) Extended life-span and stress resistance in the Drosophila mutant methuselah. *Science* 282:943–946.

17. Miller RA (2009) Cell stress and aging: new emphasis on multiplex resistance mechanisms. *J Gerontol A Biol Sci Med Sci* 64:179–182.

18. Murakami S, Salmon A, Miller RA (2003) Multiplex stress resistance in cells from long-lived dwarf mice. *FASEB J* 17:1565–1566.

19. Salmon AB et al. (2005) Fibroblast cell lines from young adult mice of long-lived mutant strains are resistant to multiple forms of stress. *Am J Physiol Endocrinol Metab* 289:E23–9.

20. Leiser SF, Salmon AB, Miller RA (2006) Correlated resistance to glucose deprivation and cytotoxic agents in fibroblast cell lines from long-lived pituitary dwarf mice. *Mech Ageing Dev* 127:821–829.

21. Maynard SP, Miller RA (2006) Fibroblasts from long-lived Snell dwarf mice are resistant to oxygen-induced in vitro growth arrest. *Aging Cell* 5:89–96.

22. Salmon AB, Sadighi Akha AA, Buffenstein R, Miller RA (2008) Fibroblasts from naked mole-rats are resistant to multiple forms of cell injury, but sensitive to peroxide, ultraviolet light, and endoplasmic reticulum stress. *J Gerontol A Biol Sci Med Sci* 63:232–241.

23. Kapahi P, Boulton ME, Kirkwood TB (1999) Positive correlation between mammalian life span and cellular resistance to stress. *Free Radic Biol Med* 26:495–500.

24. Harper JM, Salmon AB, Leiser SF, Galecki AT, Miller RA (2007) Skin-derived fibroblasts from long-lived species are resistant to some, but not all, lethal stresses and to the mitochondrial inhibitor rotenone. *Aging Cell* 6:1–13.

25. Harper JM et al. (2011) Fibroblasts from long-lived bird species are resistant to multiple forms of stress. *J Exp Biol* 214:1902–1910.

26. Tatar M, Bartke A, Antebi A (2003) The endocrine regulation of aging by insulin-like signals. *Science* 299:1346–1351.

27. de Luca C, Olefsky JM (2008) Inflammation and insulin resistance. *FEBS Lett* 582:97–105.

28. Xu J, Messina JL (2009) Crosstalk between growth hormone and insulin signaling. *Vitam Horm* 80:125–153.

29. Greer EL, Brunet A (2008) FOXO transcription factors in ageing and cancer. *Acta physiologica (Oxford, England)* 192:19–28.

30. Kenyon C, Chang J, Gensch E, Rudner A, Tabtiang R (1993) A C. elegans mutant that lives twice as long as wild type. *Nature* 366:461–464.

31. Slack C, Giannakou ME, Foley A, Goss M, Partridge L (2011) dFOXO-independent effects of reduced insulin-like signaling in Drosophila. *Aging Cell* 10:735–748.

32. Yamamoto R, Tatar M (2011) Insulin receptor substrate chico acts with the transcription factor FOXO to extend Drosophila lifespan. *Aging Cell* 10:729–732.

33. Sun L, Sadighi Akha AA, Miller RA, Harper JM (2009) Life-span extension in mice by preweaning food restriction and by methionine restriction in middle age. *J Gerontol A Biol Sci Med Sci* 64:711–722.

34. Selman C et al. (2008) Evidence for lifespan extension and delayed age-related biomarkers in insulin receptor substrate 1 null mice. *FASEB J* 22:807–818.

35. Taguchi A, Wartschow LM, White MF (2007) Brain IRS2 signaling coordinates life span and nutrient homeostasis. *Science* 317:369–372.

36. Mor A, Philips MR (2006) Compartmentalized Ras/MAPK signaling. *Annu Rev Immunol* 24:771–800.

37. Chang L, Karin M (2001) Mammalian MAP kinase signalling cascades. *Nature* 410:37–40.

38. Longo VD (2004) Ras: the other pro-aging pathway. *Science of aging knowledge environment : SAGE KE* 2004:pe36.

39. Holzenberger M et al. (2003) IGF-1 receptor regulates lifespan and resistance to oxidative stress in mice. *Nature* 421:182–187.

40. Bokov AF, Lindsey ML, Khodr C, Sabia MR, Richardson A (2009) Long-lived ames dwarf mice are resistant to chemical stressors. *J Gerontol A Biol Sci Med Sci* 64:819–827.

41. Reigart JR, Roberts JR (1999) in *Recognition and Management of Pesticide Poisonings* (US Environmental Protection Agency), pp 108–117.

42. Jones GM, Vale JA (2000) Mechanisms of toxicity, clinical features, and management of diquat poisoning: a review. *J Toxicol Clin Toxicol* 38:123–128.

43. Farrington JA, Ebert M, Land EJ, Fletcher K (1973) Bipyridylium quaternary salts and related compounds. V. Pulse radiolysis studies of the reaction of paraquat radical with oxygen. Implications for the mode of action of bipyridyl herbicides. *Biochim Biophys Acta* 314:372–381.

44. Vergara M, Smith-Wheelock M, Harper JM, Sigler R, Miller RA (2004) Hormone-treated snell dwarf mice regain fertility but remain long lived and disease resistant. *J Gerontol A Biol Sci Med Sci* 59:1244–1250.

45. Sun LY, Bokov AF, Richardson A, Miller RA (2011) Hepatic response to oxidative injury in long-lived Ames dwarf mice. *FASEB J* 25:398–408.

46. Sun LY, Al-Regaiey K, Masternak MM, Wang J, Bartke A (2005) Local expression of GH and IGF-1 in the hippocampus of GH-deficient long-lived mice. *Neurobiol Aging* 26:929–937.

47. Lithgow GJ, Miller RA (2008) in *Molecular Biology of Aging* (Cold Spring Harbor Monograph Archive).

48. Lee CK, Klopp RG, Weindruch R, Prolla TA (1999) Gene expression profile of aging and its retardation by caloric restriction. *Science* 285:1390–1393.

49. Weindruch R, Kayo T, Lee CK, Prolla TA (2001) Microarray profiling of gene expression in aging and its alteration by caloric restriction in mice. *J Nutr* 131:918S–923S.

50. Orentreich N, Matias JR, DeFelice A, Zimmerman JA (1993) Low methionine ingestion by rats extends life span. *J Nutr* 123:269–274.

51. Weindruch R, Sohal RS (1997) Seminars in medicine of the Beth Israel Deaconess Medical Center. Caloric intake and aging. *N Engl J Med* 337:986–994.

52. Coschigano KT, Clemmons D, Bellush LL, Kopchick JJ (2000) Assessment of growth parameters and life span of GHR/BP gene-disrupted mice. *Endocrinology* 141:2608–2613.

53. Harper JM et al. (2006) Stress resistance and aging: influence of genes and nutrition. *Mech Ageing Dev* 127:687–694.

54. Salmon AB, Ljungman M, Miller RA (2008) Cells from long-lived mutant mice exhibit enhanced repair of ultraviolet lesions. *J Gerontol A Biol Sci Med Sci* 63:219–231.

55. Li Y, Xu W, McBurney MW, Longo VD (2008) SirT1 inhibition reduces IGF-I/IRS-2/Ras/ERK1/2 signaling and protects neurons. *Cell Metab* 8:38–48.

56. Torres F, Quintana J, Estévez F (2010) 5,7,3“-trihydroxy-3,4-”dimethoxyflavone-induced cell death in human leukemia cells is dependent on caspases and activates the MAPK pathway. *Mol Carcinog* 49:464–475.

57. Mckay MM, Morrison DK (2007) Integrating signals from RTKs to ERK/MAPK. *Oncogene* 26:3113–3121.

58. Murphy LO, Blenis J (2006) MAPK signal specificity: the right place at the right time. *Trends Biochem Sci* 31:268–275.

59. Johnson GL, Lapadat R (2002) Mitogen-activated protein kinase pathways mediated by ERK, JNK, and p38 protein kinases. *Science* 298:1911–1912.

60. Wada T, Penninger JM (2004) Mitogen-activated protein kinases in apoptosis regulation. *Oncogene* 23:2838–2849.

61. Subramaniam S et al. (2004) ERK activation promotes neuronal degeneration predominantly through plasma membrane damage and independently of caspase-3. *J Cell Biol* 165:357–369.

62. Pryor WA (1982) Free radical biology: xenobiotics, cancer, and aging. *Ann N Y Acad Sci* 393:1–22.

63. Sukhatme VP et al. (1988) A zinc finger-encoding gene coregulated with c-fos during growth and differentiation, and after cellular depolarization. *Cell* 53:37–43.

64. Adamson ED, Mercola D (2002) Egr1 transcription factor: multiple roles in prostate tumor cell growth and survival. *Tumour Biol* 23:93–102.

65. Murphy LO, MacKeigan JP, Blenis J (2004) A network of immediate early gene products propagates subtle differences in mitogen-activated protein kinase signal amplitude and duration. *Mol Cell Biol* 24:144–153.

66. Hsieh C-C, Papaconstantinou J (2009) Dermal fibroblasts from long-lived Ames dwarf mice maintain their in vivo resistance to mitochondrial generated reactive oxygen species (ROS). *AGING* 1:784–802.

67. Amador-Noguez D et al. (2007) Alterations in xenobiotic metabolism in the long-lived Little mice. *Aging Cell* 6:453–470.

68. Kennedy MA, Rakoczy SG, Brown-Borg HM (2003) Long-living Ames dwarf mouse hepatocytes readily undergo apoptosis. *Exp Gerontol* 38:997–1008.

69. Sadighi Akha AA et al. (2011) Heightened induction of proapoptotic signals in response to endoplasmic reticulum stress in primary fibroblasts from a mouse model of longevity. *J Biol Chem* 286:30344–30351.

70. McCullough KD, Martindale JL, Klotz LO, Aw TY, Holbrook NJ (2001) Gadd153 sensitizes cells to endoplasmic reticulum stress by down-regulating Bcl2 and perturbing the cellular redox state. *Mol Cell Biol* 21:1249–1259.

71. Li J, Holbrook NJ (2004) Elevated gadd153/chop expression and enhanced c-Jun N-terminal protein kinase activation sensitizes aged cells to ER stress. *Exp Gerontol* 39:735–744.

72. Song B, Scheuner D, Ron D, Pennathur S, Kaufman RJ (2008) Chop deletion reduces oxidative stress, improves beta cell function, and promotes cell survival in multiple mouse models of diabetes. *J Clin Invest* 118:3378–3389.

73. Sierra F (2006) Is (your cellular response to) stress killing you? *J Gerontol A Biol Sci Med Sci* 61:557–561.

74. Panici JA et al. (2010) Early life growth hormone treatment shortens longevity and decreases cellular stress resistance in long-lived mutant mice. *FASEB J* 24:5073–5079.

75. Sun LY (2006) Hippocampal IGF-1 expression, neurogenesis and slowed aging: clues to longevity from mutant mice. *AGE* 28:181–189.

CHAPTER 3

Activation of genes involved in xenobiotic metabolism is a shared signature of mouse models with extended lifespan

3-1. Abstract

Xenobiotic metabolism has been proposed to play a role in modulating the rate of aging. XMEs are expressed at higher levels in calorically restricted mice (CR) and in GH/IGF-1-deficient long-lived mutant mice. In this study, we show that many phase I XME genes are similarly upregulated in additional long-lived mouse models, including “crowded litter” (CL) mice, whose lifespan has been increased by food restriction limited to the first 3 weeks of life, and in mice treated with rapamycin. Induction in the CL mice lasts at least through 22 months of age, but induction by rapamycin is transient for many of the mRNAs. Cytochrome p450s, flavin monooxygenases, hydroxyacid oxidase, and metallothioneins were found to be significantly elevated in similar proportions in each of the models of delayed aging tested, whether these are based on mutation, diet, drug treatment, or transient early intervention. The same pattern of mRNA elevation can be induced by 2 weeks of treatment with tert-butylhydroquinone, an oxidative toxin known to activate Nrf2-dependent target genes. These results suggest that elevation of phase I XMEs is a hallmark of long-lived mice and that elevation of

these mRNAs may facilitate screens for agents that could be tested for effects on health and lifespan in mice.

3-2. Introduction

Lifespan, including maximum lifespan, can be extended in mice by genetic, dietary, and pharmacological interventions. Mutations associated with reduced action of GH and/or IGF-1 can increase mouse lifespan by 40% or more (1). Ames dwarf (*Prop1*$^{df/df}$) (2) and Snell dwarf (*Pit1*$^{dw/dw}$) (3) mice carry spontaneous loss-of-function mutations that result in improper pituitary development and a reduction in somatotrophs. Growth hormone receptor knockout (*Ghr/bp*$^{-/-}$ or "GHRKO") (4) and growth hormone releasing hormone receptor (*Ghrhr*$^{lit/lit}$ or "Little") mice (3) are also long-lived compared to their respective controls, and additional mutations affecting GH and/or IGF-1 action have been shown to be associated with extended longevity (5).

Slow aging and extended lifespan can also be induced by dietary interventions. Long-term CR has been shown to extend lifespan in multiple rodent stocks (6), as well as in genetically heterogeneous mice (7). Short-term, transient nutrition restriction imposed during the developmental period prior to weaning extends lifespan in mice (8). An enlargement of litter size by 50% ("crowded litter" or CL model) to 12 pups per mother instead of the normal 8 pups per mother during the first 3 weeks of postnatal development has been shown increase median lifespan by 18% in a heterogeneous mouse population (8). In addition, these mice were reported to have lower circulating IGF-1 and maintain a

small, but significant reduction in body weight throughout adulthood (8). Ames mice on CR diets live longer than the same mutants fed ad libitum, suggesting that CR and the Ames mutation may extend lifespan at least partially through different mechanisms (9), although CR diets apparently do not further increase lifespan in GHRKO mice (10). Pharmacologic interventions that extend mouse lifespan have only recently been described, with evidence that rapamycin can extend longevity in several stocks (11-14), presumably through reduced TOR function.

In this study, we sought to identify biochemical pathways that might be regulated in similar ways in mice in which lifespan has been extended by drugs, diets, or mutations. We focused on expression of genes that encode XMEs, based on previous publications that have indicated elevated expression of these genes in slow-aging mice. Meta-analysis of CR and long-lived dwarf mice microarrays revealed that phase I enzymes, particularly cytochrome p450s, flavin monooxygenases, hydroxyacid oxidase, and metallothioneins were found to be elevated in liver tissue (15). These enzymes play a protective role against environmental toxins and interact with phase II conjugation enzymes, enhancing hydrophilicity and excretion rate of compounds, which are then exported into bile by downstream phase III transporters (16). Elevated systemic resistance to oxidative toxins, such as acetaminophen or paraquat, is a hallmark of long-lived dwarf (17-19) and diet-restricted mice (20), but has not been evaluated in CL or rapamycin-treated mice.

3-3. Materials and Methods

Animals

The CL, CR, rapamycin-treated, and tBHQ-treated mice were of UM-HET3 stock; they were the offspring of crosses between (BALB/cByJ x C57BL/6J)F1 females and (C3H/HeJ x DBA/2J)F1 males (21).

Snell dwarf (*dw/dw*) and heterozygote (*dw/+*) control mice were bred as the progeny of (DW/J x C3H/HeJ)F1 *dw/+* females and (DW/J x C3H/HeJ)F1 *dw/+* males; the sires had been treated with growth hormone and thyroxine to increase their fertility (22).

GHRKO mice and littermate controls were maintained in the laboratory of Dr. Andrzej Bartke at Southern Illinois University from stock produced by Dr. John Kopchick's group at Ohio University, as previously described (23). The genetic background of these animals is derived from 129/Ola embryonic stem cells and includes contributions from BALB/c, C57BL/6, and C3H inbred strains.

All mice evaluated in this study were male. Animals were weaned at 3 weeks of age and housed 3 mice (HET3, Snell) or 5 mice (GHRKO) per cage. All animals were given free access to food and water, except for the CR cohort. Mice were maintained using standard specific pathogen-free (SPF) husbandry techniques; sentinel animals were exposed to spent bedding on a quarterly basis to check for possible pathogens, and all such tests came up negative over the course of the study.

CL, CR, and rapamycin-treated cohorts

CL mice were generated following the procedure described previously (8). HET3 litters were culled to 8 pups (control mice) or supplemented by transfer of newborn mice to produce litters of 12 mice (CL mice). Litters were weaned at 3 weeks of age and housed thereafter at 3 mice per cage. To control for the potentially confounding effect of differing levels of nutrition experienced in utero, litters originally including fewer than 8, or more than 10, pups were not used. After weaning, both groups were fed control Purina 5LG6 chow ad libitum. CL mice were euthanized at 12 or 22 months of age.

CR mice were given 80% of the amount of food consumed by AL control mice starting at 6 weeks of age. At 10 weeks of age, CR mice were switched to 60% AL diet and then kept at that level until sacrifice at 12 months of age. Previous studies have demonstrated a robust CR effect on lifespan using this protocol (9), and a similar regimen extends longevity in HET3 mice (7).

The rapamycin-treated cohort was administered 14 ppm of microencapsulated rapamycin in 5LG6 chow, starting at 9 months of age, following the same protocol used in our previous reports (12, 13). Rapamycin-treated mice were sacrificed at 12 or 22 months of age.

tBHQ administration

Tert-butylhydroquinone (tBHQ)-treated food was prepared fresh weekly in 500 g batches in our laboratory using powdered Purina 5001 chow. tBHQ (Sigma-Aldrich) was added into powdered chow at 1% w/w. A Knox gelatin

solution (4% w/w, relative to chow weight) was prepared in ddH_2O, heated to 60°C and allowed to cool to 30°C. The gelatin solution was then added to the powdered chow/tBHQ mix and refrigerated overnight. Young adult male HET3 mice, 6 months of age, were administered 1% tBHQ-treated food, or control food prepared in the same manner without drug, for 2 weeks prior to euthanasia.

RNA isolation from liver

Liver tissue was washed with ice-cold PBS, snap frozen in liquid nitrogen, and stored at -80°C. Sectioned liver samples were suspended in TRIzol reagent (Life Technologies), homogenized for 30 s, and then sonicated for 30 s using 10 s pulse, 5 s rest intervals on ice. RNA was isolated by phenol/chloroform extraction to yield total RNA following the manufacturer's instructions. Samples were dissolved in 500 μL of RNase-free ddH_2O, and RNA concentration was quantified by spectrophotometry using a NanoDrop 1000. Samples were then stored at -80°C until later use.

Real-time RT-PCR

Quantitative real-time PCR analysis was performed by two-step reaction, by first generating cDNA with the iScript cDNA synthesis kit (Bio-Rad Laboratories). Amplification was measured using SYBR Green I (Bio-Rad Laboratories) and a RotorGene 6000 cycler (Corbett Research). After an initial denaturation step (95°C for 180 s), amplification was performed over 45 cycles of denaturation (95°C for 10 s), annealing (58°C for 6 s), and elongation (72°C for 13 s). The $\Delta\Delta C_t$ comparative method ($\Delta C_{ttarget}$ - ΔC_{tactin}) was used to determine

relative gene expression levels. Primer sequences are available in Table 3-1 and Table 3-2.

Cytochrome P450 enzymatic activity assay

CYP1A and CYP2B activity was measured by resorufin conversion from methoxyresorufin (MROD), ethoxyresorufin (EROD), or pentoxyresorufin (PROD), as previously described (24). Liver samples were collected from mice fed chow containing 1% tBHQ or control chow for 50 days that were exposed to 50 mg/kg diquat or saline for 6 h prior to dissection. Unfrozen liver samples were briefly homogenized with a Potter-Elvehjem homogenizer and suspended in sucrose buffer. Microsomes were isolated via ultracentrifugation with the commercially available Endoplasmic Reticulum Isolation Kit (ER0100; Sigma). Changes in resorufin fluorescence were measured in 96-well microtiter plates following the protocol outlined in the commercially available Cytochrome P450 2B Fluorescent Detection Kit (CYTO2B; Sigma).

Assessment of diquat-induced hepatotoxicity

Serum alanine aminotransferase (ALT) and lactate dehydrogenase (LDH) activity was measured in plasma samples collected from diquat or saline-treated male HET3 mice fed either tBHQ-treated or control chow for 50 days. ALT and LDH activity was measured using commercially available kits (Catachem, Oxford, CT, USA) in a 96-well microtiter plate following the manufacturer's recommended protocol.

Statistical Analyses

All bar graphs show mean values ± SEM, normalized to the levels seen in the corresponding control animals. Differences between treatment groups were evaluated using a two-tailed, unpaired t-test, with $p < 0.05$ as the criterion for statistical significance. Scatterplot correlation analysis was performed using Spearman's rank correlation coefficient, with $p < 0.05$ as the criterion for significance.

3-4. Results

Litter crowding during weaning results in stable upregulation of xenobiotic metabolism genes

Previous work had shown that CL mice, given limited access to food for the 3 week period between birth and weaning, lived 18% longer than control mice (8). To evaluate the extent to which patterns of gene expression in CL mice might resemble those in CR mice, we measured mRNA levels in liver for genes involved in phase I (Table 3-1) and phase II (Table 3-2) biotransformation. Of 19 such phase I mRNAs evaluated, 17 were found to be elevated in liver of 12-month-old CL mice, and 6 of these were significantly elevated in a comparison of 6 CL mice to 6 controls (Table 3-3). In parallel, we measured mRNA levels in 12-month-old CR mice of the same genetically heterogeneous stock (Table 3-4). Comparison of the mRNA levels in CL and CR mice showed a close correspondence (Figure 3-1A), with a correlation $R = 0.79$ ($p < 0.001$). These results show that a brief period of food restriction limited to the first 3 weeks of life

is sufficient to establish an altered pattern of liver gene expression that is retained for at least 11 months after the end of the intervention, and that the pattern resembles that produced by long-term CR.

To see whether similar over-expression of genes involved in phase I xenobiotic metabolism also affected mice in which slowed aging was due to genetic or pharmacologic interventions, we evaluated the same set of mRNAs in 12-month-old Snell mice, and in HET3 mice given a diet containing rapamycin (12, 13) from 9 months of age. Results shown in Figure 3-2B,C demonstrate that the pattern of genes overexpressed in CL and CR mice also characterizes age-matched Snell and rapamycin-treated mice. The gene expression pattern in the CL mice is also similar to that seen in mice exposed to cholic acid (CA), a known inducer of xenobiotic detoxification genes; Figure 3-1D compares our results from CL mice with published levels (18) for 2-4 month old mice of the C57BL/6J background, tested after 7 days of exposure to 2% CA. Means and standard errors for mRNA for the rapamycin-treated and Snell mice are listed in Table 3-5 and Table 3-6. Thus, elevation of genes involved in phase I xenobiotic detoxification is characteristic of CL, CR, Snell, and rapamycin-treated mice, and is similar to the pattern induced by short-term exposure to a bile acid.

Elevated levels of many xenobiotic metabolism genes are seen at both 12 and 22 months of age in CL mice

To see if the gene expression pattern observed in 12-month-old CL mice remained stable through adult life, we measured gene expression in 22-month-old animals and compared the mRNA levels to control mice at 12 or 22

months (Figure 3-2). All 6 phase I genes that were significantly elevated at 12 months of age in CL liver remained elevated in 22-month-old CL mice relative to 12-month-old control mice. 4 of these 6 mRNAs, i.e. Cyp2b2, Cyp2b13, Fmo3, and Hao3, were also found to be significantly higher in 22-month controls than in 12-month controls (Table 3-7). These 4 genes are thus increased in the first year of life by the CL intervention, and then in later life by the aging process itself in mice not subjected to CL. The majority of phase I enzymes that were not significantly elevated in CL mice at 12 months of age did not change at 22 months of age, but Cyp1a2 and Cyp3a41 were found to be significantly decreased in 22-month-old CL mice (Figure 3-3).

The duration of rapamycin treatment has differential effects on xenobiotic metabolism gene expression

Mice treated with rapamycin for 3 months, starting at 9 months of age, had elevated expression of 14 of the 19 phase I xenobiotic metabolism genes evaluated in liver of 12-month-old mice (Table 3-5), and 9 of these were significantly elevated compared to age-matched controls. To see whether rapamycin, like the CL intervention, leads to long-lasting activation of these mRNAs, we evaluated liver of 22-month-old mice that had been treated with rapamycin from 9 months onward. Figure 3-4 shows the results for each of the 9 mRNAs found to be significantly elevated in the 12-month-old rapamycin mice. Seven of these 9 mRNAs were at lower levels in 22-month-old rapamycin mice than they had been at 12 months of age, and 4 were significantly lower. Three genes, Cyp2c38, Cyp4a10 and Por, were at significantly lower levels in

22-month-old rapamycin-treated mice than in age-matched controls, and a fourth mRNA (Hao3) was also significantly lower in the rapamycin treated mice than in 22-month-old controls. Other mRNAs elevated by rapamycin in the 12-month-old mice, however, such as Cyp1a1 and Fmo3, remained elevated in the 22-month-old mice. Among the 9 mRNAs significantly activated by rapamycin at 12 months of age, 6 showed a significant age-associated increase among control mice, reminiscent of age-related increases in genes sensitive to CL (Figure 3-2). Additionally, Cyp2b10 and Cyp3a41, which were not significantly increased by rapamycin at 12 months of age, were found to be significantly downregulated at 22 months of age (Figure 3-5). Thus it appears that the effects of rapamycin treatment seen after 3 months are, for many genes, transient, with mRNA levels returning to baseline levels or even, in some cases, below the levels seen in young or old control mice.

The Nrf2 activator tBHQ increases xenobiotic metabolism

To see if some of mRNAs that were elevated in these slow-aging mice could be activated acutely, we evaluated hepatic phase I XME mRNAs in young adult HET3 mice after 2 weeks of exposure to tBHQ, which induces the transcription factor Nrf2 (25). All 19 of the phase I mRNAs tested showed an elevation in tBHQ-treated mice, and 13 of these showed statistically significant increases (Table 3-8). The scatterplots shown in Figure 3-6 compare the patterns of phase I xenobiotic mRNAs in tBHQ-treated mice to those of 12-month-old CR, CL, Snell, and rapamycin-treated mice, together with data from a published study

of young adult CA-treated mice (18). There are strong and significant correlations with tBHQ exposure and the pattern of mRNAs seen in the CR, CL, Snell and CA-treated models, but changes in xenobiotic metabolism in rapamycin-treated mice do not resemble those seen in tBHQ-treated mice (Figure 3-6D). For a more comprehensive test of similarities among these various models, we calculated the correlation coefficients for each of the systems studied in our laboratory, together with our data on GHRKO mice (Table 3-9) and published data for Little mice and CA-treated mice (18). Figure 3-7 tabulates these correlation coefficients, and shows the expected high correlation ($R > 0.7$) among the mutants with blocks in the GH/IGF-1 pathway, i.e. Snell, GHRKO, and Little mice. The two dietary interventions, CR and CL, are well correlated ($R > 0.5$) with one another and with each of the GH/IGF-1 mutant mice, and the same is true for mRNAs in mice subject to short-term exposure to CA (18) or tBHQ. The exception is rapamycin, for which there are significant correlations with CR, CL and CA-treated mice, but less agreement with mRNA patterns in the tBHQ-treated mice, or with the Snell, GHRKO, and Little mice.

In addition to changes in mRNA expression, we evaluated hepatic cytochrome P450 activity and liver damage in tBHQ-treated mice in response to challenge with the oxidative stressor diquat, following the same protocol described in Section 2-3. Resorufin formation from methoxyresorufin (MROD), ethoxyresorufin (EROD), and/or pentoxyresorufin ethers is indicative of CYP1A and CYP2B enzymatic activity. tBHQ-treated mice were found to have

significantly increased MROD both before and after exposure to diquat (Figure 3-8A). EROD and PROD were significantly higher in tBHQ-treated mice exposed to diquat relative to mice on control food exposed to diquat (Figure 3-8B,C). These results indicate that the Nrf2 activator tBHQ increases both XME mRNA levels and xenobiotic metabolism activity. tBHQ-treated mice exposed to an oxidative stress agent (e.g. diquat) were found to have increased hepatotoxicity (as measured by plasma ALT, LDH levels) relative to diquat-treated mice on control food (Figure 3-9), similar to Ames, Snell and GHRKO mice (19, 20). tBHQ-treated mice, like GH/IGF-1-deficient dwarf mice, may have increased liver damage in response to toxins due to an enhanced rate of xenobiotic metabolism that rapidly depletes reduced glutathione stores, and is discussed in greater detail in Section 4-2.

In addition, mice with hepatocyte-specific deletion of Keap1 (*Alb-Cre::Keap1*$^{flox/-}$) have similar elevations of XME mRNAs (26) as Snell (Figure 3-10A), GHRKO (Figure 3-10B, and Little mice (Figure 3-10C). No significant correlation in XME gene expression was observed between *Alb-Cre::Keap1*$^{flox/-}$ mice (26) and CR mice (Figure 3-10D), CL mice (Figure 3-10E), tBHQ-treated mice (Figure 3-10F), or rapamycin-treated mice (data not shown). These results indicate that the changes observed in XME gene expression in GH/IGF-1-deficient dwarf mice are a result of increased Nrf2 activity. The poor correlation between *Alb-Cre::Keap1*$^{flox/-}$ mice (26) and tBHQ-treated mice (Figure 3-10F) is paradoxical, but was performed using only 9 XME

genes, and may also be reflective of differences in the kinetics of Nrf2 activation between these two models. *Alb-Cre::Keap1*$^{flox/-}$ mice have a constitutive increase in Nrf2 activity in the liver (26), whereas tBHQ-treated mice may have a more transient pattern of Nrf2 activation in response to feeding cycles.

Phase I XME genes are similarly expressed in genetic, dietary, and pharmacological interventions that extend lifespan

Table 3-10 assembles phase I gene expression data for each of these 8 model systems, listing in each case the ratio of mRNA levels in the slow-aging mice to levels in the corresponding set of control mice. As a crude index of the extent of mRNA elevation, the table also includes the geometric mean value for the set of ratios in each column. From this perspective the elevation of phase I genes is strongest in the mutant and CR mice, which also show the largest increase in longevity, and smaller in the CL and rapamycin mice, where the longevity effect is significant but not as large as in dwarf or CR animals. Some mRNAs, including Cyp2b13, Cyp2b9, Cyp4a14, Fmo3 and Hao3 show strong elevations, at least 3-fold and as high as 7500-fold, in each of the mouse models known to be long-lived, in addition to mice treated with tBHQ or CA. Other mRNAs, however, such as Cyp1a2, show only minor and inconsistent changes.

Parallel analyses of phase II XME mRNAs

In addition to phase I XME genes, we also measured changes in phase II gene expression in CL mice (Table 3-11), CR mice (Table 3-12), rapamycin-treated mice (Table 3-13), tBHQ-treated mice (Table 3-14), Snell mice (Table

3-15), and GHRKO mice (Table 3-16), summarized in Table 3-17. Phase II XMEs were found to be slightly upregulated in CL mice (16 out of 17 genes evaluated), but only 2 genes (Gsto2, Mgst3) were significantly elevated in a comparison of 6 CL mice to 6 controls (Table 3-11). In contrast, long-term CR induced a more robust increase in expression of phase II enzymes, seen in 16 out of 17 genes, with 10 genes found to be significantly elevated in relative to control mice fed ad libitum (Table 3-12). The Nrf2 activator tBHQ also robustly induced phase II enzymes, seen in 16 out of 17 genes measured, with 8 genes reported to be elevated relative to untreated littermate control mice (Table 3-14). However, rapamycin treatment, like the CL intervention, was found to weakly induce phase II XMEs, with a small increase observed in 16 of the 17 genes evaluated. Only 3 genes (Gsto2, Mgst3, Nqo1) were found to be significantly upregulated by rapamycin in comparison to untreated control mice (Table 3-13).

Age-associated changes in 9 out of 10 phase II XMEs were also observed between 12-month-old and 22-month-old control HET3 mice, with significant increases seen in Gstm3, Gsto, and Nqo1 mRNA expression (Table 3-18). However, similar to phase I XME genes, phase II XMEs were largely unaffected by age in CL mice. Only a CL-specific decrease in Ugt1a9 expression was observed in 22-month-old mice compared to 12-month-old mice (Figure 3-11). Therefore, the CL intervention appears to induce a stable change in XME gene expression that is largely maintained at both 12 and 22 months of age. Age-associated downregulation of multiple phase II XMEs (Cyt19, Gsta2, Gsta4,

Gstt2, and Papss2) was also observed in 22-month-old mice compared to 12-month-old mice treated with rapamycin (Figure 3-12).

Phase II genes, like phase I XMEs, are elevated by multiple genetic, dietary, and pharmacological interventions that extend lifespan (Table 3-17). However, these changes are generally smaller in magnitude, with the exception of Sult2a2, which is elevated >2000-fold in Snell, GHRKO, and Little mice. Similar upregulation of phase II XME genes was only observed between Snell and Little (Figure 3-13) mice, as well as tBHQ and CA-treated mice, based on the panel of 17 genes evaluated (Figure 3-14).

3-5. Discussion

Xenobiotic metabolism enzymes have been reported to be transcriptionally upregulated in long-lived dwarf mice and mice on long-term CR (15). In this study, we show that rapamycin, tBHQ, and CL also lead to transcriptional activation of both phase I and phase II XMEs in mice, consistent with the patterns previously reported in CR and long-lived dwarf models. Whether xenobiotic metabolism activity contributes to extension of lifespan in mammals is unknown, but microarray studies in *C. elegans* support such a hypothesis (27). Based on our data, we propose that transcriptional elevation of XME genes is a common signature of delayed or decelerated aging in mice, whether based on dietary, pharmacological, developmental or genetic changes, and we suggest that activation of this and related detoxification systems may contribute to slower aging in these animal models.

Long-term CR elevates XME expression in mouse liver tissue, depending on the age of the mice and the duration of restriction (15, 28). CR extends lifespan and decreases the risk of cancer and other age-associated pathologies in rodents (6, 29, 30). Physiological and biologic studies have produced a large and growing list of differences between CR and control mice. Mice on CR have elevated antioxidant defenses (31, 32) and are resistant to multiple hepatotoxins (20, 31). The extent to which such changes contribute to increased lifespan in each case is uncertain, and the mechanism of slowed aging in CR rodents is still an area of active investigation. Whether CR can extend lifespan and delay aging in humans has not been evaluated, but an ongoing study of monkeys on CR suggests that results generated in rodents and other model organisms may also be applicable to primates (33).

Short-term CR during weaning by increasing the number of pups nursed by an individual mother produces “crowded litter” (CL) mice that are long-lived (8), presumably because of restricted nutrient availability at this early period in post-natal life. The mechanism behind CL-mediated lifespan extension is not understood, but presumably reflects stable epigenetic changes in gene expression in one or more cell types. Early, transient alterations in hormone levels can have strong, long-lasting effects on aging and lifespan. For example, short-term, intensive exposure of Ames mice to GH starting at 2 weeks of age reverses both their extended lifespan and cellular stress resistance (34). Circulating IGF-1 is reduced, at least at weaning, in CL mice (20), as it is in

young CR mice (35), suggesting that reduced GH/IGF-1 levels in early life may produce long-lasting changes that postpone aging and extend lifespan in both CL and CR mice.

The observation that diet-based interventions associated with lifespan extension upregulate XMEs led us to ask whether such changes would be seen in mice in which extended longevity was produced pharmacologically. Research conducted by the ITP (36) has shown that rapamycin extends mean and maximal lifespan in mice, whether started at 9 or 20 months of age (12, 13). Our data show that phase I gene expression is also upregulated, after 3 months of rapamycin treatment initiated at 9 months of age, in a pattern similar to that observed in CR and CL mice. Surprisingly, however, longer exposure to rapamycin (i.e. from 9 to 22 months of age) resulted in a significant repression of many of these mRNAs, in some cases to levels significantly below those seen in 12-month-old control animals. Thus, at least some of the changes in gene expression induced by rapamycin are transient, and it is not clear whether the health benefits seen in rapamycin-treated mice are due to its initial effects (such as elevation of protective enzyme levels), to compensatory down-regulation of these same genes, or to more complex feedback circuits. The transience of the effects seen in rapamycin-treated mice was not observed in aged CL mice; in the CL system, genes elevated in 12-month-old mice remained high at least through 22 months of age.

Nuclear receptors are the best-characterized regulators of phase I XMEs. A study utilizing Little mice crossed with CAR/PXR or FXR knockouts showed that FXR but not CAR or PXR is the nuclear receptor that primarily regulates phase I XME expression in Little mice (18). Mechanisms for regulation of xenobiotic metabolism have not been evaluated in other mouse models, but there is circumstantial evidence to suggest alteration of phase I gene expression by additional factors. PPAR isoforms, for example, are elevated in Ames and GHRKO liver tissue (37), and multiple Nrf2-regulated genes show increased transcription in liver of Ames, Snell, and CR mice (38-40).

Nrf2 plays a role in regulating xenobiotic metabolism by controlling XME gene expression through the ARE. During unstressed conditions, Nrf2 is sequestered in the cytosol by Keap1, which maintains Nrf2 in an inactive state, subject to rapid degradation by the proteasome. In response to oxidative stress, Nrf2/Keap1 binding is disrupted, and Nrf2 translocates to the nucleus where it acts as a transcription factor. Studies on the *C. elegans* Nrf2 ortholog *skn-1* have shown that overexpression of SKN-1 can increase worm lifespan and that *skn-1* is necessary for CR-mediated lifespan extension (41, 42). Nrf2 has also been shown to be necessary for the anti-carcinogenic effects of CR in mice (38). Hepatocyte-specific knockout of Keap1 increases Nrf2 nuclear localization and phase I XME expression in a similar pattern to that we have seen in our long-lived mice (26) and *Nrf2*$^{-/-}$ mice have lowered XME expression in the liver (24). Hepatic activation of Nrf2 is also associated with increased resistance to

acetaminophen toxicity (26). Conversely, *Nrf2*$^{-/-}$ mice are sensitive to chemical stress, suggesting that Nrf2 is a key mediator of stress resistance (43, 44).

Nrf2 can be activated by a chemically diverse group of pharmacological agents (45). Clinical studies of Nrf2 activators have reported potent chemopreventive effects, suggesting that regulation of Nrf2 activity may be a promising approach to delay cancer and possibly aging (46). Our data show that short-term exposure to tBHQ can upregulate phase I genes, and that the pattern of genes activated is similar to that seen in CR and CL mice, in mice treated with CA (18), and in GH/IGF-1-deficient dwarf mice, although correlation with gene expression patterns in rapamycin-treated mice is less striking.

The results of this study support the hypothesis that expression of xenobiotic metabolism genes is associated with many models of extended longevity in mice. An important next step is to determine whether chronic elevation of xenobiotic metabolism genes influences lifespan duration and aging. This could potentially be accomplished through pharmacological interventions with Nrf2 activators or bile acid compounds, genetic models of elevated Nrf2 activity such as the tissue-specific *Keap1*$^{-/-}$ mouse or upstream nuclear receptors that are known to regulate xenobiotic metabolism.

3-6. Acknowledgements

This work was supported by National Institute on Aging grants AG-031736, AG-024824, AG-013283 and National Institute of General Medical Sciences grant T32-GM007315, as well as by an Ellison Medical Foundation

Senior Scholar Award. We thank Lisa Burmeister and Sabrina Friedline for technical assistance, and Dr. John Kopchick for use of the GHRKO mice.

3-7. Figures

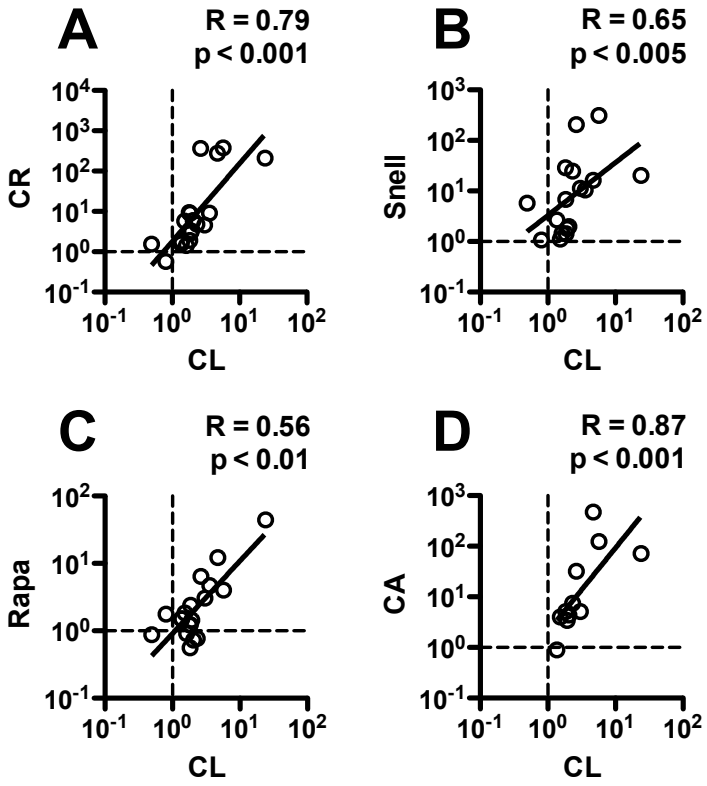

Figure 3-1. Scatterplots of mRNA levels for enzymes involved in phase I detoxification of xenobiotics in liver, expressed as ratios to their respective control mice, for CL mice as compared to (A) CR mice, (B) Snell mice, (C) rapamycin-treated mice, and (D) published effects of exposure to CA (18).

Each symbol represents a different mRNA. All mice were 12 months old, except 2-4 months for the CA group. Each panel also shows the Spearman correlation coefficient R, and its associated p-value. Calculated values are means of n = 6 experimental mice compared to n = 6 of the relevant age-matched control. Diagonal lines show best least-squares linear fit. Note that vertical axis scales differ among panels, to provide legible detail for each of the data sets compared.

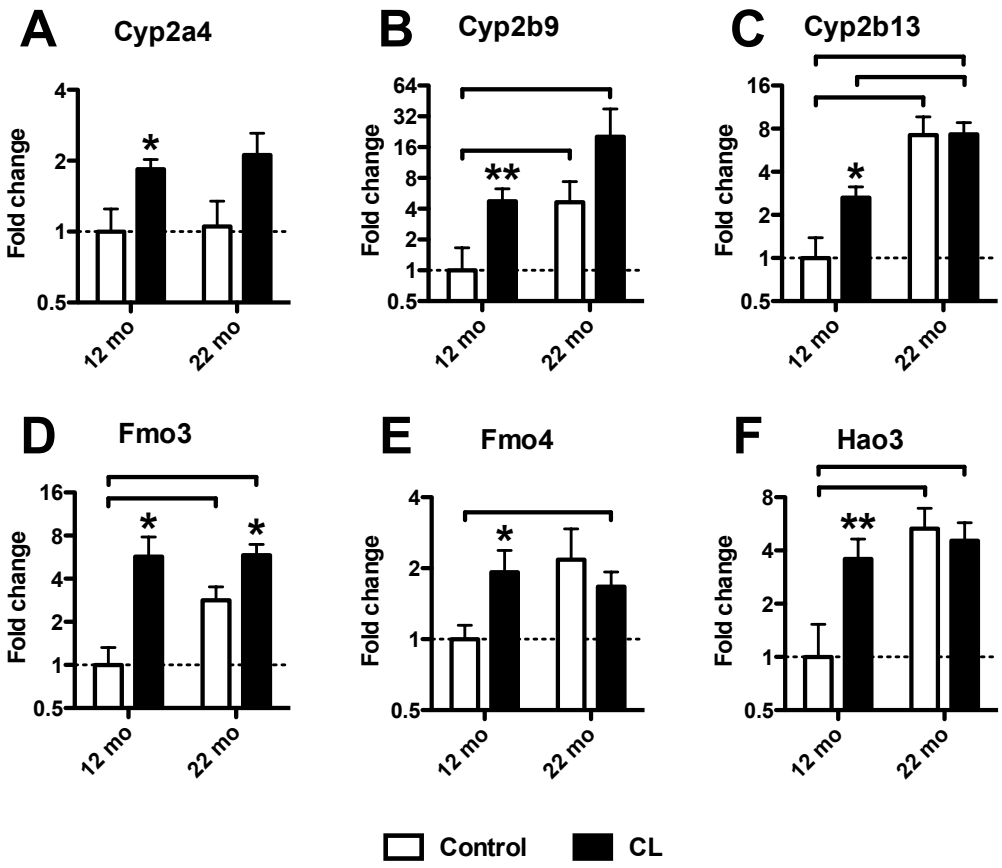

Figure 3-2. CL mice maintain elevated levels of liver phase I mRNAs through 22 months of age.

Each panel shows one of the 6 mRNA species that was significantly elevated in 12-month-old CL mice. Bars indicate mean ± SEM for CL and age-matched control mice, in each case normalized to the average level of mRNA in 12-month-old control animals. n = 6 mice per treatment; except n = 5 for 22-month-old CL mice. Asterisks over CL bars indicate significant differences from age-matched controls (two-tailed t-test; $p < 0.05$*, $p < 0.01$**). Horizontal lines indicate significant effects of age in either CL or control populations.

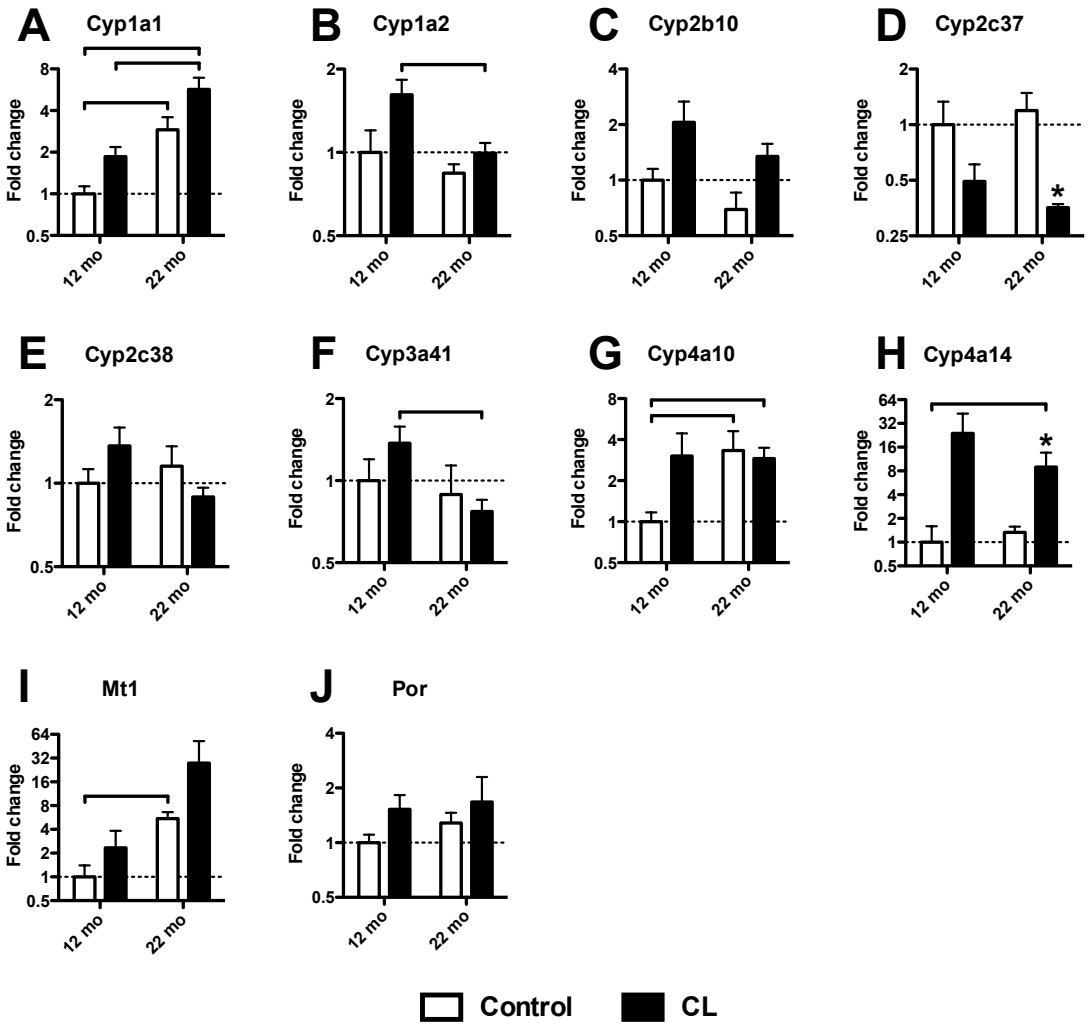

Figure 3-3. Age-associated changes of phase I xenobiotic metabolism genes that were not elevated at 12 months of age in CL mice.

Bars indicate mean ± SEM for CL and age-matched control mice, in each case normalized to the average level of mRNA in 12-month-old control animals. n = 6 mice per treatment; n = 5 for 22-month-old CL mice. Asterisks over CL bars indicate significant differences from age-matched controls (two-tailed t-test, $p < 0.05$). Horizontal lines indicate significant effects of age in either CL or control populations.

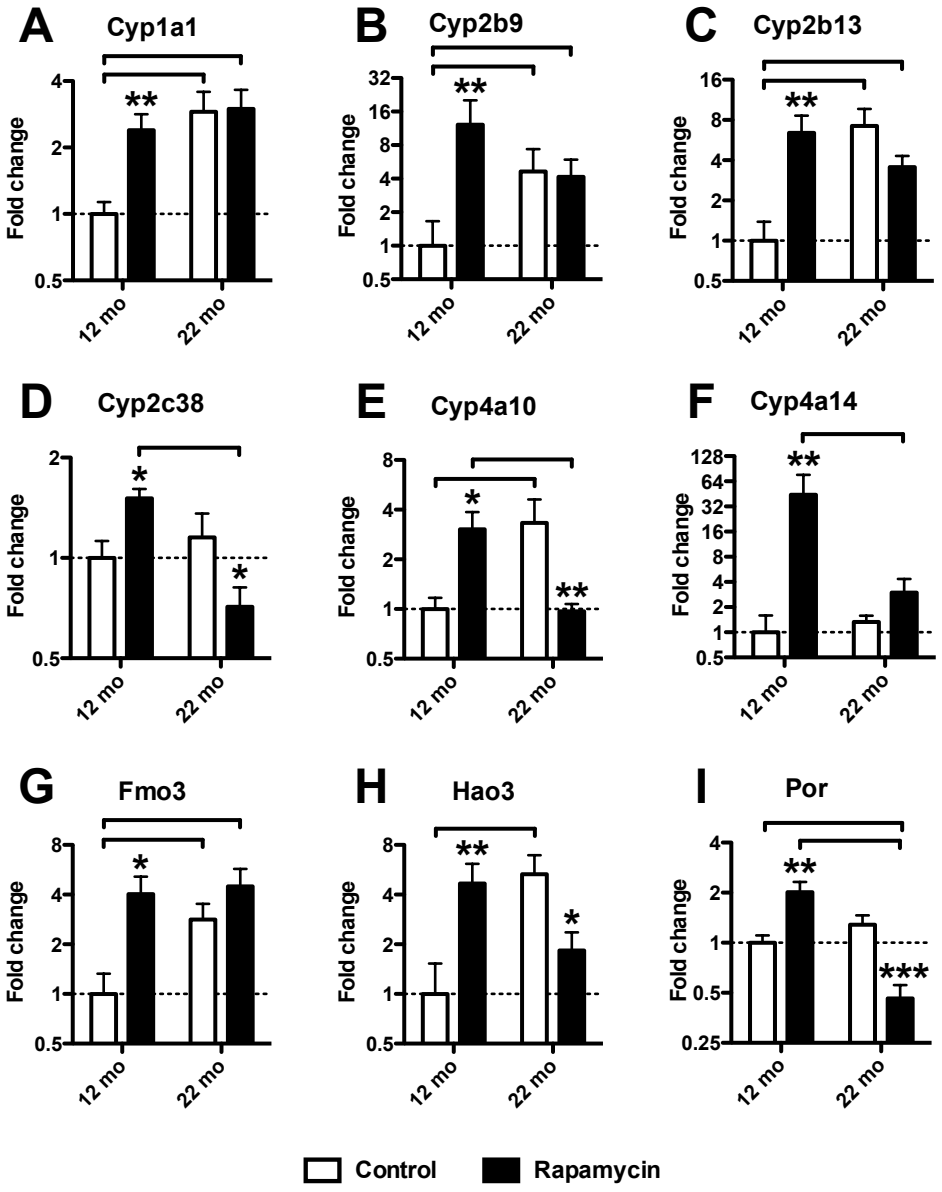

Figure 3-4. Rapamycin-dependent elevation of many phase I xenobiotic genes is reversed later in life.

Mice were given food containing rapamycin starting at 9 months of age and euthanized either at 12 or 22 months of age. Bars indicate mean ± SEM for rapamycin-treated and age-matched control mice, in each case normalized to the average level of mRNA in 12-month-old control animals. n = 6 mice per treatment. Asterisks over rapamycin bars indicate significant differences from age-matched controls (two-tailed t-test; $p < 0.05$*, $p < 0.01$**). Horizontal lines indicate significant effects of age in either rapamycin-treated or control populations.

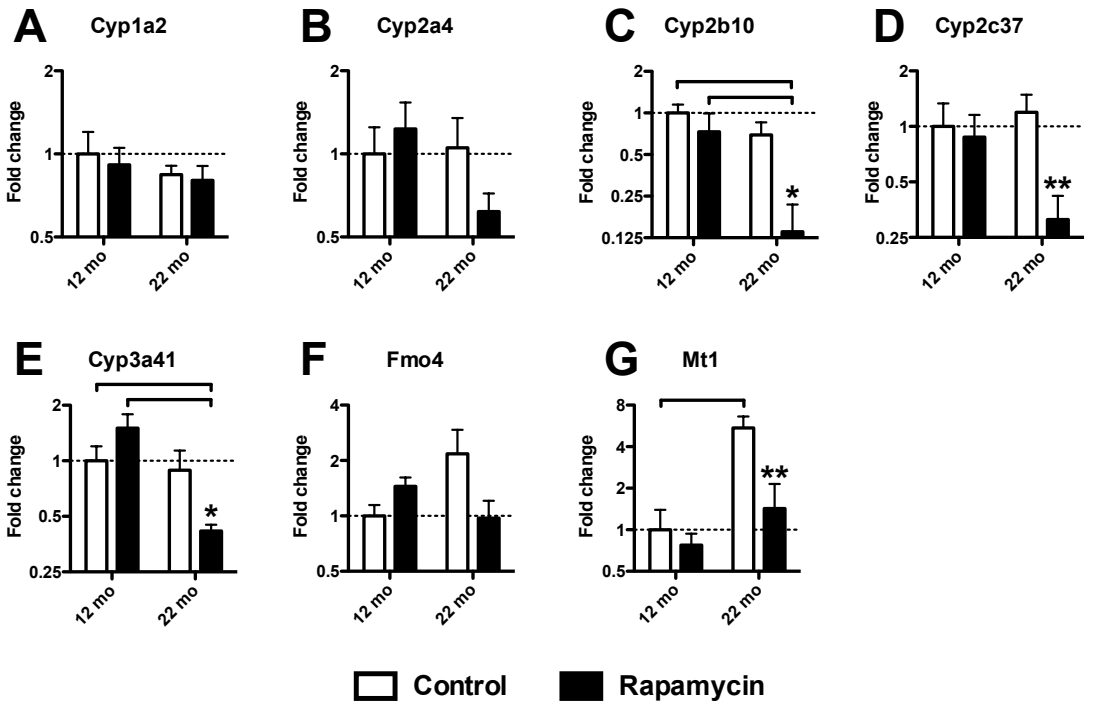

Figure 3-5. Age-associated changes of phase I xenobiotic metabolism genes that were not significantly elevated at 12 months of age in rapamycin-treated mice.

Mice were given food containing rapamycin starting at 9 months of age and sacrificed either at 12 or 22 months of age. Bars indicate mean ± SEM for rapamycin-treated and age-matched control mice, in each case normalized to the average level of mRNA in 12-month-old control animals. n = 6 mice per treatment. Asterisks over rapamycin bars indicate significant differences from age-matched controls (two-tailed t-test, $p < 0.05$). Horizontal lines indicate significant effects of age in either rapamycin-treated or control populations.

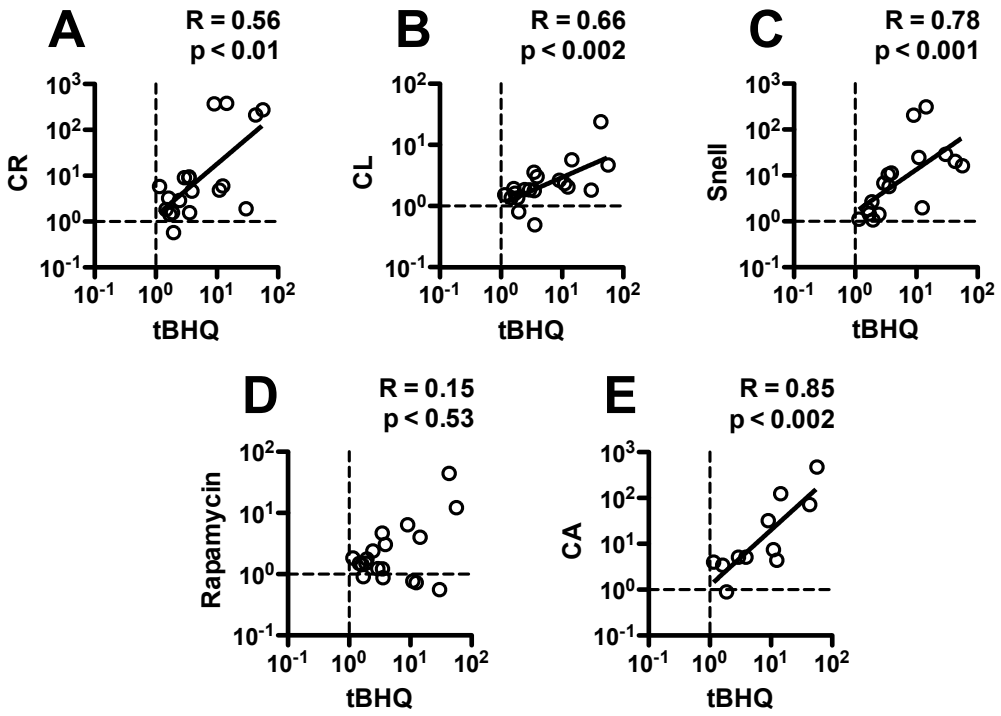

Figure 3-6. Acute exposure to tBHQ mimics mRNA patterns seen in CR, CL, Snell, and CA-treated mice, but not rapamycin-treated mice.

Scatterplots show mRNA levels for xenobiotic metabolism genes in liver of mice after 2-week exposure to tBHQ, compared to (A) CR mice, (B) CL mice, (C) Snell mice, (D) rapamycin-treated mice, and (E) CA-treated mice**.** Each symbol represents a different mRNA, plotted to show the ratio of the mean level in experimental mice to their respective controls. All mice were 12 months old, except for the published data on CA (18), which represent mice 2-4 months of age. Each panel also shows the Spearman correlation coefficient R with its associated p-value. Diagonal lines indicate least-square fits. Note that the correlation of tBHQ effects with rapamycin is not statistically significant.

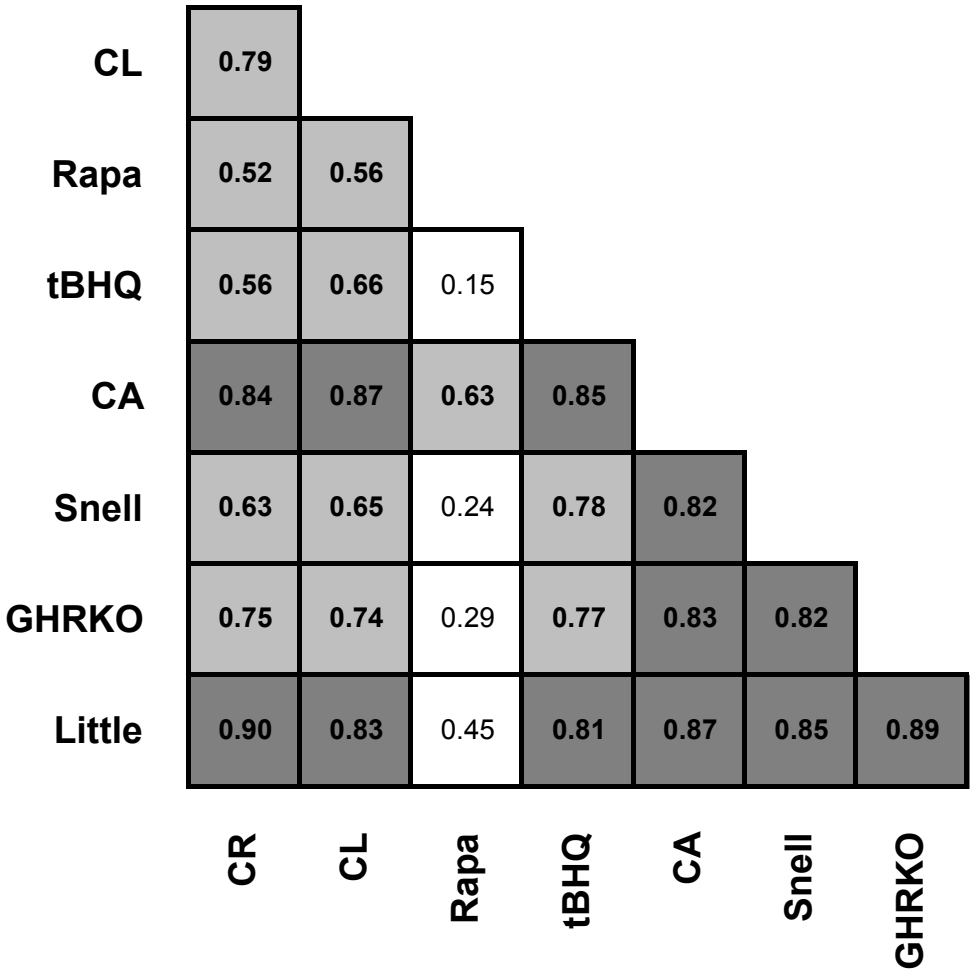

Figure 3-7. Correlation matrix of hepatic phase I xenobiotic metabolism gene expression.

Each box shows the Spearman correlation coefficient R for the populations of mice in the corresponding row and column header. Values of $R > 0.5$ are statistically significant at $p < 0.05$. Dark gray shading denotes an R-value greater than 0.8, light gray denotes an R-value ranging from 0.5 to 0.8. Note that no significant relationship was observed for the comparisons of rapamycin and tBHQ, Snell, GHRKO, or Little mice. CA and Little data were obtained from a previously published study (18).

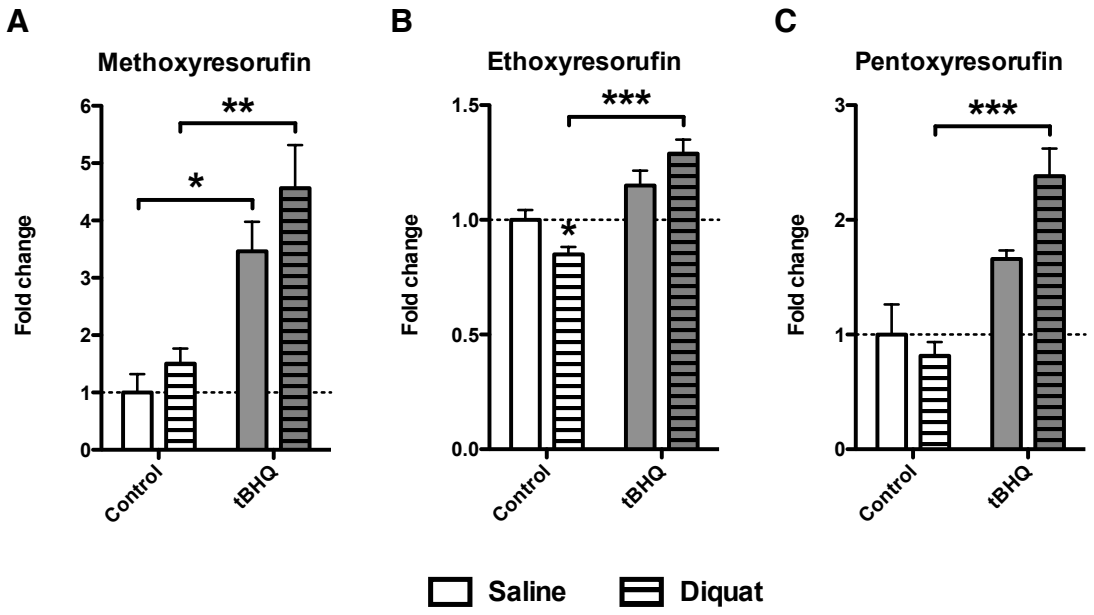

Figure 3-8. tBHQ increases functional cytochrome p450 activity.

Mice were administered 1% tBHQ in chow for 50 days and treated with 50 mg/kg diquat or saline control for 6 hours. Change in resorufin fluorescence per minute was measured in liver microsomes by spectrophotometry. Significantly higher changes in methoxyresorufin (MROD), ethoxyresorufin (EROD), and pentoxyresorufin (PROD) fluorescence were detected in the tBHQ-fed diquat-treated group compared to the control-fed diquat-treated group. Additionally, significantly higher MROD change was found between tBHQ-fed saline-treated and control-fed saline-treated mice (n = 3 saline; n = 6 diquat).

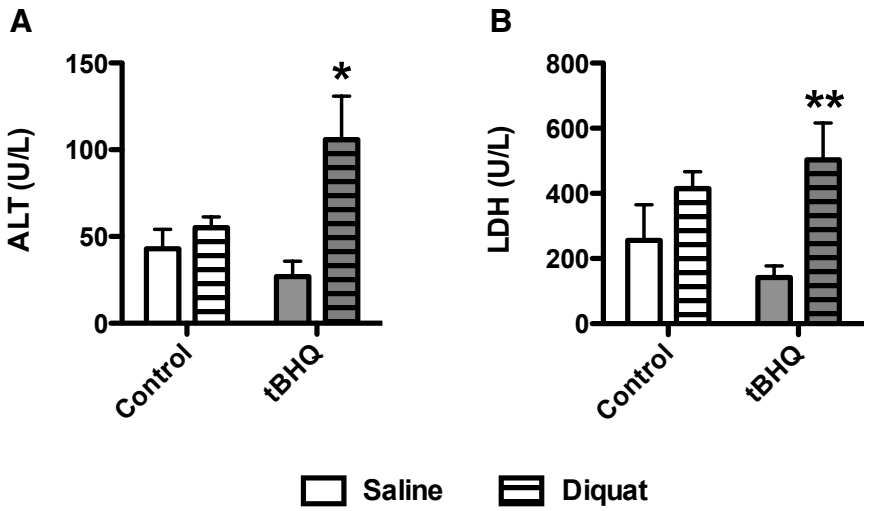

Figure 3-9. tBHQ increases sensitivity to diquat-induced oxidative stress.

Mice were administered 1% tBHQ in chow for 50 days and treated with 50 mg/kg diquat or saline control for 6 hours. tBHQ-treated mice exposed to diquat have significantly higher levels of ALT and LDH in the blood that control-fed mice (n = 3 saline; n = 6 diquat).

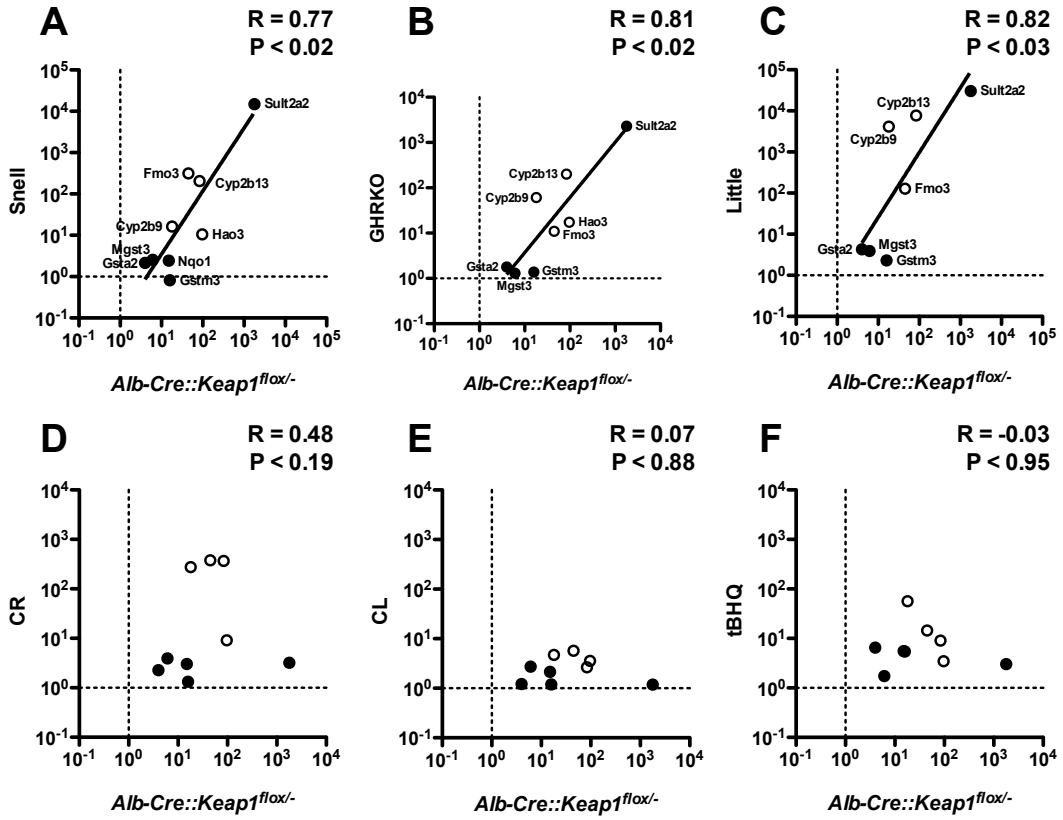

Figure 3-10. Mice with liver-specific knockout of Keap1 (*Alb-Cre::Keap1$^{flox/-}$*) have elevated expression of XME mRNAs that resemble (A-C) GH/IGF-1-deficient dwarf mice, but not (D) CR, (E) CL, or (F) tBHQ-treated mice.

Each symbol represents a different mRNA, plotted to show the ratio of the mean level in experimental mice to their respective controls. Phase I XMEs are labeled white and phase II XMEs are labeled solid black. Each panel also shows the Spearman correlation coefficient R with its associated p-value. Diagonal lines indicate least-square fits. Note that the correlations of *Alb-Cre::Keap1$^{flox/-}$* mice to CR, CL, or tBHQ-treated mice were not statistically significant. Gene expression data from Little (18) and *Alb-Cre::Keap1$^{flox/-}$* (26) mice were obtained from previously published studies.

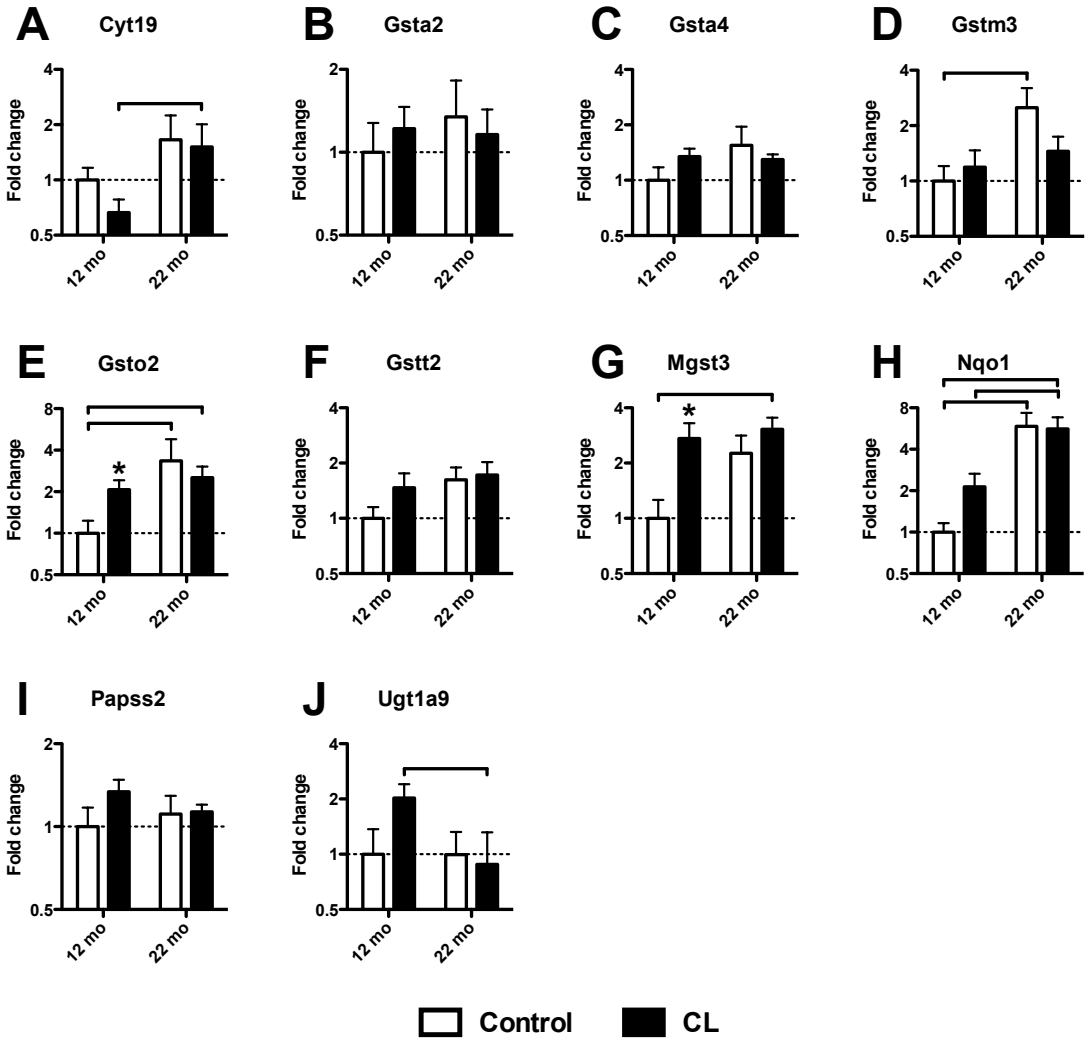

Figure 3-11. Age-associated changes of phase II xenobiotic metabolism genes in CL mice.

Bars indicate mean ± SEM for CL and age-matched control mice, in each case normalized to the average level of mRNA in 12-month-old control animals. n = 6 mice per treatment; n = 5 for 22-month-old CL mice. Asterisks over CL bars indicate significant differences from age-matched controls (two-tailed t-test, $p < 0.05$). Horizontal lines indicate significant effects of age in either CL or control populations.

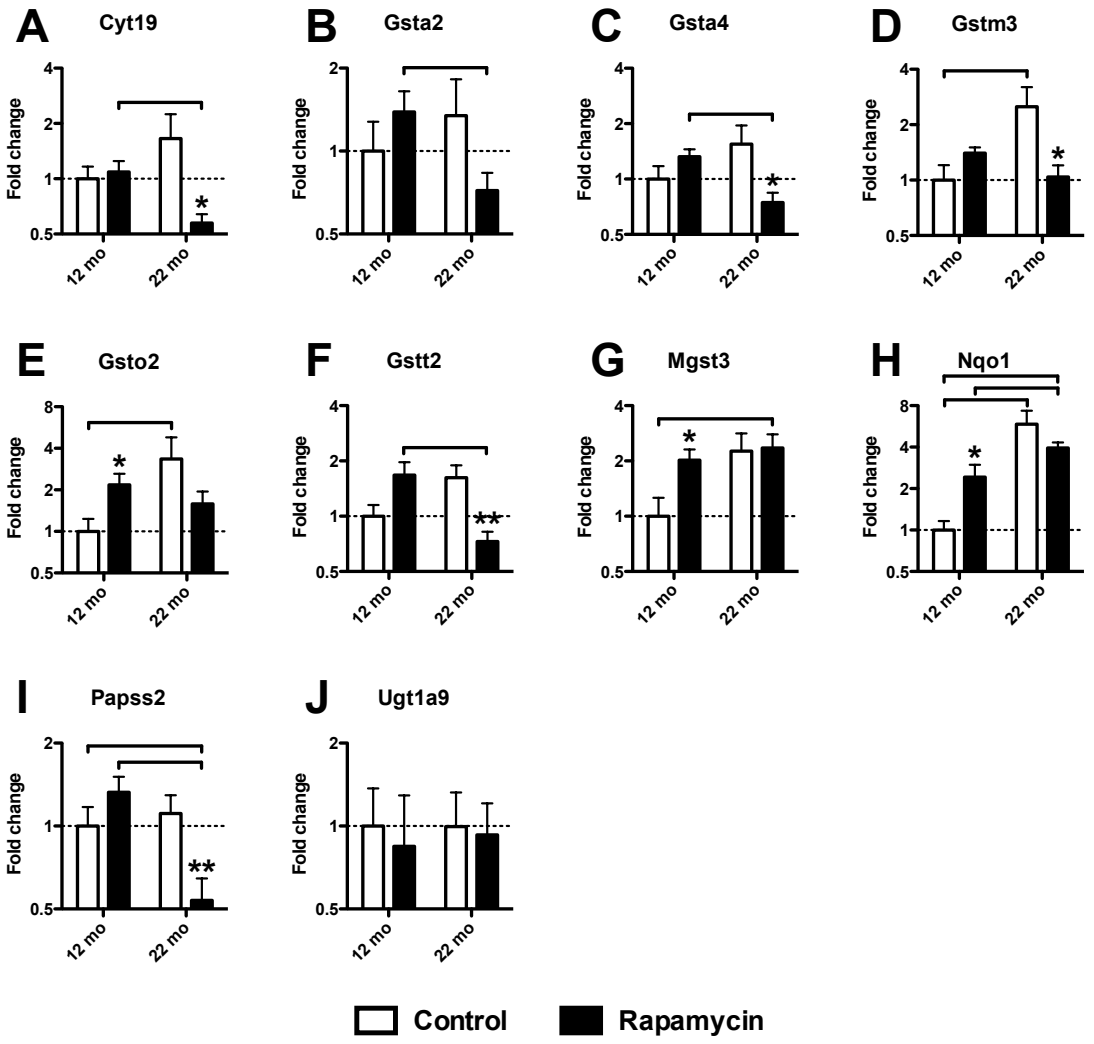

Figure 3-12. Age-associated changes of phase II xenobiotic metabolism genes in rapamycin-treated mice.

Mice were given food containing rapamycin starting at 9 months of age and sacrificed either at 12 or 22 months of age. Bars indicate mean ± SEM for rapamycin-treated and age-matched control mice, in each case normalized to the average level of mRNA in 12-month-old control animals. n = 6 mice per treatment. Asterisks over rapamycin bars indicate significant differences from age-matched controls (two-tailed t-test, $p < 0.05$). Horizontal lines indicate significant effects of age in either rapamycin-treated or control populations.

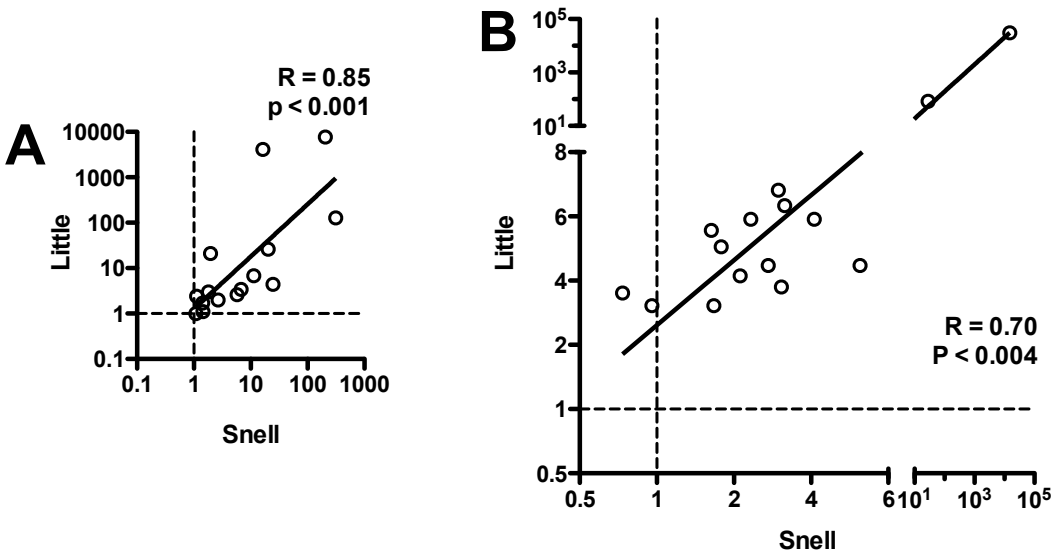

Figure 3-13. Snell and Little mice have similar (A) phase I and (B) phase II xenobiotic metabolism gene expression.

Each symbol represents a different mRNA, plotted to show the ratio of the mean level in experimental mice to their respective controls. Each panel also shows the Spearman correlation coefficient R with its associated p-value. Diagonal lines indicate least-square fits. Gene by gene comparison is available in Table 3-10 and Table 3-17.

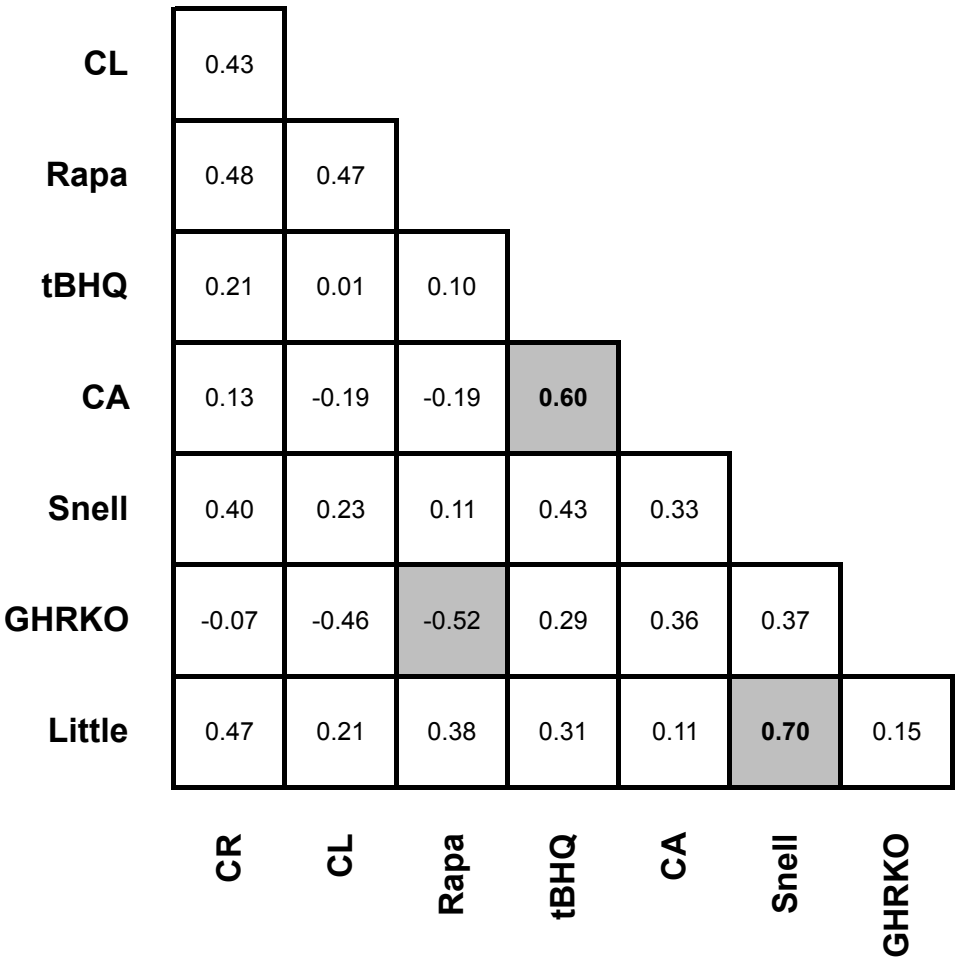

Figure 3-14. Correlation matrix of hepatic phase II xenobiotic metabolism gene expression.

Each box denotes the Spearman correlation coefficient R and is shaded if statistically significant ($p < 0.05$). Light gray shading denotes an R-value ranging from 0.5 to 0.8. Statistically significant, similar upregulation of phase II genes was observed between tBHQ and CA-treated mice, and between Snell and Little mice. Significant negative association of phase II gene expression was observed between GHRKO and rapamycin-treated mice. CA and Little mouse expression data was obtained from a previously published study (18).

3-8. Tables

Gene	Name	Forward	Reverse
Actin	β-actin (housekeeping)	CTGCTCTGGCTCCTAGCACC	CGCTCAGGAGGAGCAATGA
Cyp1a1	Cytochrome P450, family 1, subfamily a, polypeptide 1	GACTTTAAAACACGCCCGCT	GAAGACCGCATCTGCACTTG
Cyp1a2	Cytochrome P450, family 1, subfamily a, polypeptide 2	AACTCGGCCATCGACAAGAC	CAAGCCGAAGAGCATCACCT
Cyp2a4	Cytochrome P450, family 2, subfamily a, polypeptide 4	GGGCTGCATGAGGTTAAAGG	CAACCCCTGACTTGTCTGGTCT
Cyp2a5	Cytochrome P450, family 2, subfamily a, polypeptide 5	TGGTCCTGTATTCACCATCTACC	ACTACGCCATAGCCTTTGAAAA
Cyp2b10	Cytochrome P450, family 2, subfamily b, polypeptide 10	CTGCCCTTCTCAACAGGACAA	GCGCTTTCCCACAGACTTTT
Cyp2b13	Cytochrome P450, family 2, subfamily b, polypeptide 13	GCCCCACTTTTGTTGAGAATG	GCAGCTCTCTCAGAGGCACA
Cyp2b9	Cytochrome P450, family 2, subfamily b, polypeptide 9	TCCACAACTCATGCTGAGTCACT	ACACTTGGACTGTTGGGAGGA
Cyp2c37	Cytochrome P450, family 2, subfamily c, polypeptide 37	CTGCATGACAGCACGGAGTT	GTGGCCAGGGTCAAATTTCTC
Cyp2c38	Cytochrome P450, family 2, subfamily c, polypeptide 38	CAAGGAGTTCCCCAACCCA	GCGTCTAGAAAGTGGCCAGG
Cyp3a11	Cytochrome P450, family 3, subfamily a, polypeptide 11	GACAAACAAGCAGGGATGGAC	CCAAGCTGATTGCTAGGAGCA
Cyp3a41	Cytochrome P450, family 3, subfamily a, polypeptide 41	AAAGCCGCCTCGATTCTAAGC	ACTACATCCCGTGGTACAACC
Cyp4a10	Cytochrome P450, family 4, subfamily a, polypeptide 10	TGCATCAAGGAGGCCCTAAG	TCTGACAATGCCTGGGACAG
Cyp4a14	Cytochrome P450, family 4, subfamily a, polypeptide 14	AGCCAGAGCAGTTTTGGCAA	TAGGGACCAGATGGCAACATG
Fmo3	Flavin containing monooxygenase 3	AACGCCATCCTAACACAGTGG	ACGCGTCTTCATAGGCTTCAG
Fmo4	Flavin containing monooxygenase 4	CTGATCAGCCTTAATGGGTCG	TCGTGCTTGGAACTCTGTGC
Hao3	Hydroxyacid oxidase 3	ACAAGCTTTCAACATAGTGTGTGATG	TATGAATGGGACCCAAGAAGAAC
Mt1	Metallothionein 1	CCTTCTCCTCACTTACTCCGTAGCT	TCCATTCCGAGATCTGGTGAA
Mt2	Metallothionein 2	ATGCAAATGTACTTCCTGCAAGA	CTGGGAGCACTTCGCACAG
Por	Cytochrome p450 reductase	ACCCCTCGCTCCCTGTAATC	GTGGAGGTCGGCAGAAGGA

Table 3-1. Primers used for qPCR analysis: phase I genes.

Some of these sequences were previously published (18).

Gene	Name	Forward	Reverse
Cyt19	Arsenite methyltransferase	TCTTAGCCTGCTCTTCGCCA	TGGCTTTGCCACCTTCACA
Gsta2	Glutathione S-transferase, α2	CAGCCTCCCCAATGTGAAGA	GGCTTTCTCTGGCTGCCAG
Gsta4	Glutathione S-transferase, α4	GTGCAGCGTGCTTTAAGGTG	GGTGACACTGCAATTGGAACC
Gstm3	Glutathione S-transferase, μ3	TCTGCTGCAGTCCCGATTTT	TGGCCTTCAAGAACTCTGGCT
Gsto2	Glutathione S-transferase, ω2	TAAGGTCCCGCCTTTAAGCA	CTTCCGCATCTCAGCGCTA
Gstt2	Glutathione S-transferase, θ2	CTGACAGCATGGCGAGAGAG	ACACAGCTCAGCACCCAAGA
Hmox1	Heme oxygenase 1	GCCACCAAGGAGGTACACAT	GCTTGTTGCGCTCTATCTCC
Mgst3	Microsomal glutathione S-transferase 3	GGATCAGACCAGGCTTAGGCT	CACCTCAGTGGTGGCAGGAT
Nqo1	NAD(P)H dehydrogenase (quinone 1)	AGGATGGGAGGTACTCGAATC	TGCTAGAGATGACTCGGAAGG
Papss2	3'-phosphoadenosine 5'-phosphosulfate synthase 2	GGGCCCTGCCTACCCTAGA	GCTTCAGGAAATCGGAACCTCT
Sult1a1	Sulfotransferase family 1A, phenol-preferring, member 1	TGTCCTATGGGTCGTGGTACC	GTCTCAGCTCCCACCACTCC
Sult1d1	Sulfotransferase family 1D, member 1	CCTGGCACCTGGGAAGAGT	GCTCACTTGTCCAGCCATGAA
Sult1e1	Sulfotransferase family 1E, estrogen-preferring, member 1	GCAGCAGATGAAGGATTGCA	GTGGCTCAGAGCTCCATTCTAAA
Sult2a2	Sulfotransferase family 2A, DHEA-preferring, member 2	GATCGGGTTACTAATGGCTTGAA	GTCCCCAGTTGTACCTTTTCTCAT
Temt	Indolethylamine N-methyltransferase	AGCCTACGACTGGTCCTCCA	TCTCCCTCCAGCTCACATGC
Ugt1a1	UDP glucuronosyltransferase 1 family, polypeptide A1	TGGTGGAACTTGGACGGACT	CGCGCAGCAGAAAAGAATCT
Ugt1a9	UDP glucuronosyltransferase 1 family, polypeptide A9	TGTGTGGATTAATTGTCGCCA	CAAAGATCACTGATGGGAGCG

Table 3-2. Primers used for qPCR analysis: phase II genes.

Some of these sequences were previously published (18).

Gene	Fold change	SEM	N	P value
Cyp1a1	1.9	0.3	6	0.06
Cyp1a2	1.6	0.2	6	0.07
Cyp2a4	**1.8**	**0.2**	**6**	**0.03**
Cyp2a5	1.8	0.3	6	0.07
Cyp2b10	2.1	0.6	6	0.17
Cyp2b13	**2.6**	**0.5**	**6**	**0.02**
Cyp2b9	**4.7**	**1.5**	**6**	**0.004**
Cyp2c37	0.5	0.1	6	0.31
Cyp2c38	1.4	0.2	6	0.23
Cyp3a11	0.8	0.2	6	0.65
Cyp3a41	1.4	0.2	6	0.26
Cyp4a10	3.0	1.4	6	0.19
Cyp4a14	24	19	6	0.05
Fmo3	**5.7**	**2.1**	**6**	**0.02**
Fmo4	**1.9**	**0.5**	**6**	**0.04**
Hao3	**3.6**	**1.1**	**6**	**0.009**
Mt1	2.3	1.5	6	0.63
Mt2	1.8	1.4	6	0.86
Por	1.5	0.3	6	0.11

Table 3-3. Expression of mRNAs for phase I xenobiotic enzymes in liver of 12-month-old CL mice, expressed as a ratio to age-matched controls.

Fold change is expressed as a ratio to control samples normalized for each sample to β-actin levels in the same sample. SEM = standard error of the mean. n = number of mice in each group. P-values reflect two-tailed unpaired t-tests. Boldface indicates $p < 0.05$.

Gene	Fold change	SEM	N	P value
Cyp1a1	**2.9**	**0.4**	**6**	**< 0.001**
Cyp1a2	1.4	0.1	6	0.09
Cyp2a4	**9.0**	**1.8**	**6**	**< 0.001**
Cyp2a5	**9.4**	**2.2**	**6**	**< 0.001**
Cyp2b10	**6.0**	**1.2**	**6**	**< 0.001**
Cyp2b13	**368**	**359**	**6**	**0.01**
Cyp2b9	**276**	**115**	**6**	**< 0.001**
Cyp2c37	1.6	0.5	6	0.38
Cyp2c38	**1.6**	**0.2**	**6**	**0.04**
Cyp3a11	0.6	0.1	6	0.20
Cyp3a41	**1.8**	**0.2**	**6**	**0.05**
Cyp4a10	**4.6**	**1.3**	**6**	**0.002**
Cyp4a14	**210**	**76**	**6**	**< 0.001**
Fmo3	**379**	**109**	**6**	**< 0.001**
Fmo4	**3.3**	**0.5**	**6**	**< 0.001**
Hao3	**9.1**	**4.8**	**6**	**0.002**
Mt1	**4.9**	**1.6**	**6**	**0.01**
Mt2	1.9	1.4	6	0.57
Por	**5.8**	**0.9**	**6**	**< 0.001**

Table 3-4. Expression of mRNAs for phase I xenobiotic enzymes in liver of 12-month-old CR mice, expressed as a ratio to age-matched controls.

Fold change is expressed as a ratio to control samples normalized for each sample to β-actin levels in the same sample. SEM = standard error of the mean. n = number of mice in each group. P-values reflect two-tailed unpaired t-tests. Boldface indicates $p < 0.05$.

Gene	Fold change	SEM	N	P value
Cyp1a1	**2.4**	**0.4**	**6**	**0.007**
Cyp1a2	0.9	0.1	6	0.95
Cyp2a4	1.2	0.3	6	0.70
Cyp2a5	1.2	0.3	6	0.65
Cyp2b10	0.7	0.3	6	0.18
Cyp2b13	**6.4**	**2.2**	**6**	**0.005**
Cyp2b9	**12**	**8.0**	**6**	**0.009**
Cyp2c37	0.9	0.3	6	0.89
Cyp2c38	**1.5**	**0.1**	**6**	**0.02**
Cyp3a11	1.8	0.3	6	0.06
Cyp3a41	1.5	0.3	6	0.21
Cyp4a10	**3.0**	**0.8**	**6**	**0.01**
Cyp4a14	**44**	**32**	**6**	**0.007**
Fmo3	**4.0**	**1.1**	**6**	**0.006**
Fmo4	1.4	0.2	6	0.08
Hao3	**4.7**	**1.5**	**6**	**0.008**
Mt1	0.8	0.2	6	0.92
Mt2	0.6	0.2	6	0.85
Por	**1.8**	**0.3**	**6**	**0.02**

Table 3-5. Expression of mRNAs for phase I xenobiotic enzymes in liver of 12-month-old rapamycin-treated mice, expressed as a ratio to age-matched controls.

Fold change is expressed as a ratio to control samples normalized for each sample to β-actin levels in the same sample. SEM = standard error of the mean. n = number of mice in each group. P-values reflect two-tailed unpaired t-tests. Boldface indicates $p < 0.05$.

Gene	Fold change	SEM	N	P value
Cyp1a1	1.4	0.3	3	0.32
Cyp1a2	1.4	0.2	3	0.20
Cyp2a4	**6.8**	**0.5**	**3**	**0.004**
Cyp2b10	2.0	0.2	3	0.07
Cyp2b13	**205**	**42**	**3**	**< 0.001**
Cyp2b9	**16**	**1.4**	**3**	**0.003**
Cyp2c37	**5.7**	**0.5**	**3**	**0.004**
Cyp2c38	**2.7**	**0.4**	**3**	**0.005**
Cyp3a11	1.1	0.1	3	0.61
Cyp4a10	**11**	**1.0**	**3**	**0.005**
Cyp4a14	**20**	**2.8**	**3**	**0.02**
Fmo3	**314**	**52**	**3**	**< 0.001**
Fmo4	**1.8**	**0.3**	**3**	**0.03**
Hao3	**11**	**1.5**	**3**	**0.002**
Mt1	**25**	**7.5**	**3**	**0.004**
Mt2	**29**	**16**	**3**	**0.02**
Por	1.1	0.2	3	0.66

Table 3-6. Expression of mRNAs for phase I xenobiotic enzymes in liver of 6-month-old Snell mice, expressed as a ratio to age-matched controls.

Fold change is expressed as a ratio to control samples normalized for each sample to β-actin levels in the same sample. SEM = standard error of the mean. n = number of mice in each group. P-values reflect two-tailed unpaired t-tests. Boldface indicates $p < 0.05$.

Gene	Fold change	SEM	N	P value
Cyp1a1	**2.9**	**0.7**	**6**	**0.009**
Cyp1a2	0.8	0.1	6	0.81
Cyp2a4	1.1	0.3	6	0.94
Cyp2b10	0.7	0.2	6	0.20
Cyp2b13	**7.2**	**2.5**	**6**	**0.002**
Cyp2b9	**4.6**	**2.7**	**6**	**0.02**
Cyp2c37	1.2	0.3	6	0.52
Cyp2c38	1.2	0.2	6	0.57
Cyp3a41	0.9	0.2	6	0.85
Cyp4a10	**3.3**	**1.3**	**6**	**0.01**
Cyp4a14	1.3	0.2	6	0.17
Fmo3	**2.8**	**0.7**	**6**	**0.02**
Fmo4	2.2	0.8	6	0.05
Hao3	**5.3**	**1.6**	**6**	**0.004**
Mt1	**5.5**	**1.1**	**6**	**0.002**
Por	1.3	0.2	6	0.24

Table 3-7. Age-associated changes of phase I hepatic xenobiotic gene expression in control mice.

Fold change is expressed as a ratio of gene expression in 22-month-old HET3 mice to 12-month-old HET3 mice. samples normalized for each sample to β-actin levels in the same sample. SEM = standard error of the mean. n = number of mice in each group. P-values reflect two-tailed unpaired t-tests. Boldface indicates $p < 0.05$.

Gene	Fold change	SEM	N	P value
Cyp1a1	2.4	0.3	3	0.09
Cyp1a2	**1.7**	**0.1**	**3**	**0.01**
Cyp2a4	**2.9**	**0.1**	**3**	**< 0.001**
Cyp2a5	**3.5**	**0.1**	**3**	**< 0.001**
Cyp2b10	**12**	**2.5**	**3**	**< 0.001**
Cyp2b13	**9.0**	**0.9**	**3**	**0.008**
Cyp2b9	**57**	**3.5**	**3**	**< 0.001**
Cyp2c37	3.6	0.4	3	0.05
Cyp2c38	**1.9**	**0.3**	**3**	**0.02**
Cyp3a11	**1.9**	**0.4**	**3**	**0.04**
Cyp3a41	1.5	0.0	3	0.07
Cyp4a10	**3.9**	**0.2**	**3**	**< 0.001**
Cyp4a14	**43**	**6.3**	**3**	**< 0.001**
Fmo3	**14**	**4.6**	**3**	**0.01**
Fmo4	1.6	0.3	3	0.13
Hao3	3.5	1.1	3	0.12
Mt1	**11**	**4.2**	**3**	**0.02**
Mt2	**30**	**12**	**3**	**0.01**
Por	1.1	0.0	3	0.39

Table 3-8. Expression of mRNAs for phase I xenobiotic enzymes in liver of 6-month-old mice after 2 weeks of tBHQ treatment, expressed as a ratio to age-matched controls.

Fold change is expressed as a ratio to control samples normalized for each sample to β-actin levels in the same sample. SEM = standard error of the mean. n = number of mice in each group. P-values reflect two-tailed unpaired t-tests. Boldface indicates $p < 0.05$.

Gene	Fold change	SEM	N	P value
Cyp1a1	1.2	0.2	6	0.39
Cyp1a2	0.9	0.1	6	0.46
Cyp2a4	**3.5**	**0.4**	**6**	**< 0.001**
Cyp2b10	**8.8**	**0.6**	**5**	**< 0.001**
Cyp2b13	**201**	**21**	**5**	**< 0.001**
Cyp2b9	**61**	**14**	**5**	**< 0.001**
Cyp2c37	0.8	0.1	5	0.17
Cyp2c38	**2.2**	**0.3**	**6**	**0.004**
Cyp3a11	0.9	0.1	5	0.19
Cyp3a41	**0.7**	**0.1**	**5**	**0.04**
Cyp4a10	**3.1**	**0.3**	**5**	**< 0.001**
Cyp4a14	**24**	**3.6**	**5**	**< 0.001**
Fmo3	**11.0**	**3.4**	**5**	**< 0.001**
Fmo4	**1.9**	**0.2**	**5**	**0.002**
Hao3	**17**	**2.9**	**6**	**< 0.001**
Mt1	**36**	**13**	**4**	**< 0.001**
Mt2	**51**	**5.5**	**5**	**< 0.001**
Por	1.4	0.3	6	0.40

Table 3-9. Expression of mRNAs for phase I xenobiotic enzymes in liver of 6-month-old GHRKO mice, expressed as a ratio to age-matched controls.

Fold change is expressed as a ratio to control samples normalized for each sample to β-actin levels in the same sample. SEM = standard error of the mean. n = number of mice in each group. P-values reflect two-tailed unpaired t-tests. Boldface indicates $p < 0.05$.

	CR	CL	Rapa	tBHQ	CA	Little	Snell	GHRKO
Cyp1a1	**2.9**	1.9	**2.4**	2.4	—	1.7	1.4	1.2
Cyp1a2	1.4	1.6	0.9	**1.7**	—	1.1	1.4	0.9
Cyp2a4	**9.0**	**1.8**	1.2	**2.9**	**5.1**	**3.4**	**6.8**	**3.5**
Cyp2a5	**9.4**	1.8	1.2	**3.5**	—	—	—	—
Cyp2b10	**6.0**	2.1	0.7	**12**	**4.4**	**21**	2.0	**8.8**
Cyp2b13	**368**	**2.6**	**6.4**	**9.0**	**32**	**7715**	**205**	**201**
Cyp2b9	**276**	**4.7**	**12**	**57**	**473**	**4127**	**16**	**61**
Cyp2c37	1.6	0.5	0.9	3.6	—	**2.6**	**5.7**	0.8
Cyp2c38	**1.6**	1.4	**1.5**	**1.9**	0.9	**2.0**	**2.7**	**2.2**
Cyp3a11	0.6	0.8	1.8	**1.9**	—	1.0	1.1	0.9
Cyp3a41	**1.8**	1.4	1.5	1.5	—	—	—	**0.7**
Cyp4a10	**4.6**	3.0	**3.0**	**3.9**	**5.1**	**6.8**	**11**	**3.1**
Cyp4a14	**210**	24	**44**	**43**	**72**	**26**	**20**	**24**
Fmo3	**379**	**5.7**	**4.0**	**14**	**124**	**128**	**314**	**11**
Fmo4	**3.3**	**1.9**	1.4	1.6	**3.4**	**3.0**	**1.8**	**1.9**
Hao3	**9.1**	**3.6**	**4.7**	3.5	—	—	**11**	**17**
Mt1	**4.9**	2.3	0.8	**11**	**7.5**	**4.4**	**25**	**36**
Mt2	1.9	1.8	0.6	**30**	—	—	**29**	**51**
Por	**5.8**	1.5	**1.8**	1.1	**4.0**	**2.4**	1.1	1.4
Geo Mean	8.4	2.2	2.1	5.1	13	12	7.8	5.6

Table 3-10. Expression matrix of mRNAs for phase I xenobiotic metabolism enzymes in liver tissue.

Calculated values are means of gene expression as a ratio of experimental mice to age-matched control mice, normalized to β-actin levels. Samples are color coded white to gray with increasing gene expression. Boldface indicates $p < 0.05$.

Gene	Fold change	SEM	N	P value
Cyt19	0.7	0.1	6	0.16
Gsta2	1.2	0.2	6	0.46
Gsta4	1.3	0.1	6	0.20
Gstm3	1.2	0.3	6	0.68
Gsto2	**2.1**	**0.4**	**6**	**0.03**
Gstt2	1.5	0.3	6	0.16
Hmox1	1.2	0.2	6	0.52
Mgst3	**2.7**	**0.6**	**6**	**0.01**
Nqo1	2.1	0.5	6	0.05
Papss2	1.3	0.1	6	0.15
Sult1a1	1.2	0.2	6	0.36
Sult1d1	1.4	0.2	6	0.28
Sult1e1	2.2	1.0	6	0.52
Sult2a2	1.2	0.3	6	0.62
Temt	1.5	0.4	6	0.29
Ugt1a1	1.3	0.2	6	0.37
Ugt1a9	2.0	0.4	6	0.07

Table 3-11. Expression of mRNAs for phase II xenobiotic enzymes in liver of 12-month-old CL mice, expressed as a ratio to age-matched controls.

Fold change is expressed as a ratio to control samples normalized for each sample to β-actin levels in the same sample. SEM = standard error of the mean. n = number of mice in each group. P-values reflect two-tailed unpaired t-tests. Boldface indicates $p < 0.05$.

Gene	Fold change	SEM	N	P value
Cyt19	1.4	0.2	6	0.10
Gsta2	**2.3**	**0.4**	**6**	**0.03**
Gsta4	**1.9**	**0.2**	**6**	**0.02**
Gstm3	1.3	0.3	6	0.40
Gsto2	**1.9**	**0.2**	**6**	**0.01**
Gstt2	**4.3**	**0.4**	**6**	**< 0.001**
Hmox1	1.3	0.3	6	0.53
Mgst3	**3.9**	**0.7**	**6**	**0.002**
Nqo1	**3.0**	**0.7**	**6**	**0.007**
Papss2	**2.3**	**0.4**	**6**	**0.009**
Sult1a1	1.0	0.1	6	0.68
Sult1d1	1.7	0.3	6	0.07
Sult1e1	**2.0**	**0.2**	**6**	**0.03**
Sult2a2	3.2	1.7	6	0.39
Temt	**2.9**	**0.4**	**6**	**0.03**
Ugt1a1	**2.0**	**0.2**	**6**	**0.009**
Ugt1a9	2.1	0.8	6	0.36

Table 3-12. Expression of mRNAs for phase II xenobiotic enzymes in liver of 12-month-old CR mice, expressed as a ratio to age-matched controls.

Fold change is expressed as a ratio to control samples normalized for each sample to β-actin levels in the same sample. SEM = standard error of the mean. n = number of mice in each group. P-values reflect two-tailed unpaired t-tests. Boldface indicates $p < 0.05$.

Gene	Fold change	SEM	N	P value
Cyt19	1.1	0.2	6	0.72
Gsta2	1.4	0.3	6	0.26
Gsta4	1.3	0.1	6	0.21
Gstm3	1.4	0.1	6	0.15
Gsto2	**2.2**	**0.4**	**6**	**0.02**
Gstt2	1.7	0.3	6	0.08
Hmox1	1.4	0.4	6	0.42
Mgst3	**2.0**	**0.3**	**6**	**0.02**
Nqo1	**2.4**	**0.6**	**6**	**0.01**
Papss2	1.3	0.2	6	0.23
Sult1a1	1.3	0.2	6	0.17
Sult1d1	1.2	0.1	6	0.22
Sult1e1	1.6	0.4	6	0.14
Sult2a2	1.6	0.4	6	0.25
Temt	2.4	0.3	6	0.06
Ugt1a1	1.6	0.2	6	0.05
Ugt1a9	0.8	0.4	6	0.64

Table 3-13. Expression of mRNAs for phase II xenobiotic enzymes in liver of 12-month-old rapamycin-treated mice, expressed as a ratio to age-matched controls.

Fold change is expressed as a ratio to control samples normalized for each sample to β-actin levels in the same sample. SEM = standard error of the mean. n = number of mice in each group. P-values reflect two-tailed unpaired t-tests. Boldface indicates $p < 0.05$.

Gene	Fold change	SEM	N	P value
Cyt19	1.7	0.1	3	0.13
Gsta2	**6.5**	**1.4**	**3**	**0.006**
Gsta4	**1.8**	**0.1**	**3**	**0.04**
Gstm3	**5.4**	**0.3**	**3**	**0.001**
Gsto2	1.9	0.3	3	0.20
Gstt2	**1.9**	**0.1**	**3**	**< 0.001**
Hmox1	0.7	0.1	3	0.73
Mgst3	1.7	0.4	3	0.24
Nqo1	**5.5**	**0.5**	**3**	**< 0.001**
Papss2	1.3	0.2	3	0.26
Sult1a1	**1.8**	**0.1**	**3**	**0.05**
Sult1d1	1.5	0.1	3	0.13
Sult1e1	2.4	0.2	3	0.11
Sult2a2	**3.0**	**0.3**	**3**	**0.03**
Temt	1.2	0.1	3	0.32
Ugt1a1	**1.4**	**0.1**	**3**	**0.01**
Ugt1a9	2.1	0.9	3	0.26

Table 3-14. Expression of mRNAs for phase II xenobiotic enzymes in liver of 6-month-old mice after 2 weeks of tBHQ treatment, expressed as a ratio to age-matched controls.

Fold change is expressed as a ratio to control samples normalized for each sample to β-actin levels in the same sample. SEM = standard error of the mean. n = number of mice in each group. P-values reflect two-tailed unpaired t-tests. Boldface indicates $p < 0.05$.

Gene	Fold change	SEM	N	P value
Cyt19	1.6	0.2	3	0.13
Gsta2	2.1	0.2	3	0.09
Gsta4	1.4	0.1	3	0.18
Gstm3	0.8	0.1	3	0.44
Gsto2	1.5	0.2	3	0.26
Gstt2	**1.9**	**0.2**	**3**	**0.03**
Hmox1	0.5	0.0	3	0.11
Mgst3	**2.6**	**0.4**	**3**	**0.004**
Nqo1	**2.4**	**0.5**	**2**	**0.02**
Papss2	1.0	0.1	3	0.88
Sult1a1	**2.1**	**0.2**	**3**	**0.005**
Sult1d1	**3.4**	**0.3**	**3**	**0.002**
Sult1e1	**28**	**0.6**	**3**	**0.005**
Sult2a2	**14939**	**927**	**3**	**< 0.001**
Temt	**1.4**	**0.1**	**3**	**0.03**
Ugt1a1	**2.1**	**0.2**	**3**	**0.01**
Ugt1a9	1.8	0.3	3	0.08

Table 3-15. Expression of mRNAs for phase II xenobiotic enzymes in liver of 6-month-old SnellI mice, expressed as a ratio to age-matched controls.

Fold change is expressed as a ratio to control samples normalized for each sample to β-actin levels in the same sample. SEM = standard error of the mean. n = number of mice in each group. P-values reflect two-tailed unpaired t-tests. Boldface indicates $p < 0.05$.

Gene	Fold change	SEM	N	P value
Gsta2	**1.8**	**0.2**	**6**	**0.005**
Gsta4	**2.4**	**0.3**	**6**	**0.001**
Gstm3	1.4	0.5	6	0.65
Gsto2	1.1	0.3	6	0.84
Gstt2	1.2	0.1	6	0.34
Mgst3	1.3	0.1	6	0.12
Papss2	**1.8**	**0.3**	**6**	**0.05**
Sult1a1	**2.0**	**0.4**	**6**	**0.02**
Sult1d1	1.3	0.1	6	0.18
Sult1e1	**58**	**10**	**6**	**< 0.001**
Sult2a2	**2304**	**218**	**5**	**< 0.001**
Temt	1.2	0.1	6	0.43
Ugt1a1	1.5	0.2	6	0.15

Table 3-16. Expression of mRNAs for phase II xenobiotic enzymes in liver of 6-month-old GHRKO mice, expressed as a ratio to age-matched controls.

Fold change is expressed as a ratio to control samples normalized for each sample to β-actin levels in the same sample. SEM = standard error of the mean. n = number of mice in each group. P-values reflect two-tailed unpaired t-tests. Boldface indicates $p < 0.05$.

	CR	CL	Rapa	tBHQ	CA	Little	SnellI	GHRKO
Cyt19	1.4	0.7	1.1	1.7	2.2	**2.6**	1.6	—
Gsta2	**2.3**	1.2	1.4	**6.5**	**18**	**4.3**	2.1	**1.8**
Gsta4	**1.9**	1.3	1.3	**1.8**	**9.1**	**2.1**	1.4	**2.4**
Gstm3	1.3	1.2	1.4	**5.4**	**36**	**2.3**	0.8	1.4
Gsto2	**1.9**	**2.1**	**2.2**	1.9	**0.5**	**3.2**	1.5	1.1
Gstt2	**4.3**	1.5	1.7	**1.9**	**4.6**	**2.8**	**1.9**	1.2
Hmox1	1.3	1.2	1.4	0.7	—	—	0.5	—
Mgst3	**3.9**	**2.7**	**2.0**	1.7	**9.7**	**3.9**	**2.6**	1.3
Nqo1	**3.0**	2.1	**2.4**	**5.5**	—	—	**2.4**	—
Papss2	**2.3**	1.3	1.3	1.3	**2.4**	**2.1**	1.0	**1.8**
Sult1a1	1.0	1.2	1.3	**1.8**	**4.4**	**2.4**	**2.1**	**2.0**
Sult1d1	1.7	1.4	1.2	1.5	**6.8**	**2.8**	**3.4**	1.3
Sult1e1	**2.0**	2.2	1.6	2.4	5.8	**83**	**28**	**58**
Sult2a2	3.2	1.2	1.6	**3.0**	**9.3**	**30409**	**14939**	**2304**
Temt	**2.9**	1.5	2.4	1.2	0.9	**3.6**	**1.4**	1.2
Ugt1a1	**2.0**	1.3	1.6	**1.4**	4.1	**4.8**	**2.1**	1.5
Ugt1a9	2.1	2.0	0.8	2.1	—	3.9	1.8	—
Geo Mean	2.1	1.5	1.5	2.1	4.9	7.0	3.3	3.5

Table 3-17. Expression matrix of mRNAs for phase II xenobiotic metabolism enzymes in liver tissue.

Calculated values are means of gene expression as a ratio of experimental mice to age-matched control mice, normalized to β-actin levels. Samples are color coded white to gray with increasing gene expression. Boldface indicates $p < 0.05$.

Gene	Fold change	SEM	N	P value
Cyt19	1.7	0.6	6	0.31
Gsta2	1.3	0.5	6	0.55
Gsta4	1.5	0.4	6	0.24
Gstm3	**2.5**	**0.7**	**6**	**0.04**
Gsto2	**3.4**	**1.4**	**6**	**0.03**
Gstt2	1.6	0.3	6	0.07
Mgst3	2.3	0.6	6	0.05
Nqo1	**5.9**	**1.5**	**6**	**< 0.001**
Papss2	1.1	0.2	6	0.61
Ugt1a9	1.0	0.3	6	0.88

Table 3-18. Age-associated changes in hepatic phase II gene expression in control mice.

Fold change is expressed as a ratio of gene expression in 22-month-old HET3 mice to 12-month-old HET3 mice. samples normalized for each sample to β-actin levels in the same sample. SEM = standard error of the mean. n = number of mice in each group. P-values reflect two-tailed unpaired t-tests. Boldface indicates $p < 0.05$.

3-9. References

1. Bartke A (2011) Pleiotropic effects of growth hormone signaling in aging. *Trends Endocrinol Metab* 22:437–442.

2. Brown-Borg HM, Borg KE, Meliska CJ, Bartke A (1996) Dwarf mice and the ageing process. *Nature* 384:33.

3. Flurkey K, Papaconstantinou J, Miller RA, Harrison DE (2001) Lifespan extension and delayed immune and collagen aging in mutant mice with defects in growth hormone production. *Proc Natl Acad Sci USA* 98:6736–6741.

4. Coschigano KT, Clemmons D, Bellush LL, Kopchick JJ (2000) Assessment of growth parameters and life span of GHR/BP gene-disrupted mice. *Endocrinology* 141:2608–2613.

5. Bartke A (2011) Single-gene mutations and healthy ageing in mammals. *Philos Trans R Soc Lond, B, Biol Sci* 366:28–34.

6. Masoro EJ (2010) in *Calorie Restriction, Aging and Longevity*, eds Everitt AV, Rattan SIS, Couteur D, de Cabo R (Springer), pp 3–14.

7. Flurkey K, Astle CM, Harrison DE (2010) Life extension by diet restriction and N-acetyl-L-cysteine in genetically heterogeneous mice. *J Gerontol A Biol Sci Med Sci* 65:1275–1284.

8. Sun L, Sadighi Akha AA, Miller RA, Harper JM (2009) Life-span extension in mice by preweaning food restriction and by methionine restriction in middle age. *J Gerontol A Biol Sci Med Sci* 64:711–722.

9. Bartke A et al. (2001) Extending the lifespan of long-lived mice. *Nature* 414:412.

10. Bonkowski MS, Rocha JS, Masternak MM, Al-Regaiey KA, Bartke A (2006) Targeted disruption of growth hormone receptor interferes with the beneficial actions of calorie restriction. *Proc Natl Acad Sci USA* 103:7901–7905.

11. Tsang CK, Qi H, Liu LF, Zheng XFS (2007) Targeting mammalian target of rapamycin (mTOR) for health and diseases. *Drug Discov Today* 12:112–124.

12. Harrison DE et al. (2009) Rapamycin fed late in life extends lifespan in genetically heterogeneous mice. *Nature* 460:392–395.

13. Miller RA et al. (2011) Rapamycin, but not resveratrol or simvastatin, extends life span of genetically heterogeneous mice. *J Gerontol A Biol Sci Med Sci* 66:191–201.

14. Anisimov VN et al. (2011) Rapamycin increases lifespan and inhibits spontaneous tumorigenesis in inbred female mice. *Cell Cycle* 10:4230–4236.

15. Swindell WR (2007) Gene expression profiling of long-lived dwarf mice: longevity-associated genes and relationships with diet, gender and aging. *BMC Genomics* 8:353.

16. Omiecinski CJ, Vanden Heuvel JP, Perdew GH, Peters JM (2011) Xenobiotic metabolism, disposition, and regulation by receptors: from biochemical phenomenon to predictors of major toxicities. *Toxicol Sci* 120 Suppl 1:S49–75.

17. Bartke A et al. (2001) Prolonged longevity of hypopituitary dwarf mice. *Exp Gerontol* 36:21–28.

18. Amador-Noguez D et al. (2007) Alterations in xenobiotic metabolism in the long-lived Little mice. *Aging Cell* 6:453–470.

19. Bokov AF, Lindsey ML, Khodr C, Sabia MR, Richardson A (2009) Long-lived ames dwarf mice are resistant to chemical stressors. *J Gerontol A Biol Sci Med Sci* 64:819–827.

20. Harper JM et al. (2006) Stress resistance and aging: influence of genes and nutrition. *Mech Ageing Dev* 127:687–694.

21. Miller RA et al. (1999) Exotic mice as models for aging research: polemic and prospectus. *Neurobiol Aging* 20:217–231.

22. Vergara M, Smith-Wheelock M, Harper JM, Sigler R, Miller RA (2004) Hormone-treated snell dwarf mice regain fertility but remain long lived and disease resistant. *J Gerontol A Biol Sci Med Sci* 59:1244–1250.

23. Zhou Y et al. (1997) A mammalian model for Laron syndrome produced by targeted disruption of the mouse growth hormone receptor/binding protein gene (the Laron mouse). *Proc Natl Acad Sci USA* 94:13215–13220.

24. Anwar-Mohamed A et al. (2011) The effect of Nrf2 knockout on the constitutive expression of drug metabolizing enzymes and transporters in C57Bl/6 mice livers. *Toxicol In Vitro* 25:785–795.

25. Nguyen T, Sherratt PJ, Pickett CB (2003) Regulatory mechanisms controlling gene expression mediated by the antioxidant response element. *Annu Rev Pharmacol Toxicol* 43:233–260.

26. Okawa H et al. (2006) Hepatocyte-specific deletion of the keap1 gene activates Nrf2 and confers potent resistance against acute drug toxicity. *Biochem Biophys Res Commun* 339:79–88.

27. McElwee JJ, Schuster E, Blanc E, Thomas JH, Gems D (2004) Shared transcriptional signature in Caenorhabditis elegans Dauer larvae and long-lived daf-2 mutants implicates detoxification system in longevity assurance. *J Biol Chem* 279:44533–44543.

28. Swindell WR (2008) Comparative analysis of microarray data identifies common responses to caloric restriction among mouse tissues. *Mech Ageing Dev* 129:138–153.

29. McCay CM, Crowell MF, Maynard LA (1935) The effect of retarded growth upon the length of life span and upon the ultimate body size. *Nutrition* 10:63–70.

30. Weindruch R, Walford RL (1988) *The Retardation of Aging and Disease by Dietary Restriction* (Charles C Thomas, Springfield, IL).

31. Yu BP, Chung HY (2001) Stress resistance by caloric restriction for longevity. *Ann N Y Acad Sci* 928:39–47.

32. Liang H et al. (2003) Genetic mouse models of extended lifespan. *Exp Gerontol* 38:1353–1364.

33. Colman RJ et al. (2009) Caloric restriction delays disease onset and mortality in rhesus monkeys. *Science* 325:201–204.

34. Panici JA et al. (2010) Early life growth hormone treatment shortens longevity and decreases cellular stress resistance in long-lived mutant mice. *FASEB J* 24:5073–5079.

35. Sonntag WE et al. (1999) Pleiotropic effects of growth hormone and insulin-like growth factor (IGF)-1 on biological aging: inferences from moderate caloric-restricted animals. *J Gerontol A Biol Sci Med Sci* 54:B521–38.

36. Nadon NL et al. (2008) Design of aging intervention studies: the NIA interventions testing program. *AGE* 30:187–199.

37. Masternak MM, Bartke A (2007) PPARs in Calorie Restricted and Genetically Long-Lived Mice. *PPAR Res* 2007:28436.

38. Pearson KJ et al. (2008) Nrf2 mediates cancer protection but not prolongevity induced by caloric restriction. *Proceedings of the National Academy of Sciences* 105:2325–2330.

39. Leiser SF, Miller RA (2010) Nrf2 signaling, a mechanism for cellular stress resistance in long-lived mice. *Mol Cell Biol* 30:871–884.

40. Sun LY, Bokov AF, Richardson A, Miller RA (2011) Hepatic response to oxidative injury in long-lived Ames dwarf mice. *FASEB J* 25:398–408.

41. Bishop NA, Guarente L (2007) Two neurons mediate diet-restriction-induced longevity in C. elegans. *Nature* 447:545–549.

42. Tullet JMA et al. (2008) Direct inhibition of the longevity-promoting factor SKN-1 by insulin-like signaling in C. elegans. *Cell* 132:1025–1038.

43. Enomoto A et al. (2001) High sensitivity of Nrf2 knockout mice to acetaminophen hepatotoxicity associated with decreased expression of ARE-regulated drug metabolizing enzymes and antioxidant genes. *Toxicol Sci* 59:169–177.

44. Umemura T et al. (2006) A crucial role of Nrf2 in in vivo defense against oxidative damage by an environmental pollutant, pentachlorophenol. *Toxicol Sci* 90:111–119.

45. Hur W, Gray NS (2011) Small molecule modulators of antioxidant response pathway. *Curr Opin Chem Biol* 15:162–173.

46. Kensler TW, Wakabayashi N (2010) Nrf2: friend or foe for chemoprevention? *Carcinogenesis* 31:90–99.

CHAPTER 4

Conclusions

The main goal of this thesis research was to uncover specific biochemical pathways that serve to enhance protection against toxic insults in slow-aging mice. Previous work in the Miller laboratory demonstrated that primary dermal fibroblasts cultured from long-lived Snell, Ames, and GHRKO mice are resistant to multiple lethal stresses (1, 2). Snell, Ames, and GHRKO mice harbor mutations that affect circulating GH and IGF-1 action (Table 1-1). We hypothesized that downstream signal cascades controlled by GHR or IGF-1R are differentially regulated in these mice and may play a role in stress resistance.

First, we evaluated two branches controlled by IGF-1R that have been associated with stress response: (A) the PI3K-Akt pathway and (B) the Ras-MAPK pathway (3) (Chapter 2). Second, we looked for conserved alterations in XME gene expression among multiple slow-aging mouse models (Chapter 3). Expression of multiple genes involved in xenobiotic metabolism had previously been shown to be upregulated in microarray data obtained from *C. elegans*, dwarf mice, and CR mice. In addition, GH has been shown to be a negative regulator of multiple XMEs, and GH action is lower in long-lived dwarf mice. Therefore, we hypothesized that elevation of xenobiotic metabolism is a conserved phenotype of slow-aging animals.

4-1. Reprogramming during early development likely contributes to enhanced stress resistance and delayed aging in slow-aging mice

The pre-weaning period of early development appears to have a significant impact on aging and stress resistance in mice. Previous work in our laboratory has shown that the enhanced stress resistance phenotype seen in Snell dwarf fibroblasts is only observed in developmentally mature mice. Cells obtained from 4-5 day old Snell and littermate control mice have no difference in resistance to cytotoxic stress (H_2O_2, $CdCl_2$, or UV-C light), in contrast to 3-4 month old Snell mice, whose cells are resistant to multiple forms of stress (2). In addition, mice for which calories are restricted specifically during the pre-weaning period by litter crowding (CL) (12 pups/mother instead of the normal 8 pups/mother) are long-lived (4). These CL mice also have reduced circulating IGF-1 and glucose levels at weaning and a small, but statistically significant, reduction in body weight that is maintained throughout adulthood.

The specific changes associated with increased longevity and enhanced stress resistance that occur in Snell dwarf and CL mice during development have not been identified. Epigenetic reprogramming of stress response signal pathways may play a role in mediating this phenotype. Analysis of DNA methylation patterns in Snell and CL mice compared to their respective littermate controls may reveal genes that are differentially reprogrammed during weaning. The timing of this reprogramming is also not known, except that it is restricted to early development. The CL intervention can be easily manipulated, both by the number of additional pups in the crowded litters and the duration of litter

crowding. These alterations in the CL protocol may reveal specific developmental time points that play a key role in mediated CL-based lifespan extension.

4-2. Nrf2 and MAPK activity may contribute to the enhanced stress resistance phenotype observed in long-lived dwarf mice

Elevated Nrf2 and Nrf2-regulated XME gene expression has been shown to inhibit carcinogenesis and protect against multiple toxic insults (5-8). Similarly, overexpression of the Nrf2 ortholog SKN-1 also increases lifespan and stress resistance in *C. elegans* (9). Nrf2 expression declines with age in rodent and human tissues (10). Additionally, age-associated Nrf2 inhibition is observed in atherosclerosis and neurodegenerative disease models (11, 12). Transgenic mice harboring mutations that affect Nrf2 function have provided much insight into the contributions of Nrf2 in CR, as well as protection against cytotoxic damage and cancer incidence (13, 14).

Nrf2$^{-/-}$ mice undergo normal development but have a stable reduction in constitutive expression of XMEs in multiple metabolic tissues, such as the liver, intestine and forestomach (15-17). As a result, *Nrf2*$^{-/-}$ mice are extremely sensitive to numerous xenobiotics (7), including acetaminophen (18, 19), butylated hydroxytoluene (20), bleomycin (21), diesel exhaust (22), 3-NPA (23), and tobacco smoke (24, 25). *Nrf2*$^{-/-}$ mice are short-lived and develop severe multi-organ, lupus-like autoinflammation (26-28). Additionally, *Nrf2*$^{-/-}$ mice on CR have decreased protection against carcinogenesis in comparison to littermate

control CR mice, demonstrating that Nrf2 activity mediates some of the beneficial effects of CR (29).

Conversely, Nrf2 activity can be increased by genetic knockout of its negative regulator, Keap1. However, whole body Keap1-null mutations are embryonic lethal in mice, due to hyperkeratosis of the esophagus and forestomach, as a consequence of Nrf2-mediated overexpression of keratins and loricrin (30). Embryonic lethality can be avoided through tissue-specific knockout of Keap1 with the loxP/Cre recombinase technique. Mice with hepatocyte-specific deletion of Keap1 (*Alb-Cre::Keap1*$^{flox/-}$) are viable, have elevated expression of both phase I and phase II XME genes that are also induced in GH/IGF-1-deficient dwarf mice, and are resistant to acute drug toxicity induced by acetaminophen (31).

Paradoxically, Snell and GHRKO mice have been reported to be sensitive to acetaminophen (32), while Little mice, like *Alb-Cre::Keap1*$^{flox/-}$ mice, have been reported to be resistant to acetaminophen-induced hepatotoxicity (33). The reason for this observed phenotypic difference is not known but may be due in part to age-associated sensitivity to toxins (*Alb-Cre::Keap1*$^{flox/-}$ mice were 5-6 weeks old, Little mice were 2-4 months old; Snell mice were 5-9 months old, GHRKO mice were 10 months old), differences in redox buffering capacity, intracellular levels of reduced glutathione (32), or elevations in pro-apoptotic signal cascades (34). It has been proposed that a propensity for increased

apoptosis of damaged proliferative tissues, such as the liver, may serve to rapidly regenerate fresh and undamaged cells (35).

The direct contribution of Nrf2 to stress resistance in long-lived dwarf mice has not been tested. Indirect evidence from our laboratory using fibroblast cultures treated with the Nrf2 activator sodium arsenite support the idea that Nrf2 acts as a potent enhancer of stress resistance in these mice. Primary skin-derived fibroblasts were pretreated with a low dose of sodium arsenite (5 μM for 24 h) to activate Nrf2, and then exposed to lethal doses of cytotoxic stress ($CdCl_2$, H_2O_2, paraquat, UV-C light). Pretreatment with sodium arsenite was found to enhance the resistance of littermate control fibroblasts to a similar level as Snell dwarf cells in response to each of these stresses (36). In addition, Nrf2 protein levels are dramatically elevated in liver tissue of Ames (34) and Snell (Sun LY, personal communication) mice exposed to diquat. These findings support a role of Nrf2 in mediating stress resistance in dwarf mice, but a direct role for Nrf2 cannot be claimed until stress resistance has been evaluated in dwarf mice lacking Nrf2. We propose that Snell dwarf mice crossed with *Nrf2*$^{-/-}$ mice would produce offspring that have attenuated multiplex cellular stress resistance in fibroblasts and increased sensitivity to xenobiotic-induced stress (e.g. acetaminophen, diquat challenge) in vivo.

The ERK MAPK pathway has also been shown to contribute to stress resistance in mammals, although analysis of ERK1 and ERK2-null mice have not provided as much insight as genetic manipulations of Nrf2 and Keap1.

ERK1$^{-/-}$ mice have been shown to be resistant to high-fat diet induced obesity and the occurrence of skin carcinoma in response to 9,10-dimethylbenz(a)anthracene or 12-O-tetradecanoylphorbol-13-acetate treatment (37-39). *ERK1*$^{-/-}$ mice retain functional ERK2 protein but effectively have a knockdown of total ERK1/2. *ERK2*$^{-/-}$ mice are embryonic lethal, and this has been attributed to the difference in ERK2 protein expression relative to ERK1. ERK2 has been reported to be more highly expressed than ERK1, by a factor of ~1.5-fold (39, 40). However, mice with conditional ERK2 alleles have been reported to be viable (41, 42), including mice with hepatocyte-specific deletion (43).

We attempted to pharmacologically attenuate the ERK pathway in Snell and littermate control fibroblasts with the MEK inhibitor PD98059 and measure resistance to H_2O_2 stress (data not shown). The initial findings of this experiment were that MEK inhibition selectively raised the resistance to H_2O_2 of normal fibroblasts to that observed in Snell dwarf fibroblasts. However, this experiment was not reproducible upon repeated attempts. Therefore, it remains inconclusive as to whether reduced ERK activation enhances stress resistance in fibroblasts. Genetic knockout of ERK in Snell mice by crossing with the aforementioned ERK knockout strains may better address the question of whether ERK activation contributes to stress resistance than pharmacological approaches. Additionally, the contribution of altered hepatic ERK signaling to stress resistance in GH/IGF-1-deficient dwarf mice could be tested in vivo by knocking out ERK

specifically in the liver using an *Alb-Cre::ERK2*$^{fl/fl}$ stock. Inactivation of the upstream Ras signaling component RasGrf1 has been shown to extend lifespan in mice, and reduce basal levels of oxidative stress markers (44), but survival in response to an oxidative stress (e.g. diquat or paraquat) has not been evaluated in these mice.

4-3. Comparative approaches to identify pro-aging signal networks

Comparative analysis of microarrays

Comparative analysis of microarray datasets may reveal shared signatures in gene expression across multiple models that would otherwise be missed in analysis of individual array datasets. Xenobiotic metabolism genes were shown to be similarly upregulated in Snell, Ames, GHRKO, and Little mice through a comparative approach (45). This method is also applicable outside the context of aging, but is particularly useful for identifying shared alterations in gene expression to dietary and pharmacological interventions that extend lifespan. This approach can also be applied to analysis of array data from multiple tissue types, which may aid in the search for biochemical pathways that are differentially regulated throughout multiple tissues in slow-aging mice.

A potentially powerful new tool for biogerontologists is a comparative, "genetical-genomics" approach (46) that combines gene expression microarray data from differing genetic backgrounds with corresponding lifespan data. Compatible gene expression array (46) and lifespan (47) datasets have been published for 21 strains of BxD mice. Interestingly, combined analysis of these

datasets reported a positive correlation between lifespan and mRNA expression for multiple XME genes (e.g. Cyp4a14, Fmo3, Hao3). This type of analysis may help identify genes associated with increased lifespan that cannot be easily studied through the use of transgenic mouse models. For example, there are hundreds of genes involved in xenobiotic metabolism with varying levels of redundancy. To date, no genetic mutation in the xenobiotic metabolism pathway has been shown to increase lifespan. With this comparative genetical-genomics approach, genes that have a significant correlation with lifespan (e.g. XMEs), both negative or positive, may serve as potential candidates for future lifespan studies in transgenic mice.

Comparative cellular biogerontology

Thus far, the vast majority of experiments on aging in mammals have been performed in a single species at a time. Evolution through natural selection has produced phylogenetically related species that differ in the rate of aging. Comparative analysis of species-specific differences in pro-aging molecular signaling pathways has largely been unexplored (48). Primary skin-derived fibroblasts can be cultured from biopsies of multiple species of birds and mammals (49-51). Resistance to multiple forms of cytotoxic stress has been reported to be to positively associated with maximal lifespan in birds ($CdCl_2$, MMS, paraquat) (48, 52) and mammals ($CdCl_2$, H_2O_2) (50). Cultured fibroblasts from long-lived dwarf mice have been reported to have altered MAPK signaling (53), Nrf2 signaling (36), ER stress response (54, 55), DNA repair (54), plasma

membrane redox system (PMRS) activity (50, 56), TOR signaling (Yasumura and Miller, unpublished), and autophagy (Wang and Miller, unpublished). Whether changes in these pathways, such as diminished ERK phosphorylation, increased LC3-II expression, or altered downstream TOR signaling, correlate with maximal lifespan in birds and mammals is a promising subject of future study.

4-4. Age-associated changes in XME expression observed in rapamycin-treated mice may be due to differences in TOR complex inhibition

Prolonged exposure to rapamycin causes glucose intolerance and insulin resistance in mice (57) and humans (58). Rapamycin was initially reported to selectively inhibit TORC1 (59, 60), but recent work has shown that chronic rapamycin also inhibits TORC2 in mice (57, 61). Specific inhibition of TORC1 (by deletion of *Raptor*) or TORC2 (by deletion of *Rictor*) demonstrate that rapamycin-mediated lifespan extension is dependent on TORC1, and that chronic rapamycin treatment activates TORC2, which is responsible for the previously observed metabolic abnormalities (57). Similarly, RNAi-mediated knockdown of TORC1 extends lifespan in *C. elegans* in a *skn-1* and *daf-16*-dependent manner. However, rapamycin-mediated lifespan extension has been shown to be dependent upon *skn-1* but not *daf-16* and appears to inhibit both TORC1 and TORC2 (Blackwell TK, personal communication). Based on these worm longevity experiments, rapamycin may extend lifespan through Nrf2 activation in mice, which may also possibly explain how XME genes are induced in response to rapamycin treatment. However, it should be noted that poor correlation between

rapamycin and tBHQ-treated mice was observed for both phase I and II biotransformation genes in our analysis. Additionally, these studies may help resolve the discrepancy seen in XME gene expression data from mice treated with rapamycin for 3 months (12 months of age) and 13 months (22 months of age) (Figure 3-4; Figure 3-12). Downregulation of multiple XMEs in rapamycin-treated mice at 22 months of age, that were previously shown to be upregulated at 12 months of age (Figure 3-4), may be due to increased activation of the Akt signal cascade by TORC2, which may affect Nrf2 activation or Jak/Stat-mediated nuclear receptor activation through crosstalk with the GHR signal cascade (62).

4-5. Reductions in GH signaling may enhance xenobiotic metabolism in long-lived dwarf mice

Regulation of xenobiotic metabolism is influenced by numerous factors, including age, diet, sex, and hormones (63). As previously mentioned in Chapter 3, mice with mutations that affect GH and/or IGF-1 responsiveness have a shared pattern of increased XME gene expression (45). GH is known to be a potent negative regulator of many XME genes, particularly cytochrome P450s (63, 64). The observed differences in XME genes are proposed to be influenced by GH or IGF-1, and not thyroid hormone (TH), since Snell and GHRKO mice have different concentrations of TH (65, 66) but similar patterns of XME expression. However, there are some observed differences in XME gene expression between Snell and GHRKO mice (e.g. Cyp2b9, Cyp4a10, Fmo3, Sult2a2) (Table 3-10 and Table 3-17) that could be potentially attributed to

differences in TH metabolism. Similarly, Hsp genes are known to be differentially regulated at the mRNA level between Snell and GHRKO mice in multiple tissues (67). This observed genotype-specific difference may also be due to differences in the circulating levels of GH, prolactin, and/or TSH.

Similar elevations in expression of XME mRNAs are observed in Snell, GHRKO, and Little mice (Figure 3-1). If a reduction in GH-stimulated pathways mediate this effect, then no such changes should be observed in mice without altered circulating levels of GH. We tested this hypothesis, albeit indirectly in long-lived mice that do not have altered circulating GH, by comparing XME gene expression in liver samples from long-lived PAPPA-KO (Figure 4-1A) and macrophage inhibitory factor knockout (MIFKO) (Figure 4-1B) mice to their respective littermate controls. No significant change in a panel of 5 mRNAs shown to be elevated in GH/IGF-1-deficient mice (Cyp2b9, Cyp2b10, Cyp2b13, Cyp4a10, and Cyp4a14) was observed in either PAPPA-KO or MIFKO mice. Future analysis of XME expression in dwarf mice treated with GH or transgenic mice that overexpress GH (GH-Tg) will better address the role of GH in the regulation of XME expression in long-lived mice.

In addition, the effects of GH signaling on hepatic xenobiotic metabolism may be tissue-specific in long-lived mice. We are in the process of addressing this question with tissue-specific knockout of the GH receptor (GHR). Liver-specific knockout of GHR increases some but not all of the XME genes observed to be altered in whole body GHR-null mice (Table 3-9 and Table 3-16). No

change was observed in Cyp4a10, Cyp4a14, Fmo3, and Mt1 expression in liver-specific GHRKO mice (Sun LY, personal communication), although these mRNAs are elevated in whole body GHRKO mice (Table 3-9). No change was observed in a panel of hepatic XME genes that are elevated in whole body GHRKO mice in fat-specific or muscle-specific GHRKO mice (Sun LY, personal communication). These data suggest that specific impairment of GHR in the liver results in an increase in hepatic XME gene expression. However, the mechanism of how GHR signaling regulates xenobiotic metabolism is still not well defined.

The signal transducer and activator of transcription (STAT) pathway has been implicated in mediating GHR-regulated effects on xenobiotic metabolism. GH secretion from the pituitary is sexually dimorphic in rodents (68). Adult males release GH in discrete pulses every ~3.5 h, with little or no GH detectable between pulses. In contrast, females secrete GH more frequently, resulting in a continuous level of GH that is lower than peak pulsatile GH levels observed in males (69, 70). STAT5b has been shown to regulate GH-mediated sexual dimorphism of cytochrome P450 enzymes (71, 72), but the downstream regulatory cascade activated by STAT5b that controls hepatic P450 expression is not well understood (Figure 4-2). We propose that STAT5b signaling may regulate nuclear receptor activity or Nrf2 activation through an unidentified pathway. In addition, IGF-1R signaling may potentially influence STAT5b activity through crosstalk with the GHR signaling pathway (62).

As mentioned above, sexual dimorphism has been observed in the regulation of XME genes, primarily with regard to cytochrome P450 enzymes (63, 73). In unpublished studies, we have noted sexual dimorphism for XME mRNA levels in the HET3 mice used to generate the CR, CL, and tBHQ-treated mice described in Chapter 3. Females were found to have increased basal expression of multiple phase I (Cyp1a1, Cyp2a4, Cyp2b13, Cyp4a10, Cyp4a14) and phase II (Mgst3, Nqo1, Sult2a2) genes (Figure 4-3) compared to age-matched male controls. Preliminary analysis of sex-based effects on XME gene expression in Snell and GHRKO mice is currently in progress. Interestingly, multiple genes that are elevated in male GHRKO mice relative to littermate control mice (e.g. Cyp2b9, Cyp2b10, Cyp2b13, Cyp4a10, Sulta2) are expressed at a similar level in both female littermate control and GHRKO mice (Sun LY, personal communication), at levels similar to those seen in male GHRKO mice and thus much higher than levels in male control mice. Since both male and female GHRKO mice are long-lived, these data argue against a role for elevated xenobiotic metabolism in delaying aging, at least in females. However, additional studies that measure directly measure xenobiotic metabolism activity rather than simply gene expression are required before such a conclusion can be drawn. Regardless, sexual dimorphism of xenobiotic metabolism is relevant in the context of pharmacological-based lifespan extension studies. Observed gender-specific effects in longevity (74-77) may be a result of sex-specific differences in

drug metabolism, and sexual dimorphism is also observed in response to many common drugs in humans (78, 79).

4-6. Pharmacological activation of Nrf2 may be a promising new approach to delay aging in mice

The isothiocyanate sulforaphane (SFN), a naturally occurring organosulfur compound found in broccoli, is a potent activator of Nrf2 (80). SFN is the best characterized Nrf2 activator, and is thought to activate Nrf2 by oxidation of the Cys151 residue of Keap1, similar to tBHQ (81, 82). SFN has potent anticancer properties, and was recently identified as an inhibitor of cancer stem cell formation (83). We attempted to measure changes in XME gene expression in response to dietary SFN but were plagued by degradation of the compound during food preparation (data not shown). This was observed with two SFN variants in mice treated at the University of Michigan: synthesized D,L-sulforaphane (Toronto Research Chemicals #S699115) and natural chiral product L-sulforaphane (LKT Laboratories #S8046). Therefore, although SFN is a promising candidate for inclusion in a future ITP lifespan study, the stability problem must first be resolved.

Protandim (LifeVantage Corporation, Sandy, UT, USA) is an herbal supplement comprised of milk thistle, bacopa, ashwagandha, green tea, and turmeric extracts. IP injection of this supplement in rats was reported to increase Nrf2 and heme oxygenase 1 levels in cardiac tissue (84). In addition, Protandim was shown to protect against two-stage skin carcinogenesis in mice (85) and

decrease lipid peroxidation byproducts detected as thiobarbituric acid-reacting substances (TBARS) in plasma in a human clinical study (86). We found that HET3 mice administered 1% w/w Protandim in chow for 4 weeks had elevated expression of multiple XME mRNAs in kidney tissue (Figure 4-4) but not liver tissue (data not shown), with no observed signs of ill health. Protandim appears to maintain potency during food preparation and may be a good candidate for testing in a future ITP longevity study.

4-7. Final remarks

One of the major goals of aging research is to develop new therapeutics that can slow the aging process in humans. Although an effective anti-aging drug has not yet been developed for humans, research on long-lived mice and invertebrates implicate IGF-1 and GH as key hormones that influence the aging process. The experiments presented in this thesis suggest that differential regulation of MAPKs (Chapter 2) and xenobiotic metabolism (Chapter 3), potentially in response to altered GH and/or IGF-1 action, contribute to the regulation of stress resistance in mice Figure 4-2. While additional research is required to conclusively demonstrate that disruption of GH or IGF-1, elevated xenobiotic metabolism, or other interventions (e.g. rapamycin, CR mimetics) can effectively slow aging in humans, this work represents a small step toward that goal.

4-8. Figures

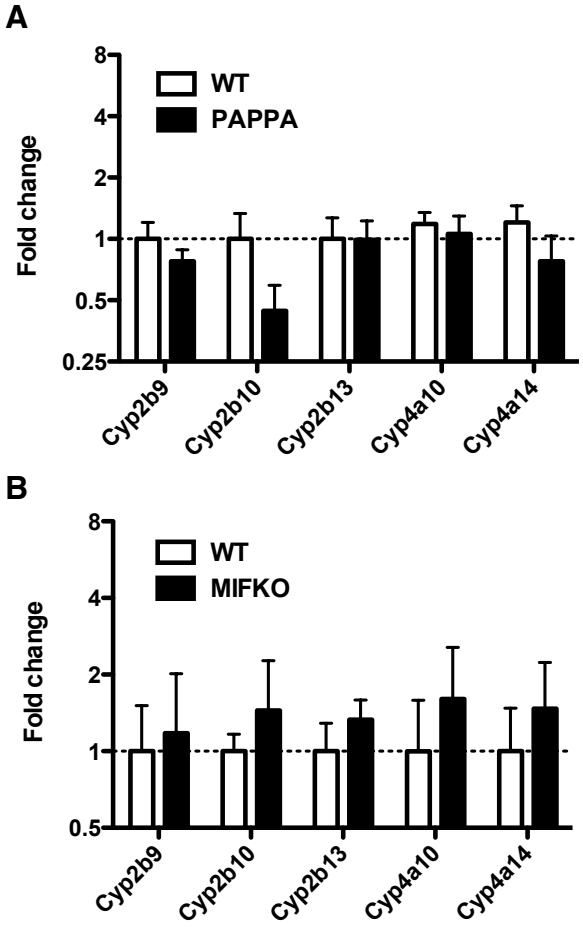

Figure 4-1. Long-lived PAPPA-KO (87) and MIFKO (88) mice do not have altered hepatic xenobiotic metabolism gene expression.

No significant difference in expression of Cyp2b9, Cyp2b10, Cyp2b13, Cyp4a10, or Cyp4a14 was observed in male, young adult PAPPA-KO or MIFKO mice. Bars indicate mean ± SEM for (A) PAPPA-KO and (B) MIFKO mice along with age-matched littermate control mice, in each case normalized to the average level of mRNA in the littermate control animals (n = 3).

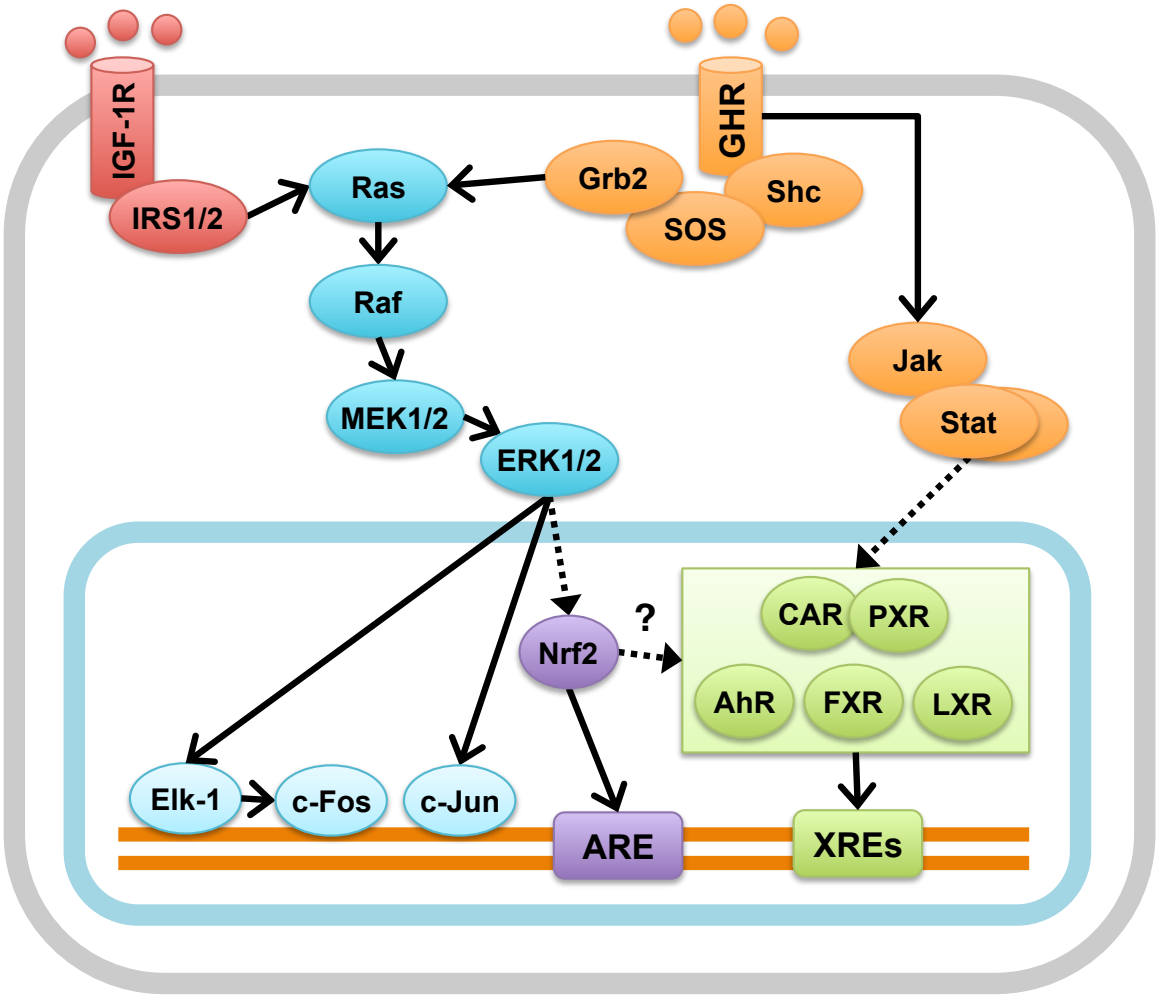

Figure 4-2. Model of IGF-1R and GHR-mediated regulation of xenobiotic metabolism and the ERK signal cascade.

Multiple XME genes are negatively regulated by GH in a STAT5b-dependent manner (63, 89). The downstream regulators of STAT5b that influence XME gene expression have not been identified but likely influence nuclear receptor (e.g. CAR, PXR, AhR, FXR, and/or LXR) activity. Nuclear receptors regulate XME gene expression through multiple binding sites, including XREM (90-92), PBREM (93, 94), and PPRE (95). Nrf2 regulates XME transcription through the ARE binding sequence (7) but may also regulate nuclear receptor activity (31, 96). ERK activity is regulated by the IGF-1R receptor through the IRS-Ras-Raf-MEK cascade (97). ERK is known to directly regulate Elk-1 (which regulates c-Fos) and c-Jun IEGs (98), and has been proposed to regulate Nrf2 activity (99).

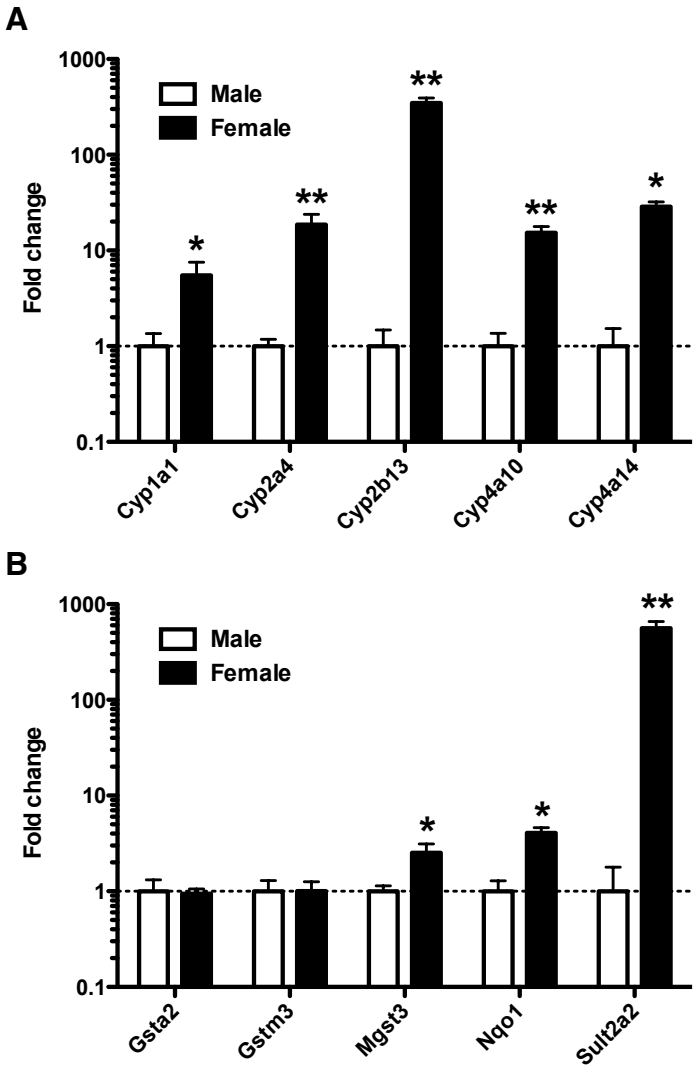

Figure 4-3. Sexual dimorphism of (A) phase I and (B) phase II XME RNAs in HET3 mouse liver tissue.

Bars indicate mean ± SEM for male and female mice, in each case normalized to the average level of mRNA in the male mice. Significant elevation of phase I (Cyp1a1, Cyp2a4, Cyp2b13, Cyp4a10, and Cyp4a14) and phase II (Mgst3, Nqo1, Sult2a2) was observed in female mice compared to male mice (n = 3; $p < 0.05$*; $p < 0.01$**).

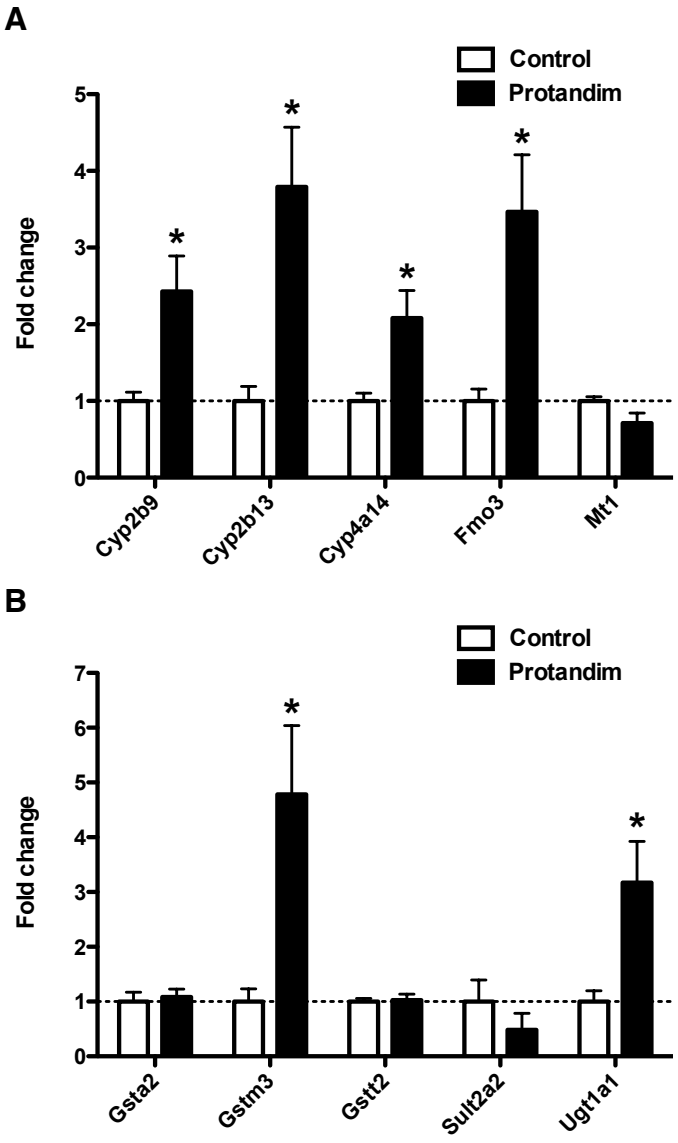

Figure 4-4. Short-term Protandim treatment increases (A) phase I and (B) phase II mRNA levels in mouse kidney tissue.

Male HET3 mice were treated with 1% (w/w) Protandim in chow for 4 weeks. Bars indicate mean ± SEM for Protandim-treated and age-matched littermate control mice, in each case normalized to the average level of mRNA in the littermate control animals. Significant elevation of multiple phase I (Cyp2b9, Cyp2b13, Cyp4a14, Fmo3) and phase II (Gstm3, Ugt1a1) genes was observed in response to Protandim treatment ($n = 6$; $p < 0.05$*)

4-9. References

1. Murakami S, Salmon A, Miller RA (2003) Multiplex stress resistance in cells from long-lived dwarf mice. *FASEB J* 17:1565–1566.

2. Salmon AB et al. (2005) Fibroblast cell lines from young adult mice of long-lived mutant strains are resistant to multiple forms of stress. *Am J Physiol Endocrinol Metab* 289:E23–9.

3. de Luca C, Olefsky JM (2008) Inflammation and insulin resistance. *FEBS Lett* 582:97–105.

4. Sun L, Sadighi Akha AA, Miller RA, Harper JM (2009) Life-span extension in mice by preweaning food restriction and by methionine restriction in middle age. *J Gerontol A Biol Sci Med Sci* 64:711–722.

5. Kwak MK et al. (2001) Role of phase 2 enzyme induction in chemoprotection by dithiolethiones. *Mutat Res* 480-481:305–315.

6. Kwak M-K, Wakabayashi N, Kensler TW (2004) Chemoprevention through the Keap1-Nrf2 signaling pathway by phase 2 enzyme inducers. *Mutat Res* 555:133–148.

7. Kensler TW, Wakabayashi N, Biswal S (2007) Cell survival responses to environmental stresses via the Keap1-Nrf2-ARE pathway. *Annu Rev Pharmacol Toxicol* 47:89–116.

8. Osburn WO, Kensler TW (2008) Nrf2 signaling: an adaptive response pathway for protection against environmental toxic insults. *Mutat Res* 659:31–39.

9. Tullet JMA et al. (2008) Direct inhibition of the longevity-promoting factor SKN-1 by insulin-like signaling in C. elegans. *Cell* 132:1025–1038.

10. Suh JH et al. (2004) Decline in transcriptional activity of Nrf2 causes age-related loss of glutathione synthesis, which is reversible with lipoic acid. *Proc Natl Acad Sci USA* 101:3381–3386.

11. Praticò D, Delanty N (2000) Oxidative injury in diseases of the central nervous system: focus on Alzheimer's disease. *Am J Med* 109:577–585.

12. Jenner P (2003) Oxidative stress in Parkinson's disease. *Ann Neurol* 53 Suppl 3:S26–36; discussion S36–8.

13. Hayes JD, McMahon M (2009) NRF2 and KEAP1 mutations: permanent activation of an adaptive response in cancer. *Trends Biochem Sci* 34:176–188.

14. Martín-Montalvo A, Villalba JM, Navas P, de Cabo R (2011) NRF2, cancer and calorie restriction. *Oncogene* 30:505–520.

15. Hayes JD et al. (2000) The Nrf2 transcription factor contributes both to the basal expression of glutathione S-transferases in mouse liver and to their induction by the chemopreventive synthetic antioxidants, butylated hydroxyanisole and ethoxyquin. *Biochem Soc Trans* 28:33–41.

16. McMahon M et al. (2001) The Cap“n”Collar basic leucine zipper transcription factor Nrf2 (NF-E2 p45-related factor 2) controls both constitutive and inducible expression of intestinal detoxification and glutathione biosynthetic enzymes. *Cancer Res* 61:3299–3307.

17. Thimmulappa RK et al. (2002) Identification of Nrf2-regulated genes induced by the chemopreventive agent sulforaphane by oligonucleotide microarray. *Cancer Res* 62:5196–5203.

18. Chan K, Han XD, Kan YW (2001) An important function of Nrf2 in combating oxidative stress: detoxification of acetaminophen. *Proc Natl Acad Sci USA* 98:4611–4616.

19. Enomoto A et al. (2001) High sensitivity of Nrf2 knockout mice to acetaminophen hepatotoxicity associated with decreased expression of ARE-regulated drug metabolizing enzymes and antioxidant genes. *Toxicol Sci* 59:169–177.

20. Chan K, Kan YW (1999) Nrf2 is essential for protection against acute pulmonary injury in mice. *Proc Natl Acad Sci USA* 96:12731–12736.

21. Cho H-Y, Reddy SPM, Yamamoto M, Kleeberger SR (2004) The transcription factor NRF2 protects against pulmonary fibrosis. *FASEB J* 18:1258–1260.

22. Aoki Y et al. (2001) Accelerated DNA adduct formation in the lung of the Nrf2 knockout mouse exposed to diesel exhaust. *Toxicol Appl Pharmacol* 173:154–160.

23. Shih AY et al. (2005) Induction of the Nrf2-driven antioxidant response confers neuroprotection during mitochondrial stress in vivo. *J Biol Chem* 280:22925–22936.

24. Rangasamy T et al. (2004) Genetic ablation of Nrf2 enhances susceptibility to cigarette smoke-induced emphysema in mice. *J Clin Invest* 114:1248–1259.

25. Iizuka T et al. (2005) Nrf2-deficient mice are highly susceptible to cigarette smoke-induced emphysema. *Genes Cells* 10:1113–1125.

26. Yoh K et al. (2001) Nrf2-deficient female mice develop lupus-like autoimmune nephritis. *Kidney Int* 60:1343–1353.

27. Li J, Stein TD, Johnson JA (2004) Genetic dissection of systemic autoimmune disease in Nrf2-deficient mice. *Physiol Genomics* 18:261–272.

28. Ma Q, Battelli L, Hubbs AF (2006) Multiorgan autoimmune inflammation, enhanced lymphoproliferation, and impaired homeostasis of reactive oxygen species in mice lacking the antioxidant-activated transcription factor Nrf2. *Am J Pathol* 168:1960–1974.

29. Pearson KJ et al. (2008) Nrf2 mediates cancer protection but not prolongevity induced by caloric restriction. *Proceedings of the National Academy of Sciences* 105:2325–2330.

30. Wakabayashi N et al. (2003) Keap1-null mutation leads to postnatal lethality due to constitutive Nrf2 activation. *Nat Genet* 35:238–245.

31. Okawa H et al. (2006) Hepatocyte-specific deletion of the keap1 gene activates Nrf2 and confers potent resistance against acute drug toxicity. *Biochem Biophys Res Commun* 339:79–88.

32. Harper JM et al. (2006) Stress resistance and aging: influence of genes and nutrition. *Mech Ageing Dev* 127:687–694.

33. Amador-Noguez D et al. (2007) Alterations in xenobiotic metabolism in the long-lived Little mice. *Aging Cell* 6:453–470.

34. Sun LY, Bokov AF, Richardson A, Miller RA (2011) Hepatic response to oxidative injury in long-lived Ames dwarf mice. *FASEB J* 25:398–408.

35. Sierra F (2006) Is (your cellular response to) stress killing you? *J Gerontol A Biol Sci Med Sci* 61:557–561.

36. Leiser SF, Miller RA (2010) Nrf2 signaling, a mechanism for cellular stress resistance in long-lived mice. *Mol Cell Biol* 30:871–884.

37. Bost F et al. (2005) The extracellular signal-regulated kinase isoform ERK1 is specifically required for in vitro and in vivo adipogenesis. *Diabetes* 54:402–411.

38. Bourcier C et al. (2006) p44 mitogen-activated protein kinase (extracellular signal-regulated kinase 1)-dependent signaling contributes to epithelial skin carcinogenesis. *Cancer Res* 66:2700–2707.

39. Lefloch R, Pouysségur J, Lenormand P (2009) Total ERK1/2 activity regulates cell proliferation. *Cell Cycle* 8:705–711.

40. Lefloch R, Pouysségur J, Lenormand P (2008) Single and combined silencing of ERK1 and ERK2 reveals their positive contribution to growth signaling depending on their expression levels. *Mol Cell Biol* 28:511–527.

41. Fischer AM, Katayama CD, Pagès G, Pouysségur J, Hedrick SM (2005) The role of erk1 and erk2 in multiple stages of T cell development. *Immunity* 23:431–443.

42. Samuels IS et al. (2008) Deletion of ERK2 mitogen-activated protein kinase identifies its key roles in cortical neurogenesis and cognitive function. *J Neurosci* 28:6983–6995.

43. Kujiraoka T et al. (2011) Hepatic ERK Protects From Endothelial Dysfunction With The Suppression Of Hepatic Steatosis In Mice Fed High-fat And High-sucrose Diet. *Circulation* 124:A14925. Available at: http://circ.ahajournals.org/cgi/content/meeting_abstract/124/21_MeetingAbstracts/A14925.

44. Borrás C et al. (2011) RasGrf1 deficiency delays aging in mice. *AGING* 3:262–276.

45. Swindell WR (2007) Gene expression profiling of long-lived dwarf mice: longevity-associated genes and relationships with diet, gender and aging. *BMC Genomics* 8:353.

46. Williams RBH et al. (2006) Normalization procedures and detection of linkage signal in genetical-genomics experiments. *Nat Genet* 38:855–6; author reply 856–9.

47. Gelman R, Watson A, Bronson R, Yunis E (1988) Murine chromosomal regions correlated with longevity. *Genetics* 118:693–704.

48. Miller RA, Williams JB, Kiklevich JV, Austad S, Harper JM (2011) Comparative cellular biogerontology: primer and prospectus. *Ageing Res Rev* 10:181–190.

49. Hart RW, Setlow RB (1974) Correlation between deoxyribonucleic acid excision-repair and life-span in a number of mammalian species. *Proc Natl Acad Sci USA* 71:2169–2173.

50. Harper JM, Salmon AB, Leiser SF, Galecki AT, Miller RA (2007) Skin-derived fibroblasts from long-lived species are resistant to some, but not

all, lethal stresses and to the mitochondrial inhibitor rotenone. *Aging Cell* 6:1–13.

51. Salmon AB, Sadighi Akha AA, Buffenstein R, Miller RA (2008) Fibroblasts from naked mole-rats are resistant to multiple forms of cell injury, but sensitive to peroxide, ultraviolet light, and endoplasmic reticulum stress. *J Gerontol A Biol Sci Med Sci* 63:232–241.

52. Harper JM et al. (2011) Fibroblasts from long-lived bird species are resistant to multiple forms of stress. *J Exp Biol* 214:1902–1910.

53. Sun LY, Steinbaugh MJ, Masternak MM, Bartke A, Miller RA (2009) Fibroblasts from long-lived mutant mice show diminished ERK1/2 phosphorylation but exaggerated induction of immediate early genes. *Free Radic Biol Med* 47:1753–1761.

54. Salmon AB, Ljungman M, Miller RA (2008) Cells from long-lived mutant mice exhibit enhanced repair of ultraviolet lesions. *J Gerontol A Biol Sci Med Sci* 63:219–231.

55. Sadighi Akha AA et al. (2011) Heightened induction of proapoptotic signals in response to endoplasmic reticulum stress in primary fibroblasts from a mouse model of longevity. *J Biol Chem* 286:30344–30351.

56. Leiser SF, Salmon AB, Miller RA (2006) Correlated resistance to glucose deprivation and cytotoxic agents in fibroblast cell lines from long-lived pituitary dwarf mice. *Mech Ageing Dev* 127:821–829.

57. Lamming DW et al. (2012) Rapamycin-induced insulin resistance is mediated by mTORC2 loss and uncoupled from longevity. *Science* 335:1638–1643.

58. Houde VP et al. (2010) Chronic rapamycin treatment causes glucose intolerance and hyperlipidemia by upregulating hepatic gluconeogenesis and impairing lipid deposition in adipose tissue. *Diabetes* 59:1338–1348.

59. Loewith R et al. (2002) Two TOR complexes, only one of which is rapamycin sensitive, have distinct roles in cell growth control. *Mol Cell* 10:457–468.

60. Jacinto E et al. (2004) Mammalian TOR complex 2 controls the actin cytoskeleton and is rapamycin insensitive. *Nat Cell Biol* 6:1122–1128.

61. Hughes KJ, Kennedy BK (2012) Cell biology. Rapamycin paradox resolved. *Science* 335:1578–1579.

62. Xu J, Messina JL (2009) Crosstalk between growth hormone and insulin signaling. *Vitam Horm* 80:125–153.

63. Waxman DJ, Holloway MG (2009) Sex differences in the expression of hepatic drug metabolizing enzymes. *Mol Pharmacol* 76:215–228.

64. Waxman DJ, O'Connor C (2006) Growth hormone regulation of sex-dependent liver gene expression. *Mol Endocrinol* 20:2613–2629.

65. Flurkey K, Papaconstantinou J, Miller RA, Harrison DE (2001) Lifespan extension and delayed immune and collagen aging in mutant mice with defects in growth hormone production. *Proc Natl Acad Sci USA* 98:6736–6741.

66. Vergara M, Smith-Wheelock M, Harper JM, Sigler R, Miller RA (2004) Hormone-treated snell dwarf mice regain fertility but remain long lived and disease resistant. *J Gerontol A Biol Sci Med Sci* 59:1244–1250.

67. Swindell WR et al. (2009) Endocrine regulation of heat shock protein mRNA levels in long-lived dwarf mice. *Mech Ageing Dev* 130:393–400.

68. Kato R (1974) Sex-related differences in drug metabolism. *Drug Metab Rev* 3:1–32.

69. Tannenbaum GS, Martin JB (1976) Evidence for an endogenous ultradian rhythm governing growth hormone secretion in the rat. *Endocrinology* 98:562–570.

70. Edén S (1979) Age- and sex-related differences in episodic growth hormone secretion in the rat. *Endocrinology* 105:555–560.

71. Park SH, Liu X, Hennighausen L, Davey HW, Waxman DJ (1999) Distinctive roles of STAT5a and STAT5b in sexual dimorphism of hepatic P450 gene expression. Impact of STAT5a gene disruption. *J Biol Chem* 274:7421–7430.

72. Holloway MG, Laz EV, Waxman DJ (2006) Codependence of growth hormone-responsive, sexually dimorphic hepatic gene expression on signal transducer and activator of transcription 5b and hepatic nuclear factor 4alpha. *Mol Endocrinol* 20:647–660.

73. Waxman DJ, Chang TKH (2005) in *Cytochrome P450*, ed Ortiz de Montellano PR (Kluwer Academic/Plenum Publishers), pp 347–376. Available at: http://dx.doi.org/10.1007/0-387-27447-2_9.

74. Holzenberger M et al. (2003) IGF-1 receptor regulates lifespan and resistance to oxidative stress in mice. *Nature* 421:182–187.

75. Selman C et al. (2008) Evidence for lifespan extension and delayed age-related biomarkers in insulin receptor substrate 1 null mice. *FASEB J* 22:807–818.

76. Selman C et al. (2009) Ribosomal protein S6 kinase 1 signaling regulates mammalian life span. *Science* 326:140–144.

77. Harrison DE et al. (2009) Rapamycin fed late in life extends lifespan in genetically heterogeneous mice. *Nature* 460:392–395.

78. Gandhi M, Aweeka F, Greenblatt RM, Blaschke TF (2004) Sex differences in pharmacokinetics and pharmacodynamics. *Annu Rev Pharmacol Toxicol* 44:499–523.

79. Schwartz JB (2007) The current state of knowledge on age, sex, and their interactions on clinical pharmacology. *Clin Pharmacol Ther* 82:87–96.

80. Guerrero-Beltrán CE et al. (2010) Protective effect of sulforaphane against cisplatin-induced mitochondrial alterations and impairment in the activity of NAD(P)H: quinone oxidoreductase 1 and γ glutamyl cysteine ligase: studies in mitochondria isolated from rat kidney and in LLC-PK1 cells. *Toxicol Lett* 199:80–92.

81. Hong F, Freeman ML, Liebler DC (2005) Identification of sensor cysteines in human Keap1 modified by the cancer chemopreventive agent sulforaphane. *Chem Res Toxicol* 18:1917–1926.

82. Sekhar KR, Rachakonda G, Freeman ML (2010) Cysteine-based regulation of the CUL3 adaptor protein Keap1. *Toxicol Appl Pharmacol* 244:21–26.

83. Li Y et al. (2010) Sulforaphane, a dietary component of broccoli/broccoli sprouts, inhibits breast cancer stem cells. *Clin Cancer Res* 16:2580–2590.

84. Bogaard HJ et al. (2009) Chronic pulmonary artery pressure elevation is insufficient to explain right heart failure. *Circulation* 120:1951–1960.

85. Liu J et al. (2009) Protandim, a fundamentally new antioxidant approach in chemoprevention using mouse two-stage skin carcinogenesis as a model. *PLoS ONE* 4:e5284.

86. Nelson SK, Bose SK, Grunwald GK, Myhill P, Mccord JM (2006) The induction of human superoxide dismutase and catalase in vivo: a

fundamentally new approach to antioxidant therapy. *Free Radic Biol Med* 40:341–347.

87. Conover CA, Bale LK (2007) Loss of pregnancy-associated plasma protein A extends lifespan in mice. *Aging Cell* 6:727–729.

88. Harper JM, Wilkinson JE, Miller RA (2010) Macrophage migration inhibitory factor-knockout mice are long lived and respond to caloric restriction. *FASEB J* 24:2436–2442.

89. Zhang Y, Laz EV, Waxman DJ (2012) Dynamic, sex-differential STAT5 and BCL6 binding to sex-biased, growth hormone-regulated genes in adult mouse liver. *Mol Cell Biol* 32:880–896.

90. Mangelsdorf DJ, Evans RM (1995) The RXR heterodimers and orphan receptors. *Cell* 83:841–850.

91. Goodwin B, Hodgson E, Liddle C (1999) The orphan human pregnane X receptor mediates the transcriptional activation of CYP3A4 by rifampicin through a distal enhancer module. *Mol Pharmacol* 56:1329–1339.

92. Goodwin B, Redinbo MR, Kliewer SA (2002) Regulation of cyp3a gene transcription by the pregnane x receptor. *Annu Rev Pharmacol Toxicol* 42:1–23.

93. Trottier E, Belzil A, Stoltz C, Anderson A (1995) Localization of a phenobarbital-responsive element (PBRE) in the 5'-flanking region of the rat CYP2B2 gene. *Gene* 158:263–268.

94. Honkakoski P, Negishi M (1997) Characterization of a phenobarbital-responsive enhancer module in mouse P450 Cyp2b10 gene. *J Biol Chem* 272:14943–14949.

95. Tugwood JD et al. (1992) The mouse peroxisome proliferator activated receptor recognizes a response element in the 5' flanking sequence of the rat acyl CoA oxidase gene. *EMBO J* 11:433–439.

96. Anwar-Mohamed A et al. (2011) The effect of Nrf2 knockout on the constitutive expression of drug metabolizing enzymes and transporters in C57Bl/6 mice livers. *Toxicol In Vitro* 25:785–795.

97. Mckay MM, Morrison DK (2007) Integrating signals from RTKs to ERK/MAPK. *Oncogene* 26:3113–3121.

98. Murphy LO, MacKeigan JP, Blenis J (2004) A network of immediate early gene products propagates subtle differences in mitogen-activated protein kinase signal amplitude and duration. *Mol Cell Biol* 24:144–153.

99. Owuor ED, Kong A-NT (2002) Antioxidants and oxidants regulated signal transduction pathways. *Biochem Pharmacol* 64:765–770.